UiT The Arctic University of Norway

Faculty of Biosciences Fisheries and Economics
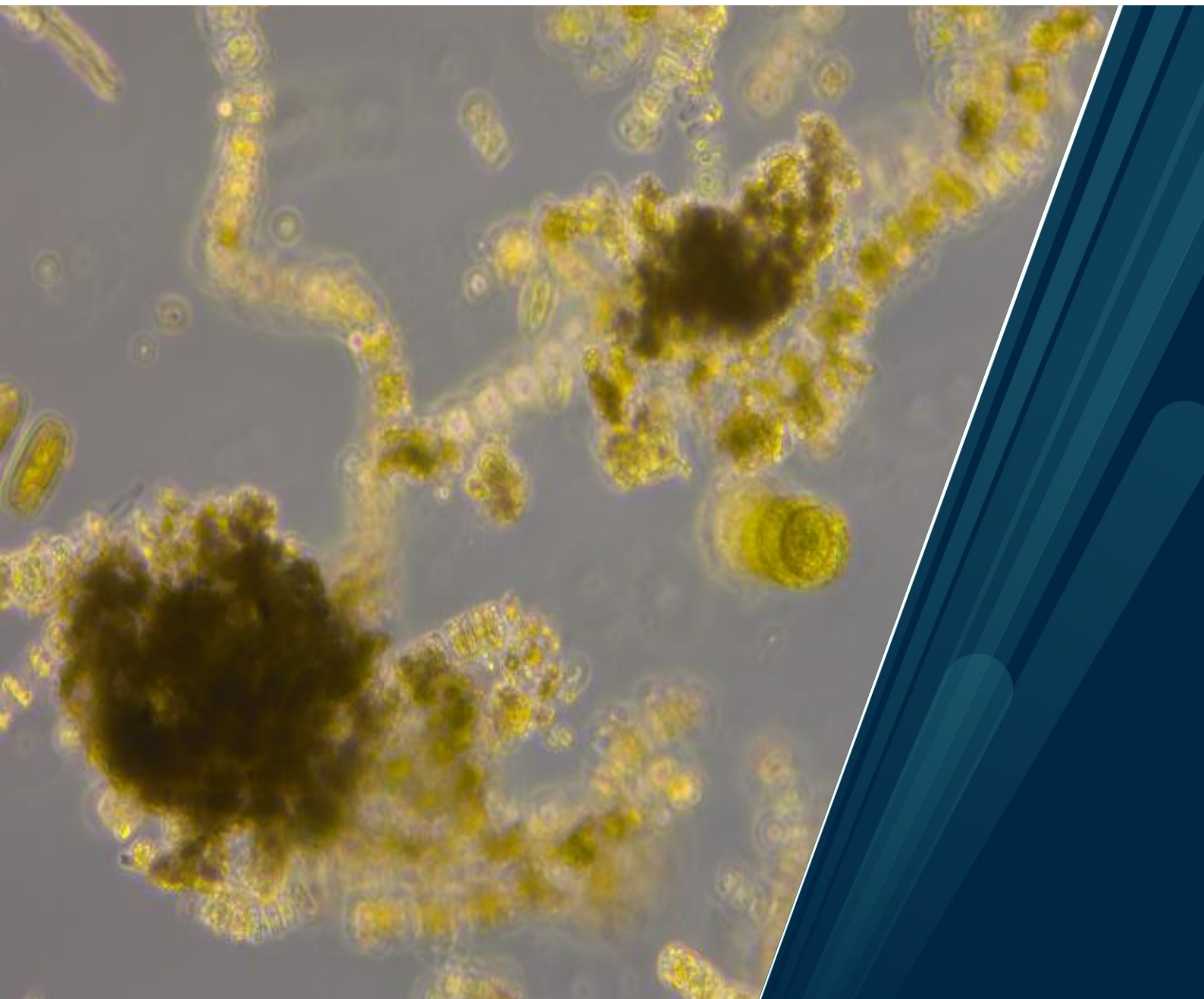
Department of Arctic and Marine Biology

Aspects of the biological carbon pump in the Atlantic sector of the Arctic

Aggregation, vertical flux and pelagic-benthic coupling

Yasemin Vicdan Bodur

A dissertation for the degree of Philosophiae Doctor – March 2024

Aspects of the biological carbon pump in the Atlantic sector of the Arctic

Aggregation, vertical flux and pelagic-benthic coupling

Yasemin Vicdan Bodur

A dissertation for the degree of Philosophiae Doctor
March 2024

Faculty of Biosciences, Fisheries and Economics
Department of Arctic and Marine Biology

Acknowledgements

Table of Contents

Summary

The biological carbon pump (BCP) is an essential component of the earth's carbon cycle. It facilitates the uptake of atmospheric CO_2 by the surface ocean, provides an essential food source for organisms in the deep and at the bottom of the ocean, and enables the storage and sequestration of carbon at the seafloor. The BCP is mainly driven by the gravitational settling of particulate organic matter (POM), transporting carbon that escapes pelagic remineralization below the euphotic zone. In the Arctic, the BCP is subject to strong changes due to climate change. The sea-ice concentration and extent are decreasing, and the influence of boreal water masses and coastal runoff are increasing. Arctic shelves experience a seasonal shift with earlier onset of ice melt and a longer open-water period, changes in mixing regimes and increased concentrations of dissolved organic matter (DOM). These changes will have implications for Arctic marine ecosystems and hence, the BCP. It is postulated that under a longer open-water period, concentrations, composition and characteristics of sinking particles will reflect pelagic summer conditions for a longer time during the year. However, it is yet unclear how or whether the magnitude and efficiency of pelagic carbon export from the pelagic zone will change, and with that how benthic communities will be affected by changes in food supply or composition (i.e., how tightly the pelagic and benthic realm will be coupled). Moreover, the DOM and POM are under constant dynamic change, and the contribution of DOM to the BCP under different environmental conditions is yet unresolved, which makes it difficult to estimate the influence of changing DOM concentrations and composition on the BCP. A holistic view on the Arctic BCP is often hampered by the lack of interdisciplinarity. To address some of these issues, this thesis integrates findings from benthos on an Arctic outflow shelf, a vertical flux study on an inflow shelf, and DOM aggregation experiments in a sub-Arctic fjord that combine marine chemistry and ecology.

Field work was conducted in three regions in the Atlantic sector of the Arctic. For the benthic study (**Paper I**), the fieldwork occurred between September and October 2017 on the Northeast Greenland shelf, and samples were taken with multicorers or benthic landers to characterize the benthic infaunal communities (bacteria, meiofauna, macrofauna) and their environment. The identified patterns were compared to studies conducted in the 1990s to detect possible changes in benthic communities. For **Paper II**, vertical flux was investigated in August and December 2019, and March and May 2021 in the northwestern Barents Sea along a revisited transect in the marginal ice zone (MIZ). Sediment traps were used for sampling and parameters were taken that characterize the seasonal and spatial composition and magnitude of vertical flux. In **Paper III**, seasonal aggregation patterns and processes in the DOM-POM continuum were investigated. For this, fieldwork was conducted in Gáranasvuotna/Ramfjorden, a sub-Arctic fjord in Sápmi/Northern Norway due to its easy accessibility and conditions representative for the Arctic Barents Sea. A set of biogeochemical parameters were sampled on a monthly basis between September 2020 and August 2021 to characterize the ecosystem and its seasonal cycle in the fjord. Aggregation experiments were conducted every second month. The sampled fjord water was filtered through a GF/F filter (0.7 µm pore size), and subsequently incubated in roller tanks for 36 h. Samples for dissolved and particulate organic parameters were taken before and after the incubation to determine changes in the two different organic matter pools over the course of the incubation.

On the Northeast Greenland shelf, benthic communities (meio- and macrofauna) showed a separation between the northern region, which is influenced by a polynya, and the southern and glacier-influenced region. However, this separation was not significant and less distinct when compared to results from the 1990s. Samples taken in 1992 and 1993 showed clear differences in terms of their benthic community composition between the northern and the southern region, and they were mainly driven by food availability at the seafloor (benthic pigment concentrations). Moreover, we found higher meiofauna and lower macrofauna abundances since the 1990s, along with a decrease in benthic pigment concentrations. We postulated that the amount and/or the composition of sinking organic matter had probably changed compared to the 1990s, leading to lower food availability at the seafloor.

Following the hypothesis that the BCP will reflect a prolonged "summer" scenario in a future Arctic, we postulate that vertical flux patterns under different environmental conditions can be used for explaining changing food availability for benthos. In the northwestern Barents Sea, we found that vertical flux was highly seasonal, and its composition between May and August differed considerably, with fresh and diatom-derived material sinking out in spring and increasing degradation towards summer. Moreover, higher concentrations of suspended particles in August, but no increase in vertical flux, point towards lower export efficiency compared to May. However, strong spatial gradients in vertical flux magnitude revealed that a range of seasonal scenarios spanning from winter to peak-bloom were present along the transect during May. By contrast, in August, vertical flux magnitude and composition were more similar across stations and represented a post-bloom scenario along the transect. This spatial variability was driven by sea-ice cover and the influence of Atlantic Water in concert and makes it difficult to compare the overall export magnitude between a spring and a summer scenario.

To further elucidate mechanisms affecting particle dynamics, we investigated the aggregation patterns of DOM as an overlooked contributor to the pelagic particle pool. We found increased particulate carbon concentrations in filtered water in April, June, and September, and confirm previous findings showing that DOM has the potential to aggregate when biological productivity is high. The highest aggregation potential was found during the summer period. During winter (December, February), we measured decreased particulate carbon concentrations in filtered water, pointing towards a dissolution of particles. Aggregation in September was accompanied by an increase in molecular weight of molecules <1 kDa, and a decrease in DOM lability. In December and February, on the other hand, DOM molecular weight decreased, and lability increased.

To integrate the findings of the three papers in the synthesis of this thesis, different mechanisms of the BCP are presented, and pelagic-benthic coupling processes are compared across different Arctic shelf regions. The fresh, diatom-derived organic matter exported during spring possibly enforces a strong pelagic-benthic coupling in the MIZ and productive polynyas. In a future ice-free, prolonged summer period in the MIZ, organic matter may be more degraded for a longer time. Together with a lower magnitude of export, these changes can result in a shift in benthic communities, from macrobenthic suspension feeders towards a domination of smaller, facultative meiofauna, and a homogenization of benthic communities. However, a "weakening" or "tightening" of pelagic-benthic coupling on Arctic shelves will depend on a range of factors. The main mechanisms are identified as (1) the degree of vertical flux regulation by grazing or microbial degradation, (2) short-circuiting processes such as vertical mixing, (3) processes that lead to increased particle concentrations and the potential for particles to sink, such as aggregation or ballasting. Under a summer scenario, the contribution of DOM to the

particulate pool may increase, serving as one factor that increases particle concentrations in the water column and could possibly contribute to vertical flux. Heterotrophic activity in the water column may increase, but zooplankton fecal pellets may mediate the sinking of small particles. Ultimately, the mixing regime will determine whether slow sinking particles can be transported physically to depth or will be retained above the thermo- or pycnocline. A "tightening" or "weakening" of pelagic-benthic coupling will vary across different Arctic shelf regions, as these mechanisms contribute at different scales to the regulation of vertical flux and the BCP. Finally, the thesis provides one of the few contributions on vertical flux and processes in the DOM-POM continuum during the Arctic winter. To get a comprehensive picture of the Arctic BCP and its possible responses to climate change, it is important to integrate studies from different disciplines.

Supervisors

Prof. Marit Reigstad

Prof. Paul E. Renaud

Publication list

List of papers in this thesis

I Benthic ecosystem changes suggest weakened pelagic-benthic coupling on an Arctic outflow shelf (Northeast Greenland)

II Seasonal patterns of vertical flux in the northwestern Barents Sea under Atlantic Water influence and sea-ice decline

III Contrasting seasonal patterns in particle aggregation and DOM transformation in a sub-Arctic fjord

Author contributions

	Paper I	**Paper II**	**Paper III**
Concept and idea	UB, YVB, FW, JF	MR, YVB	YVB, MGD
Study design and methods	UB, FW, JF	YVB, MR, PER	MGD, YVB, MAA, MLP
Data gathering	YVB, LL, LDCM, UB, FW, JF, TK	YVB, LG, MM, MAA, AMD, AT	YVB, MGD, MAA, SK, JH, UD, TKI, MLP
Manuscript preparation	YB, PER, UB	YVB, PER, MR	YVB, MGD
Input to manuscript writing and development	YVB, UB, PER, WGA, LL, LDCM, FW, JF, MWK, TK	YVB, PER, MR, MM, MAA, PA, AHHR, LG, AMD, AT	MGD, YVB, MLP, MAA, MLP, SK, OM, MR, JH, UD, TKI

Agnieska Tatarek (AT)
Angelika H. H. Renner (AHHR)
Anna Maria Dąbrowska (AMD)
Frank Wenzhoefer (FW)
Janine Felden (JF)
Jeffrey Hawkes (JH)
Lidia Lins (LL)
Luana Da Costa Monteira (LDCM)
Lucie Goraguer (LG)
Marit Reigstad (MR)
Martí Amargant-Arumí (MAA)
Maria Guadalupe Digernes (MGD)
Maria Lund Paulsen (MLP)
Maria Włodarska-Kowalczuk (MWK)
Miriam Marquardt (MM)

Oliver Mueller (OM)
Paul E. Renaud (PER)
Philipp Assmy (PA)
Stephen Koehler (SK)
Thomas Krumpen (TK)
Tobias Kieland (TKI)
Ulrike Braeckman (UB)
Ulrike Dietrich (UD)
William G. Ambrose (WA)
Yasemin V. Bodur (YVB)

Associated Datasets

Bodur, Yasemin V., Martí Amargant-Arumí, and Marit Reigstad. "Downward Vertical Flux of Size-Fractionated Chlorophyll-a and Phaeopigments in the Northern Barents Sea during May 2021, Nansen Legacy Cruise 2021704 Q2." UiT The Arctic University of Norway, 2023. https://doi.org/10.11582/2023.00105.

Bodur, Yasemin V., Anna Maria Dąbrowska, Agnieska Tatarek, Józef Maria Wiktor, Lucie Goraguer, Martí Amargant-Arumí, and Marit Reigstad. "Downward Vertical Flux of Protist Cells and Biomass in the Northern Barents Sea during May 2021, Nansen Legacy Cruise 2021704 Q2." UiT The Arctic University of Norway, 2023. https://doi.org/10.11582/2023.00091.

Bodur, Yasemin V., Anna Maria Dąbrowska, Agnieska Tatarek, Józef Maria Wiktor, Lucie Goraguer, Martí Amargant-Arumí, and Marit Reigstad. "Downward Vertical Flux of Protist Cells and Biomass in the Northern Barents Sea during August 2019, Nansen Legacy Cruise 2019706 Q3." UiT The Arctic University of Norway, 2023. https://doi.org/10.11582/2023.00088.

Bodur, Yasemin V., Anna Maria Dąbrowska, Agnieska Tatarek, Józef Maria Wiktor, Lucie Goraguer, Martí Amargant-Arumí, and Marit Reigstad. "Downward Vertical Flux of Protist Cells and Biomass in the Northern Barents Sea during December 2019, Nansen Legacy Cruise 2019711 Q4." UiT The Arctic University of Norway, 2023. https://doi.org/10.11582/2023.00089.

Bodur, Yasemin V., Anna Maria Dąbrowska, Agnieska Tatarek, Józef Maria Wiktor, Lucie Goraguer, Martí Amargant-Arumí, and Marit Reigstad. "Downward Vertical Flux of Protist Cells and Biomass in the Northern Barents Sea during March 2021, Nansen Legacy Cruise 2021703 Q1." UiT The Arctic University of Norway, 2023. https://doi.org/10.11582/2023.00090.

Bodur, Yasemin V., Anna Maria Dąbrowska, Agnieska Tatarek, Józef Maria Wiktor, Lucie Goraguer, Ulrike Dietrich, Camilla Svensen, and Marit Reigstad. "Downward Vertical Flux of Protist Cells and Biomass in the Northern Barents Sea during August 2018, Nansen Legacy Cruise 2018707 JC 1-2." UiT The Arctic University of Norway, 2023. https://doi.org/10.11582/2023.00087.

Bodur, Yasemin V., Martí Amargant-Arumí, and Marit Reigstad. "Downward Fecal Pellet Flux Measured from Short-Term Sediment Traps during August 2019 in the Northern Barents Sea as Part of the Nansen Legacy Project, Cruise 2019706 Q3." UiT The Arctic University of Norway, 2023. https://doi.org/10.11582/2023.00108.

Bodur, Yasemin V., Martí Amargant-Arumí, and Marit Reigstad. "Downward Fecal Pellet Flux Measured from Short-Term Sediment Traps during December in the Northern Barents Sea as Part of the Nansen Legacy Project, Cruise 2019711 Q4." UiT The Arctic University of Norway, 2023. https://doi.org/10.11582/2023.00106.

Bodur, Yasemin V., Martí Amargant-Arumí, and Marit Reigstad. "Downward Fecal Pellet Flux Measured from Short-Term Sediment Traps during March 2021 in the Northern Barents Sea as Part of the Nansen Legacy Project, Cruise 2021703 Q1." UiT The Arctic University of Norway, 2023. https://doi.org/10.11582/2023.00086.

Bodur, Yasemin V., Martí Amargant-Arumí, and Marit Reigstad. "Downward Fecal Pellet Flux Measured from Short-Term Sediment Traps during May 2021 in the Northern Barents Sea as Part of the Nansen Legacy Project, Cruise 2021704 Q2." UiT The Arctic University of Norway, 2023. https://doi.org/10.11582/2023.00107.

Bodur, Yasemin V., Martí Amargant-Arumí, and Marit Reigstad. "Downward Vertical Flux of Size-Fractionated Chlorophyll-a and Phaeopigments in the Northern Barents Sea during August 2019, Nansen Legacy Cruise 2019706 Q3." UiT The Arctic University of Norway, 2023. https://doi.org/10.11582/2023.00102.

Bodur, Yasemin V., Martí Amargant-Arumí, and Marit Reigstad. "Downward Vertical Flux of Size-Fractionated Chlorophyll-a and Phaeopigments in the Northern Barents Sea during December 2019, Nansen Legacy Cruise 2019711 Q4." UiT The Arctic University of Norway, 2023. https://doi.org/10.11582/2023.00103.

Bodur, Yasemin V., Martí Amargant-Arumí, and Marit Reigstad. "Downward Vertical Flux of Size-Fractionated Chlorophyll-a and Phaeopigments in the Northern Barents Sea during March 2021, Nansen Legacy Cruise 2021703 Q1." UiT The Arctic University of Norway, 2023. https://doi.org/10.11582/2023.00104.

Bodur, Yasemin V., Ulrike Dietrich, Camilla Svensen, and Marit Reigstad. "Downward Vertical Flux of Size-Fractionated Chlorophyll-a and Phaeopigments in the Northern Barents Sea during August 2018, Nansen Legacy Cruise 2018707 JC 1-2." UiT The Arctic University of Norway, 2023. https://doi.org/10.11582/2023.00101.

Bodur, Yasemin V., Miriam Marquardt, Paul Dubourg, Martí Amargant, and Marit Reigstad. "Downward Vertical Flux of Particulate Organic Carbon (POC) and Nitrogen (PON) in the Northern Barents Sea during May 2021, Nansen Legacy Cruise 2021704 Q2." UiT The Arctic University of Norway, 2023. https://doi.org/10.11582/2023.00096.

Bodur, Yasemin V., Miriam Marquardt, Paul Dubourg, Martí Amargant-Arumí, and Marit Reigstad. "Downward Vertical Flux of Particulate Organic Carbon (POC) and Nitrogen (PON) in the Northern Barents Sea during August 2019, Nansen Legacy Cruise 2019706 Q3." UiT The Arctic University of Norway, 2023. https://doi.org/10.11582/2023.00093.

Bodur, Yasemin V., Miriam Marquardt, Paul Dubourg, Martí Amargant-Arumí, and Marit Reigstad. "Downward Vertical Flux of Particulate Organic Carbon (POC) and Nitrogen (PON) in the Northern Barents Sea during December 2019, Nansen Legacy Cruise 2019711 Q4." UiT The Arctic University of Norway, 2023. https://doi.org/10.11582/2023.00094.

Bodur, Yasemin V., Miriam Marquardt, Paul Dubourg, Martí Amargant-Arumí, and Marit Reigstad. "Downward Vertical Flux of Particulate Organic Carbon (POC) and Nitrogen (PON) in the Northern Barents Sea during March 2021, Nansen Legacy Cruise 2021703 Q1." UiT The Arctic University of Norway, 2023. https://doi.org/10.11582/2023.00095.

Bodur, Yasemin V., Miriam Marquardt, Paul Dubourg, Ulrike Dietrich, Camilla Svensen, and Marit Reigstad. "Downward Vertical Flux of Particulate Organic Carbon (POC) and Nitrogen (PON) in the Northern Barents Sea during August 2018, Nansen Legacy Cruise 2018707 J/C 1-2." UiT The Arctic University of Norway, 2023. https://doi.org/10.11582/2023.00092.

Bodur, Yasemin V., Paul E. Renaud, Martí Amargant-Arumí, and Marit Reigstad. "Stable Isotopic Composition (d13C and d15N) of Sinking Particulate Matter Measured from Short-Term Sediment Traps in the Northern Barents Sea during August 2019, Nansen Legacy Cruise 2019706 Q3." UiT The Arctic University of Norway, 2023. https://doi.org/10.11582/2023.00097.

Bodur, Yasemin V., Paul E. Renaud, Martí Amargant-Arumí, and Marit Reigstad. "Stable Isotopic Composition (d13C and d15N) of Sinking Particulate Matter Measured from Short-Term Sediment Traps in the Northern Barents Sea during December 2019, Nansen Legacy Cruise

2019711 Q4.” UiT The Arctic University of Norway, 2023.
https://doi.org/10.11582/2023.00098.

Bodur, Yasemin V., Paul E. Renaud, Martí Amargant-Arumí, and Marit Reigstad. “Stable Isotopic
Composition (d13C and d15N) of Sinking Particulate Matter Measured from Short-Term
Sediment Traps in the Northern Barents Sea during March 2021, Nansen Legacy Cruise
2021703 Q1.” UiT The Arctic University of Norway, 2023.
https://doi.org/10.11582/2023.00099.

Bodur, Yasemin V., Paul E. Renaud, Martí Amargant-Arumí, and Marit Reigstad. “Stable Isotopic
Composition (d13C and d15N) of Sinking Particulate Matter Measured from Short-Term
Sediment Traps in the Northern Barents Sea during May 2021, Nansen Legacy Cruise 2021704
Q2.” UiT The Arctic University of Norway, 2023. https://doi.org/10.11582/2023.00100.

Bodur, Yasemin V., Kajetan Deja, Barbara Górska, Monika Kędra, Piotr Kukliński, Joanna
Legeżyńska, Joanna Pawlowska, Marta Ronowicz, Maria Włodarska-Kowalczuk, and Ulrike
Braeckman. “Benthic Macrofauna and Foraminifera (>500 Mm) Diversity, Abundance and
Biomass on the Northeast Greenland (NEG) Shelf Sediments during POLARSTERN Cruise
PS109.” PANGAEA, 2023. https://doi.pangaea.de/10.1594/PANGAEA.959134.

Bodur, Yasemin V., Janine Felden, and Ulrike Braeckman. “Single Prokaryotic Cell Abundances of
the Northeast Greenland (NEG) Shelf Sediments from POLARSTERN Cruise PS109.”
PANGAEA, 2023. https://doi.pangaea.de/10.1594/PANGAEA.959552.

Braeckman, Ulrike. “Ex Situ Total Nutrient Fluxes of the Northeast Greenland (NEG) Shelf
Sediments from POLARSTERN Cruise PS109.” PANGAEA, 2023.
https://doi.pangaea.de/10.1594/PANGAEA.959547.

Braeckman, Ulrike. “Grain Size Analysis of the Northeast Greenland (NEG) Shelf Sediments from
POLARSTERN Cruise PS109.” PANGAEA, 2023.
https://doi.pangaea.de/10.1594/PANGAEA.959546.

Braeckman, Ulrike. “Porosity of the Northeast Greenland (NEG) Shelf Sediments from
POLARSTERN Cruise PS109.” PANGAEA, 2023.
https://doi.pangaea.de/10.1594/PANGAEA.959550.

Braeckman, Ulrike. “Sedimentary Pigments on the Northeast Greenland (NEG) Shelf from Polarstern
Cruise PS109.” PANGAEA, 2023. https://doi.pangaea.de/10.1594/PANGAEA.959548.

Braeckman, Ulrike. “Total Organic Nitrogen (TON) and Total Organic Carbon (TOC) Concentration
of the Northeast Greenland (NEG) Shelf Sediments from POLARSTERN Cruise PS109.”
PANGAEA, 2023. https://doi.pangaea.de/10.1594/PANGAEA.959554.

Braeckman, Ulrike, and Janine Felden. “Porewater Nutrients of the Northeast Greenland (NEG) Shelf
Sediments from POLARSTERN Cruise PS109.” PANGAEA, 2023.
https://doi.pangaea.de/10.1594/PANGAEA.959549.

Braeckman, Ulrike, and Frank Wenzhöfer. “Ex Situ Total Oxygen Uptake of the Northeast Greenland
(NEG) Shelf Sediments from POLARSTERN Cruise PS109.” PANGAEA, 2023.
https://doi.pangaea.de/10.1594/PANGAEA.959553.

Da Costa Monteiro, Luana, Lidia Lins, and Ulrike Braeckman. “Benthic Meiofauna Diversity on the
Northeast Greenland (NEG) Shelf during POLARSTERN Cruise PS109.” PANGAEA, 2023.
https://doi.pangaea.de/10.1594/PANGAEA.959357.

Da Costa Monteiro, Luana, Lidia Lins, and Ulrike Braeckman. "Nematoda Diversity and Functional Feeding Groups on the Northeast Greenland (NEG) Shelf during POLARSTERN Cruise PS109." PANGAEA, 2023. https://doi.pangaea.de/10.1594/PANGAEA.959351.

Felden, Janine, Frank Wenzhöfer, and Ulrike Braeckman. "Ex Situ Diffusive Oxygen Uptake of the Northeast Greenland (NEG) Shelf Sediments from POLARSTERN Cruise PS109." PANGAEA, 2023. https://doi.pangaea.de/10.1594/PANGAEA.959545.

Marquardt, Miriam, Yasemin V. Bodur, Paul Dubourg, and Marit Reigstad. "Concentration of Particulate Organic Carbon (POC) and Particulate Organic Nitrogen (PON) from the Sea Water and Sea Ice in the Northern Barents Sea as Part of the Nansen Legacy Project, Cruise 2019706 Q3." Archive2014, 2022. https://doi.org/10.11582/2022.00055.

Marquardt, Miriam, Yasemin V. Bodur, Paul Dubourg, and Marit Reigstad. "Concentration of Particulate Organic Carbon (POC) and Particulate Organic Nitrogen (PON) from the Sea Water and Sea Ice in the Northern Barents Sea as Part of the Nansen Legacy Project, Cruise 2019711 Q4." Archive2014, 2022. https://doi.org/10.11582/2022.00048.

Marquardt, Miriam, Yasemin V. Bodur, Paul Dubourg, and Marit Reigstad. "Concentration of Particulate Organic Carbon (POC) and Particulate Organic Nitrogen (PON) from the Sea Water and Sea Ice in the Northern Barents Sea as Part of the Nansen Legacy Project, Cruise 2021703 Q1." Archive2014, 2022. https://doi.org/10.11582/2022.00053.

Marquardt, Miriam, Yasemin V. Bodur, Paul Dubourg, and Marit Reigstad. "Concentration of Particulate Organic Carbon (POC) and Particulate Organic Nitrogen (PON) from the Sea Water and Sea Ice in the Northern Barents Sea as Part of the Nansen Legacy Project, Cruise 2021704 Q2." Archive2014, 2022. https://doi.org/10.11582/2022.00054.

List of abbreviations

AI$_{mod}$: modified Aromaticity Index
AIS: automatic identification system
AODC: acridine orange direct counting
AW: Atlantic Water
BCP: biological carbon pump
CA: correspondence analysis
Chl-*a*: Chlorophyll-*a*
cDOM: colored dissolved organic matter
CTD: conductivity, temperature, density
DIC: dissolved inorganic carbon
DOC: dissolved organic carbon
DOM: dissolved organic matter
DOU: diffusive oxygen uptake
EGC: East Greenland Current
EPS: exopolymeric substance
F: filtered water
FCM: flow cytometry
H/C: hydrogen to carbon ratio
HNA: high nucleic acid
LNA: low nucleic acid
MIZ: marginal ice zone
MUC: multicorer
MW: molecular weight
NEG: Northeast Greenland Shelf
NCC: Norwegian Coastal Current
NEW: Northeast Water Polynya
O/C: oxygen to carbon ratio
OM: organic matter
PCA: principal component analysis
PIM: particulate inorganic matter
PN: particulate nitrogen
POC: particulate organic carbon
POM: particulate organic matter
PW: Polar Water
SIMPROF: similarity profile routine
TEP: transparent exopolyer particles
TDN: total dissolved nitrogen
TN: total nitrogen
TOU: total oxygen uptake
TOC: total organic carbon
TPM: total particulate matter
UF: unfiltered water
WoRMS: World Register of Marine Species

List of figures

1 Introduction

About a third to a fourth of anthropogenic CO_2 emissions is taken up by the global oceans (Friedlingstein et al., 2019; Heinze et al., 2015; Marinov and Sarmiento, 2004; Sarmiento and Gruber, 2006). High latitude oceans play an especially important role for reducing atmospheric carbon concentrations (Takahashi et al., 2009). The Arctic Ocean is the smallest ocean, comprising about 4% of the global ocean surface. Nevertheless, it is estimated that it accounts for about 4-8% of the global oceanic carbon uptake (Christensen et al., 2017; CMEMS, 2024; Smedsrud et al., 2022). Compared to other areas in the world, climate change-driven transitions are most pronounced in the Arctic (summarized in IPCC, 2023), and the effects of these changes on the carbon uptake capacity and its mechanisms in the Arctic Ocean are yet to be resolved.

1.1 The oceanic carbon pumps

The uptake and storage of natural and anthropogenic CO_2 in the ocean is controlled by the oceanic carbon pumps (Iversen, 2023; Sarmiento and Gruber, 2006). The physical carbon pump, also referred to as the solubility pump, is driven by the difference in the partial pressure between the ocean surface and the atmosphere. When CO_2 is taken up by seawater, it is present in the form of dissolved inorganic carbon (DIC). Polar and subpolar areas are strong sinks for atmospheric CO_2, because cold water has a higher potential for its uptake, and DIC-rich surface waters are transported to the deep ocean in these areas via the thermohaline circulation (Marinov and Sarmiento, 2004). The biological carbon pump (BCP), on the other hand, describes the conversion of DIC into organic matter by phytoplankton through photosynthesis (soft-tissue pump) or into calcium carbonate by marine calcifying organisms (hard-tissue or carbonate pump), and the subsequent transport of this material to deeper layers (Iversen, 2023). A part of this carbon is buried at the seafloor and with that, removed from further cycling. As a result, the BCP lowers DIC concentrations in the surface ocean, thus creating a vertical gradient towards the deep ocean and promoting the uptake of atmospheric CO_2 at the surface. Without the soft-tissue pump, CO_2 concentrations in the atmosphere would be twice as high as during pre-industrial times (Heinze et al., 2015). Moreover, the soft-tissue pump (hereafter referred to as BCP) provides benthic organisms at the seafloor with food, while the benthos in turn remineralizes the organic matter (OM) and releases inorganic nutrients back into the water column, where it can be used by primary producers at the ocean surface once again.

1.1.1 Vertical flux

The gravitational sinking of particulate organic matter (POM) is usually referred to as "vertical flux", while "carbon export" defines the amount of organic carbon that escapes a specified depth, usually below the euphotic layer. The majority of the carbon that is photosynthetically fixed by phytoplankton undergoes different pathways other than being exported from the surface ocean to deeper layers: Most of it is channeled through the food web, recycled back to CO_2 by phytoplankton itself or heterotrophic organisms, or converted to dissolved organic matter (DOM) (Iversen, 2023). As a result, sinking particulate material is usually strongly retained (and thus, vertical flux is attenuated) in the upper ocean before a fraction of this material is exported from the euphotic layer and ends up at the seafloor (Martin et al., 1987; Turner, 2015; Figure 1). Particles that sink constitute of various organic and

Box 1: Trapping sinking particles

Sediment traps are a tool that is used for collecting vertically settling particles. Different shapes and configurations are possible, depending on the exact purpose. Bottom-moored, funnel-shaped long-term sediment traps, for example, are often deployed for time periods of up to a year and used for capturing interannual variations in vertical flux at a specific location. They collect particles at one depth which settle into bottles that are rotating at pre-programmed timeframes over the sampling period. Due to the long deployment period, the bottles are filled with a preservative. This can, however, alter the chemical composition of the trapped material. Moreover, particles can accumulate on the inner funnel wall and/or turbulence and mixing in the funnel can flush them out, therefore funnel-shaped traps often underestimate particle flux (Baker et al., 2020; Gardner, 1985, 1980).
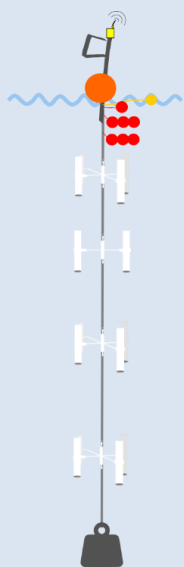
Gimballed, cylinder-shaped sediment traps (see illustration to the left) have been found to be more efficient at capturing sinking particles in the upper ocean compared to funnel-shaped (and other shapes of) sediment traps (Baker et al., 2020; Gardner, 1985, 1980), as turbulence at the trap opening is reduced. The most important factor for trapping efficiency of cylindrical traps is not the opening diameter or size, but the aspect ratio A (A = H/D; where H = cylinder height and D = opening diameter), which should be ideally >5 (Blomqvist, 1981; Buesseler et al., 2007; Hargrave and Burns, 1979).

Under high current velocities, moored sediment traps under-trap sinking particles (Buesseler et al., 2007). Therefore, another aspect that increases trapping efficiency besides the shape is leaving the sediment traps to drift freely (Siegel et al., 2008). It further reduces turbulence due to current shear. In surface-attached, drifting sediment traps, the traps can be attached at different depths on a long mooring (see illustration to the left). This allows for studying the depth gradient of vertical flux. Free drift can be achieved by adding floatation at the surface that balances out the weight of the mooring. The mooring can be deployed in open water, in ice leads or attached to sea-ice floes. An automatic identification system (AIS) ensures the spatial tracking of the mooring. However, current shear cannot fully be ruled out for surface-attached sediment traps because deeper currents usually do not match surface currents or sea-ice drift (Andreassen and Wassmann, 1998). Neutrally buoyant sediment traps were designed to further reduce the effect of horizontal shear (Buesseler et al., 2000).

Ultimately, it is important to keep in mind that the sampling efficiency varies between sediment trap types, and the trapping of bulk material, its composition and the amount of organisms that actively swim into the trap ("swimmers") can vary from trap to trap and depending on the physical conditions. There are no standardizations or accuracy controls for the trapping efficiency of sediment traps (Buesseler et al., 2007). Often, trapping efficiency is calibrated with radionuclide particle scavenging (Coppola et al., 2002); however, they do not always show the same pattern as sediment traps (Buesseler et al., 2007; Lalande et al., 2008). Therefore, different sediment trap configurations are used for different purposes.

inorganic material. Examples for organic material are decaying phytoplankton, fecal pellets produced by grazing zooplankton, detritus and/or DOM of high molecular weight that can act as a sticky glue and

promote aggregation. Inorganic material such as dust, calcium carbonate or gypsum can act as ballast and facilitate particle sinking rates or scavenging of DOM (De La Rocha et al., 2008; Iversen and Robert, 2015; Lombard et al., 2013; Wollenburg et al., 2018). One of the most common methods to measure vertical flux and its components are sediment traps (Box 1).

1.1.2 Pelagic-benthic coupling

The fraction (or the amount) of OM that ultimately arrives at the seafloor determines how tightly coupled the pelagic and benthic environments are. If most of the material is regenerated in the pelagic realm and little arrives at the seafloor, this coupling is weak, and it is usually reflected in lower abundance and richness of benthic communities. While vertical flux is tightly linked to pelagic processes and with that, especially at high latitudes highly seasonal and of ephemeral nature, the seafloor integrates processes across longer temporal and spatial scales and is thus rather affected by long-term changes (Jordà-Molina et al., 2023; Szczepanek et al., 2021; Ziegler et al., 2023).

1.1.3 Mismatch between deep ocean carbon demand and export

Essentially, the seafloor, as well as the deep ocean, depend on primary production and its export below the euphotic layer. However, the estimated carbon demand of benthos in the deep Arctic Ocean and of bacteria in the Deep Sea often exceed estimations of carbon export, often by twofold (Burd et al., 2010; Wiedmann et al., 2020). Accordingly, it is worth exploring other export mechanisms than gravitational settling alone (Figure 1). For example, OM present at the seafloor does not necessarily originate from the surface waters right above. The physical environment determines the trajectories of organic and inorganic particles, and the particles are often horizontally transported across large areas in the water column (Siegel et al., 2008; Wekerle et al., 2018) or along the seafloor (Rogge et al., 2022). Physical subduction of particles through the "mixed-layer pump" , eddies, or vertical migration of mesozooplankton that transport carbon up and down the water column can have patchy occurrences, and cannot be measured with common sediment trap deployments (Boyd et al., 2019). Carbon that has been channeled through higher trophic levels can end up rapidly sinking to the seafloor through large settling events of e.g. carcasses from deceased animals (Hoving et al., 2022; Sokolova, 1994), or larvacean houses (Robison et al., 2005). These settling events are seldomly matched by the deployment of sediment traps. Moreover, the vast pool of DOM in the ocean provides a high potential for an additional particle source which is often overlooked (Engel et al., 2004). Dissolved and particulate organic matter are mostly treated as distinct entities in biogeochemistry, separated operationally by size (filter pore size between 0.2–0.7 µm); however, the two fractions are in constant dynamic change with each other (He et al., 2016; Verdugo et al., 2004; Verdugo and Santschi, 2010). Carbon that has been converted to dissolved organic carbon (DOC) can still aggregate and form particles that potentially can sink, or act as a "glue" that keeps aggregates stuck together and facilitate their sinking (He et al., 2016).
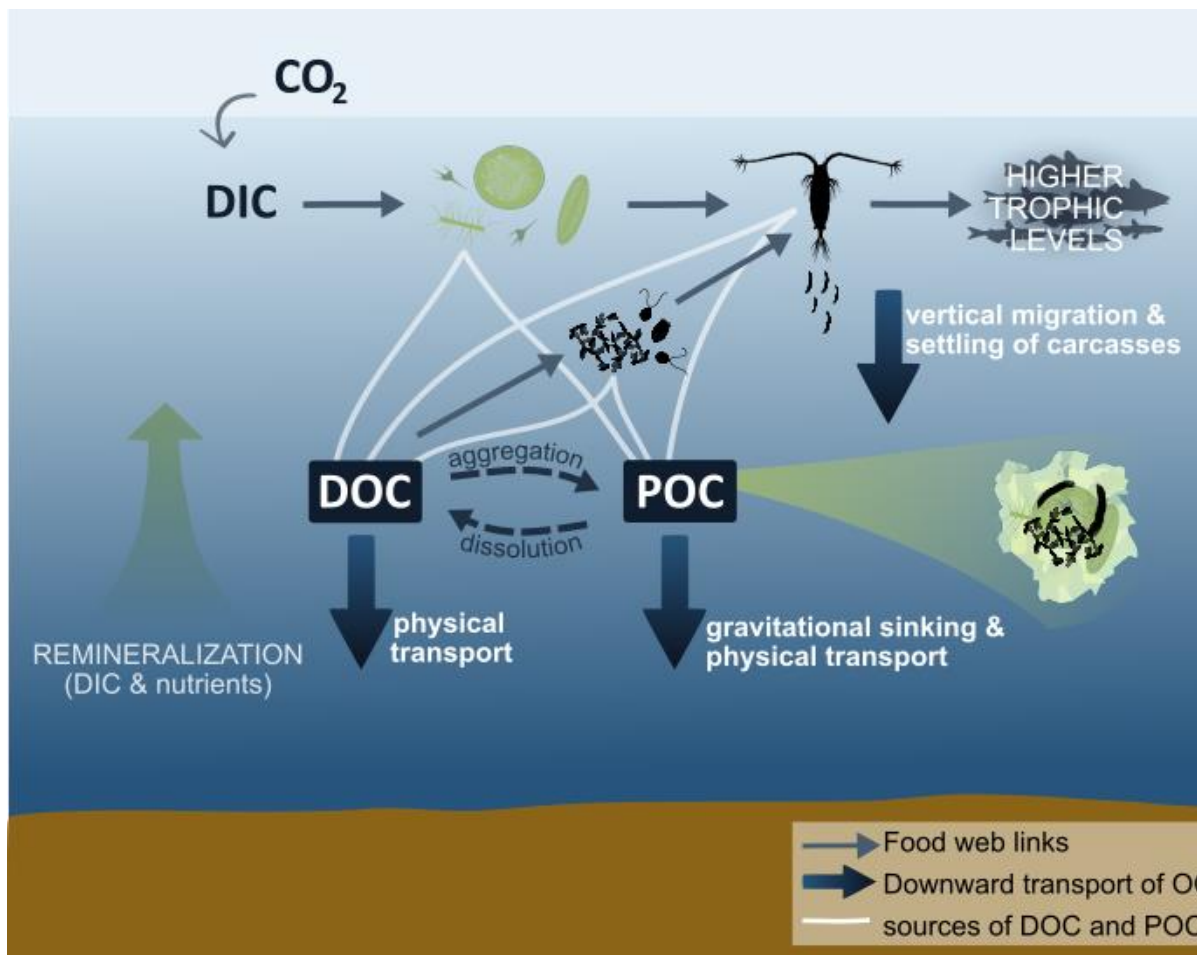
Figure 1: Carbon pathways within the biological carbon pump. DIC is fixed by phytoplankton through photosynthesis and converted to particulate organic carbon (POC), which is taken up by zooplankton and further channeled through higher trophic levels via the classical food web. Dissolved organic carbon (DOC) is produced additionally by phytoplankton through excretion or cell lysis, or by other organisms through feeding, excretion, or senescence. Carbon is "returned" to the food web by the microbial loop through the uptake of DOC by bacteria. DOC and POC pools are in constant exchange through aggregation and dissolution processes. Several mechanisms lead to the export of organic carbon from surface layers and the escape of its remineralization in the food web: gravitational sinking or physical transport of aggregates; physical transport or aggregation, and subsequent downward transport of DOC; vertical migration and settling of carcasses of zooplankton and higher trophic levels.

1.1.4 Aggregation in marine ecosystems

There are different pathways to aggregation. Particle-to-particle aggregation occurs when particles collide, usually through differential settling or shear, forming larger and denser particles that can sink more efficiently (Burd and Jackson, 2009). Another way is through phase-shifts of dissolved molecules, for example due to changes in temperature, pH or salinity (Chin et al., 1998; Verdugo et al., 2004). Small molecules can then form DOM of large molecular weight, which can aggregate and form particles (Engel et al., 2004; Passow, 2000). Transparent exopolymeric particles (TEP) play an important role for both processes. These gel-like substances, the "grey zone" between particulate and dissolved material, are highly sticky and act as glue between particles. TEPs are formed by exopolymeric substances (EPS); polysaccharide-rich dissolved organic molecules that are excreted by phytoplankton

and can rapidly form TEP (Passow, 2002). EPS often accumulate under increasing nutrient limitation and/or with increasing concentrations of senescent cells, as is the case during post-bloom conditions in summer (Engel, 2000; Hellebust, 1965; Mague et al., 1980; Mari and Burd, 1998; Myklestad, 1995; Thornton, 2002). Molecular phase shifts can already be triggered by small changes in the environment (Chin et al., 1998; He et al., 2016). This suggests a high seasonality of processes in the DOM-POM continuum, as well as possible implications induced by climate change.

1.2 The Arctic biological carbon pump and its seasonal variations

At high latitudes, the BCP is strongly driven by seasonal processes. As it is mainly fueled by primary production, it is controlled by the availability of light and sea-ice cover. While annually integrated primary production increases towards lower latitudes, the fraction of primary production that is transferred to the benthos is overall highest at higher latitudes (Petersen and Curtis, 1980; Weber et al., 2016). In tropical regions, the constant light availability might fuel primary production throughout the year, though at lower levels because of thermal stratification and nutrient limitation. The constant food availability can sustain a grazer population year-round (Henson et al., 2019). Polar ecosystems, on the other hand, are strongly light-limited during winter, and the ocean interior is characterized by deep convection. This redistributes nutrients in the water column which remain at the surface until the return of the sunlight, and then fuel strong bursts of primary production. Therefore, strong seasonality in polar regions can result in a mismatch between grazers and primary production (Cushing, 1975; Daase et al., 2021).

1.2.1 The seasonal cycle in the Arctic

During winter, little OM is suspended in the water column, regenerative processes dominate and consequently vertical flux is at a minimum (Olli et al., 2002). Once the light returns, intense, but highly ephemeral blooms can occur. Hotspots for vertical flux and pelagic-benthic coupling in the Arctic are coastal areas and fjords, inflow shelves, marginal sea ice zones (MIZ) and polynyas (Carmack and Wassmann, 2006; Piepenburg, 2005). On Arctic shelf seas (Box 2), although the light is back, the incident sunlight can still be blocked by sea ice and phytoplankton blooms can be delayed. Nevertheless, ice algae can thrive within the sea ice under low light conditions (Kvernvik et al., 2021). Therefore, at the MIZ, intense phytoplankton blooms can be preceded by ice algal blooms, utilizing the abundant nutrient sources in the beginning of the spring period (Leu et al., 2015). Large and fresh, diatom-derived aggregates can settle rapidly to the seafloor during spring. Highest export of OM below the euphotic zone has been measured during spring blooms, when diatoms escape the upper pelagic zone ungrazed (Dybwad et al., 2021; Reigstad et al., 2008). With increasing nutrient deficiency towards summer, smaller cells and heterotrophic organisms dominate the pelagic zone. This is reflected in the sinking material, which consists of amorphous (unidentifiable), regenerated particles that are more difficult to characterize (Trudnowska et al., 2021). However, a sufficient amount of small particles, or POM packed into fast-sinking fecal pellets, can still contribute to vertical flux (Wiedmann, 2014).

1.3 Climate change in the Arctic

Studying the BCP in Arctic marine ecosystems is particularly important because the Arctic Ocean plays a crucial role in taking up carbon from the atmosphere (Anderson et al., 1998; Smedsrud et al., 2022),

Box 2: A short introduction to the Arctic Ocean

The Arctic Ocean is a mediterranean sea, almost completely enclosed by the northern Eurasian and North American landmasses. The Fram Strait in the northern Atlantic and the Bering Strait in the northern Pacific separate these two continents and connect the Arctic Ocean to its adjacent seas through the inflow of Atlantic and Pacific water masses. Approximately 50% of the Arctic Ocean is continental shelf seas and is seasonally ice-covered, while the other 50% is comprised of slopes, ridges and basins in the deep Arctic Ocean (Bluhm et al., 2015; Carmack and Wassmann, 2006; see also Figure 3). Two productive inflow shelves lie in the pathway of the warm and saline Atlantic and Pacific water masses: the Barents Sea, a shelf sea of about 300 m deep, receives the Atlantic Water (AW) inflow, while the shallow Chukchi Sea (about 80 m deep) is influenced by fresher Pacific Water. The Arctic Ocean receives its main freshwater input from the river discharge onto the interior shelves: the Beaufort Sea, and the East Siberian, Kara and Laptev Seas (Carmack et al., 2015). Although the Arctic Ocean constitutes only 1% of global ocean volume, it receives 10% of the global river discharge. Melting of sea ice and glaciers, especially from Greenland, permafrost thaw and precipitation are additional freshwater sources to the Arctic Ocean. The only exit for freshwater, sea ice and modified boreal water masses from the Arctic Ocean is through the outflow shelves in the Canadian Arctic and east and west of Greenland (Bluhm et al., 2015; Carmack et al., 2015; Carmack and Wassmann, 2006).

Figure modified after Wassman 2020 and Carmack & Wassmann 2006. Red arrows: inflow of Pacific and Atlantic Water. Blue arrows: outflow of Arctic water.

and this uptake has increased by 30% since the last century (Smedsrud et al., 2022). Moreover, increasing air and seawater temperatures, decreasing sea-ice concentration, thickness and age, increasing freshwater influence through permafrost thaw, glacial melt and enhanced coastal runoff are all acting in concert on Arctic seas and, consequently, their ecosystems (summarized in Meredith et al., 2019). The range of simulated and observed atmospheric warming in the Arctic is from 1.5 to 4.5 times the global mean warming ("polar amplification"; Comiso and Hall, 2014; Holland and Bitz, 2003; Previdi et al., 2021; Rantanen et al., 2022). Similarly, the Arctic Ocean is warming faster than the global average (Shu et al., 2022). The summer sea-ice extent is declining at a fast pace, such that the Arctic Ocean has lost 50% of its sea-ice extent since the 1980s (Meier et al., 2023) and is predicted to become sea-ice-free during summer already from the next decade on (Johannessen et al., 2004; Onarheim et al., 2018; Stroeve and Notz, 2018). The Arctic Ocean and its coastlines become increasingly accessible to

humans and human activities beyond its native communities, and anthropogenic impacts intensify (Ng et al., 2018 and references therein; Bartsch et al., 2021).

1.3.1 Sea-ice decline and inflow of boreal waters

The overall decrease in average sea-ice thickness and concentration across the Arctic leads to a shift of the ice edge further north, resulting in part of the Arctic Ocean becoming ice-free earlier during the year. Consequently, in the future primary production is expected to start earlier in the seasonal ice zones, and a prolongation of the productive period is expected (Wassmann and Reigstad, 2011). The marginal ice zone, which is a light-limited system, is turning into a more boreal, nutrient-limited system. This "borealization" (Polyakov et al., 2020a) is moreover driven by the increased inflow of the Atlantic (AW) and Pacific water masses (Skagseth et al., 2008). The inflow of these warm water masses does not only introduce heat and salt, increasing the melting of sea ice and marine-terminating glaciers (Carr et al., 2017; Schaffer et al., 2020; Smedsrud et al., 2022). It also transport nutrients, introduce DOM (Anderson and Amon, 2015), and lead to the expansion of boreal phytoplankton communities (Hegseth and Sundfjord, 2008; Neukermans et al., 2018; Oziel et al., 2020; Vernet et al., 2019; Zhang et al., 2023) and organisms of higher trophic levels (Fossheim et al., 2015; Gluchowska et al., 2017; Hunt et al., 2016; Renaud et al., 2015).

1.3.2 Changing mixing regimes

The increasing discharge of coastal rivers, permafrost thaw, groundwater discharge and glacial melt increase the freshwater content in the Arctic Ocean (Brown et al., 2020). With increasing freshwater input, sea-ice retreat and the influence of Atlantic and Pacific Waters, the mixing regimes of Arctic seas are expected to change, with implications for primary production. Studies based on satellite measurements and models show increases in primary production throughout the Arctic (Frey, 2017; Frey et al., 2022; Lewis et al., 2020; Oziel et al., 2022). However, primary production on outflow shelves either decreased or did not show a trend (Arrigo and van Dijken, 2015). Moreover, *in situ* measurements of Chlorophyll-*a* (Chl-*a*) and particulate organic carbon (POC) during the last 25 years did not show this trend of increasing primary production (Nöthig et al., 2020). In parts of the Arctic, the water column may remain or become increasingly stratified and nutrients will be limited in the upper ocean, decreasing primary production (McLaughlin and Carmack, 2010; Nummelin et al., 2016). In the Beaufort Gyre within the Amerasian Basin, for example, the increase of surface freshwater resulted in an increase of stratification (Polyakov et al., 2023). Similarly, the Northeast Greenland (NEG) shelf is becoming increasingly more stratified due to terrestrial runoff, glacial and sea-ice melt, and freshwater export from the Arctic Ocean (Sejr et al., 2017). Other parts of the Arctic will experience more mixing through sea-ice retreat and increased wind forcing (Carmack and Chapman, 2003; Rainville and Woodgate, 2009; Tremblay et al., 2011). This will redistribute nutrients up and particles down through the water column, with consequences for primary production and pelagic-benthic coupling (Polyakov et al., 2020b; Slagstad et al., 2015). Earlier onset of primary production is expected for the high Arctic (Ardyna and Arrigo, 2020), as well as for seasonally ice-covered fjords (Vonnahme et al., 2022). In the Eurasian basin, stratification decreased in the last decade due to the increased inflow and shoaling of AW (Polyakov et al., 2023, 2020b, 2017). Nutriclines in the Barents Sea are shoaling and winter ventilation is increasing (Lind et al., 2018). However, at high latitudes above 80°N, mixing in autumn

due to delayed sea-ice formation which could support substantial autumn blooms might start too late into the polar night (Lundesgaard et al., 2022; Renner et al., 2023).

With uncertainties in future primary production patterns across the Arctic Ocean, the implications of a decrease in sea ice and a longer vegetative season on the BCP and pelagic-benthic coupling are difficult to estimate. On one hand, compared to ice-free regions, export from sea-ice-covered regions can be higher in the beginning of the productive period when fresh, diatom-rich particles of sympagic or early pelagic origin can sink rapidly to the seafloor (Fadeev et al., 2021). Sympagic production can be a substantial food source for the entire food web, including benthos (Koch et al. 2023). With a longer ice-free period, more OM will likely be recycled within the pelagic zone, with less food of lower quality for benthic communities (Wassmann and Reigstad, 2011). On the other hand, sea-ice melt derived stratification can lead to a high attenuation of vertical flux at the surface, and in well-mixed, open-water areas vertical flux can be higher (Amargant-Arumí et al., 2024; Reigstad et al., 2008; von Appen et al., 2021). On other Arctic shelf regions, an increase in pelagic-benthic coupling in response to a prolonged productive period are predicted (Cochrane et al., 2009; Olivier et al., 2020).

1.3.3 Implications for the DOM-POM continuum

Environmental and biological changes in the Arctic Ocean also affect concentrations and the molecular composition of DOM in marine ecosystems, with consequences for the microbial loop and DOM-POM interactions (Nguyen et al., 2022). Terrestrial runoff is a major source of DOC in the Arctic Ocean, and the surface oceans are accumulating substantial amounts of terrigenous DOM (Anderson and Amon, 2015). Because phytoplankton are one of the main sources of labile DOM, changes in primary production and protist community compositions would likely also change the concentrations and composition of DOM in the Arctic Ocean (Nguyen et al., 2022). Melting sea ice alters the DOM composition of the surface water, because it contains higher quantities of DOM compared to the surrounding seawater (Nguyen et al., 2022). Other processes such as the inflow of Pacific and Atlantic Water, atmospheric deposition and efflux from sediment similarly contain high quantities of DOM with a distinct composition differing from marine DOM (summarized in Nguyen et al., 2022). The effect of these changes on particle dynamics, and with that on the BCP are difficult to assess. This is because little is known about processes in the DOM-POM continuum under contrasting environmental conditions, and most observations have been carried out in the laboratory only. Combined field and lab studies are scarce (Riley, 1963; Sheldon et al., 1967), and processes are often analyzed from a pure chemistry or pure ecological viewpoint; seldomly the two fields are combined.

1.3.4 Regional variability

In the end, particle dynamics, vertical flux and the export of OM from the euphotic zone depend on a multitude of drivers besides the magnitude of primary production, such as the protist community composition, aggregation, grazing efficiency, fecal pellet production and export, the microbial loop, and the physical environment (Iversen, 2023). Differing physical and biological settings at the different Arctic shelves influence particle interactions, vertical flux, and ultimately pelagic-benthic coupling in varying manners. This means that Arctic regions will be affected in different ways by climate change.

The Arctic is characterized by high seasonality and interannual variability. Accordingly, it is challenging to evaluate the effects of long-term environmental and biological changes on the BCP. It is

yet unclear how or whether the efficiency of carbon export from the pelagic zone will change, and with that, how benthic communities will be affected by changes in food supply or composition. Moreover, the contribution of DOM to the BCP under different environmental conditions is yet unresolved, which makes it difficult to estimate the influence of changing DOM concentrations and composition on the BCP. Studying seasonal patterns could help to elucidate future trends, since it gives us the possibility to explore extremes of the environment, representing different scenarios of primary production and pelagic processes impacting the BCP. Benthic communities, on the other hand, integrate environmental and biological changes over larger time scales (Ziegler et al., 2023). Accordingly benthic communities can be useful as long-term indicators: Monitoring short-term and long-term patterns in the pelagic realm and the benthos thus could help us elucidating climate-change induced alterations in carbon flow within the Arctic marine ecosystem.

2 Thesis aims

The overall objective of this thesis was to discuss the functioning of the biological carbon pump (BCP) and pelagic-benthic coupling under a prolonged sea-ice free, open water scenario in the Arctic marginal ice zone. All papers have in common that the study sites were revisited over a temporal scale (seasonal, **Papers II** and **III**; and annual, **Paper I**) to study the effect of environmental contrasts on different aspects of the BCP. The dependency of benthic communities on the BCP on the Northeast Greenland shelf are presented in **Paper I**, followed by a discussion of the effects of a possible weakening of pelagic-benthic coupling since the 1990s. In **Paper II**, we explore how the amount and composition of vertical flux changes with depth along the marginal ice zone, and across different seasons in the northwestern Barents Sea, discussing some regulatory mechanisms of the BCP. **Paper III** investigates the seasonal potential of dissolved organic matter to aggregate and with that, contribute to the particulate pool. In the synthesis of this thesis, the results from the different papers are integrated to get a holistic understanding of some mechanisms of the BCP and pelagic-benthic coupling in the Arctic.
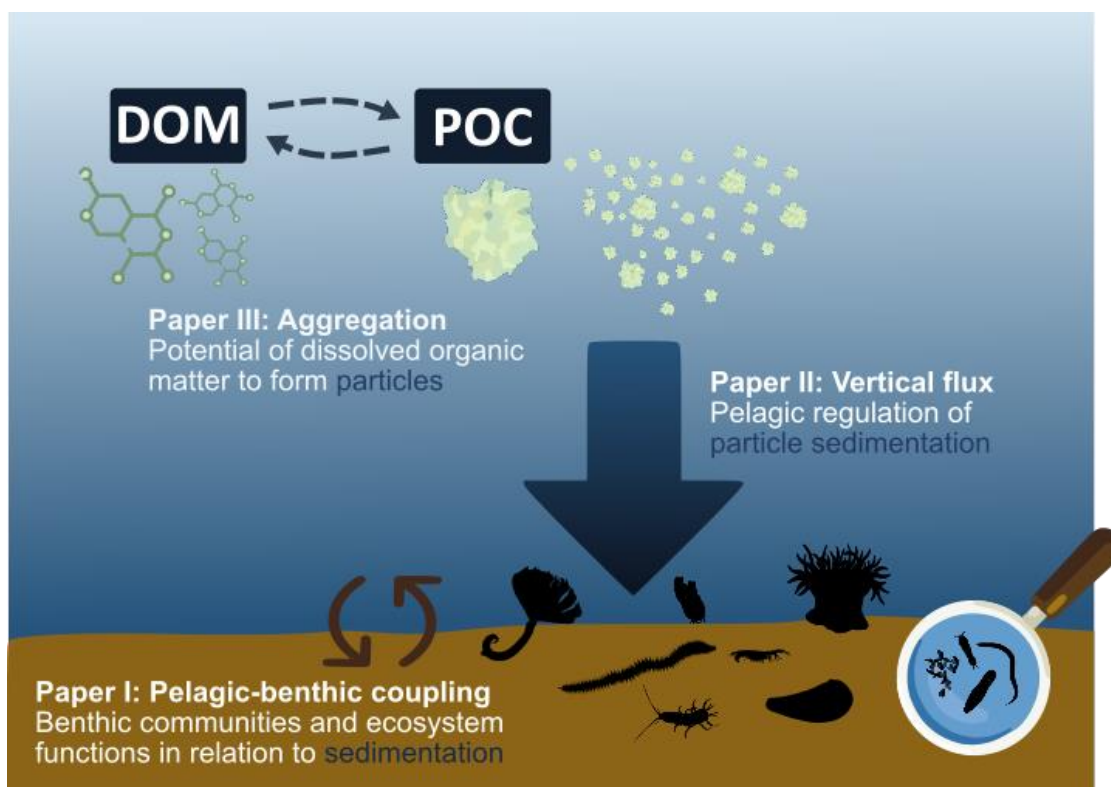
Figure 2: Conceptual representation of the topics covered in the papers included in this thesis.

2.1 Research questions

Paper I

I. Is food availability at the seafloor the main driver of benthic communities on the NEG shelf, as it was in the 1990s?

II. How have benthic communities and the food availability at the seafloor changed since the 1990s?

Paper II

I. How does the amount and the composition of vertical flux change across different depths, a latitudinal gradient across the MIZ and different seasons in the northwestern Barents Sea?

II. What are possible regulatory mechanisms for the changes observed?

Paper III

I. In which season does organic matter aggregate (or dissolve), and with that, contribute to (or reduce) the particulate carbon pool?

II. How does DOM change its characteristics during aggregation (or dissolution) processes?

In the **synthesis** of this thesis, the findings of the included papers are integrated, addressing the following overarching questions:

- What are the main regulating mechanisms of the Arctic BCP and how do they differ across different Arctic shelves? (**Paper II**)
- How important is DOM aggregation as a mechanism of the BCP? (**Paper III**)
- What are the processes and mechanisms that could lead to a weakening (or a tightening) of pelagic-benthic coupling in a future Arctic? (**Paper I, II**)
- How do particle dynamics and vertical flux in the Arctic winter differ from the Arctic spring and summer? (**Paper II, III**)

3 Methods

3.1 Study region

This thesis focused on processes of the biological carbon pump in a sub-Arctic fjord (Ramfjorden, Tromsø), the Northeast Greenland shelf and the Barents Sea shelf. Accordingly, the environmental conditions within the Atlantic sector of the Arctic are described in more detail.
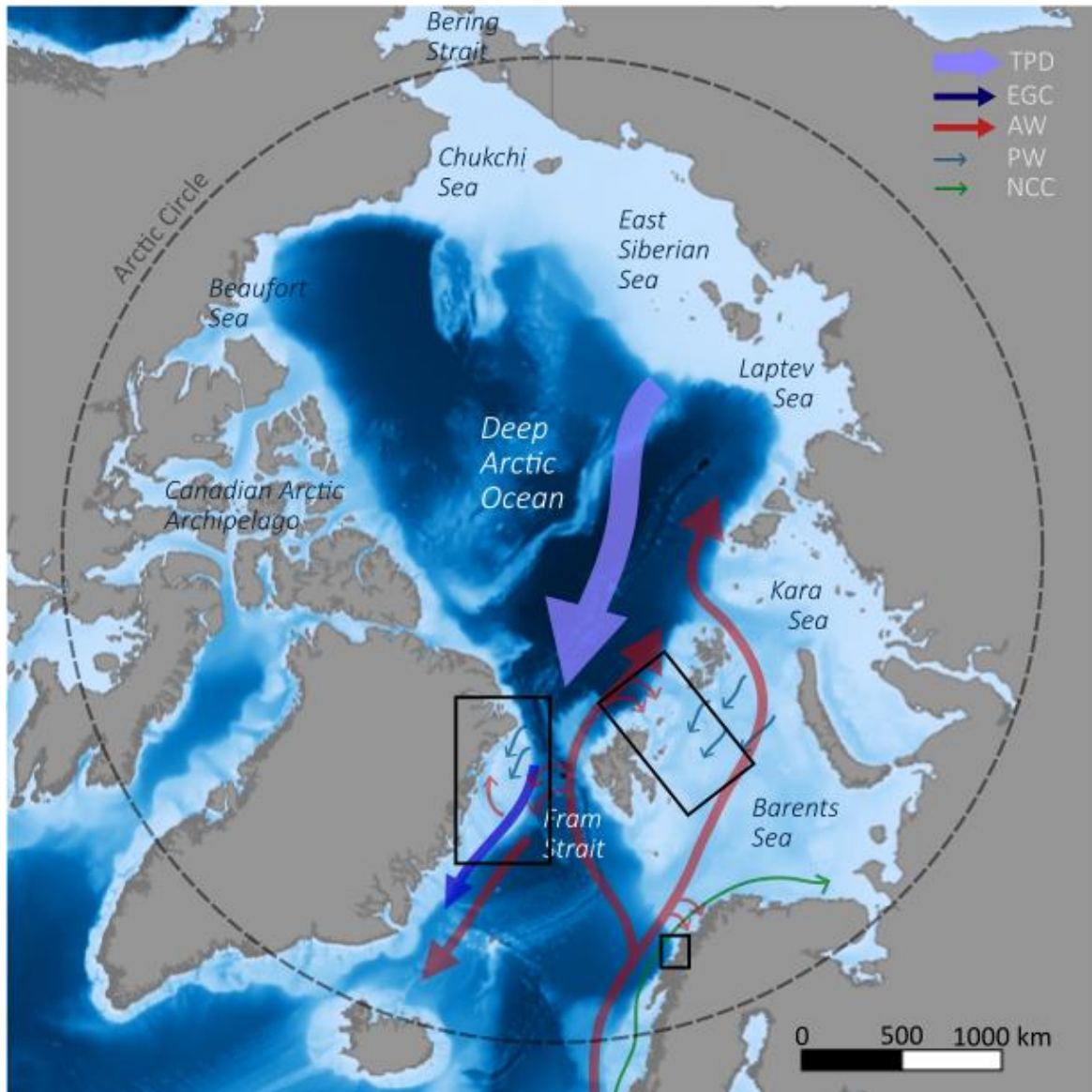
Figure 3: Overview of the Arctic Ocean and the study areas. The study areas are shown in black rectangles, with conceptual patterns of ocean currents in the Atlantic sector of the Arctic that are relevant for this work: Transpolar Drift (TPD), East Greenland Current (EGC), Atlantic Water (AW), surface Polar Water (PW), Norwegian Coastal Current (NCC). Bathymetry was taken from the International Bathymetric Chart of the Arctic Ocean Version 4 (Jakobsson et al., 2020), and land polygons from Open Street Map (2023).

3.1.1 A highway through the Arctic: The inflow and circulation of Atlantic Water in the Atlantic sector of the Arctic

Atlantic Water (AW) flowing towards the Arctic is a poleward extension of the Gulf Stream (Skagseth et al., 2008). Its pathway into and within the Arctic Ocean is determined by bathymetry and largely follows continental shelf breaks (Aagaard, 1989). Its advection onto the shelves depends on deeper bathymetric trough systems. The main branch of the AW follows northwards along the Norwegian continental shelf (Figure 3). Along the Norwegian coast, part of it mixes with or flows underneath the shallower Norwegian Coastal Current (NCC). Both currents influence the oceanographic setting of the coastal fjords (Sætre, 1999). The AW flows further north along the Barents Sea continental shelf and splits into two branches, with its main branch entering the central Barents Sea through the Barents Sea Opening between mainland Norway and Bjørnøya, continuing eastwards (Ingvaldsen et al., 2002, 2004; Schauer et al., 2002). It is separated from cold and fresh waters of Arctic origin by the Polar Front (Figure 1 in **Paper II**). The second AW branch enters the Arctic Ocean via Fram Strait (Figure 3), following the northern boundary of the Barents Sea continental slope west and then north of Svalbard (Beszczynska-Möller et al., 2012; Schauer et al., 2004). From there, AW continues eastward and enters the northern Barents Sea through two troughs on either side of Kvitøya (Lind and Ingvaldsen, 2012; Lundesgaard et al., 2022) (Figure 1 in **Paper II**). Before entering the Arctic Ocean, about half of the AW recirculates within Fram Strait, joining the East Greenland Current (EGC) and flowing southward along the Greenland continental shelf break (de Steur et al., 2014; Hattermann et al., 2016; Rudels et al., 2005). From there, it is partly advected onto the Northeast Greenland shelf, circulating in a clockwise (anticyclonic) pattern within the deep trough system on the shelf (Arndt et al., 2015; Bourke et al., 1987; Schaffer et al., 2020) (Figure 1 in **Paper I**). A switch in the atmospheric Arctic Dipole resulted in an increase of AW inflow through the Barents Sea Opening since the last decade, while the inflow through the Fram Strait has decreased (Polyakov et al., 2023).

3.1.2 Sea ice: a declining, but highly variable feature

The sea ice in the Arctic shrinks to its minimum extent in September (7.7–4.7 Mio km^2), and expands to its maximum extent in March (14.3–16.3 Mio km^2), with an area of the size of Australia melting and growing anew on an annual basis (Lund-Hansen et al., 2020); however, this pattern is highly dynamic on a yearly basis. The outer margin of the sea-ice extent reaches mostly to the northern regions of the Arctic shelves. These regions lie therefore in the seasonal ice zone and are characterized by strong environmental gradients during the seasonal cycle. Sea-ice concentration and thickness are decreasing across the Arctic, with the Barents Sea being the region with the strongest sea-ice loss and possible sea-ice free winters already before the end of this century (Årthun et al., 2021). Nevertheless, the negative trend of sea-ice concentration across the Arctic underlies interannual and decadal variability. In the Barents Sea, the advection of sea ice from the eastern Eurasian Arctic drives the interannual variability in sea-ice concentration, while the AW inflow hinders sea-ice formation locally, thus maintaining long open water periods within the AW pathway even under low air temperatures (Lundesgaard et al., 2021). Due to borealization, the stratification in the northern Barents Sea is decreasing (Lind et al., 2018). In the Amerasian Basin, the switch from a negative to a positive Arctic Dipole phase in 2007 resulted in an increase of surface freshwater content since the last century, and with that an increase of stratification and sea-ice area within this region (Polyakov et al., 2023). The majority of sea ice that is exported leaves the Arctic through the Fram Strait via the East Greenland Current (Serreze et al., 2006). This makes sea

ice conditions on the NEG shelf intra- and interannually highly variable. The ice export through Fram Strait has intensified (Polyakov et al., 2023); however, the exported sea ice is getting younger, thinner and more uniform (Krumpen et al., 2019; Sumata et al., 2022). While in the Barents Sea, the import of sea ice from the East Siberian and Laptev Seas is the main freshwater source in this region (Ellingsen et al., 2009; Lind et al., 2018; Lundesgaard et al., 2022), the NEG shelf is additionally strongly influenced by glacial meltwater from Greenland's largest marine-terminating glacier (79⁰N Glacier) and the Zachariæ Isstrøm (Schaffer et al., 2017). Due to increasing glacial melt, together with the export of melting sea ice with the EGC, and the increased inflow of AW, the NEG shelf is subject to strong upper ocean stratification (Sejr et al., 2017).

Changes in sea-ice thickness, age and concentration, along with increasing inflow of boreal waters and increasing open water areas also impact polynyas across the Arctic (Smith and Barber, 2007). Polynyas are open water features within a completely sea-ice covered area. They can be important for local biological production, as light can be available early on in an area where it is otherwise blocked by ice, and mixing regimes can differ within the polynya compared to the surrounding waters. With decreasing sea ice, many polynyas are expected to disappear during summer or decrease in size, become more boreal in character or rather act as marginal ice zones than true polynyas (Smith and Barber, 2007).

3.1.3 Detailed description of the study sites

The study site for **Paper I** comprised the area between 77°N and 81°N on the Northeast Greenland (NEG) shelf (Figure 1 in **Paper I**). Two oceanic troughs, namely the Westwind Trough in the northern part of the shelf, and the Norske Trough in the southern part, half-encircle shallow banks of water depths <200 m (Arndt et al., 2015; Jakobsson et al., 2020). Atlantic Water (AW) from the EGC enters the NEG shelf through the Norske Trough and circulates in an anticyclonic pattern within this trough system (Bourke et al., 1987; Schaffer et al., 2017). The inflowing AW promotes subglacial melting of the largest marine-terminating glacier of Greenland, the Nioghalvfjerdsfjorden glacier (79°N Glacier; (Mayer et al., 2000; Schaffer et al., 2017; Straneo et al., 2012). AW then leaves the glacier cavity as modified AW and flows eastward through the Westwind Trough. In the period between 1979–1999 and 2000–2016, the Norske Trough experienced a temperature increase of 0.5°C because of increasing influence of AW on the NEG shelf (Schaffer et al., 2017; 2020; Mayer et al., 2018). In the Westwind Trough, the Northeast Water (NEW) Polynya extended to an area of approximately 44,000 km² (Wadhams, 1981) between 79⁰N and 81⁰20'N and between the NEG coast and the shelf break. It was described to be confined by the Ob Bank Ice Barrier in its northern, and the Nørske Øer Ice Barrier in its southern part (Minnett et al., 1997). While in winter, the NEW functions as a latent heat polynya, formed by strong coastal northwesterly winds that push sea ice away and form an open water area, in summer the anticyclonic circulation on the NEG shelf advects sea ice out of the NEW Polynya. The resupply of new ice is constrained by the Nørske Øer Ice Barrier in the south (Minnett et al., 1997). However, during the last century, sea-ice conditions became more variable in this area and the land-fast ice structures are breaking up more often (Sneed and Hamilton, 2016), and the polynya was described to be "morphed into the Marginal Ice Zone" (ISSI, 2008).

Sampling stations for **Paper II** were located along a transect along the 30°E meridian (Process stations P1-P7) between 75° and 85°N, covering a latitudinal gradient across the seasonally ice-covered northwestern Barents Sea (Figure 1 in **Paper II**). Four stations were located on the shelf (P1, P2, P4,

P5; 160–60 m), one station was located at the northern Barents Sea shelf break (P6; varying between 790–1550 m) and one in the deep Nansen Basin (P7; 3300–3400 m). The southernmost station P1 (76⁰N Latitude) was located south of the Polar Front, where it was strongly influenced by AW and permanently ice-free, while the sea-ice cover between 77-82⁰N is interannually variable. The northernmost stations P6 and P7 (81-82⁰N) are located within the northern branch of AW inflow, which is heating the upper water layers and thus sea-ice presence can be reduced compared to lower latitudes. During 2018, which was a "low-ice year" (Amargant-Arumí et al., 2024), P6 and P7 were ice-covered only in December and January and ice-free for the rest of the year, while the locations 77–80⁰N were ice-covered between December and May (Steer and Divine, 2023). 2019, on the other hand, was a "high-ice year" (Amargant-Arumí et al., 2024). Stations P5-P6 were ice-covered almost year-round, while Stations P2–P4 were ice-covered until the end of June (Steer and Divine, 2023).

Arctic regions are difficult to access, especially if a study requires high sampling frequency such as for seasonal investigations. Because we wanted to investigate the seasonality of aggregation patterns in the Arctic, we conducted sampling for **Paper III** at the mouth of a sub-Arctic fjord (Gáranasvuotna/Ramfjorden, 69°31'34" N, 19°1'33.0" E) in Sápmi/Northern Norway (Figure 1 in **Paper III**). Ramfjorden is a western sidearm of Báhccavuotna (Balsfjorden), where intensive investigations have shown that physical and ecological conditions are highly comparable to the Barents Sea shelf (Degerlund and Eilertsen, 2010; Eilertsen et al., 1981; Tande, 1991). Phytoplankton community structure and bloom seasonality are representative for Arctic conditions (Eilertsen and Taasen, 1981).

The station in Ramfjorden was about 130 m deep. The inner part of Ramfjorden (about 20 m deep) can be ice-covered between late January until April/May due to the heavy freshwater inflow (O'Sadnick et al., 2020). Especially in autumn/early winter, the surface of the fjord is freshened by river runoff (Vonnahme et al., 2022), which can freeze at the surface in the inner part. However, the outermost part of Ramfjorden, where our sampling station was located was sea-ice free throughout the year.

3.2 Sample collection

3.2.1 Field work

Samples for **Paper I** were collected between September and October 2017 with camera-equipped multicorers (MUC) and autonomous benthic landers on the seasonally ice-covered Northeast Greenland shelf along the trough system and at the 79⁰N Glacier. Benthic community parameters (bacterial abundance, meiofauna and macrofauna communities) were sampled along parameters for sediment solid-phase (granulometry, porosity, sedimentary pigments (Chlorophyll-*a* (Chl-*a*), fucoxanthin and phaeopigments), total organic carbon (TOC) and total nitrogen (TN)), porewater (dissolved inorganic carbon and nutrients) and oxygen fluxes (total and diffusive oxygen uptake) from MUC and Lander deployments.

For **Paper II**, short-term drifting sediment traps (Box 1) were deployed in the northwestern Barents Sea along the station transect P1–P7 during four different seasons (August 2019, December 2019, March 2021 and May 2021). Two or four cylinders were deployed at each depth (30, 40, 60, 90, 120 and 200 m). The deployment period varied between 18 and 38 h, with longer deployment times when low fluxes were expected (December and March). After retrieval, the cylinders from each depth were pooled

and samples for particulate organic carbon (POC) and particulate nitrogen (PN), size-fractionated (0.7 µm and 10 µm) Chlorophyll-*a* (Chl-*a*) and Phaeopigments, protist cell and biomass fluxes, fecal pellet fluxes and stable isotopes were taken.

Samples for **Paper III** were taken on a monthly basis in the mouth of Ramfjorden between September 2020 and September 2021. A CTD was deployed in the beginning of each sampling campaign to obtain seasonal variations in temperature, salinity, fluorescence, turbidity, and oxygen saturation at the station throughout the water column. Subsequently, GoFlos were used to sample seawater at 5 m depth for a set of biogeochemical parameters (nutrients, total dissolved nitrogen (TDN), dissolved organic carbon (DOC), dissolved organic matter characterization (DOM), colored DOM (cDOM), extracellular polymeric substances (EPS), POC and PN, size-fractionated Chl-*a* and Phaeopigments, total particulate matter (TPM), flow cytometry (FCM) and protist community composition).

For **Paper III**, every second month three additional GoFlos were taken in Ramfjorden for water that was used for the aggregation experiments. The sampled water was filtered through a 90 µm mesh to remove larger grazers, and then the water from each of the GoFlos was equally distributed among three acid-rinsed containers that were packed in dark plastic bags to protect from light until they were brought ashore (Figure 4a). The containers were stored in a cold room (4°C) at dark until processing (within a couple of hours after bringing them ashore). All sampling equipment was acid-rinsed (plastic ware), combusted (glass ware) or sonicated (metal ware) prior to use to minimize contamination. The water of two containers was pooled and pressure-filtered through a single layer (September–December) or a double layer (February–August) of pre-combusted GF/F filters (0.7 µm, Whatman, diameter: 130 mm). The effect of a single or a double layer of filters was tested in January with water taken at the same station, and the results and a short discussion are presented in Figure S1 in **Paper III**. The water from the third container was channeled through the filtration system, but without a filter to treat the filtered and unfiltered water in the same way and to account for possible coagulation during the filtration process. Subsequently, the filtered (F) and unfiltered (UF) water was sampled for EPS, FCM, DOC and DOM characterization before it was distributed equally with sample splitters among roller tanks (Figure 4c). Each month, the tanks were distributed randomly on roller tables and rolled at 3 rpm for 36 h. At the end of the incubation, each tank was sampled for EPS and FCM after it was homogenized by gentle turning. Subsequently, all tanks were connected to an air-tight peristaltic filtration system to ensure minimal contamination (Figure 4d). POC/PN samples were collected through syringe filter holders with pre-combusted GF/F filters that were attached in-line, and the filtrate was collected in graduated cylinders capped with stoppers with air filters. The filtrate was then used to sample for DOC and DOM characterization.

3.2.2 Experimental work
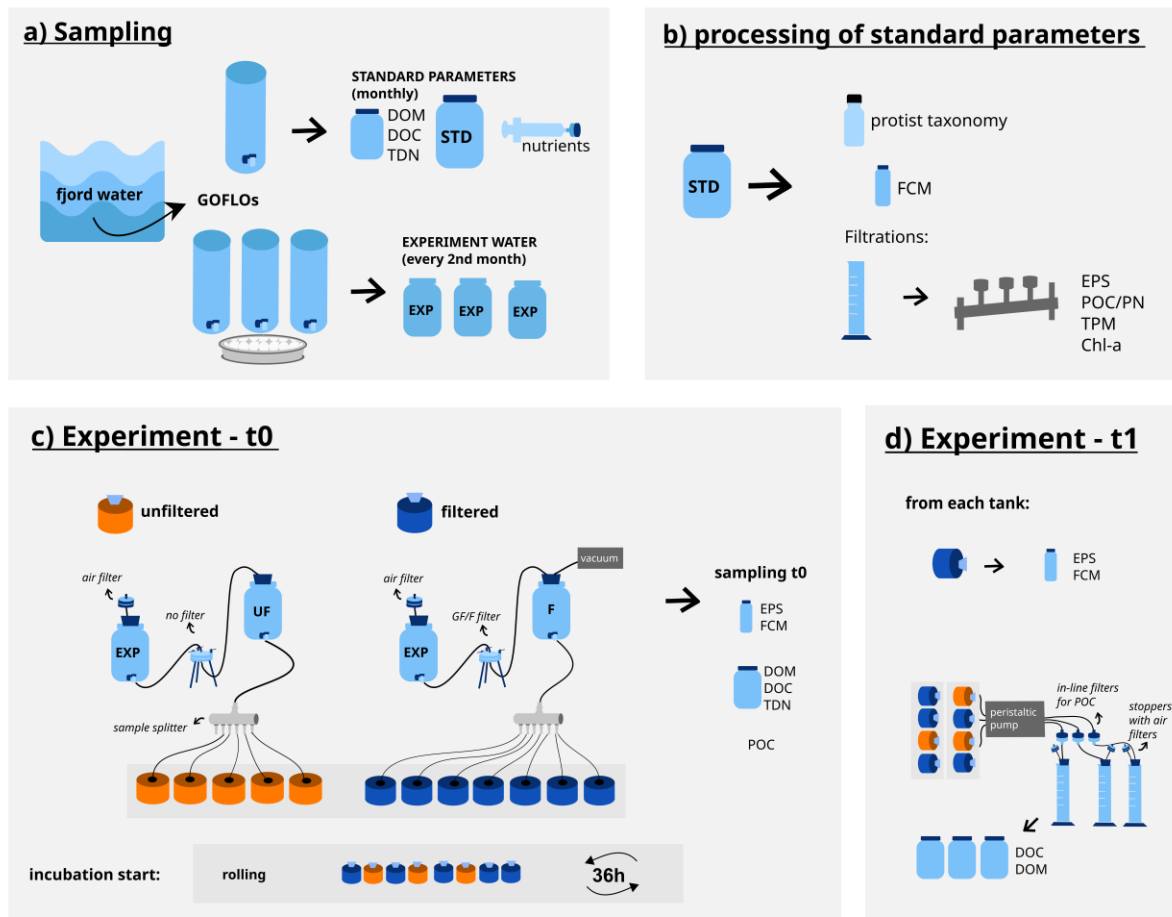
Figure 4 (Figure 2 in **Paper III**): **Sample processing and experimental setup for Paper III**.

3.3 Sample processing and analysis

3.3.1 Pelagic biogeochemical parameters

An overview of all analyzed parameters is given in Figure 5. Nutrients were syringe-filtered through a 0.2 µm filter, and the filtrate was frozen at -20°C until further analysis. Concentrations of dissolved silicate, nitrate, nitrite and phosphate were measured with a QuAAtro nutrient analyzer (SEAL Analytical). Samples for dissolved organic carbon (DOC) were filtered on GF/F filters (0.7 µm, Whatman, pre combusted), acidified and then stored at 6°C until analysis. DOC determination was performed via high temperature catalytic oxidation method using a Total Organic Carbon Analyzer (TOC-L CPH/CPN™, Shimadzu). Dissolved organic matter (DOM) extraction was performed using solid phase extraction following Dittmar et al. (2008). DOM samples were then analyzed for their chemical characterization (Box 3) by high performance liquid chromatography coupled to high-resolution mass spectrometry (HPLC-HRMS). Samples for exopolymeric substances (EPS) were filtered onto 0.4 µm polycarbonate filters. Following the colorimetric method by Dubois et al. (1956), a mixture of phenol and concentrated sulfuric acid was used to extract material from the filter to

determine total carbohydrates in the sample. A spectrophotometer (UV-6300PC, VWR) was used to measure the absorbance of the solution at 485 nm.
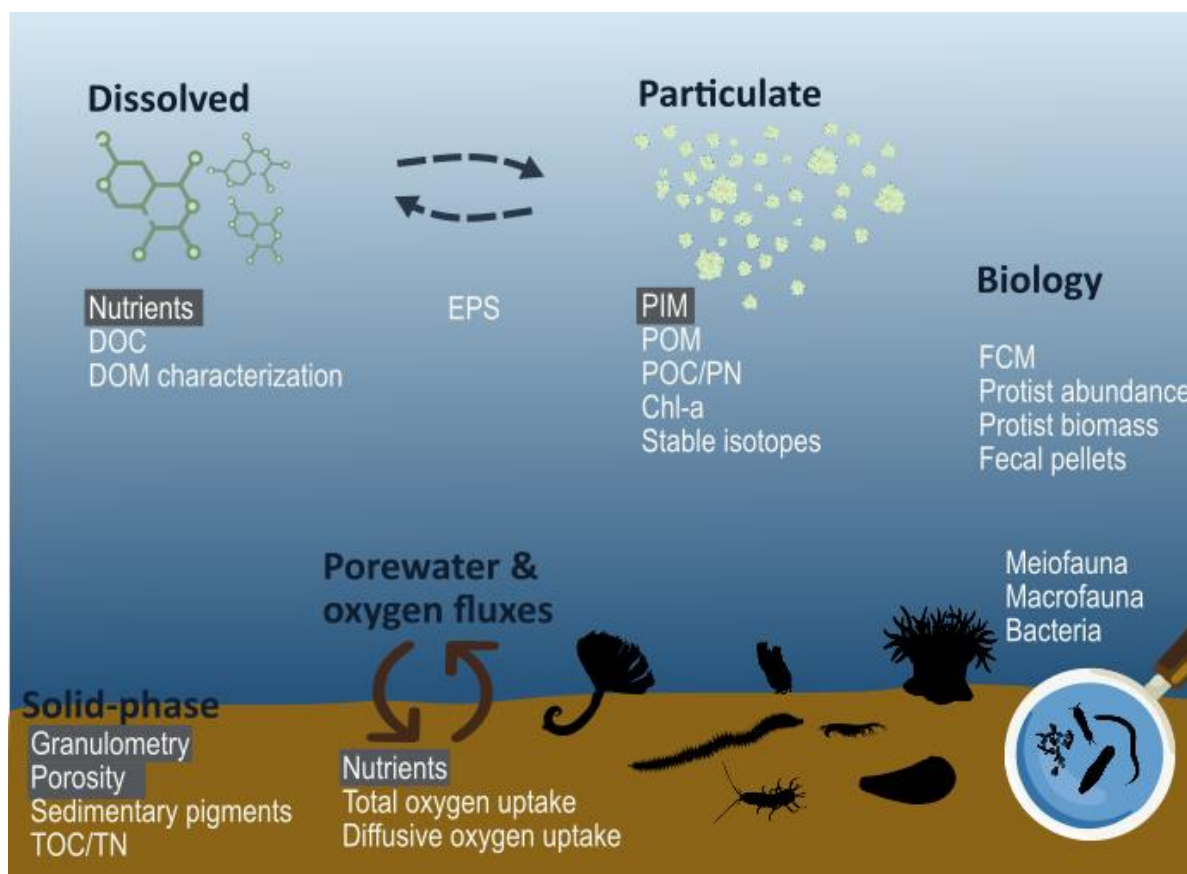
Figure 5: Overview of all parameters analyzed in this thesis. Parameters highlighted in grey are measured inorganic components. Abbreviations are dissolved organic carbon (DOC), dissolved organic matter (DOM), extrapolymeric substances (EPS), particulate inorganic matter (PIM), particulate organic matter (POM), particulate organic carbon and particulate nitrogen (POC/PN), Chlorophyll-*a* (Chl-*a*), flow cytometry (FCM), sedimentary total organic carbon and total nitrogen (TOC/TN).

Samples for TPM (including the particulate inorganic (PIM) and organic matter (POM) components), were filtered in triplicates on pre-weighed, combusted GF/F filters (Whatman). The filters were placed in aluminum trays, dried for 24 h at 60ºC and subsequently weighed on a microbalance for the determination of TPM. Afterwards, they were combusted for 7 h at 450ºC and weighed again to determine PIM. The difference between TPM and PIM was calculated as POM. Samples for stable isotopes, particulate organic carbon (POC) and particulate nitrogen (PN) were filtered through pre-combusted GF/F filters (0.7 µm, Whatman), folded and packed in pre-combusted aluminum foil and subsequently frozen at -20ºC (-80ºC for stable isotopes). For POC/PN analyses, the filters were placed in glass tubes, dried at 60ºC for 24 h and then acid-fumed for 24 h to remove all inorganic carbon and dried again at 60ºC for 24 h. Finally, the samples were packed in tin capsules and measured with a CHN elemental analyser (Exeter Analytical). For stable isotopes, samples were packed into pre-weighed tin cups, and subsequently measured with an elemental analyzer coupled with a mass spectrometer (Thermo Fisher Scientific). For size-fractionated (0.7 µm and 10 µm) Chl-*a* and Phaeopigments, samples were filtered on 0.7 µm GF/F filters (Whatman) and 10 µm polycarbonate filters (Whatman). The filters were immediately transferred to tubes with 100% methanol and placed in the fridge for 12-

24 h for extraction. Subsequently, they were analyzed with a pre-calibrated Turner Design AU-10 fluorometer or a Turner Triology before and after acidification with 5% HCl.

Box 3: An ecologist's guide for DOM Characterization

DOM Proxy	Description	Explanation	References
O/C ratio	Average oxygen to carbon atomic ratio	If the compound has been in the water for a long time and/or gone through bacterial/chemical processes, oxygen is added. Higher O/C values therefore indicate a decrease of DOM bioavailability, or compounds of older age. Terrestrial DOM also contains more oxygen relative to marine DOM.	Flerus et al. (2012)
H/C ratio	Hydrogen to carbon atomic ratio	A measure for the relative hydrogen saturation. Hydrogen bonds are easier to break up; therefore, higher H/C values indicate higher DOM bioavailability.	Cai and Jiao (2023) and references therein
AI_{mod} (Aromaticity index)	Poly-aromatic hydrocarbons	More aromatic rings in DOM molecules lead to a higher $AI_{[mod]}$ and indicate low bioavailability and high recalcitrance. DOM of high $AI_{[mod]}$ are mostly found in deep waters.	Koch & Dittmar (2006)
MW	Intensity weighted average molecular weight	A measure for the size of DOM molecules which give insight into reactivity.	Flerus et al. (2012)

3.3.2 Sediment solid-phase parameters

Samples for granulometry, porosity and sedimentary pigments (Chl-*a,* phaeopigments (phaeophorbide *a* and phaeophytin *a* and fucoxanthin) were taken from 1cm sediment slices from the MUC cores or from the landers. Pigment samples were stored at -80ºC for later analysis. Grain size spectra were assessed by laser diffraction (Malvern Instruments, Malvern, UK; Braeckman, 2023a). For porosity, the wet mass of the sediment samples was measured, and then dried at 60ºC. Afterwards, porosity was calculated by the difference between the wet and dry mass of the samples after Dalsgaard et al. (2000; Braeckman, 2023b). Sedimentary pigments were analyzed using high performance liquid chromatography after Wright et al. (2005; Braeckman, 2023c). For TOC and TN, the sediment sample was acidified with hydrochloric acid to remove inorganic carbon prior to analysis. Percent TOC and TN were determined in sediments dried at 250°C using a ELTRA CS2000 Carbon Analyzer (Braeckman, 2023d).

3.3.3 Sediment porewater parameters and oxygen fluxes

For porewater extractions, MUC cores with pre-drilled holes were mounted on the MUC prior to deployment. Samples for DIC, nutrients, sulfate and sulfide concentrations were extracted from the porewater with Rhizon samplers (Rhizosphere). For DIC, porewater was transferred to glass vials, treated with $HgCl_2$ and then stored at 4ºC. DIC concentrations were measured using a flow injection system equipped with the Spark Optimas auto-sampler. To determine nutrient concentrations (phosphate, silicate, ammonium, nitrate and nitrite), porewater was transferred to acid-washed Sarstedt vials and stored at -20°C. In the lab, samples were analyzed with a Continuous Segmented Flow Analyser (QuAAtro39, SEAL Analytical; Braeckman and Felden, 2023).

For the *ex situ* determination of diffusive (DOU) and total oxygen uptake (TOU), MUC cores were transferred to a temperature-controlled water bath. The overlying water was homogenized with a magnetic stirrer and aerated. Two oxygen optodes (Pyroscience, Firesting) mounted on an autonomous microprofiler module measured simultaneously oxygen microprofiles through the sediment for DOU. After microprofiling, total oxygen uptake (TOU) was assessed from the decrease in oxygen concentration in the overlying water over time for approximately 48 h (at least 36 h) with an oxygen optode (Pyroscience, Firesting) that measured the oxygen concentration continuously in the overlying water (measuring interval of 60 s). TOU was assessed as the decrease in oxygen concentration in the water phase that was measured. The incubation was terminated at ≤80% initial $[O_2]$ (Braeckman and Wenzhöfer, 2023). DOU and TOU were additionally measured autonomously *in situ* with benthic landers at selected stations. Details are described in **Paper I**.

3.3.4 Pelagic and benthic community parameters

For the determination of suspended bacteria, virus, pico- and nano-sized phytoplankton abundances, flow cytometry was used on samples taken from the water column in Ramfjorden. 5 ml were directly transferred to a scintillation vial, fixed with glutaraldehyde (0.5% final concentration) and frozen at -80°C until analysis. Afterwards, the samples were thawed and the abundances of pico- and nanophytoplankton were directly analyzed with an Acoustic Focusing Flow Cytometer (Attune, Applied Biosystems by Life Technologies). The populations of phytoplankton were grouped based on their pigmentation on biplots of green vs. red fluorescence. Bacteria and viruses were assessed by staining their DNA with SYBR-green I and grouped on biplots based on side scatter vs. green fluorescence. The ratio of high nucleic acid (HNA) to low nucleic acid (LNA) bacteria was used as an indicator for relative bacterial activity.

Bacterial abundances in the sediment were assessed by the Acridine Orange direct count (AODC) method. 1 cm slices of the upper 5cm sediment surface were transferred into scintillation vials and then fixed with a formaldehyde-artificial seawater solution. Afterwards, the samples were diluted and filtered through 0.2 µm polycarbonate filters (Whatman) and stained with a 0.001% acridine orange solution after Hobbie et al. (1977). For the estimation of single cell abundances, at least 30 grids from 2 replicate samples were counted with a Zeiss Axiophot microscope (Germany) and a 100x oil immersion objective lens (Zeiss Plan-Apochromat, Germany; Bodur et al., 2023a).

For the determination of suspended protist biomass and abundance, 100 ml sampled from the GoFlos (Ramfjorden) was transferred to a brown glass bottle and then fixed with a glutaraldehyde-lugol solution

for later protist examination. The same was done for samples taken from sediment traps. Protists, including phyto- and protozooplankton, were identified to the lowest possible taxonomic level in accordance with the World Register of Marine Species (WoRMS) and counted under an inverted light microscope (Nikon Eclipse TE-300 and Ti-S) using the Utermöhl method (Edler and Elbrächter, 2010; Utermöhl, 1958). Abundances were converted to carbon biomass based on published geometric relationships for biovolume conversion (Hillebrand et al., 1999) and biovolume to carbon conversion factors (Menden-Deuer and Lessard, 2000).

250 ml from sediment traps were taken for fecal pellet analysis and fixed with hexamethylenetetramine-buffered 37% formaldehyde for microscopic identification. In the lab, 25–100 ml were subsampled and settled in an Utermöhl sedimentation chamber. Fecal pellets were counted, the width and length of each pellet was measured and attributed to their origin (Calanoid copepods, appendicularians, euphausiids, chaetognaths). The carbon content of each fecal pellet was estimated using volume-to-carbon relationships using empirical conversion factors detailed in **Paper II**.

Meiofauna and macrofaunal communities were sampled at the end of the *ex situ* TOU measurements. The MUC cores were opened, and the sediment was sampled with a cut-off 10 mL syringe (area 1.89 cm²) and stored in 4% seawater-buffered formaldehyde for meiofauna. Macrofauna was collected by sieving the leftover sediment over a 500 µm mesh, stored in a Kautex bottle and fixed with the same formaldehyde solution. After meiofauna was extracted in the lab by centrifugation, meiobenthic individuals were identified to higher taxonomic levels and enumerated in accordance with WoRMS. Subsequently, nematodes were picked and transferred to separate glass slides for identification based in genus level. Macrofauna individuals were identified to the lowest taxonomic level and their blotted wet formalin weight was determined.

3.4 Data analyses

For all papers, multivariate analysis techniques were used to explore the differences between the samples along locations (**Paper I** and **II**), seasons (**Paper II** and **III**) and depths (**Paper II**).

For **Paper I**, a similarity profile routine (SIMPROF; Clarke et al., 2008) was used to explore how the stations sampled on the Northeast Greenland shelf grouped based on environmental parameters. SIMPROF identified 4 distinct groups ("sites"). Subsequently, correspondence analyses (CA) were applied to macrofauna and meiofauna communities, respectively, to visualize the grouping between stations. A Kruskal-Wallis test was applied on each dataset to test whether the benthic communities grouped according to the sites identified by SIMPROF. Finally, one additional CA was applied to Polychaeta data from 2017 and Polychaeta data sampled in 1992 (family level), formerly published in Ambrose and Renaud (1995); Piepenburg et al. (1997), to see how the communities differed between 2017 and the 1990s. The same was applied to Nematoda data (on genus level).

For **Paper II**, a CA was applied to protist flux communities to investigate how the protists sinking out during the different season differed from each other. To distinguish which protist groups were dominant during the seasons, the identified protists at species level were attributed to groups (ciliates, dinoflagellates, other flagellates, *Phaeocystis* sp. and diatoms) and plotted on top of the ordination. Subsequently, a principal component analysis (PCA) was applied to bulk vertical flux parameters in order to describe how they differed between each station and season. Afterwards, environmental and

suspended biological parameters were plotted on top to visualize how they may be related to the flux parameters.

In **Paper III**, a SIMPROF was applied to determine how the monthly sampling points were separated based on biogeochemical field data from Ramfjorden. A PCA was applied to the same data in order to visualize the seasonal progression of the marine ecosystem in Ramfjorden. Another PCA was applied to the DOM molecular weight at the start and the end of the experiment in September, October, December and January to demonstrate how the DOM molecular weight changed in the course of the experiment.

4 Key findings and summary of the results

Paper I: Benthic ecosystem changes suggest weakened pelagic-benthic coupling on an Arctic outflow shelf (Northeast Greenland)

In **Paper I** we investigated benthic communities and their functions on the Northeast Greenland Shelf (Figure 1 in **Paper I**), a remote outflow shelf where the last benthic studies were carried out during the 1990s. 17 stations across the NEG shelf were sampled with a multicorer and/or an autonomous lander between September and October 2017, including some stations close to the 79ºN Glacier. Benthic community parameters (macrofauna, meiofauna, bacteria) were analyzed along with their functions (total and diffusive oxygen uptake) and environmental variables (porosity, granulometry, sedimentary pigments, total organic carbon and total nitrogen (TOC/TN), porewater chemistry) from each station. A SIMPROF analysis revealed that based on the environmental variables, the stations could be grouped into 4 sites: Westwind Trough, Norske Trough, Belgica Bank and close to the 79ºN Glacier. Benthic pigment concentrations, including fucoxanthin (an accessory pigment of diatoms), as well as TOC, porewater silicate (indicative of diatom-derived remineralization), ammonia and nitrite concentrations and bacterial cell abundances were highest in the Westwind Trough. This suggests a higher benthic activity and a tighter pelagic-benthic coupling in the Westwind Trough compared to the Glacier, Norske Trough and Belgica Bank. Total abundances of macrofauna and meiofauna were highest in the outer parts of the shelf compared to locations adjacent to the Glacier and the inner shelf stations (e.g., macrofauna: 1,964–2,952 versus 18–1,381 individuals m^{-2}). Two Correspondence Analyses (CA) performed separately for macrofauna and meiofauna communities revealed that the benthic communities were mainly separated between the Westwind versus the Glacier and Norske Trough (Figure 6a, b). Macrofauna and meiofauna community structures were mainly driven by food availability. However, a Kruskal-Wallis Test did not show a significant distinction of macrobenthic (or meiobenthic) communities between sites. This is in contrast to results from the 1990s, when macro- and meiobenthos showed a clear distinction between the Westwind and the Norske Trough. The results suggest a homogenization of benthic communities across the NEG shelf since the 1990s. Subsequently, CAs based on Polychaeta (on family level) and Nematoda (on genus level) from 2017 and the 1990s were performed to analyze how these communities might have changed during the last 24 years. In both cases, the sampling years separated clearly along the first CA axis. Overall, Polychaeta densities were about 5 times lower in 2017 compared to the 1990s, while Nematoda densities were about 3 times higher (Figure 6c, d). We found a decreased Polychaeta and an increased Nematoda diversity across the shelf, and a different community structure of Nematoda genera. These changes were accompanied by warmer bottom water temperatures, an increased number of sea-ice-free days, and decreased sediment pigment concentrations that were one order of magnitude lower in 2017 compared to the 1990s (Figure 6e, f). A shift from macrofauna to meiofauna and a homogenization of benthic communities across the shelf suggest that pelagic-benthic coupling might have weakened since the 1990s.
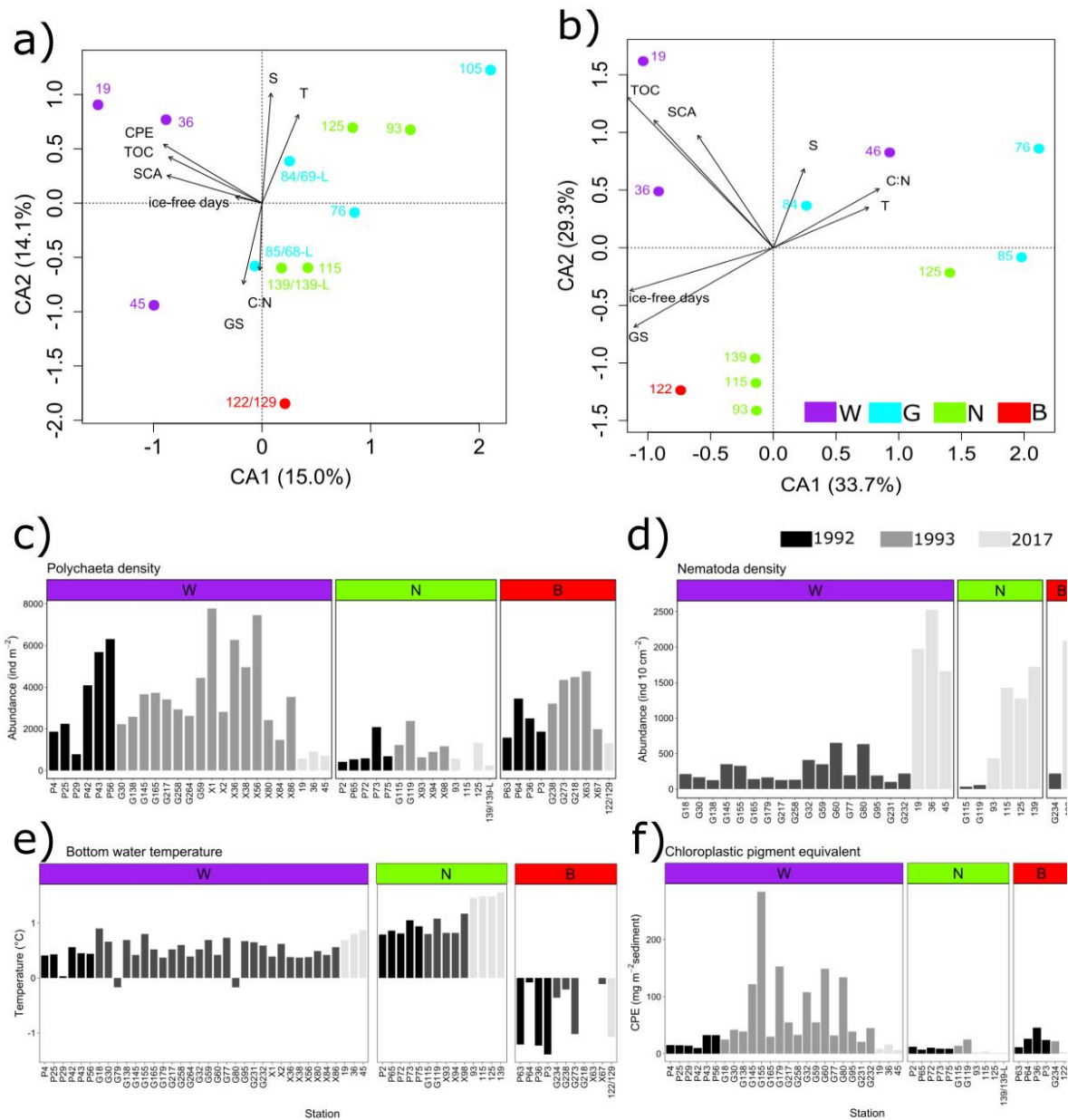
Figure 6 (Figures 5a, b and 6a, b, e, f in **Paper I**)**: Results from Paper I.** Visualization of the Correspondence Analysis for macrofauna (a) and meiofauna (b) abundances with environmental parameters fitted on top, and comparison of (c) Polychaeta density, (d) Nematoda density, (e) bottom water temperature and (f) benthic pigment concentrations between 1992, 1993 and 2017. Colors represent the 4 sites statistically identified by the SIMPROF analysis based on standardized environmental data (Figure S5): Westwind Trough (W), 79ºN Glacier (G), Norske Trough (N), and Belgica Bank (B). Tested environmental parameters are number of sea-ice-free days (ice-free days), sediment TOC:TN ratio (C:N), chloroplastic pigment equivalent (CPE), grain size (GS), single cell abundances (SCA), bottom water salinity (S) and temperature (T).

Paper II: Seasonal patterns of vertical flux in the northwestern Barents Sea under Atlantic Water influence and sea-ice decline

For **Paper II**, we studied the composition and magnitude of vertical flux in the seasonal ice zone of the northwestern Barents Sea across different seasons. To characterize the composition and amount of vertical flux, short-term drifting, surface-attached sediment traps were deployed in August and December 2019, and in March and May 2021 along a latitudinal transect between 75º and 85ºN east of Svalbard (Figure 1 in **Paper II**). After each deployment, samples for particulate organic carbon and particulate nitrogen (POC/PN), size-fractionated Chl-*a*, fecal pellets and stable isotopes were taken. The stable isotope analysis revealed a strong separation of sinking material between seasons along the $\delta^{15}N$ axis, indicating a gradient of decreasing organic matter quality from spring to winter. A separation between stations along the $\delta^{13}C$ axis, especially during May, indicated a spatial gradient related to local productivity within the season. We found that during winter (December and March) vertical flux was very low, and smaller, heterotrophic protist cells, especially dinoflagellates, dominated the vertical flux, mirroring the standing stocks of protist communities (Figure 7a). During spring, vertical flux across the northwestern Barents Sea was highly variable and strongly related to the sea-ice edge and Atlantic Water influence. The sinking particles at the two Atlantic Water-influenced, most productive stations were Chl-*a*-rich, mainly composed of diatoms, and had low POC:PN ratios. Less productive stations in May were still in a winter/pre-bloom stage, with high POC:PN ratios, low Chl-*a* flux and dominated by flagellates and ciliates (Figures 7a, b). In August, vertical flux across the transect was more homogenous in terms of magnitude and composition (Figure 7b). The sinking particles were composed of smaller cells, especially dinoflagellates, and Chl-*a* flux was lower compared to May, indicating a decreasing "freshness" of organic matter from spring to summer. The concentration of suspended particles was higher than in spring, suggesting a more efficient retention system during August.

The results confirm a strong seasonality of vertical flux in the northern Barents Sea, with lowest magnitude and quality during winter and highest quality in May. While the magnitude of vertical flux was high in May and August compared to winter, there were strong compositional differences between spring and summer. Ultimately, seasonality in the northern Barents Sea is driven by the inflow of AW and sea ice in concert, and high vertical flux can occur under pack ice within the AW pathway.
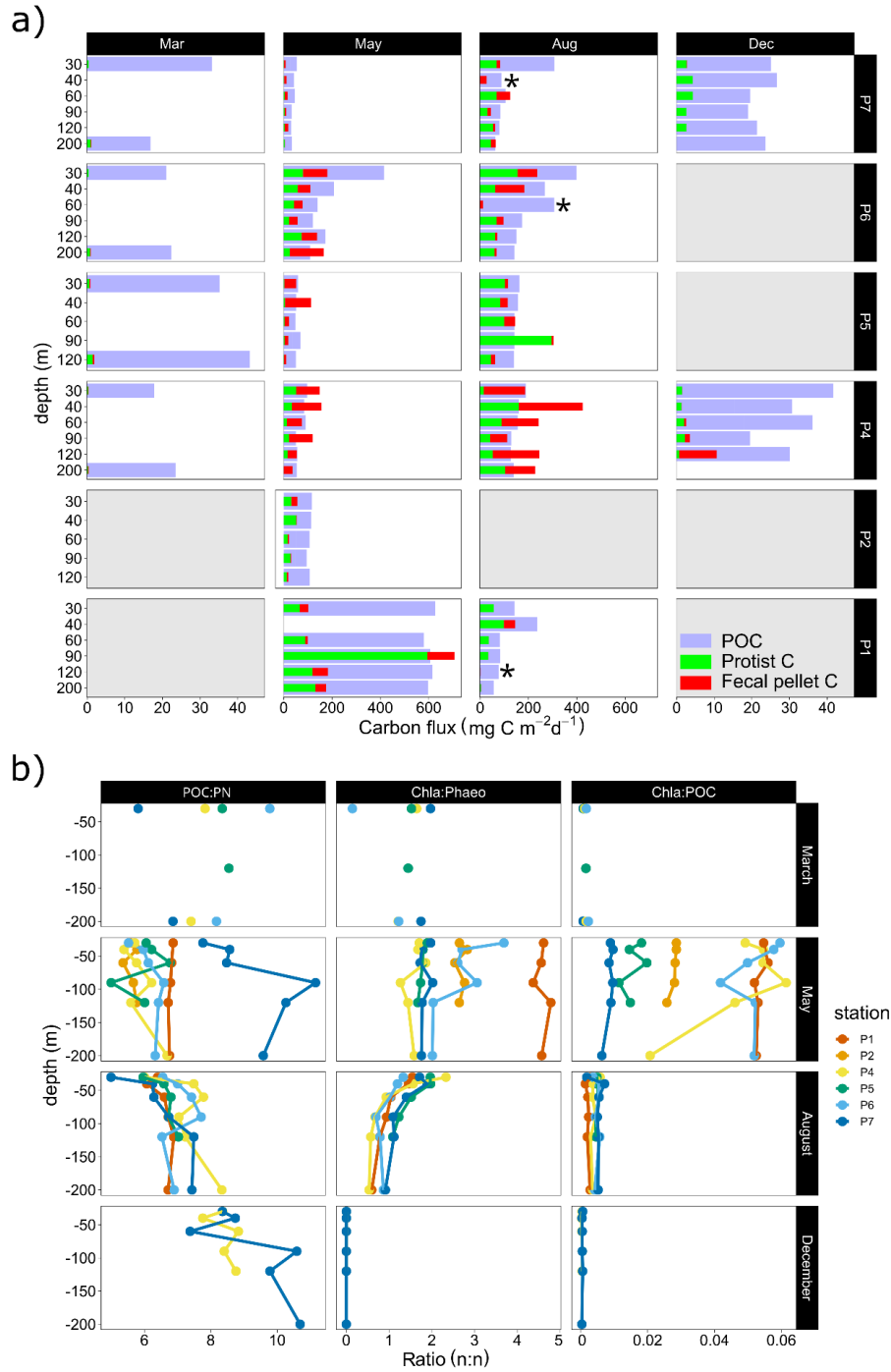
Figure 7 (Figures 5 and 6 in **Paper II**)**: Results from Paper II.** (a) Measured particulate organic carbon flux (blue bars) and carbon flux estimates of protists (green) and fecal pellets (red); and (b) POC:PN, Chl-*a*:Phaeopigments and Chl-*a*:POC ratios of vertical flux across all seasons and stations in the northwestern Barents Sea.

Paper III: Contrasting seasonal patterns in particle aggregation and DOM transformation in a sub-Arctic fjord

For **Paper III**, we studied the continuum between the particulate and dissolved fractions across different seasons within a sub-Arctic fjord (Ramfjorden, Tromsø; Figure 1 in **Paper III**). We carried out aggregation experiments between September 2020 and August 2021 every second month. Part of the water was filtered through a GF/F filter, while the other part was left unfiltered. The filtered (F) and unfiltered (UF) water each was subsampled for POC, DOC, extracellular polymeric substances (EPS), dissolved organic matter (DOM) characterization and flow cytometry (FCM) before it was filled into roller tanks that were rotated at 3 rpm. After 36 h the incubation was terminated, and all tanks were subsampled for the same parameters. In addition to the experiment, we deployed a CTD and collected biogeochemical parameters at the sampling station every month to record the seasonal development within the fjord. In April, June, and September, when the system was productive, we measured increased POC concentrations in both, F and UF treatments at the end relative to the start of the experiment (Figure 8a). However, aggregation was higher under post-bloom conditions in June and September compared to spring bloom conditions in April. During winter, in December and February, POC concentrations decreased in both treatments relative to the start of the experiment. The trends were similar in filtered and unfiltered treatments, underlining that during the productive period, a substantial fraction of POC could originate from aggregation within the DOM pool, while in winter, processes reducing particles seem to be dominant. Although bacterial abundances were only increasing in June and August, bacterial activity was increasing in all treatments throughout the year. We also found an increase in lability of DOM during POM dissolution after incubation in winter, which was reflected by an increase in hydrogen to carbon ratios (H/C), and a decrease in average oxygen to carbon ratios (O/C) and modified aromaticity index ($AI_{[mod]}$), together with a decrease in molecular weight of DOM compounds (Figure 8c, d, e, f). The opposite DOM compositional patterns were observed with aggregation in September. DOM compounds were converted to more recalcitrant compounds as shown by a decrease in average H/C ratios, an increase in $AI_{[mod]}$ and O/C, and an increase in average molecular weight of compounds.

We demonstrated that in a sub-Arctic fjord, transitions in the DOM-POM continuum underlie seasonal variations in the ecosystem. While aggregation seems to be the dominant process between spring-autumn, during winter particle dissolution seems to prevail. Comparing the DOM molecular composition between autumn and winter revealed that during the aggregation process in autumn, DOM lability and molecular weight increased, while in winter DOM lability increased and MW decreased within the small molecular (<1 kDa) fraction. These findings suggest that physical (aggregation) and biological (degradation) processes drive processes the DOM-POM continuum in concert, and their relative influence is driven by ecological, physical and chemical conditions in the environment.
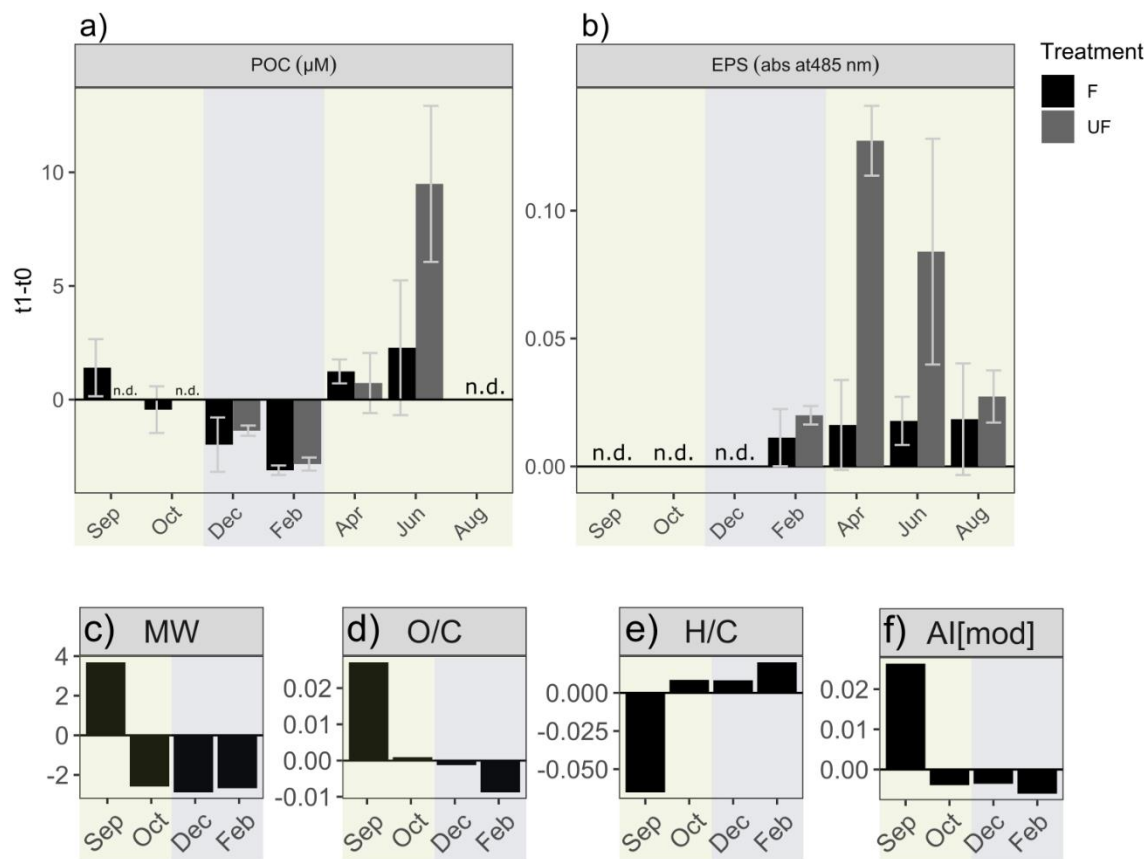
Figure 8 (Figures 4a, b, 5a, b, c, d in **Paper III**): **Results from Paper III.** Change of (a) concentrations in particulate organic carbon (POC) and (b) relative absorption of extracellular polymeric particles (EPS) in filtered (F) and unfiltered water (UF); and change in intensity weighed average of molecular weight (MW; c), oxygen to carbon ratio (O/C; d), hydrogen to carbon ratio (H/C; e) and modified aromaticity index (AI[mod]; f) in filtered (F) water. The background colors indicate the statistically identified winter (blue) and productive (green) period, respectively.

5 Synthesis and discussion

To understand pelagic-benthic coupling and its mechanisms in a changing Arctic, it is important to combine the pelagic and the benthic "perspectives" on the biological carbon pump (BCP). In the following synthesis, I integrate the findings of the diverse, but highly connected aspects of the BCP addressed in the papers included in this thesis. The synthesis consists of three parts: In the first part, I outline the benthic dependency on the BCP using the example of benthic communities on the NEG shelf (**Paper I**). I will then present some of the mechanisms that regulate vertical flux (**Paper II** and **Paper III**) and with that, the BCP in the Arctic, and give some examples for pelagic-benthic coupling from some Arctic shelf regions. In the second part, I will present the changes in the benthic communities on the NEG shelf since the 1990s (**Paper III**), and subsequently discuss drivers that could lead to a weakening, or a tightening of pelagic-benthic coupling in the Arctic by means of the mechanisms described before. Finally, I will give some insights into processes of the BCP during the polar night, as this thesis provides one of the few contributions for this time of the year.

5.1 The biological carbon pump in the Arctic and its mechanisms

5.1.1 The benthic perspective: Benthic communities depend on the biological carbon pump

Benthic communities are mainly driven by food availability at the seafloor. On Arctic shelf seas and in the deep sea, sedimentary organic matter (OM) is largely supplied by vertical flux from the euphotic zone (Graf, 1989; Wiedmann et al., 2020). High concentrations of organic carbon and little degradation of pigments in the sediment can lead to high benthic abundance, biomass, remineralization and/or taxonomic, functional and food-web diversity (Blanchard et al., 2013; Denisenko et al., 2003; Link et al., 2013b, 2013a; Mäkelä et al., 2017a; Morata et al., 2008; Oleszczuk et al., 2023; Szczepanek et al., 2021). Especially diatom-derived food is utilized most efficiently by benthos (Braeckman et al., 2018).

On the NEG shelf, we found increased benthic abundance and biomass in the Westwind Trough together with higher sedimentary pigment content (including Fucoxanthin, an accessory pigment found in diatoms), and porewater silicate concentrations (indicative of diatom-derived remineralization) compared to the southern region (Figures S3 and 4 in **Paper I**). It suggests that the Westwind Trough received a higher amount of diatom-derived OM. In the 1990s, higher primary production (Pesant et al., 2002, 1996) and lower pelagic degradation (Ashjian et al., 1995) has been described for the NEW Polynya, located in the Westwind Trough, compared to the surrounding areas, resulting in a tighter pelagic-benthic coupling within the area (Ambrose and Renaud, 1995; Brandt, 1995; Hobson et al., 1996; Piepenburg et al., 1997). During spring, OM export was dominated by diatoms, with patches of the filament-forming under-ice diatom *Melosira arctica* sinking out occasionally (Bauerfeind et al., 1997; Gutt, 1995). Higher benthic pigment concentrations in the NEW Polynya compared to the surrounding areas suggest that a substantial fraction of fresh material was sinking out and was incorporated into the benthic food web (Ambrose and Renaud, 1995; Hobson et al., 1996).

5.1.2 The pelagic perspective: The biological carbon pump is driven by vertical flux

The presence of organic matter at the seafloor in terms of quantity and quality often reflects primary production patterns in the water column (Cochrane et al., 2009; Morata and Renaud, 2008). Vertical flux during the spring bloom is often related to the rapid export of fresh algal material (**Paper II**; Dybwad et al., 2021; Olli et al., 2002; Reigstad et al., 2008). This is reflected in the low degradation in sedimentary pigments in spring, while in summer, more degraded material is available at the seafloor (Morata and Renaud, 2008). Fresh OM matter pulses are quickly incorporated into the benthic food web (Boetius et al., 2013; Morata et al., 2015, 2011). In our study, the "freshness" of sinking OM in May was demonstrated by lowest δ^{15}N stable isotopic signatures, higher Chl-*a* flux as well as higher Chl-*a*:Phaeopigment and Chl-*a*:POC ratios compared to the other sampling periods (August, December, March; Figures 3, 4 and 6 in **Paper II**). Moreover, diatoms were dominating the sinking material at the most productive stations (P1 and P6; Figure 7 in **Paper II**). As the bloom progresses, however, the abundance of diatoms decreases, and smaller phytoplankton, heterotrophic protists and fecal pellets dominate the composition of the sinking OM. The change in composition is accompanied by a decrease in "freshness" of the bulk material, shown by increasing C:N ratios and δ^{15}N stable isotopic signatures, and lower Chl-*a* flux, Chl-*a*:Phaeopigment and Chl-*a*:POC ratios (**Paper II**; Dybwad et al., 2021; Reigstad et al., 2008; Trudnowska et al., 2021).

In the Barents Sea, benthic biomass is highest at locations where annual primary productivity and carbon export are highest as well (Reigstad et al., 2011). There is a positive correlation between primary production and vertical flux of carbon at 90 m (Reigstad et al., 2008), as well as the vertical flux of pigments at 90 m and sediment pigment concentrations (Renaud et al., 2008). In the Northern Bering and Chukchi Seas, areas with high suspended Chl-*a* concentrations exhibit high sedimentary oxygen consumption, organic carbon content and benthic biomass (Grebmeier et al., 2006a). However, high export can occur in low production regimes, often in the early stages of a spring bloom and typical for high latitudes, and at other locations, low export can be measured despite high production (Henson et al., 2019). A variety of biotic and abiotic mechanisms in the pelagic realm regulate the vertical flux, and with that the export to the benthos.

5.1.2.1 Mechanisms for spatial and temporal variability in vertical flux

Grazing and fecal pellet flux

The grazing pressure in the water column defines whether little OM ("retention system") or a lot of OM ("export system") is exported to the seafloor. Because OM is increasingly remineralized in the pelagic zone from spring to summer, the system usually shifts towards a "retention system" (Wassmann, 1998). On a global scale, carbon export decreases with increasing picophytoplankton, small zooplankton and bacterial abundances (Henson et al., 2019).

On the other hand, zooplankton can also mediate sinking flux by packaging OM into fecal pellets that can sink more efficiently to the seafloor (Miquel et al., 2015; Turner, 2015; Wexels Riser et al., 2007). The contribution of fecal pellets to vertical flux relative to protist cells can increase from spring to summer (Caron et al., 2004; Figures 5 and 8a in **Paper II**). Coprorhexy (fragmentation of fecal pellets) makes fecal pellets susceptible to degradation by bacteria and protists (Iversen and Poulsen, 2007), and

in the Barents Sea, retention of fecal pellets can be higher in AW than in Polar Water (Wexels Riser et al., 2002). Other studies found that during post-bloom scenarios small and slowly sinking particles such as *Phaeocystis* are packaged and exported to greater depth through fecal pellets (**Paper II**; Dybwad et al., 2022, 2021; von Appen et al., 2021; Wiedmann, 2015). Their role seems temporally and spatially variable, and conclusions differ between studies; however, it is clear that the importance of fecal pellets for vertical flux is higher during summer, when OM in the pelagic zone consists of small, degraded and slow-sinking particles, and a "mediator" is required for increasing the export efficiency.

The influence of sea ice and Atlantic Water in the northwestern Barents Sea

The presence of sea ice drives strong spatial variability of vertical flux in the MIZ, especially during the "spring" period. In the northern Barents Sea, peak blooms can occur between May-July, depending on the location (Reigstad et al., 2008). South of the MIZ, local blooms often occur earlier in the year compared to areas north of the MIZ, following the northward retreat of the sea ice (Castro de la Guardia et al., 2023). This demonstrates the high variability of "spring" seasonality in a highly dynamic, seasonally sea-ice-covered area such as the Barents Sea. During our field campaign for **Paper II** in May, the ice edge reached as far south as Station P2 (77.5°N). Indeed, at that time we measured highest fluxes at the southernmost open-water station P1 (605 mg $C^{-2} d^{-1}$ at 90 m, 30–60 km away from the sea-ice edge, Figure 2 in **Paper II**) and lowest fluxes at the northernmost ice-covered station P7 (2.9 mg $C^{-2} d^{-1}$ at 90m). In August, when the sea-ice edge was further north around P5, the northernmost stations P6 and P7 displayed highest POC fluxes while P1 displayed lowest vertical flux from a strongly retentive system, following the retreat of the sea-ice edge. Moreover, in contrast to the strong spatial heterogeneity of vertical flux during spring (POC fluxes between 32–605 mg $C^{-2} d^{-1}$ at 90 m), vertical flux was more comparable in terms of magnitude and composition across the transect in August, when a large part of the transect was ice-free (**Paper II**). The range of measured POC flux in August was 82–221 mg $C m^{-2} d^{-1}$ at 90 m (Figure 2 in **Paper II**). The spatial variability in vertical flux probably mirrored the supporting role of sea ice as a driver for spatial diversity in vertical flux.

However, the relationship between sea ice and export in the peak bloom period is not always trivial. During May, we also measured high diatom-derived vertical flux at the ice-covered station P6, which was located, similar to P1, within the AW pathway. We concluded that the classic seasonality pattern driven by the ice edge retreat is intersected by the inflow of AW and the local sea-ice variability. The sea-ice concentration north of Svalbard, which lies in the AW pathway where P6 and P7 are located, is highly variable compared to the northern shelf (Stations P2–P5) (Steer and Divine, 2023). During fieldwork in March, we observed sea smoke in large ice leads at P6 and P7, which is indicative of warm AW heating the upper ocean and melting sea ice from below. Locations influenced by AW probably receive more nutrients, as well as experience earlier and more incident light due to temporary open-water areas and leads, thus blooms can occure earlier, even compared to locations further south.

Depth, stratification and mixing

Sea ice can influence vertical flux patterns in two different ways. It controls the timing of the spring bloom as described above, and meltwater-derived stratification can lead to a stabilization of the water column, and thus to high biological productivity ("critical depth hypothesis"; Sverdrup, 1953) that can rapidly be exported. Conversely, sea-ice-melt-derived stratification can also result in a strong attenuation of vertical flux, with most of the particles being retained at the pycnocline (Reigstad et al.,

2008; von Appen et al., 2021; Wiedmann, 2015). During May, while we measured high POC export below 200 m at the mixed, open-water station P1, fluxes at the ice-covered station P6 were strongly attenuated (Figure 2 in **Paper II;** >600 mg C m^{-2} d^{-1} at P1 vs <150 mg C^{-2} d^{-1} at P6). This attenuation pattern became also evident in a study where we compared pelagic production and export in two contrasting "summer" scenarios across the same transect (Amargant-Arumí et al., 2024). In August 2019, a "high ice year", the transect was more affected by meltwater-derived stratification compared to August 2018, which was in a "low ice year". Although vertical flux in August 2019 was higher at the surface, it was also stronger attenuated, resulting in a similar amount of OM exported at 200 m across the transect between the two years (Amargant-Arumí et al., 2024). Mixing events in open water are not only important for bringing nutrients closer to the surface to fuel primary production (Ardyna et al., 2014; Castro de la Guardia et al., 2023), but are also highly relevant for the export of carbon from the euphotic zone and pelagic-benthic coupling, transporting particles down in the water column and escaping grazing pressure (Pesant et al., 2002; von Appen et al., 2021). The "mixed-layer pump" is especially typical for high-latitude ecosystems and can transport large fractions of particles below the euphotic layer (Dall'Olmo et al., 2016). Consequently, highest export in the northwestern Barents Sea during spring does not necessarily occur under sea-ice conditions, but also in a mixed open-water area (**Paper II**; Reigstad et al., 2008; Wiedmann, 2015).

Aggregation

Aggregation of fresh diatom cells to large particles can play an important role for the rapid downward transport of OM (Thornton, 2002). Ice algal material from melting sea ice can rapidly be deposited and provide large amounts of fresh OM at the seafloor (Boetius et al., 2013; Trudnowska et al., 2021). On the NEG shelf, the diatom *Melosira arctica* produces sticky mucilage, and these large strands may collect other particles, thus enhancing sedimentation of suspended, slowly sinking particles (Bauerfeind et al., 1997). Aggregation of cells, fecal pellets and detritus is usually promoted by colloidal or gel-like DOM of high molecular weight, such as EPS and TEP. DOM of low molecular weight can rapidly transform into these colloids/gels, depending on physical, chemical or biological conditions (Chin et al., 1998). However, little is known about the seasonal changes of these transitions.

Under spring bloom conditions in Ramfjorden (April), we measured very little aggregation of POC in our experiment in unfiltered (UF) water compared to during a second bloom peak in June (increase of 0.7 and 9.5 µM POC, respectively; Figure 4 in **Paper III**). This was the case even though POC concentrations before the incubation (t0) were higher in April than in June (18.6 µM and 7.7 µM, respectively). However, EPS concentrations in the field as well as at t0 in the experiment were more than twice as high in June compared to April (Figures S2 and S4 in **Paper III**). This demonstrates the importance of EPS as a mediator for particle-to-particle aggregation, and probably for sorption of DOM onto particles.

Phase shifts of DOM and subsequent aggregation of large molecular compounds can additionally contribute to the particle pool in the pelagic zone (Verdugo et al., 2004). Just as for UF water, we also measured little aggregation in April from the dissolved pool (increase of 1.2 µM POC in filtered (F) water). While in April, aggregation from the dissolved pool accounted for 1.7% of the POC concentration measured *in situ*, in June and in September this process accounted for 2.9% and 7.9% of *in situ* POC, respectively (Figures 4 and S3 in **Paper III**). This points towards little contribution of

DOM to the particulate pool under peak bloom conditions, and an increased potential of particles originating from the dissolved pool in the post-bloom period.

During the post-bloom period, particles in the water column are mainly composed of fecal pellets and amorphous, unidentifiable material, which indicates a mix of degraded cells and sticky DOM material (**Paper II**). EPS accumulate under increasing nutrient limitation and/or with increasing concentrations of senescent cells, as is the case during post-bloom conditions (Engel, 2000; Hellebust, 1965; Mague et al., 1980; Myklestad, 1995; Passow, 2002; Thornton, 2002). This increases the aggregation potential from the dissolved pool during summer (Figure 4b in **Paper III**). Although not all particles sink, aggregation plays an important role for the export of particles from the euphotic zone. Moreover, aggregation occurs most readily under high particle concentrations, which is the case under post-bloom conditions during summer as well (Burd and Jackson, 2009). Flocculation and ballasting through minerals, trapped in sticky EPS matrices, can additionally drive highest vertical export during autumn in glacially-impacted fjords or on riverine influenced interior shelves (Forest et al., 2013; Wiedmann et al., 2016), underlining the importance of aggregation processes.

5.1.3 Pelagic-benthic coupling and its definition

While food availability at the seafloor and benthic activity (e.g. oxygen consumption, bioturbation) can reflect seasonal gradients in vertical flux, these gradients, regulated by different mechanisms in the pelagic realm, are not directly incorporated into benthic communities. In the northwestern Barents Sea, despite the strong seasonality of vertical flux, benthos did not show a seasonality in terms of community composition, abundance, biomass (Jordà-Molina et al., 2023) or stable isotopic signature (Ziegler et al., 2023). Benthic communities were rather driven by bathymetric parameters, and were separated between the shelf and the slope/basin (Jordà-Molina et al., 2023). Benthic communities change over longer timescales (Soltwedel et al., 2016), rather integrating systematic changes in vertical flux (e.g., longer sea-ice-free periods over several years, shifts in pelagic primary producers or secondary consumers). Accordingly, benthos is a useful tool to detect long-term changes in vertical flux. Studying pelagic regulation patterns along environmental gradients in turn can address possible reasons for changes in benthic ecosystems. Therefore, it is important to combine the pelagic and the benthic "perspectives" when addressing pelagic-benthic coupling.

However, combining the two fields bears some challenges for the definition of "pelagic-benthic coupling". Does, for example, a system with high export efficiency (i.e., a relatively large part of primary production is exported to the seafloor), but little primary production necessarily mean a tight pelagic-benthic coupling? And what about a system where sinking OM is highly recycled, but a similar amount is exported as in the former scenario? From a pelagic perspective, little remineralization of OM in the pelagic zone, regardless of the amount of production, would mean an efficient BCP where production and grazing are decoupled, and the "connectedness" with the benthos is high; thus, a tighter pelagic-benthic coupling. From a benthic perspective, however, what matters is not the fraction of OM that is exported, but the overall amount that reaches the seafloor.

The same question arises when considering the quality of the sinking OM. Is pelagic-benthic coupling tightening or weakening in a system in which bulk export of carbon increases but the quality of the exported matter decreases (e.g. through increased primary production, but also high pelagic

degradation)? Here again, from a "pelagic perspective" we could argue for a weakened pelagic-benthic coupling, as the degradation of the sinking material is increasing. From a "benthic perspective", however, it is unclear whether the decreased quality of the food matters, if overall food availability increases. These issues are important to keep in mind when comparing pelagic-benthic coupling across different spatial and temporal scales, and when discussing pelagic-benthic coupling in a future warmer Arctic with less sea ice.

5.1.3.1 Panarctic examples for pelagic-benthic coupling

High productivity and export: The inflow shelves and the North Water Polynya

Figure 9 displays a compilation of short-term sediment trap studies across the Arctic, showing that inflow shelves (Bering, Chukchi and Barents Seas) exhibit highest peaks of POC downward fluxes (up to 2200, 1390 and 766 mg C m^{-2} d^{-1}, respectively; O'Daly et al., 2020; Olli et al., 2002). This is because of the export of high spring primary production on inflow shelves, which accounts for two thirds of total primary production in the Arctic Ocean (Carmack and Wassmann, 2006). In the similarly highly productive North Water Polynya, peak blooms and subsequent high vertical flux (up to 680 mg C m^{-2} d^{-1}) occur a little later in June/July and are followed by the downward transport of fresh diatom-derived OM (Amiel et al., 2002; Michel et al., 2002; Figure 6). These productive sites (Bering, Chukchi and Barent Seas, as well as the North Water Polynya) showed similar seasonal patterns, with downward flux of diatoms in the beginning of the bloom period, followed by increasingly regenerated material and an increased contribution of fecal pellets towards summer. The production on inflow shelves is largely fueled by the inflow of the Pacific (PW) and Atlantic (AW) water masses which carry along high levels of nutrients, but also allochthonous OM, and this is reflected in benthic food availability and community parameters. In accordance, the inflow shelves also exhibit highest benthic biomass across Arctic shelves (<10–500 g wet weight m^{-2} in the Barents Sea (Wassmann et al., 2006) and 38–2800 g wet weight m^{-2} in the Bering and Chukchi Seas (Grebmeier et al., 2006a), respectively).

The Chukchi Sea is seasonally strongly stratified and vertical mixing is lower than in the Barents Sea (Carmack and Wassmann, 2006). Nevertheless, peak fluxes, as well as benthic biomass are higher than in the Barents Sea (Figure 9). This is because the Chukchi Sea is a shallow shelf. Abundance and biomass of benthos (meiofauna, macrofauna and megafauna; except for bacteria) decrease with depth because of decreased food input with increasing distance of the seafloor to the surface production (Meyer et al., 2015; Rex et al., 2006). At deep locations, OM spends a longer time being degraded within the water column. With increasing depth, benthic biomass and size distribution decreases, with meiofauna dominating over macrofauna (Górska et al., 2020). Moreover, in the Chukchi Sea, the pelagic ecosystem is weaker compared to the Barents Sea (Blanchard et al., 2013; Cooper and Grebmeier, 2018; Grebmeier et al., 2006a); therefore, a substantial amount arrives ungrazed at the seafloor. In the Barents Sea, the pelagic food web has a strong ecological role (Dalpadado et al., 2014; Ellingsen et al., 2008). High zooplankton standing stocks, enforced by the advection with AW, have a high grazing capacity and sustain a substantial fish biomass. Advection of zooplankton with Pacific Water is lower than through AW in the Atlantic Arctic (Carmack and Wassmann, 2006).

Export mediated through river runoff and aggregation: the interior shelves

The interior shelves exhibit peak fluxes later in the season during summer, and of lower magnitude than the inflow shelves (Figure 9; up to 92 mg C m^{-2} d^{-1} in the Kara Sea; Drits et al., 2017), with decreasing peak fluxes along the Laptev and East Siberian Seas; and up to 260 mg C m^{-2} d^{-1} in the Beaufort Sea; Juul-Pedersen et al., 2010). However, it needs to be noted that little information about the Eastern Arctic is available in English scientific literature, which is why not many data points are included for these regions in Figure 9.

In the Beaufort Sea, primary production is lower compared to the inflow shelves (Sakshaug, 2004). The shelf is sea-ice-covered until May, after which the melt season starts, together with increased river discharge (Barber and Hanesiak, 2004; Forest et al., 2013). This creates a strongly stratified water column during the productive season. Productivity is dependent on the breaking of this stratification by wind-driven coastal or shelf-break upwelling, which can promote occasional primary production bursts (Tremblay et al., 2011) and subsequent vertical flux. Inorganic material is a large contributor to particle fluxes on the shelf, due to the river inflow (Forest et al., 2013; O'Brien et al., 2006), and benthic communities on the shelf receive a large fraction of their food input by terrestrial sources (Carmack and Wassmann, 2006; Morata et al., 2008). Riverine minerals entangled in EPS matrices ballast the sinking OM, resulting in the largest export by small, detritus-derived particles (Forest et al., 2013; Sallon et al., 2011). Vertical flux beyond the shelf and at the shelf break is driven to a larger extent by marine, allochthonous production under shelf upwelling events. These events, by contrast, favor the production of large, fresh particles (Forest et al., 2013). Zooplankton are strong flux regulators (Juul-Pedersen et al., 2010). Benthic communities on the Mackenzie Shelf are driven by pigment concentrations and their freshness at the seafloor (Link et al., 2013a; Morata et al., 2008), which might indicate a dependency on marine-derived primary production. With retreating sea ice, increasing wind and upwelling events as well as increasing river input, vertical flux might increase in this region (Forest et al., 2013; Tremblay et al., 2011).

Pelagic-benthic coupling on an oligotrophic outflow shelf: Northeast Greenland

The productive period on the NEG shelf was described to be between May and August (Smith et al., 1997). A summary of the physical setting on the NEG shelf was presented in Section 3.1. Unfortunately, the study by Bauerfeind et al. (1997) provides the only available comprehensive flux measurements on the NEG shelf, derived from moored long-term sediment traps. Annual fluxes measured with these traps in the NEW Polynya during the 1990s were within the range of long-term sediment trap measurements north and northeast of Svalbard (975 vs 592 and 1381 mg C m^{-2} yr^{-1}; respectively; Bauerfeind et al., 1997; Dybwad et al., 2022). In Figure 9, short-term sediment trap data from the southern shelf (Norske Trough) are included (M. Reigstad, unpublished data), with fluxes between 7–12 mg C m^{-2} d^{-1}, probably representing pre-bloom conditions (note that vertical flux magnitudes systematically differ between drifting short-term and moored long-term sediment traps; see Box 1). During the 1990s, although fresh material was mainly sinking out in spring (June), long-term sediment trap measurements showed highest vertical flux during the post-bloom period between August and October, driven by fecal pellets and appendicularian houses (Bauerfeind et al., 1997). Nevertheless, the authors state that occasional food fall events such as *M. arctica* patches, as observed frequently underneath the ice during the 1990s (Gutt, 1995), were probably not captured by the moored sediment traps. Isotopic analysis of benthic organisms in the NEW Polynya showed that they incorporated fresh, diatom-derived food (Hobson et

al., 1996), which supports that such food fall events from melting sea ice were not an exception. Due to the decreasing thickness and age of sea ice exported through Fram Strait (Krumpen et al., 2019; Sumata et al., 2022), it is doubtful whether such large ice algal patches are sinking out as frequent as observed during the 1990s.

5.2 Future implications for the Arctic biological carbon pump

5.2.1 A shift in benthic communities?

The effect of changes in environmental and anthropogenic drivers on benthic ecosystems is most pronounced in the Atlantic Artic (Jørgensen et al., 2017). In **Paper I,** we hypothesize that on the NEG shelf, a shift in today's benthic communities has taken place relative to 24 years ago. The observed increase in Nematoda abundance and diversity, and the decrease in Polychaeta abundance in 2017 compared to the 1990s were accompanied by increased bottom water temperatures (Schaffer et al., 2017) and significantly lower sedimentary pigment concentrations (Figure 6 in **Paper I**). This indicates that the quantity and/or the quality of OM reaching the seafloor on the NEG shelf could have possibly changed since the 1990s. While meiofauna mainly feeds on bacterial and reworked food sources, macrofauna relies on fresh organic matter sinking out of the euphotic zone (Górska et al., 2020; Ingels et al., 2010; Oleszczuk et al., 2023, 2021). Under decreasing food input or freshness, macrofauna communities can shift from suspension or deposit feeders to facultative feeding species (Meadows et al., 2019).

Decreased pigment concentrations in the sediments could be a seasonal signal because the quantity and quality of OM sinking to the seafloor is intra-annually highly variable (**Paper II**; Dybwad et al., 2021; Olli et al., 2002; Reigstad et al., 2008). This seasonal signal can be reflected in the amount of pigments in the sediments (Renaud et al., 2008), although it is usually dampened or characterized by a time-lag at the seafloor relative to the water column (Morata et al., 2011; Szczepanek et al., 2021; Ziegler et al., 2023). Nevertheless, the time of sampling during September and October 2017 on the NEG shelf was in the period with highest export of OM within the NEW Polynya (between August–October), at least as observed during the 1990s (Bauerfeind et al., 1997). Therefore, we would expect the highest pigment concentrations during the sampling period in 2017. Moreover, while benthic respiration can vary on a seasonal basis (Link et al., 2011; Renaud et al., 2007), benthic community parameters (abundance and biomass) do less so. The integration of ecosystem processes over longer time scales by benthic community patterns indicates that the quantity and/or the quality of the organic matter supply to the seafloor has changed. This could mean either reduced primary production on the NEG shelf in general, or a higher retention in the water column due to a stronger coupling to the pelagic realm.
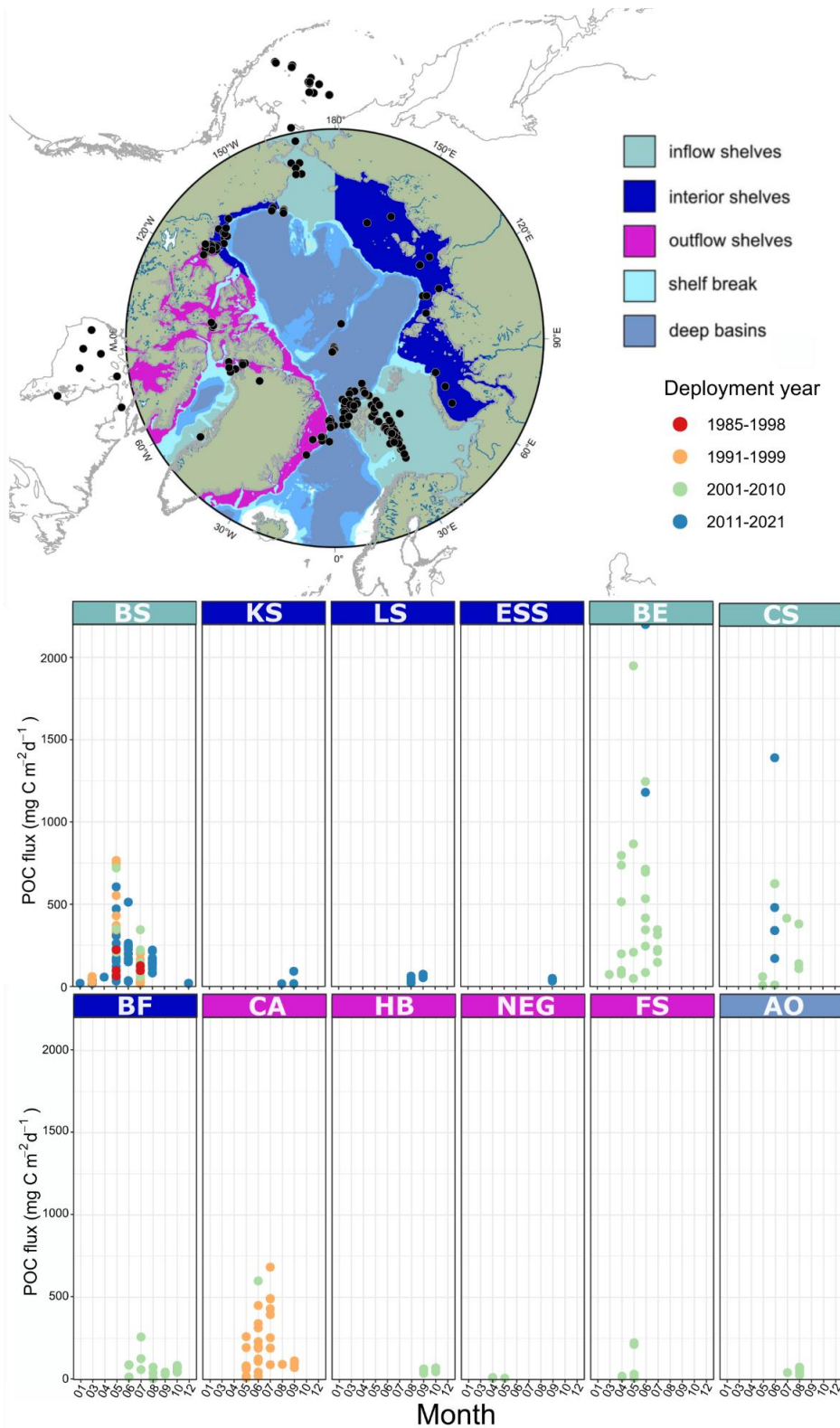
Figure 9: Comparison of POC flux measured with short-term sediment traps across the Arctic Ocean. Depicted are Barents Sea (BS), Kara Sea (KS), Laptev Sea (LS), East Siberian Sea (ESS), Bering Sea (BE), Chukchi Sea (CS), Beaufort Sea (BF), Canadian Arctic Archipelago (CA), Hud-son Bay (HB), Northeast Greenland Shelf (NEG), Fram Strait (FS), deep Arctic Ocean (AO). Figure modified after Wassmann et al., 2020). The used data and their references are presented in Table S1.

Another aspect we noticed in **Paper I** was a homogenization of benthic communities across the NEG shelf: while in the 1990s the benthic communities were highly separated between the Westwind and the Norske Trough (Ambrose and Renaud, 1995; Piepenburg et al., 1997) — a reflection of the presence of the NEW Polynya in the Westwind and the mostly ice-covered Norske Trough — , in 2017 this clear spatial pattern became diluted (Figure 5 in **Paper I**). We rather observed higher macrofauna and meiofauna abundances at the outer shelf, decreasing towards the inner shelf and with proximity to the glacier. This pattern could reflect a possible "borealization" of the shelf. Arctic benthos shows higher functional diversity and trophic levels, while temperate benthos has fewer trophic links (Silberberger et al., 2024). A similar pattern of homogenization of benthic communities in 2006 compared to the 1990s has been observed in an Arctic fjord, associated to stronger inflow of AW and decreased glacial influence (Kędra et al., 2010). The diversity of functional traits may decrease with warming temperatures in the Arctic (Meyer et al., 2015). Besides the increase of AW influence on the NEG shelf (Schaffer et al., 2017), sea ice exported with the East Greenland Current became thinner and more variable in recent years (Sumata et al., 2022), probably resulting in similar upper ocean features between the Norske and the Westwind Trough. This comes along with a disappearance of the NEW Polynya (ISSI, 2008), which was important for the productivity in the region (Pesant et al., 2002; Piepenburg et al., 1997).

If the sinking OM would consist of regenerated particles for a longer period of time in a future scenario with an early summer- and prolonged open-water season, increased primary production across the Arctic Ocean would not necessarily fuel the BCP, as particles would increasingly accumulate and get recycled within the water column. Moreover, it might lead to changes in pelagic-benthic coupling, changing patterns in benthic communities over longer timescales. A shift from a pelagic-benthic coupled system to a pelagic-dominated system has been projected for Arctic shelf systems with earlier ice-melt and increasing open-water periods (Carmack and Wassmann, 2006; Moore and Stabeno, 2015; Wassmann and Reigstad, 2011). Weaker pelagic-benthic coupling in warmer years or with less sea ice has been described for some areas in the Bering Sea (Grebmeier et al., 2006b) and the Chukchi Borderland (Zhulay et al., 2023). According to indigenous knowledge from the Alaskan Inuit Circumpolar Council, benthic prey decreased in walrus stomachs, while pelagic fish species increased, along with a larger proportion of sand (Jørgensen et al., 2017).

5.2.2 Can vertical flux in a summer scenario explain changes in benthic communities?

To understand the mechanisms that could lead to a weakening of pelagic-benthic coupling, it is worth contrasting vertical flux patterns during spring and summer, as we did for **Paper II** in the northwestern Barents Sea. Late- or post-bloom scenarios are generally characterized by a high concentration of particles in the water column but also higher retention and lower sinking rates of particles compared to peak bloom scenarios (Wassmann, 1998; **Paper II**). This suggests a lower export efficiency during summer. Moreover, in **Paper II** we found that the composition and amount of vertical flux was more homogenous across the transect during summer (August), in contrast to the high spatial heterogeneity of vertical flux during spring (May). The amount and composition of vertical flux reflects pelagic ecosystem processes, and the higher degradation of sinking OM demonstrates higher pelagic activity

and increasing dominance of heterotrophs, as we showed in Kohlbach et al. (2023). Along the same transect, primary and bacterial production become increasingly uniform in magnitude with the retreat of sea ice (Amargant-Arumí et al., 2024). These findings suggest that the quality of sinking OM will change in the future, with probable implications for benthic communities.

Dybwad et al. (2022) compared the annual cycle of vertical flux of a seasonally ice-covered and a permanently ice-free location north and east of Svalbard. As expected, the composition of vertical flux between the two locations differed highly from each other, with more diatom-derived flux in the seasonally ice-covered location, and more fecal pellets and higher C:N ratios at the open-water location. However, annual vertical flux was higher at the permanently open-water station. At locations under low-ice conditions or earlier ice break-up, OM at the seafloor can be more regenerated and bacterially reworked while more fresh microalgal OM can be found at the seafloor at locations where sea ice retreats later in the year; however, the feeding plasticity of benthic communities across these locations can be preserved (Kędra et al., 2021; Ziegler et al., 2023). In the Barents Sea, benthic biomass is higher in the southern, AW-influenced and sea-ice-free region, as well as at the Polar Front. Biomasses are comparatively lower in the seasonally ice-covered northern Barents Sea (Cochrane et al., 2009). In the NOW Polynya, the duration of phytoplankton blooms increased due to an earlier bloom onset, but the bloom intensity decreased (Marchese et al., 2017). Benthic communities, however, seem to receive a higher food input because of the longer duration and/or a mismatch with pelagic grazers due to the earlier bloom onset (Mäkelä et al., 2017a; Olivier et al., 2020). These relationships between enhanced vertical flux and/or benthic biomass coupled to open water might seem contrary to Fadeev et al. (2021)'s observations, who found a negative relationship between the distance to sea-ice cover and POC flux at 200m in the Fram Strait. However, it is important to note that the authors found this relationship only during early spring (March–May), but not during summer (June–August), where also peaks of vertical flux were observed. In the NEW Polynya, no relationship (positive or negative) between primary production and open water was found because the ice cover in the area is extremely variable (Smith Jr., 1995).

5.2.3 Consequences for pelagic-benthic coupling

The examples demonstrate that the future of the BCP, and with that pelagic-benthic coupling, will depend on a range of interconnected factors and therefore differ from region to region (see Figure 10 for a summary). It is also important to distinguish between possible changes in particle composition and in the overall magnitude of sinking particles. While the contribution of ice algae will probably decrease with decreasing sea-ice concentration and age, the effect of these changes on benthos remains unclear. Although Arctic ecosystems seem to depend to a large extent on ice algal material (Koch et al., 2023), field experiments have shown that benthic uptake was not different with addition of ice or pelagic diatoms (Mäkelä et al., 2017b). This might indicate that from a benthic perspective, as long as fresh, diatom-derived OM is exported, it does not matter whether it is sea-ice- or pelagic-originating.

A factor that will likely determine the quality and the quantity of sinking particles is vertical mixing, as it transports nutrients up and particles down the water column, escaping pelagic grazing. Temperate regions are characterized by strong winds, and the mixed-layer pump transports small particles efficiently to depth in these regions (Dall'Olmo and Mork, 2014; Giering et al., 2016), where it can account for 23% of exported POC, and in some cases more than 100% (Dall'Olmo et al., 2016). If some

Arctic regions become more temperate in character, the "mixed-layer pump" might play an important role for carbon export. With less sea ice and more AW influence, the northern Barents Sea is getting increasingly mixed (Lind et al., 2018) and the storm frequency is increasing (Rainville and Woodgate, 2009). A deeper mixed layer can even result in pelagic diatom blooms in open water that are rapidly transported to the seafloor (von Appen et al., 2021; **Paper II**). Vertical mixing will be more important during summer when vertical flux is strongly regulated by heterotrophic processes, and nutrients in the upper ocean are limited. However, while with decreasing sea-ice cover, mixing could increase in the shelf region of the Barents Sea, autumn mixing in the northern Barents Sea above 80ºN (around Station P6) could occur too late into the dark season before significant autumn blooms could be generated (Renner et al., 2023). Several areas in the Arctic may also become increasingly stratified, which will reduce primary production due to nutrient limitation at the surface, and keep particles trapped above the upper pycnocline. Thermal stratification, for example, may occur in the southern Barents Sea (Hordoir et al., 2022), ultimately reducing pelagic-benthic coupling in this area (Wassmann and Reigstad, 2011). The NEG shelf is already becoming increasingly stratified due to freshening through sea-ice melt and increased coastal runoff (Sejr et al., 2017). This might be, together with the disappearance of the NEW Polynya, another reason for the weakening of pelagic-benthic coupling we described in **Paper I**.
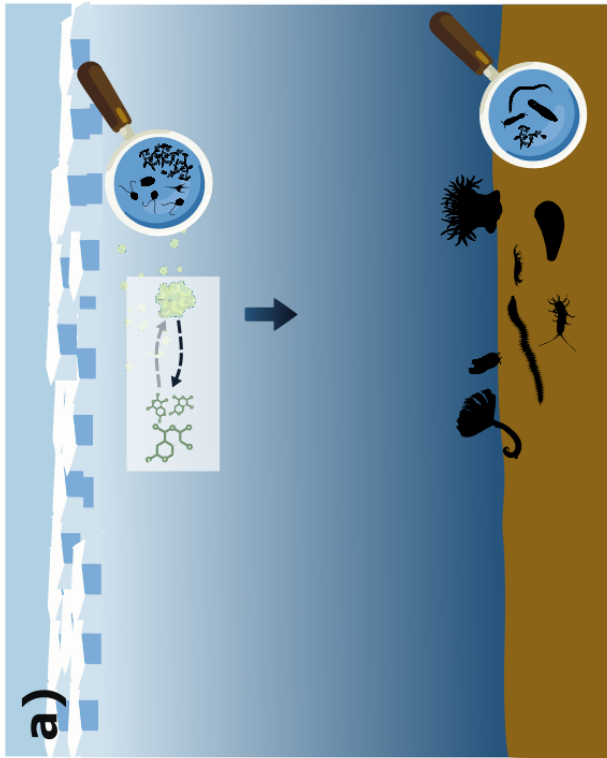
Factors that increase the particle abundance in the water column (fecal pellet concentrations, aggregation, ballasting through riverine minerals) generally increase towards summer. The example of the Beaufort Sea demonstrates how their importance might increase under prolonged open-water and "summer-like" conditions. Efficient carbon export of small particles can occur under summer, post-bloom conditions through the repackaging of OM into fecal pellets (Wexels Riser et al., 2007; Wiedmann, 2015), or through aggregation of smaller particles and detritus (O'Daly et al., 2020). Ultimately, water depth will be an important factor, because pelagic remineralization of smaller particles will increase, and with a lower water depth OM will be susceptible to degradation for a shorter time in the water column before it arrives at the seafloor.

## 5.3 Vertical flux during the polar night

Little is known about particle dynamics and vertical flux during the Arctic winter. The polar night was, for a long time, considered a quiet period in the Arctic Ocean. Observations since the last decade show high biological activity across all ecosystem levels during winter (Berge et al., 2015b, 2015a; Darnis et al., 2012). Arctic winter microbial communities differ substantially from spring and summer communities and are active (Marquardt et al., 2016; Vonnahme et al., 2022; Wietz et al., 2021) and thus should influence the remineralization of particles during this time of the year even if their concentration is low. Deployments of short-term sediment traps during winter in the SIZ are challenging, and few studies exist (Dybwad et al., 2021; Olli et al., 2002).

In the absence of light, heterotrophic processes dominate in the pelagic zone. Lowest levels of suspended POC are present during winter (Marquardt et al., 2022a, 2022b). This results in a very efficient retention system, and in the Barents Sea the lowest vertical flux is measured during the winter period (Dybwad et al., 2021; Olli et al., 2002 **Paper II**). In line with the observations of a highly heterotrophic system and high retention, in Ramfjorden we documented a dissolution of particles in December and February during our experiment (**Paper III**). This contrasted with the observations in April, June and September, when aggregation processes dominated. This finding is also in contrast to

studies in temperate regions, where particle formation from the dissolved pool also occurred during winter (Riley, 1963; Sheldon et al., 1967), where light is not limited. The decrease in particulates occurred together with an increase in lability of dissolved organic matter, as shown by the increase of H/C ratios and decrease of O/C ratios (**Paper III**).

Key

copepods	bacteria
fecal pellets	pelagic heterotrophs
suspension feeding macrofauna	diatoms
facultative macrofauna	autotrophs/ mixotrophs
Nematoda	DOM
vertical flux	POM
stratification mixing	minerals

a) **Winter scenario:** During winter, vertical flux is lowest in the year and dominated by small heterotrophic ciliates and flagellates. Processes in the DOM-POM continuum are dominated by particle dissolution, and little organic matter reaches the benthos.
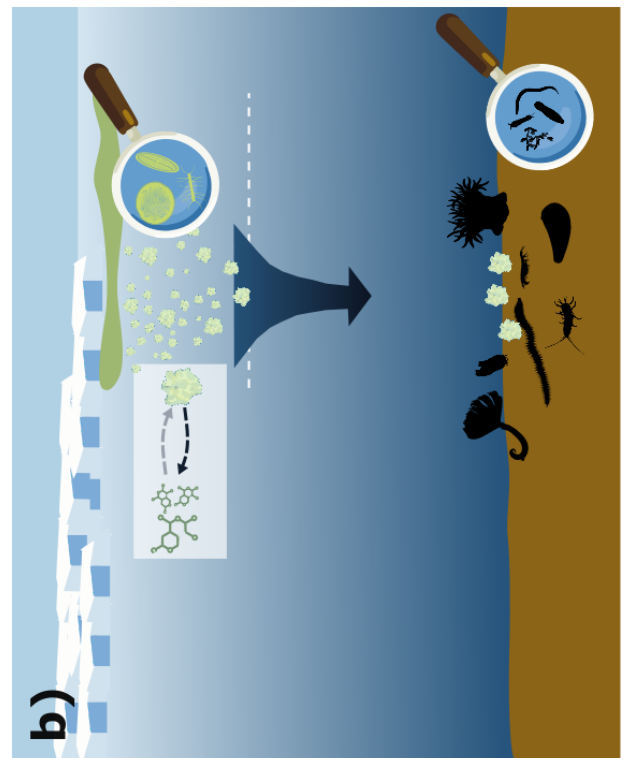
b) **Spring scenario:** Spring blooms at the marginal ice zone are characterized by high vertical flux dominated by diatoms and often a grazer mismatch, leading to strong pulses of fresh organic matter. Sea-ice melt derived stratification can retain particles above the upper pycnocline even under high productivity; however, a substantial amount of fresh, diatom-rich organic matter can reach the seafloor, sustaining the benthic community. Processes in the DOM-POM continuum are dominated by aggregation, but DOM contributes little to the particle pool.
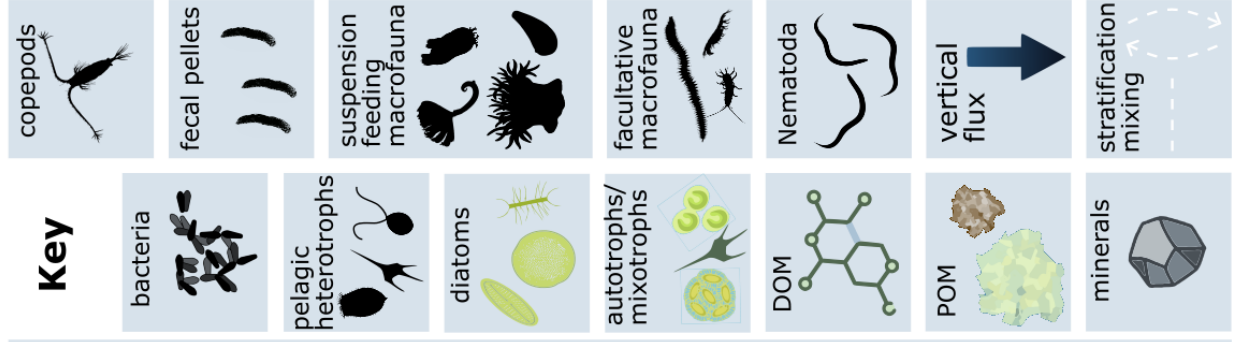
Summer scenario I (increased pelagic-benthic coupling): The concentration of suspended particles in the pelagic is high, but regenerative processes are dominant. The contribution of DOM to the POM pool increases. Phytoplankton communities are dominated by small cells and heterotrophs.

A sufficient amount can be transported to the seafloor if mixing occurs, organic matter transport is facilitated by fecal pellets, ballasting and aggregation, and the water depth is shallow. The material arriving at the seafloor may be more degraded, but high feeding plasticity in benthic communities may account for a change in food composition. Accordingly, a longer productive season can uphold pelagic-benthic coupling, or even tighten it.
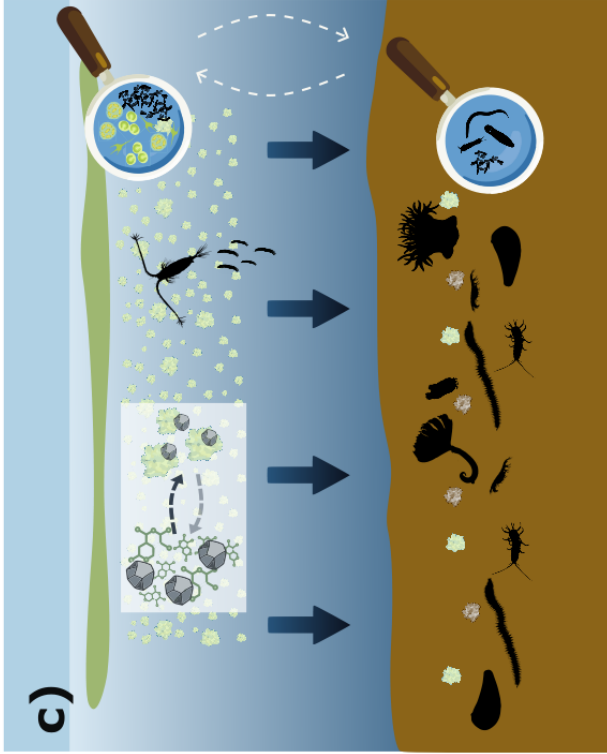
Summer scenario II (decreased pelagic-benthic coupling): Organic matter is retained in the upper water column through strong stratification, grazing and microbial degradation, including the break-down of fecal pellets. No ballasting occurs to mediate the downward transport of aggregates. This may induce changes in benthic communities towards a decrease of benthic macrofauna abundance (especially suspension feeders), while the importance of small, facultative metazoans (especially nematodes) and bacteria in benthic communities may increase.
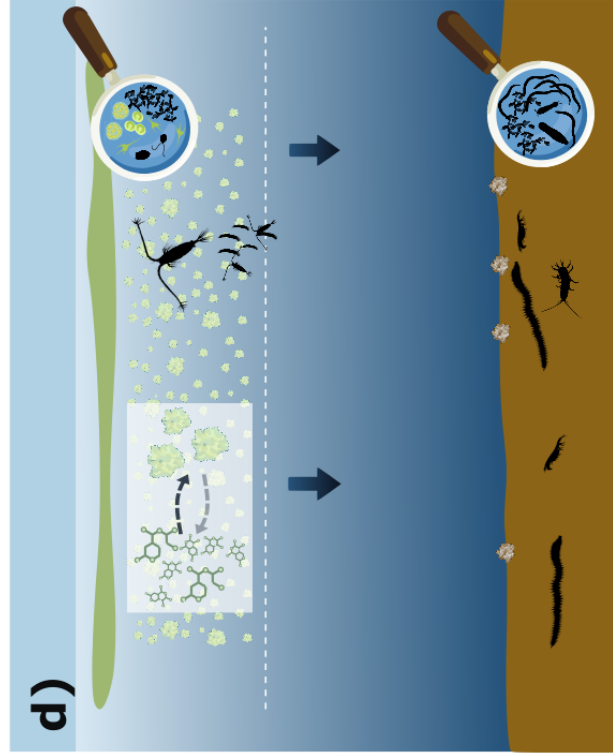

Figure 10: Conceptual diagram summarizing the dis-cussion. Winter-spring seasonality of the bio-logical carbon pump in the marginal ice zone (a, b), and hypothesized changes for a future "prolonged summer season" summarizing the processes that lead to a tightening (c) or a weakening (d) of pelagic-benthic coupling.

6 Conclusions and outlook

Benthic communities on Arctic shelves and in the deep sea depend on the organic matter exported from primary production in the upper ocean (**Paper I**). For a given level of primary production, the amount and composition of the OM exported to the seafloor is determined by a range of mechanisms in the pelagic zone. These mechanisms include (1) the degree of regulation through grazing and microbial degradation; (2) factors that increase particle concentrations and the potential for particles to sink, such as aggregation, fecal pellet production and ballasting; (3) short-circuiting of vertical flux through mixing events. In the different Arctic shelf regions, these mechanisms contribute at different scales to the regulation of vertical flux, which suggests that changes in pelagic-benthic coupling will differ on regional levels. Pelagic-benthic coupling is generally "tight" on inflow shelves and in productive polynyas, as primary production is high, bypassing grazing pressure and sinking out in a large fraction (Cochrane et al., 2009; Grebmeier et al., 2006a; Mäkelä et al., 2017a; Michel et al., 2002; O'Daly et al., 2020; Olli et al., 2002). On interior shelves, ballasting by riverine minerals and aggregation play an important role for vertical flux (Drits et al., 2017; Forest et al., 2013). In the Northeast Water Polynya on the Northeast Greenland Shelf (outflow shelf), ice-algal patches melting from the exported sea ice through Fram Strait were probably important for a tight connection between the pelagic and the benthic realms, as well as sinking appendicularian houses during the summer period (Ambrose and Renaud, 1995; Bauerfeind et al., 1997; Gutt, 1995; Hobson et al., 1996).

In the northwestern Barents Sea, we also identified strong seasonal gradients in vertical flux patterns. Under summer conditions, regenerative processes in the pelagic zone are more dominant, which is reflected in a vertical flux of less fresh, more flagellate-dominated material, in contrast to spring, when vertical flux is dominated by strong pulses of fresh, diatom-derived OM exported to the seafloor (**Paper II**). Summer is also characterized by a reduced vertical flux efficiency because of higher particle concentrations in the water, but no increase in vertical flux relative to May. As we have shown in **Paper III**, the contribution of DOM to the particulate pool through aggregation increases towards the summer period. The seasonality of vertical flux is determined by sea ice and AW, especially during May: May was characterized by a wide span of pelagic conditions from winter to peak bloom scenarios across the study locations, while in August, pelagic conditions were more similar across the transect, mostly representing post-bloom conditions. This was reflected in vertical flux patterns.

With a prolonged summer period, an increase in primary production across the Arctic Ocean has been predicted. However, increases in primary production will not necessarily result in increased carbon export from the upper ocean (Wassmann et al., 2003). The bulk of carbon may be retained in the euphotic zone due to intensive biological remineralization or stratification. This stresses the importance of studying OM turnover mechanisms (**Paper III**) and regeneration processes of vertical flux in the upper pelagic zone **(Paper II)**. Benthic communities, on the other hand, integrate processes over longer time scales (**Paper I**); and as such they serve as powerful ecosystem indicators for changes in oceanic biogeochemical cycles.

The results of this thesis suggest that the composition of vertical flux will likely reflect summer conditions for a longer period under earlier sea-ice melt and later freeze-up. We hypothesize a weakening of pelagic-benthic coupling since the 1990s on the Northeast Greenland (NEG) shelf and explain changes in the benthic community with prolonged summer conditions, increased stratification and/or the disappearance of the NEW Polynya. A decrease in primary production and/or increase in OM

retention in the pelagic zone may lead to decreased or more regenerated OM reaching the seafloor, and may favor smaller-sized, facultative benthos (**Paper I**; Meadows et al., 2019).

Comparing pelagic-benthic coupling and regulatory mechanisms of vertical flux across different regions suggests that Arctic shelves will most likely respond in different ways to climate change-induced effects on the biological carbon pump (BCP). Zooplankton and bacteria are strong vertical flux regulators, and their influence might increase with the increased influence of Pacific and Atlantic water masses. However, zooplankton can also package slowly sinking particles into fast-sinking fecal pellets. With an enhanced influence of boreal water masses, coastal runoff and increased primary production, the contribution of DOM to the particulate pool through aggregation will likely increase further, as will the input of riverine ballasting minerals. In a prolonged summer scenario, the mixing regime will be highly important as a short-circuiting mechanism and for breaking possible thermal stratification. Ultimately, while an overall decrease in food availability at the seafloor will likely change the structure of benthic communities, it is unclear how a change in food composition will affect benthic communities and their species composition, as laboratory and field studies show contrasting results (Braeckman et al., 2018; Mäkelä et al., 2017b; Morata et al., 2011; Sun et al., 2009).

Finally, seasonal processes in the DOM-POM continuum should receive more attention, because the two entities are in constant dynamic change. Dynamics in the DOM-POM continuum might change in a future fresher, warmer Arctic, and we lack the understanding about the implications for the BCP. It should be noted that this thesis presented an overview of the BCP in the Arctic with the focus on vertical settling mechanisms of organic particles. Other mechanisms that can contribute significantly to the BCP such as horizontal advection, vertical migration of zooplankton and other processes were not discussed. When addressing the fate of the BCP in a future Arctic, it is important to take all these processes into account.

7 References

Aagaard, K., 1989. A synthesis of the Arctic Ocean circulation. Rapp. Procès-Verbaux La Réun. (1903–1991) 188. https://doi.org/10.17895/ices.pub.19279133

Amargant-Arumí, M., Müller, O., Bodur, Y.V., Ntinou, I.-V., Vonnahme, T., Assmy, P., Kohlbach, D., Chierici, M., Jones, E., Olsen, L.M., Tsagaraki, T.M., Reigstad, M., Bratbak, G., Gradinger, R., 2024. Interannual differences in sea ice regime in the north-western Barents Sea cause major changes in summer pelagic production and export mechanisms. Prog. Oceanogr. 103178. https://doi.org/10.1016/j.pocean.2023.103178

Ambrose, W.G., Renaud, P.E., 1995. Benthic response to water column productivity patterns: Evidence for benthic-pelagic coupling in the Northeast Water Polynya. J. Geophys. Res. Oceans 100. https://doi.org/10.1029/94JC01982

Amiel, D., Cochran, J.K., Hirschberg, D.J., 2002. 234Th/238U disequilibrium as an indicator of the seasonal export flux of particulate organic carbon in the North Water. Deep Sea Res. Part II Top. Stud. Oceanogr., The International North Water Polynya Study 49. https://doi.org/10.1016/S0967-0645(02)00185-6

Anderson, L.G., Amon, R.M.W., 2015. DOM in the Arctic Ocean, in: Hansell, D.A., Carlson, C.A. (Eds.), Biogeochemistry of marine dissolved organic matter. Elsevier, pp. 609–633. https://doi.org/10.1016/B978-0-12-405940-5.00014-5

Anderson, L.G., Olsson, K., Chierici, M., 1998. A carbon budget for the Arctic Ocean. Glob. Biogeochem. Cycles 12. https://doi.org/10.1029/98GB01372

Andreassen, I., Wassmann, P., 1998. Vertical flux of phytoplankton and particulate biogenic matter in the marginal ice zone of the Barents Sea in May 1993. Mar. Ecol. Prog. Ser. 170. https://doi.org/10.3354/meps170001

Ardyna, M., Arrigo, K.R., 2020. Phytoplankton dynamics in a changing Arctic Ocean. Nat. Clim. Change 10. https://doi.org/10.1038/s41558-020-0905-y

Ardyna, M., Babin, M., Gosselin, M., Devred, E., Rainville, L., Tremblay, J.-É., 2014. Recent Arctic Ocean sea ice loss triggers novel fall phytoplankton blooms. Geophys. Res. Lett. 41. https://doi.org/10.1002/2014GL061047

Arndt, J.E., Jokat, W., Dorschel, B., Myklebust, R., Dowdeswell, J.A., Evans, J., 2015. A new bathymetry of the Northeast Greenland continental shelf: Constraints on glacial and other processes. Geochem. Geophys. Geosystems 16. https://doi.org/10.1002/2015GC005931

Arrigo, K.R., van Dijken, G.L., 2015. Continued increases in Arctic Ocean primary production. Prog. Oceanogr. 136. https://doi.org/10.1016/j.pocean.2015.05.002

Årthun, M., Onarheim, I.H., Dörr, J., Eldevik, T., 2021. The seasonal and regional transition to an ice-free Arctic. Geophys. Res. Lett. 48. https://doi.org/10.1029/2020GL090825

Ashjian, C.J., Smith, S.L., Lane, P.V.Z., 1995. The Northeast Water Polynya during summer 1992: Distribution and aspects of secondary production of copepods. J. Geophys. Res. Oceans 100. https://doi.org/10.1029/94JC02199

Baker, C.A., Estapa, M.L., Iversen, M., Lampitt, R., Buesseler, K., 2020. Are all sediment traps created equal? An intercomparison study of carbon export methodologies at the PAP-SO site. Prog. Oceanogr. 184. https://doi.org/10.1016/j.pocean.2020.102317

Barber, D.G., Hanesiak, J.M., 2004. Meteorological forcing of sea ice concentrations in the southern Beaufort Sea over the period 1979 to 2000. J. Geophys. Res. Oceans 109. https://doi.org/10.1029/2003JC002027

Bartsch, A., Pointner, G., Nitze, I., Efimova, A., Jakober, D., Ley, S., Högström, E., Grosse, G., Schweitzer, P., 2021. Expanding infrastructure and growing anthropogenic impacts along Arctic coasts. Environ. Res. Lett. 16. https://doi.org/10.1088/1748-9326/ac3176

Bauerfeind, E., Garrity, C., Krumbholz, M., Ramseier, R.O., Voβ, M., 1997. Seasonal variability of sediment trap collections in the Northeast Water Polynya. Part 2. Biochemical and microscopic composition of sedimenting matter. J. Mar. Syst. 10. https://doi.org/10.1016/S0924-7963(96)00069-3

Berge, J., Daase, M., Renaud, P.E., Ambrose, W.G., Darnis, G., Last, K.S., Leu, E., Cohen, J.H., Johnsen, G., Moline, M.A., Cottier, F., Varpe, Ø., Shunatova, N., Bałazy, P., Morata, N., Massabuau, J.-C., Falk-Petersen, S., Kosobokova, K., Hoppe, C.J.M., Węsławski, J.M., Kukliński, P., Legeżyńska, J., Nikishina, D., Cusa, M., Kędra, M., Włodarska-Kowalczuk, M., Vogedes, D., Camus, L., Tran, D., Michaud, E., Gabrielsen, T.M., Granovitch, A., Gonchar, A., Krapp, R., Callesen, T.A., 2015a. Unexpected levels of biological activity during the polar night offer new perspectives on a warming Arctic. Curr. Biol. 25. https://doi.org/10.1016/j.cub.2015.08.024

Berge, J., Renaud, P.E., Darnis, G., Cottier, F., Last, K., Gabrielsen, T.M., Johnsen, G., Seuthe, L., Weslawski, J.M., Leu, E., Moline, M., Nahrgang, J., Søreide, J.E., Varpe, Ø., Lønne, O.J., Daase, M., Falk-Petersen, S., 2015b. In the dark: A review of ecosystem processes during the Arctic polar night. Prog. Oceanogr., Overarching perspectives of contemporary and future ecosystems in the Arctic Ocean 139. https://doi.org/10.1016/j.pocean.2015.08.005

Beszczynska-Möller, A., Fahrbach, E., Schauer, U., Hansen, E., 2012. Variability in Atlantic water temperature and transport at the entrance to the Arctic Ocean, 1997–2010. ICES J. Mar. Sci. 69. https://doi.org/10.1093/icesjms/fss056

Blanchard, A.L., Parris, C.L., Knowlton, A.L., Wade, N.R., 2013. Benthic ecology of the northeastern Chukchi Sea. Part I. Environmental characteristics and macrofaunal community structure, 2008–2010. Cont. Shelf Res., Seasonal and interannual dynamics of the northeastern Chukchi Sea Ecosystem 67. https://doi.org/10.1016/j.csr.2013.04.021

Blomqvist, S., 1981. Sediment trapping—A subaquatic in situ experiment. Limnol. Oceanogr. 26. https://doi.org/10.4319/lo.1981.26.3.0585

Bluhm, B.A., Kosobokova, K.N., Carmack, E.C., 2015. A tale of two basins: An integrated physical and biological perspective of the deep Arctic Ocean. Prog. Oceanogr., Overarching perspectives of contemporary and future ecosystems in the Arctic Ocean 139. https://doi.org/10.1016/j.pocean.2015.07.011

Bodur, Y.V., Felden, J., Braeckman, U., 2023. Single prokaryotic cell abundances of the Northeast Greenland (NEG) shelf sediments from POLARSTERN cruise PS109.

Boetius, A., Albrecht, S., Bakker, K., Bienhold, C., Felden, J., Fernández-Méndez, M., Hendricks, S., Katlein, C., Lalande, C., Krumpen, T., Nicolaus, M., Peeken, I., Rabe, B., Rogacheva, A., Rybakova, E., Somavilla, R., Wenzhöfer, F., Party, R.P.A.-3-S.S., 2013. Export of algal biomass from the melting arctic sea ice. Science 339. https://doi.org/10.1126/science.1231346

Bourke, R.H., Newton, J.L., Paquette, R.G., Tunnicliffe, M.D., 1987. Circulation and water masses of the East Greenland shelf. J. Geophys. Res. Oceans 92. https://doi.org/10.1029/JC092iC07p06729

Boyd, P.W., Claustre, H., Levy, M., Siegel, D.A., Weber, T., 2019. Multi-faceted particle pumps drive carbon sequestration in the ocean. Nature 568. https://doi.org/10.1038/s41586-019-1098-2

Braeckman, U., 2023a. Grain size analysis of the Northeast Greenland (NEG) shelf sediments from POLARSTERN cruise PS109. PANGAEA. https://doi.pangaea.de/10.1594/PANGAEA.959546

Braeckman, U., 2023b. Porosity of the Northeast Greenland (NEG) shelf sediments from POLARSTERN cruise PS109. PANGAEA. https://doi.pangaea.de/10.1594/PANGAEA.959550

Braeckman, U., 2023c. Sedimentary pigments on the Northeast Greenland (NEG) Shelf from Polarstern cruise PS109. PANGAEA. https://doi.pangaea.de/10.1594/PANGAEA.959548

Braeckman, U., 2023d. Total organic nitrogen (TON) and total organic carbon (TOC) concentration of the Northeast Greenland (NEG) shelf sediments from POLARSTERN cruise PS109. PANGAEA. https://doi.pangaea.de/10.1594/PANGAEA.959554

Braeckman, U., Felden, J., 2023. Porewater nutrients of the Northeast Greenland (NEG) shelf sediments from POLARSTERN cruise PS109. PANGAEA. https://doi.pangaea.de/10.1594/PANGAEA.959549

Braeckman, U., Janssen, F., Lavik, G., Elvert, M., Marchant, H., Buckner, C., Bienhold, C., Wenzhöfer, F., 2018. Carbon and nitrogen turnover in the Arctic deep sea: in situ benthic community response to diatom and coccolithophorid phytodetritus. Biogeosciences Discuss. 15. https://doi.org/10.5194/bg-2018-264

Braeckman, U., Wenzhöfer, F., 2023. Ex situ total oxygen uptake of the Northeast Greenland (NEG) shelf sediments from POLARSTERN cruise PS109. PANGAEA. https://doi.pangaea.de/10.1594/PANGAEA.959553

Brandt, A., 1995. Peracarid fauna (Crustacea, Malacostraca) of the Northeast Water Polynya off Greenland: documenting close benthic-pelagic coupling in the Westwind Trough. Mar. Ecol. Prog. Ser. 121. https://doi.org/10.3354/meps121039

Brown, K.A., Holding, J.M., Carmack, E.C., 2020. Understanding regional and seasonal variability is key to gaining a pan-Arctic perspective on Arctic Ocean freshening. Front. Mar. Sci. 7. https://doi.org/10.3389/fmars.2020.00606

Buesseler, K., N. Antia, A., Chen, M., Fowler, S., Gardner, W., Gustafsson, O., Harada, K., Michaels, A., van der Loeff, M.R., Sarin, M.M., K. Steinberg, D., Trull, T., 2007. An assessment of the use of sediment traps for estimating upper ocean particle fluxes. J. Mar. Res. 65. https://doi.org/10.1357/002224007781567621

Buesseler, K.O., Steinberg, D.K., Michaels, A.F., Johnson, R.J., Andrews, J.E., Valdes, J.R., Price, J.F., 2000. A comparison of the quantity and composition of material caught in a neutrally buoyant versus surface-tethered sediment trap. Deep Sea Res. Part Oceanogr. Res. Pap. 47. https://doi.org/10.1016/S0967-0637(99)00056-4

Burd, A.B., Hansell, D.A., Steinberg, D.K., Anderson, T.R., Arístegui, J., Baltar, F., Beaupré, S.R., Buesseler, K.O., DeHairs, F., Jackson, G.A., Kadko, D.C., Koppelmann, R., Lampitt, R.S., Nagata, T., Reinthaler, T., Robinson, C., Robison, B.H., Tamburini, C., Tanaka, T., 2010. Assessing the apparent imbalance between geochemical and biochemical indicators of meso- and bathypelagic biological activity: What the @$#! is wrong with present calculations of carbon budgets? Deep Sea Res. Part II Top. Stud. Oceanogr., Ecological and Biogeochemical Interactions in the Dark Ocean 57. https://doi.org/10.1016/j.dsr2.2010.02.022

Burd, A.B., Jackson, G.A., 2009. Particle Aggregation. Annu. Rev. Mar. Sci. 1. https://doi.org/10.1146/annurev.marine.010908.163904

Cai, R., Jiao, N., 2023. Recalcitrant dissolved organic matter and its major production and removal processes in the ocean. Deep Sea Res. Part I Oceanogr. 191. https://doi.org/10.1016/j.dsr.2022.103922

Carmack, E., Chapman, D.C., 2003. Wind-driven shelf/basin exchange on an Arctic shelf: The joint roles of ice cover extent and shelf-break bathymetry. Geophys. Res. Lett. 30. https://doi.org/10.1029/2003GL017526

Carmack, E., Wassmann, P., 2006. Food webs and physical–biological coupling on pan-Arctic shelves: Unifying concepts and comprehensive perspectives. Prog. Oceanogr., Structure and function of contemporary food webs on Arctic shelves: a pan-Arctic comparison 71. https://doi.org/10.1016/j.pocean.2006.10.004

Carmack, E., Winsor, P., Williams, W., 2015. The contiguous panarctic Riverine Coastal Domain: A unifying concept. Prog. Oceanogr., Overarching perspectives of contemporary and future ecosystems in the Arctic Ocean 139. https://doi.org/10.1016/j.pocean.2015.07.014

Caron, G., Michel, C., Gosselin, M., 2004. Seasonal contributions of phytoplankton and fecal pellets to the organic carbon sinking flux in the North Water (northern Baffin Bay). Mar. Ecol. Prog. Ser. 283. https://doi.org/10.3354/meps283001

Carr, J.R., Stokes, C.R., Vieli, A., 2017. Threefold increase in marine-terminating outlet glacier retreat rates across the Atlantic Arctic: 1992–2010. Ann. Glaciol. 58. https://doi.org/10.1017/aog.2017.3

Castro de la Guardia, L., Hernández Fariñas, T., Marchese, C., Amargant-Arumí, M., Myers, P.G., Bélanger, S., Assmy, P., Gradinger, R., Duarte, P., 2023. Assessing net primary production in the northwestern Barents Sea using in situ, remote sensing and modelling approaches. Prog. Oceanogr. 219. https://doi.org/10.1016/j.pocean.2023.103160

Chin, W.-C., Orellana, M.V., Verdugo, P., 1998. Spontaneous assembly of marine dissolved organic matter into polymer gels. Nature 391. https://doi.org/10.1038/35345

Christensen, T.R., Rysgaard, S., Bendtsen, J., Else, B., Glud, R.N., van Huissteden, K., Parmentier, F.-J.W., Sachs, T., Vonk, J.E., 2017. Arctic Carbon Cycling, in: Snow, water, ice and permafrost in the Arctic. Arctic Monitoring Assessment Program (AMAP), Oslo, Norway, pp. 203–218.

Clarke, K.R., Somerfield, P.J., Gorley, R.N., 2008. Testing of null hypotheses in exploratory community analyses: similarity profiles and biota-environment linkage. J. Exp. Mar. Biol. Ecol., Marine ecology: A tribute to the life and work of John S. Gray 366. https://doi.org/10.1016/j.jembe.2008.07.009

CMEMS, 2024. Ocean Carbon Uptake [WWW Document]. Copernic. Mar. Serv. URL https://marine.copernicus.eu/ocean-climate-portal/ocean-carbon-uptake (accessed 2.7.24).

Cochrane, S.K.J., Denisenko, S.G., Renaud, P.E., Emblow, C.S., Ambrose Jr, W.G., Ellingsen, I.H., Skarḥhamar, J., 2009. Benthic macrofauna and productivity regimes in the Barents Sea—ecological implications in a changing Arctic. J. Sea Res. 61.

Comiso, J.C., Hall, D.K., 2014. Climate trends in the Arctic as observed from space. Wiley Interdiscip. Rev. Clim. Change 5. https://doi.org/10.1002/wcc.277

Cooper, L.W., Grebmeier, J.M., 2018. Deposition patterns on the Chukchi shelf using radionuclide inventories in relation to surface sediment characteristics. Deep Sea Res. Part II Top. Stud. Oceanogr. 152. https://doi.org/10.1016/j.dsr2.2018.01.009

Coppola, L., Roy-Barman, M., Wassmann, P., Mulsow, S., Jeandel, C., 2002. Calibration of sediment traps and particulate organic carbon export using 234Th in the Barents Sea. Mar. Chem. 80. https://doi.org/10.1016/S0304-4203(02)00071-3

Cushing, D.H., 1975. Marine Ecology and Fisheries. Cambridge University Press.

Daase, M., Berge, J., Søreide, J.E., Falk-Petersen, S., 2021. Ecology of Arctic Pelagic Communities, in: Thomas, D.N. (Ed.), Arctic Ecology. Wiley, pp. 219–259. https://doi.org/10.1002/9781118846582.ch9

Dall'Olmo, G., Dingle, J., Polimene, L., Brewin, R.J.W., Claustre, H., 2016. Substantial energy input to the mesopelagic ecosystem from the seasonal mixed-layer pump. Nat. Geosci. 9. https://doi.org/10.1038/ngeo2818

Dall'Olmo, G., Mork, K.A., 2014. Carbon export by small particles in the Norwegian Sea. Geophys. Res. Lett. 41. https://doi.org/10.1002/2014GL059244

Dalsgaard, T., Nielsen, L.P., Brotas, V., Viaroli, P., Underwood, G., Nedwell, D., Sundbäck, K., Rysgaard, S., Miles, A., Bartoli, M., Dong, L., Thornton, D., Ottosen, L., Castaldelli, G., Risgaard-Petersen, N., 2000. Protocol handbook for NICE-Nitrogen cycling in estuaries: A project under the EU research programme, Marine Science and Technology (MAST III). National Environmental Research Institute, Denmark.

Darnis, G., Robert, D., Pomerleau, C., Link, H., Archambault, P., Nelson, R.J., Geoffroy, M., Tremblay, J.-É., Lovejoy, C., Ferguson, S.H., Hunt, B.P.V., Fortier, L., 2012. Current state and trends in Canadian Arctic marine ecosystems: II. Heterotrophic food web, pelagic-benthic coupling, and biodiversity. Clim. Change 115. https://doi.org/10.1007/s10584-012-0483-8

De La Rocha, C.L., Nowald, N., Passow, U., 2008. Interactions between diatom aggregates, minerals, particulate organic carbon, and dissolved organic matter: Further implications for the ballast hypothesis. Glob. Biogeochem. Cycles 22. https://doi.org/10.1029/2007GB003156

de Steur, L., Hansen, E., Mauritzen, C., Beszczynska-Möller, A., Fahrbach, E., 2014. Impact of recirculation on the East Greenland Current in Fram Strait: Results from moored current meter measurements between 1997 and 2009. Deep Sea Res. Part Oceanogr. Res. Pap. 92. https://doi.org/10.1016/j.dsr.2014.05.018

Degerlund, M., Eilertsen, H.C., 2010. Main species characteristics of phytoplankton spring blooms in NE Atlantic and Arctic waters (68–80° N). Estuaries Coasts 33. https://doi.org/10.1007/s12237-009-9167-7

Denisenko, S., Denisenko, N., Lehtonen, K., Andersin, A., Laine, A., 2003. Macrozoobenthos of the Pechora Sea (SE Barents Sea): community structure and spatial distribution in relation to environmental conditions. Mar. Ecol. Prog. Ser. 258. https://doi.org/10.3354/meps258109

Dittmar, T., Koch, B., Hertkorn, N., Kattner, G., 2008. A simple and efficient method for the solid-phase extraction of dissolved organic matter (SPE-DOM) from seawater. Limnol. Oceanogr. Methods 6. https://doi.org/10.4319/lom.2008.6.230

Drits, A.V., Kravchishina, M.D., Pasternak, A.F., Novigatsky, A.N., Dara, O.M., Flint, M.V., 2017. Role of zooplankton in the vertical mass flux in the Kara and Laptev Seas in fall. Oceanology 57. https://doi.org/10.1134/S0001437017060029

Dybwad, C., Assmy, P., Olsen, L.M., Peeken, I., Nikolopoulos, A., Krumpen, T., Randelhoff, A., Tatarek, A., Wiktor, J.M., Reigstad, M., 2021. Carbon export in the seasonal sea ice zone north of Svalbard from winter to late summer. Front. Mar. Sci. 7. https://doi.org/10.3389/fmars.2020.525800

Dybwad, C., Lalande, C., Bodur, Y.V., Henley, S.F., Cottier, F., Ershova, E.A., Hobbs, L., Last, K.S., Dąbrowska, A.M., Reigstad, M., 2022. The influence of sea ice cover and Atlantic Water advection on annual particle export north of Svalbard. J. Geophys. Res. Oceans 127. https://doi.org/10.1029/2022JC018897

Edler, L., Elbrächter, M., 2010. The Utermöhl method for quantitative phytoplankton analysis, in: Microscopic and Molecular Methods for Quantitative Phytoplankton Analysis. Unesco Pub., pp. 13–20.

Eilertsen, H.C., Falk-Petersen, S., Hopkins, C.C.E., Tande, K., 1981. Ecological investigations on the plankton community of Balsfjorden, northern Norway: program for the project, study area, topography, and physical environment. Sarsia 66.

Eilertsen, H.Chr., Taasen, J.P., 1981. Investigations on the plankton community of Balsfjorden, Northern Norway. The phytoplankton 1976–1978. Abundance, species composition, and succession. Sarsia 66. https://doi.org/10.1080/00364827.1984.10420584

Ellingsen, I., Slagstad, D., Sundfjord, A., 2009. Modification of water masses in the Barents Sea and its coupling to ice dynamics: a model study. Ocean Dyn. 59. https://doi.org/10.1007/s10236-009-0230-5

Engel, A., 2000. The role of transparent exopolymer particles (TEP) in the increase in apparent particle stickiness (α) during the decline of a diatom bloom. J. Plankton Res. 22.

Engel, A., Thoms, S., Riebesell, U., Rochelle-Newall, E., Zondervan, I., 2004. Polysaccharide aggregation as a potential sink of marine dissolved organic carbon. Nature 428. https://doi.org/10.1038/nature02453

Fadeev, E., Rogge, A., Ramondenc, S., Nöthig, E.-M., Wekerle, C., Bienhold, C., Salter, I., Waite, A.M., Hehemann, L., Boetius, A., Iversen, M.H., 2021. Sea ice presence is linked to higher carbon export and vertical microbial connectivity in the Eurasian Arctic Ocean. Commun. Biol. 4. https://doi.org/10.1038/s42003-021-02776-w

Flerus, R., Lechtenfeld, O.J., Koch, B.P., McCallister, S.L., Schmitt-Kopplin, P., Benner, R., Kaiser, K., Kattner, G., 2012. A molecular perspective on the ageing of marine dissolved organic matter. Biogeosci. 9. 1 https://doi.org/0.5194/bg-9-1935-2012

Forest, A., Babin, M., Stemmann, L., Picheral, M., Sampei, M., Fortier, L., Gratton, Y., Bélanger, S., Devred, E., Sahlin, J., Doxaran, D., Joux, F., Ortega-Retuerta, E., Martín, J., Jeffrey, W.H., Gasser, B., Carlos Miquel, J., 2013. Ecosystem function and particle flux dynamics across the Mackenzie Shelf (Beaufort Sea, Arctic Ocean): an integrative analysis of spatial variability and biophysical forcings. Biogeosciences 10. https://doi.org/10.5194/bg-10-2833-2013

Fossheim, M., Primicerio, R., Johannesen, E., Ingvaldsen, R.B., Aschan, M.M., Dolgov, A.V., 2015. Recent warming leads to a rapid borealization of fish communities in the Arctic. Nat. Clim. Change 5. https://doi.org/10.1038/nclimate2647

Frey, K.E., 2017. Arctic Ocean Primary Productivity. Arct. Rep. Card 2017 NOAA Httpwww Arct. Noaa GovReport-CardReport-Card-2017ArtMID7798ArticleID701Arctic-Ocean-Prim.-Product.

Frey, K.E., Comiso, J.C., Cooper, L.W., Garcia-Eidell, C., Grebmeier, J.M., Stock, L.V., 2022. Arctic Ocean primary productivity: The response of marine algae to climate warming and sea ice decline. https://doi.org/10.25923/0JE1-TE61

Friedlingstein, P., Jones, M.W., O'Sullivan, M., Andrew, R.M., Hauck, J., Peters, G.P., Peters, W., Pongratz, J., Sitch, S., Le Quéré, C., Bakker, D.C.E., Canadell, J.G., Ciais, P., Jackson, R.B., Anthoni, P., Barbero, L., Bastos, A., Bastrikov, V., Becker, M., Bopp, L., Buitenhuis, E., Chandra, N., Chevallier, F., Chini, L.P., Currie, K.I., Feely, R.A., Gehlen, M., Gilfillan, D., Gkritzalis, T., Goll, D.S., Gruber, N., Gutekunst, S., Harris, I., Haverd, V., Houghton, R.A., Hurtt, G., Ilyina, T., Jain, A.K., Joetzjer, E., Kaplan, J.O., Kato, E., Klein Goldewijk, K., Korsbakken, J.I., Landschützer, P., Lauvset, S.K., Lefèvre, N., Lenton, A., Lienert, S., Lombardozzi, D., Marland, G., McGuire, P.C., Melton, J.R., Metzl, N., Munro, D.R., Nabel, J.E.M.S., Nakaoka, S.-I., Neill, C., Omar, A.M., Ono, T., Peregon, A., Pierrot, D., Poulter, B., Rehder, G., Resplandy, L., Robertson, E., Rödenbeck, C., Séférian, R., Schwinger, J., Smith, N., Tans, P.P., Tian, H., Tilbrook, B., Tubiello, F.N., van der Werf, G.R., Wiltshire, A.J., Zaehle, S., 2019. Global carbon budget 2019. Earth Syst. Sci. Data 11. https://doi.org/10.5194/essd-11-1783-2019

Gardner, W.D., 1985. The effect of tilt on sediment trap efficiency. Deep Sea Res. Part Oceanogr. Res. Pap. 32. https://doi.org/10.1016/0198-0149(85)90083-4

Gardner, W.D., 1980. Sediment trap dynamics and calibration: a laboratory evaluation. J. Mar. Res. 38.

Giering, S.L.C., Sanders, R., Martin, A.P., Lindemann, C., Möller, K.O., Daniels, C.J., Mayor, D.J., St. John, M.A., 2016. High export via small particles before the onset of the North Atlantic spring bloom. J. Geophys. Res. Oceans 121. https://doi.org/10.1002/2016JC012048

Gluchowska, M., Dalpadado, P., Beszczynska-Möller, A., Olszewska, A., Ingvaldsen, R.B., Kwasniewski, S., 2017. Interannual zooplankton variability in the main pathways of the Atlantic water flow into the Arctic Ocean (Fram Strait and Barents Sea branches). ICES J. Mar. Sci. 74. https://doi.org/10.1093/icesjms/fsx033

Górska, B., Soltwedel, T., Schewe, I., Włodarska-Kowalczuk, M., 2020. Bathymetric trends in biomass size spectra, carbon demand, and production of Arctic benthos (76-5561 m, Fram Strait). Prog. Oceanogr. 186. https://doi.org/10.1016/j.pocean.2020.102370

Graf, G., 1989. Benthic-pelagic coupling in a deep-sea benthic community. Nature 341. https://doi.org/10.1038/341437a0

Grebmeier, J.M., Cooper, L.W., Feder, H.M., Sirenko, B.I., 2006a. Ecosystem dynamics of the Pacific-influenced Northern Bering and Chukchi Seas in the Amerasian Arctic. Prog. Oceanogr. 71. https://doi.org/10.1016/j.pocean.2006.10.001

Grebmeier, J.M., Overland, J.E., Moore, S.E., Farley, E.V., Carmack, E.C., Cooper, L.W., Frey, K.E., Helle, J.H., McLaughlin, F.A., Mcnutt, S.L., 2006b. A major ecosystem shift in the Northern Bering Sea. Science 311. https://doi.org/10.1126/science.1121365

Gutt, J., 1995. The occurrence of sub-ice algal aggregations off northeast Greenland. Polar Biol. 15. https://doi.org/10.1007/BF00239844

Hargrave, B.T., Burns, N.M., 1979. Assessment of sediment trap collection efficiency. Limnol. Oceanogr. 24. https://doi.org/10.4319/lo.1979.24.6.1124

Hattermann, T., Isachsen, P.E., Appen, W.-J. von, Albretsen, J., Sundfjord, A., 2016. Eddy-driven recirculation of Atlantic Water in Fram Strait. Geophys. Res. Lett. 43. https://doi.org/10.1002/2016GL068323

He, W., Chen, M., Schlautman, M.A., Hur, J., 2016. Dynamic exchanges between DOM and POM pools in coastal and inland aquatic ecosystems: A review. Sci. Total Environ. 551–552. https://doi.org/10.1016/j.scitotenv.2016.02.031

Hegseth, E.N., Sundfjord, A., 2008. Intrusion and blooming of Atlantic phytoplankton species in the high Arctic. J. Mar. Syst. 74. https://doi.org/10.1016/j.jmarsys.2007.11.011

Heinze, C., Meyer, S., Goris, N., Anderson, L., Steinfeldt, R., Chang, N., Le Quéré, C., Bakker, D.C.E., 2015. The ocean carbon sink – impacts, vulnerabilities and challenges. Earth Syst. Dyn. 6. https://doi.org/10.5194/esd-6-327-2015

Hellebust, J.A., 1965. Excretion of some organic compounds by marine phytoplankton. Limnol. Oceanogr. 10. https://doi.org/10.4319/lo.1965.10.2.0192

Henson, S., Le Moigne, F., Giering, S., 2019. Drivers of carbon export efficiency in the global ocean. Glob. Biogeochem. Cycles 33. https://doi.org/10.1029/2018GB006158

Hillebrand, H., Dürselen, C.-D., Kirschtel, D., Pollingher, U., Zohary, T., 1999. Biovolume calculation for pelagic and benthic microalgae. J. Phycol. 35. https://doi.org/10.1046/j.1529-8817.1999.3520403.x

Hobbie, J.E., Daley, R.J., Jasper, S., 1977. Use of nuclepore filters for counting bacteria by fluorescence microscopy. Appl. Environ. Microbiol. 33.

Hobson, K.A., Ambrose, W.G., Renaud, P.R., 1996. Sources of primary production, benthicpelagic coupling, and trophic relationships within the northeast Water Polynya: insights from 13C and 15N analysis. Oceanogr. Lit. Rev. 7.

Holland, M.M., Bitz, C.M., 2003. Polar amplification of climate change in coupled models. Clim. Dyn. 21. https://doi.org/10.1007/s00382-003-0332-6

Hordoir, R., Skagseth, Ø., Ingvaldsen, R.B., Sandø, A.B., Löptien, U., Dietze, H., Gierisch, A.M.U., Assmann, K.M., Lundesgaard, Ø., Lind, S., 2022. Changes in Arctic

stratification and mixed layer depth cycle: A Modeling Analysis. J. Geophys. Res. Oceans 127. https://doi.org/10.1029/2021JC017270

Hoving, H.J.T., Amon, D., Bodur, Y., Haeckel, M., Jones, D.O.B., Neitzel, P., Simon-Lledó, E., Smith, C.R., Stauffer, J.B., Sweetman, A.K., Purser, A., 2022. The abyssal voyage of the argonauts: Deep-sea in situ observations reveal the contribution of cephalopod egg cases to the carbon pump. Deep Sea Res. Part Oceanogr. Res. Pap. 183. https://doi.org/10.1016/j.dsr.2022.103719

Hunt, G.L., Drinkwater, K.F., Arrigo, K., Berge, J., Daly, K.L., Danielson, S., Daase, M., Hop, H., Isla, E., Karnovsky, N., Laidre, K., Mueter, F.J., Murphy, E.J., Renaud, P.E., Smith, W.O., Trathan, P., Turner, J., Wolf-Gladrow, D., 2016. Advection in polar and sub-polar environments: Impacts on high latitude marine ecosystems. Prog. Oceanogr. 149. https://doi.org/10.1016/j.pocean.2016.10.004

Ingels, J., Van den Driessche, P., De Mesel, I., Vanhove, S., Moens, T., Vanreusel, A., 2010. Preferred use of bacteria over phytoplankton by deep-sea nematodes in polar regions. Mar. Ecol. Prog. Ser. 406. https://doi.org/10.3354/meps08535

Ingvaldsen, R., Loeng, H., Asplin, L., 2002. Variability in the Atlantic inflow to the Barents Sea based on a one-year time series from moored current meters. Cont. Shelf Res. 22. https://doi.org/10.1016/S0278-4343(01)00070-X

Ingvaldsen, R.B., Asplin, L., Loeng, H., 2004. The seasonal cycle in the Atlantic transport to the Barents Sea during the years 1997–2001. Cont. Shelf Res. 24. https://doi.org/10.1016/j.csr.2004.02.011

IPCC, 2023. Climate Change 2022 – Impacts, adaptation and vulnerability: Working group II contribution to the sixth assessment report of the Intergovernmental Panel on Climate Change. Cambridge University Press. https://doi.org/10.1017/9781009325844

ISSI, 2008. Arctic change and polynyas: Focus on the Northeast Water Polynya and North Water Polynya/Nares Strait system team [WWW Document]. URL http://www.issibern.ch/teams/Polynya/ (accessed 2.11.18).

Iversen, M., Poulsen, L., 2007. Coprorhexy, coprophagy, and coprochaly in the copepods Calanus helgolandicus, Pseudocalanus elongatus, and Oithona similis. Mar. Ecol. Prog. Ser. 350. https://doi.org/10.3354/meps07095

Iversen, M.H., 2023. Carbon export in the ocean: A biologist's perspective. Annu. Rev. Mar. Sci. 15. https://doi.org/10.1146/annurev-marine-032122-035153

Iversen, M.H., Robert, M.L., 2015. Ballasting effects of smectite on aggregate formation and export from a natural plankton community. Mar. Chem., Particles in aquatic environments: from invisible exopolymers to sinking aggregates 175. https://doi.org/10.1016/j.marchem.2015.04.009

Jakobsson, M., Mayer, L.A., Bringensparr, C., Castro, C.F., Mohammad, R., Johnson, P., Ketter, T., Accettella, D., Amblas, D., An, L., Arndt, J.E., Canals, M., Casamor, J.L., Chauché, N., Coakley, B., Danielson, S., Demarte, M., Dickson, M.-L., Dorschel, B., Dowdeswell, J.A., Dreutter, S., Fremand, A.C., Gallant, D., Hall, J.K., Hehemann, L., Hodnesdal, H., Hong, J., Ivaldi, R., Kane, E., Klaucke, I., Krawczyk, D.W., Kristoffersen, Y., Kuipers, B.R., Millan, R., Masetti, G., Morlighem, M., Noormets, R., Prescott, M.M., Rebesco, M., Rignot, E., Semiletov, I., Tate, A.J., Travaglini, P., Velicogna, I., Weatherall, P., Weinrebe, W., Willis, J.K., Wood, M., Zarayskaya, Y., Zhang, T., Zimmermann, M., Zinglersen, K.B., 2020. The International Bathymetric Chart of the Arctic Ocean Version 4.0. Sci. Data 7. https://doi.org/10.1038/s41597-020-0520-9

Johannessen, O.M., Bengtsson, L., Miles, M.W., Kuzmina, S.I., Semenov, V.A., Alekseev, G.V., Nagurnyi, A.P., Zakharov, V.F., Bobylev, L.P., Pettersson, L.H., Hasselmann, K., Cattle, H.P., 2004. Arctic climate change: observed and modelled temperature and sea-ice

variability. Tellus Dyn. Meteorol. Oceanogr. 56. https://doi.org/10.3402/tellusa.v56i4.14418

Jordà-Molina, È., Sen, A., Bluhm, B.A., Renaud, P.E., Włodarska-Kowalczuk, M., Legeżyńska, J., Oleszczuk, B., Reiss, H., 2023. Lack of strong seasonality in macrobenthic communities from the northern Barents Sea shelf and Nansen Basin. Prog. Oceanogr. 219. https://doi.org/10.1016/j.pocean.2023.103150

Jørgensen, L.L., Archambault, P., Blicher, M.E., Denisenko, N.V., Guðmundsson, G., Iken, K., Roy, V., Sørensen, J., Anisimova, N., Behe, C., Bluhm, B.A., Denisenko, S.G., Metcalf, V., Olafsdóttir, S., Schiøtte, T., Tendal, O., Ravelo, A.M., Kędra, M., Piepenburg, D., 2017. Benthos, in: CAFF (Ed.), State of the arctic marine biodiversity report. Conservation of Arctic Flora and Fauna International Secretariat, Akureyri, Iceland, pp. 85–104.

Juul-Pedersen, T., Michel, C., Gosselin, M., 2010. Sinking export of particulate organic material from the euphotic zone in the eastern Beaufort Sea. Mar. Ecol. Prog. Ser. 410. https://doi.org/10.3354/meps08608

Kędra, M., Cooper, L.W., Silberberger, M.J., Zhang, M., Biasatti, D., Grebmeier, J.M., 2021. Organic carbon source variability in Arctic bivalves as deduced from the compound specific carbon isotopic composition of amino acids. J. Mar. Syst. 219. https://doi.org/10.1016/j.jmarsys.2021.103547

Kędra, M., Włodarska-Kowalczuk, M., Węsławski, J.M., 2010. Decadal change in macrobenthic soft-bottom community structure in a high Arctic fjord (Kongsfjorden, Svalbard). Polar Biol. 33. https://doi.org/10.1007/s00300-009-0679-1

Koch, C.W., Brown, T.A., Amiraux, R., Ruiz-Gonzalez, C., MacCorquodale, M., Yunda-Guarin, G.A., Kohlbach, D., Loseto, L.L., Rosenberg, B., Hussey, N.E., Ferguson, S.H., Yurkowski, D.J., 2023. Year-round utilization of sea ice-associated carbon in Arctic ecosystems. Nat. Commun. 14. https://doi.org/10.1038/s41467-023-37612-8

Koch, B.P., Dittmar, T., 2006. From mass to structure: an aromaticity index for high-resolution mass data of natural organic matter. Rapid Commun. Mass Spectrom. 20. https://doi.org/10.1002/rcm.2386

Kohlbach, D., Goraguer, L., Bodur, Y.V., Müller, O., Amargant-Arumí, M., Blix, K., Bratbak, G., Chierici, M., Dąbrowska, A.M., Dietrich, U., Edvardsen, B., García, L.M., Gradinger, R., Hop, H., Jones, E., Lundesgaard, Ø., Olsen, L.M., Reigstad, M., Saubrekka, K., Tatarek, A., Wiktor, J.M., Wold, A., Assmy, P., 2023. Earlier sea-ice melt extends the oligotrophic summer period in the Barents Sea with low algal biomass and associated low vertical flux. Prog. Oceanogr. 213. https://doi.org/10.1016/j.pocean.2023.103018

Krumpen, T., Belter, H.J., Boetius, A., Damm, E., Haas, C., Hendricks, S., Nicolaus, M., Nöthig, E.-M., Paul, S., Peeken, I., Ricker, R., Stein, R., 2019. Arctic warming interrupts the Transpolar Drift and affects long-range transport of sea ice and ice-rafted matter. Sci. Rep. 9. https://doi.org/10.1038/s41598-019-41456-y

Kvernvik, A.C., Hoppe, C.J.M., Greenacre, M., Verbiest, S., Wiktor, J.M., Gabrielsen, T.M., Reigstad, M., Leu, E., 2021. Arctic sea ice algae differ markedly from phytoplankton in their ecophysiological characteristics. Mar. Ecol. Prog. Ser. 666. https://doi.org/10.3354/meps13675

Lalande, C., Moran, S.B., Wassmann, P., Grebmeier, J.M., Cooper, L.W., 2008. 234Th-derived particulate organic carbon fluxes in the northern Barents Sea with comparison to drifting sediment trap fluxes. J. Mar. Syst. 73. https://doi.org/10.1016/j.jmarsys.2007.09.004

Leu, E., Mundy, C.J., Assmy, P., Campbell, K., Gabrielsen, T.M., Gosselin, M., Juul-Pedersen, T., Gradinger, R., 2015. Arctic spring awakening – Steering principles behind the phenology of vernal ice algal blooms. Prog. Oceanogr., Overarching perspectives of

contemporary and future ecosystems in the Arctic Ocean 139. https://doi.org/10.1016/j.pocean.2015.07.012

Lewis, K.M., van Dijken, G.L., Arrigo, K.R., 2020. Changes in phytoplankton concentration now drive increased Arctic Ocean primary production. Science 369. https://doi.org/10.1126/science.aay8380

Lind, S., Ingvaldsen, R.B., 2012. Variability and impacts of Atlantic Water entering the Barents Sea from the north. Deep Sea Res. Part Oceanogr. Res. Pap. 62. https://doi.org/10.1016/j.dsr.2011.12.007

Lind, S., Ingvaldsen, R.B., Furevik, T., 2018. Arctic warming hotspot in the northern Barents Sea linked to declining sea-ice import. Nat. Clim. Change 8. https://doi.org/10.1038/s41558-018-0205-y

Link, H., Archambault, P., Tamelander, T., Renaud, P.E., Piepenburg, D., 2011. Spring-to-summer changes and regional variability of benthic processes in the western Canadian Arctic. Polar Biol. 34. https://doi.org/10.1007/s00300-011-1046-6

Link, H., Chaillou, G., Forest, A., Piepenburg, D., Archambault, P., 2013a. Multivariate benthic ecosystem functioning in the Arctic - benthic fluxes explained by environmental parameters in the southeastern Beaufort Sea. Biogeosciences 10. https://doi.org/10.5194/bg-10-5911-2013

Link, H., Piepenburg, D., Archambault, P., 2013b. Are Hotspots always hotspots? The relationship between diversity, \resource and ecosystem functions in the Arctic. PLoS ONE 8. https://doi.org/10.1371/journal.pone.0074077

Lombard, F., Guidi, L., Kiørboe, T., 2013. Effect of type and concentration of ballasting particles on sinking rate of marine snow produced by the appendicularian Oikopleura dioica. PLOS ONE 8. https://doi.org/10.1371/journal.pone.0075676

Lundesgaard, Ø., Sundfjord, A., Lind, S., Nilsen, F., Renner, A.H.H., 2022. Import of Atlantic Water and sea ice controls the ocean environment in the northern Barents Sea. Ocean Sci. 18. https://doi.org/10.5194/os-18-1389-2022

Lundesgaard, Ø., Sundfjord, A., Renner, A.H.H., 2021. Drivers of interannual sea ice concentration variability in the Atlantic Water inflow region north of Svalbard. J. Geophys. Res. Oceans 126. https://doi.org/10.1029/2020JC016522

Lund-Hansen, L.C., Søgaard, D.H., Sorrell, B.K., Gradinger, R., Meiners, K.M., 2020. Sea Ice in a Climate Change Context, in: Lund-Hansen, L.C., Søgaard, D.H., Sorrell, B.K., Gradinger, R., Meiners, K.M. (Eds.), Arctic Sea Ice Ecology: Seasonal dynamics in algal and bacterial productivity. Springer, pp. 103–130.

Mague, T.H., Friberg, E., Hughes, D.J., Morris, I., 1980. Extracellular release of carbon by marine phytoplankton; a physiological approach1. Limnol. Oceanogr. 25. https://doi.org/10.4319/lo.1980.25.2.0262

Mäkelä, A., Witte, U., Archambault, P., 2017a. Benthic macroinfaunal community structure, resource utilisation and trophic relationships in two Canadian Arctic Archipelago polynyas. PLOS ONE 12. https://doi.org/10.1371/journal.pone.0183034

Mäkelä, A., Witte, U., Archambault, P., 2017b. Ice algae vs. phytoplankton: resource utilization by Arctic deep sea macroinfauna revealed through isotope labelling experiments. Mar. Ecol. Prog. Ser. 572. https://doi.org/10.3354/meps12157

Marchese, C., Albouy, C., Tremblay, J.-É., Dumont, D., D'Ortenzio, F., Vissault, S., Bélanger, S., 2017. Changes in phytoplankton bloom phenology over the North Water (NOW) polynya: a response to changing environmental conditions. Polar Biol. 40. https://doi.org/10.1007/s00300-017-2095-2

Mari, X., Burd, A., 1998. Seasonal size spectra of transparent exopolymeric particles (TEP) in a coastal sea and comparison with those predicted using coagulation theory. Mar. Ecol. Prog. Ser. 163. https://doi.org/10.3354/meps163063

Marinov, I., Sarmiento, J.L., 2004. The role of the oceans in the global carbon cycle: An overview, in: Follows, M., Oguz, T. (Eds.), The ocean carbon cycle and climate. Springer Netherlands, Dordrecht, pp. 251–295. https://doi.org/10.1007/978-1-4020-2087-2_8

Marquardt, M., Bodur, Y.V., Dubourg, P., Reigstad, M., 2022a. Concentration of particulate organic carbon (POC) and particulate organic nitrogen (PON) from the sea water and sea ice in the northern Barents Sea as part of the Nansen Legacy project, Cruise 2019711 Q4. https://doi.org/10.11582/2022.00048

Marquardt, M., Bodur, Y.V., Dubourg, P., Reigstad, M., 2022b. Concentration of particulate organic carbon (POC) and particulate organic nitrogen (PON) from the sea water and sea ice in the northern Barents Sea as part of the Nansen Legacy project, Cruise 2021703 Q1. https://doi.org/10.11582/2022.00053

Marquardt, M., Vader, A., Stübner, E.I., Reigstad, M., Gabrielsen, T.M., 2016. Strong seasonality of marine microbial eukaryotes in a high-Arctic fjord (Isfjorden, in West Spitsbergen, Norway). Appl. Environ. Microbiol. 82. https://doi.org/10.1128/AEM.03208-15

Martin, J.H., Knauer, G.A., Karl, D.M., Broenkow, W.W., 1987. VERTEX: Carbon cycling in the northeast Pacific. Deep Sea Res. Part Oceanogr. Res. Pap. 34. https://doi.org/10.1016/0198-0149(87)90086-0

Mayer, C., Reeh, N., Jung-Rothenhäusler, F., Huybrechts, P., Oerter, H., 2000. The subglacial cavity and implied dynamics under Nioghalvfjerdsfjorden Glacier, NE-Greenland. Geophys. Res. Lett. 27. https://doi.org/10.1029/2000GL011514

McLaughlin, F.A., Carmack, E.C., 2010. Deepening of the nutricline and chlorophyll maximum in the Canada Basin interior, 2003–2009. Geophys. Res. Lett. 37. https://doi.org/10.1029/2010GL045459

Meadows, C.A., Grebmeier, J.M., Kidwell, S.M., 2019. High-latitude benthic bivalve biomass and recent climate change: Testing the power of live-dead discordance in the Pacific Arctic. Deep Sea Res. Part II Top. Stud. Oceanogr. 162. https://doi.org/10.1016/j.dsr2.2019.04.005

Meier, W.N., Petty, A., Hendricks, S., Kaleschke, L., Divine, D., Farrell, S., Gerland, S., Perovich, D.K., Ricker, R., Tian-Kunze, X., Webster, M., 2023. Sea Ice (Arctic Report Card: Update for 2023), Arctic Report Cards. National Oceanic and Atmospheric Administration (NOAA).

Menden-Deuer, S., Lessard, E.J., 2000. Carbon to volume relationships for dinoflagellates, diatoms, and other protist plankton. Limnol. Oceanogr. 45. https://doi.org/10.4319/lo.2000.45.3.0569

Meredith, M., Sommerkorn, M., Cassota, S., Derksen, C., Ekaykin, A., Hollowed, A., Kofinas, G., Mackintosh, A., Melbourne-Thomas, J., Muelbert, M.M.C., Ottersen, G., Pritchard, H., Schuur, E.A.G., 2019. Polar Regions, in: Pörtner, H.O., Roberts, D.C., Masson-Delmotte, V., Zhai, P., Tignor, M., Poloczanska, E.S., Mintenbeck, K., Alegría, A., Nicolai, M., Okem, A., Petzold, J., Rama, B., Weyer, N.M. (Eds.), IPCC Special Report on the Ocean and Cryosphere in a Changing Climate. Cambridge University Press, pp. 203–320. https://doi.org/10.1017/9781009157964

Meyer, K.S., Sweetman, A.K., Young, C.M., Renaud, P.E., 2015. Environmental factors structuring Arctic megabenthos—a case study from a shelf and two fjords. Front. Mar. Sci. 2. https://doi.org/10.3389/fmars.2015.00022

Michel, C., Gosselin, M., Nozais, C., 2002. Preferential sinking export of biogenic silica during the spring and summer in the North Water Polynya (northern Baffin Bay): Temperature or biological control? J. Geophys. Res. Oceans 107. https://doi.org/10.1029/2000JC000408

Minnett, P.J., Bignami, F., Böhm, E., Budéus, G., Galbraith, P.S., Gudmandsen, P., Hopkins, T.S., Ingram, R.G., Johnson, M.A., Niebauer, H.J., Ramseier, R.O., Schneider, W., 1997. A summary of the formation and seasonal progression of the Northeast Water Polynya. J. Mar. Syst. 10. https://doi.org/10.1016/S0924-7963(96)00060-7

Miquel, J.-C., Gasser, B., Martín, J., Marec, C., Babin, M., Fortier, L., Forest, A., 2015. Downward particle flux and carbon export in the Beaufort Sea, Arctic Ocean; the role of zooplankton. Biogeosciences 12. https://doi.org/10.5194/bg-12-5103-2015

Moore, S.E., Stabeno, P.J., 2015. Synthesis of Arctic Research (SOAR) in marine ecosystems of the Pacific Arctic. Prog. Oceanogr., Synthesis of Arctic Research (SOAR) 136. https://doi.org/10.1016/j.pocean.2015.05.017

Morata, N., Michaud, E., Włodarska-Kowalczuk, M., 2015. Impact of early food input on the Arctic benthos activities during the polar night. Polar Biol. 38. https://doi.org/10.1007/s00300-013-1414-5

Morata, N., Poulin, M., Renaud, P.E., 2011. A multiple biomarker approach to tracking the fate of an ice algal bloom to the sea floor. Polar Biol. 34. https://doi.org/10.1007/s00300-010-0863-3

Morata, N., Renaud, P., Brugel, S., Hobson, K., Johnson, B., 2008. Spatial and seasonal variations in the pelagic–benthic coupling of the southeastern Beaufort Sea revealed by sedimentary biomarkers. Mar. Ecol. Prog. Ser. 371. https://doi.org/10.3354/meps07677

Morata, N., Renaud, P.E., 2008. Sedimentary pigments in the western Barents Sea: A reflection of pelagic–benthic coupling? Deep Sea Res. Part II Top. Stud. Oceanogr. 55. https://doi.org/10.1016/j.dsr2.2008.05.004

Myklestad, S.M., 1995. Release of extracellular products by phytoplankton with special emphasis on polysaccharides. Sci. Total Environ., Marine Mucilages 165. https://doi.org/10.1016/0048-9697(95)04549-G

Neukermans, G., Oziel, L., Babin, M., 2018. Increased intrusion of warming Atlantic water leads to rapid expansion of temperate phytoplankton in the Arctic. Glob. Change Biol. 24. https://doi.org/10.1111/gcb.14075

Ng, A.K.Y., Andrews, J., Babb, D., Lin, Y., Becker, A., 2018. Implications of climate change for shipping: Opening the Arctic seas. WIREs Clim. Change 9. https://doi.org/10.1002/wcc.507

Nguyen, H.T., Lee, Y.M., Hong, J.K., Hong, S., Chen, M., Hur, J., 2022. Climate warming-driven changes in the flux of dissolved organic matter and its effects on bacterial communities in the Arctic Ocean: A review. Front. Mar. Sci. 9. https://doi.org/10.3389/fmars.2022.968583

Nöthig, E.-M., Ramondenc, S., Haas, A., Hehemann, L., Walter, A., Bracher, A., Lalande, C., Metfies, K., Peeken, I., Bauerfeind, E., Boetius, A., 2020. Summertime Chlorophyll a and particulate organic carbon standing stocks in surface waters of the Fram Strait and the Arctic Ocean (1991–2015). Front. Mar. Sci. 7. https://doi.org/10.3389/fmars.2020.00350

Nummelin, A., Ilicak, M., Li, C., Smedsrud, L.H., 2016. Consequences of future increased Arctic runoff on Arctic Ocean stratification, circulation, and sea ice cover. J. Geophys. Res. Oceans 121. https://doi.org/10.1002/2015JC011156

O'Brien, M.C., Macdonald, R.W., Melling, H., Iseki, K., 2006. Particle fluxes and geochemistry on the Canadian Beaufort Shelf: Implications for sediment transport and deposition. Cont. Shelf Res. 26. https://doi.org/10.1016/j.csr.2005.09.007

O'Daly, S.H., Danielson, S.L., Hardy, S.M., Hopcroft, R.R., Lalande, C., Stockwell, D.A., McDonnell, A.M.P., 2020. Extraordinary carbon fluxes on the shallow Pacific Arctic shelf during a remarkably warm and low sea ice period. Front. Mar. Sci. 7. https://doi.org/10.3389/fmars.2020.548931

Oleszczuk, B., Grzelak, K., Kędra, M., 2021. Community structure and productivity of Arctic benthic fauna across depth gradients during springtime. Deep Sea Res. Part Oceanogr. Res. Pap. 170. https://doi.org/10.1016/j.dsr.2020.103457

Oleszczuk, B., Silberberger, M.J., Grzelak, K., Winogradow, A., Dybwad, C., Peeken, I., Wiedmann, I., Kędra, M., 2023. Macrofauna and meiofauna food-web structure from Arctic fjords to deep Arctic Ocean during spring: A stable isotope approach. Ecol. Indic. 154. https://doi.org/10.1016/j.ecolind.2023.110487

Olivier, F., Gaillard, B., Thébault, J., Meziane, T., Tremblay, R., Dumont, D., Bélanger, S., Gosselin, M., Jolivet, A., Chauvaud, L., Martel, A.L., Rysgaard, S., Olivier, A.-H., Pettré, J., Mars, J., Gerber, S., Archambault, P., 2020. Shells of the bivalve Astarte moerchi give new evidence of a strong pelagic-benthic coupling shift occurring since the late 1970s in the North Water polynya. Philos. Trans. R. Soc. Math. Phys. Eng. Sci. 378. https://doi.org/10.1098/rsta.2019.0353

Olli, K., Wexels Riser, C., Wassmann, P., Ratkova, T., Arashkevich, E., Pasternak, A., 2002. Seasonal variation in vertical flux of biogenic matter in the marginal ice zone and the central Barents Sea. J. Mar. Syst., Seasonal C-cycling variability in the open and ice-covered waters of the Barents Sea 38. https://doi.org/10.1016/S0924-7963(02)00177-X

Onarheim, I.H., Eldevik, T., Smedsrud, L.H., Stroeve, J.C., 2018. Seasonal and regional manifestation of arctic sea ice loss. J. Clim. 31. https://doi.org/10.1175/JCLI-D-17-0427.1

Open Street Map, 2023. Land polygons [WWW Document]. URL https://osmdata.openstreetmap.de/data/land-polygons.html (accessed 9.22.23).

O'Sadnick, M., Petrich, C., Brekke, C., Skarðhamar, J., 2020. Ice extent in sub-arctic fjords and coastal areas from 2001 to 2019 analyzed from MODIS imagery. Ann. Glaciol. 1–17. https://doi.org/10.1017/aog.2020.34

Oziel, L., Baudena, A., Ardyna, M., Massicotte, P., Randelhoff, A., Sallée, J.-B., Ingvaldsen, R.B., Devred, E., Babin, M., 2020. Faster Atlantic currents drive poleward expansion of temperate phytoplankton in the Arctic Ocean. Nat. Commun. 11. https://doi.org/10.1038/s41467-020-15485-5

Oziel, L., Massicotte, P., Babin, M., Devred, E., 2022. Decadal changes in Arctic Ocean Chlorophyll a: Bridging ocean color observations from the 1980s to present time. Remote Sens. Environ. 275. https://doi.org/10.1016/j.rse.2022.113020

Passow, U., 2002. Transparent exopolymer particles (TEP) in aquatic environments. Prog. Oceanogr. 55. https://doi.org/10.1016/S0079-6611(02)00138-6

Passow, U., 2000. Formation of transparent exopolymer particles, TEP, from dissolved precursor material. Mar. Ecol. Prog. Ser. 192. https://doi.org/10.3354/meps192001

Pesant, S., Legendre, L., Gosselin, M., Bauerfeind, E., Budéus, G., 2002. Wind-triggered events of phytoplankton downward flux in the Northeast Water Polynya. J. Mar. Syst. 31. https://doi.org/10.1016/S0924-7963(01)00065-3

Pesant, S., Legendre, L., Gosselin, M., Smith, R., Kattner, G., Ramseier, R., 1996. Size-differential regimes of phytoplankton production in the Northeast Water Polynya (77*-81*N). Mar. Ecol. Prog. Ser. 142. https://doi.org/10.3354/meps142075

Petersen, G.H., Curtis, M.A., 1980. Differences in energy flow through major components of subarctic, temperate and tropical marine sheif ecosystems. Dana 1.

Piepenburg, D., 2005. Recent research on Arctic benthos: Common notions need to be revised. Polar Biol. 28. https://doi.org/10.1007/s00300-005-0013-5

Piepenburg, D., Ambrose, W.G., Brandt, A., Renaud, P.E., Ahrens, M.J., Jensen, P., 1997. Benthic community patterns reflect water column processes in the Northeast Water polynya (Greenland). J. Mar. Syst. 10. https://doi.org/10.1016/S0924-7963(96)00050-4

Polyakov, I.V., Alkire, M.B., Bluhm, B.A., Brown, K.A., Carmack, E.C., Chierici, M., Danielson, S.L., Ellingsen, I., Ershova, E.A., Gårdfeldt, K., Ingvaldsen, R.B., Pnyushkov, A.V., Slagstad, D., Wassmann, P., 2020a. Borealization of the Arctic Ocean in response to anomalous advection from sub-arctic seas. Front. Mar. Sci. 7. https://doi.org/10.3389/fmars.2020.00491

Polyakov, I.V., Ingvaldsen, R.B., Pnyushkov, A.V., Bhatt, U.S., Francis, J.A., Janout, M., Kwok, R., Skagseth, Ø., 2023. Fluctuating Atlantic inflows modulate Arctic atlantification. Science 381. https://doi.org/10.1126/science.adh5158

Polyakov, I.V., Pnyushkov, A.V., Alkire, M.B., Ashik, I.M., Baumann, T.M., Carmack, E.C., Goszczko, I., Guthrie, J., Ivanov, V.V., Kanzow, T., Krishfield, R., Kwok, R., Sundfjord, A., Morison, J., Rember, R., Yulin, A., 2017. Greater role for Atlantic inflows on sea-ice loss in the Eurasian Basin of the Arctic Ocean. Science 356. https://doi.org/10.1126/science.aai8204

Polyakov, I.V., Rippeth, T.P., Fer, I., Alkire, M.B., Baumann, T.M., Carmack, E.C., Ingvaldsen, R., Ivanov, V.V., Janout, M., Lind, S., Padman, L., Pnyushkov, A.V., Rember, R., 2020b. Weakening of cold halocline layer exposes sea ice to oceanic heat in the eastern Arctic Ocean. J. Clim. 33. https://doi.org/10.1175/JCLI-D-19-0976.1

Previdi, M., Smith, K.L., Polvani, L.M., 2021. Arctic amplification of climate change: a review of underlying mechanisms. Environ. Res. Lett. 16. https://doi.org/10.1088/1748-9326/ac1c29

Rainville, L., Woodgate, R.A., 2009. Observations of internal wave generation in the seasonally ice-free Arctic. Geophys. Res. Lett. 36. https://doi.org/10.1029/2009GL041291

Rantanen, M., Karpechko, A.Y., Lipponen, A., Nordling, K., Hyvärinen, O., Ruosteenoja, K., Vihma, T., Laaksonen, A., 2022. The Arctic has warmed nearly four times faster than the globe since 1979. Commun. Earth Environ. 3. https://doi.org/10.1038/s43247-022-00498-3

Reigstad, M., Carroll, J., Slagstad, D., Ellingsen, I., Wassmann, P., 2011. Intra-regional comparison of productivity, carbon flux and ecosystem composition within the northern Barents Sea. Prog. Oceanogr., Arctic Marine Ecosystems in an Era of Rapid Climate Change 90. https://doi.org/10.1016/j.pocean.2011.02.005

Reigstad, M., Wexels Riser, C., Wassmann, P., Ratkova, T., 2008. Vertical export of particulate organic carbon: Attenuation, composition and loss rates in the northern Barents Sea. Deep Sea Res. Part II Top. Stud. Oceanogr. 55. https://doi.org/10.1016/j.dsr2.2008.05.007

Renaud, P.E., Morata, N., Carroll, M.L., Denisenko, S.G., Reigstad, M., 2008. Pelagic–benthic coupling in the western Barents Sea: Processes and time scales. Deep Sea Res. Part II Top. Stud. Oceanogr. 55. https://doi.org/10.1016/j.dsr2.2008.05.017

Renaud, P.E., Riedel, A., Michel, C., Morata, N., Gosselin, M., Juul-Pedersen, T., Chiuchiolo, A., 2007. Seasonal variation in benthic community oxygen demand: A response to an ice algal bloom in the Beaufort Sea, Canadian Arctic? J. Mar. Syst. 67. https://doi.org/10.1016/j.jmarsys.2006.07.006

Renaud, P.E., Sejr, M.K., Bluhm, B.A., Sirenko, B., Ellingsen, I.H., 2015. The future of Arctic benthos: Expansion, invasion, and biodiversity. Prog. Oceanogr., Overarching perspectives of contemporary and future ecosystems in the Arctic Ocean 139. https://doi.org/10.1016/j.pocean.2015.07.007

Renner, A.H.H., Bailey, A., Reigstad, M., Sundfjord, A., Chierici, M., Jones, E.M., 2023. Hydrography, inorganic nutrients and chlorophyll a linked to sea ice cover in the Atlantic Water inflow region north of Svalbard. Prog. Oceanogr. 103162. https://doi.org/10.1016/j.pocean.2023.103162

Rex, M.A., Etter, R.J., Morris, J.S., Crouse, J., McClain, C.R., Johnson, N.A., Stuart, C.T., Deming, J.W., Thies, R., Avery, R., 2006. Global bathymetric patterns of standing stock and body size in the deep-sea benthos. Mar. Ecol. Prog. Ser. 317. https://doi.org/10.3354/meps317001

Riley, G.A., 1963. Organic Aggregates in seawater and the dynamics of their formation and utilization. Limnol. Oceanogr. 8. https://doi.org/10.4319/lo.1963.8.4.0372

Robison, B.H., Reisenbichler, K.R., Sherlock, R.E., 2005. Giant larvacean houses: Rapid carbon transport to the deep sea floor. Science 308. https://doi.org/10.1126/science.1109104

Rogge, A., Janout, M., Loginova, N., Trudnowska, E., Hörstmann, C., Wekerle, C., Oziel, L., Schourup-Kristensen, V., Ruiz-Castillo, E., Schulz, K., Povazhnyy, V.V., Iversen, M.H., Waite, A.M., 2022. Carbon dioxide sink in the Arctic Ocean from cross-shelf transport of dense Barents Sea water. Nat. Geosci. https://doi.org/10.1038/s41561-022-01069-z

Rudels, B., Björk, G., Nilsson, J., Winsor, P., Lake, I., Nohr, C., 2005. The interaction between waters from the Arctic Ocean and the Nordic Seas north of Fram Strait and along the East Greenland Current: results from the Arctic Ocean-02 Oden expedition. J. Mar. Syst. 55. https://doi.org/10.1016/j.jmarsys.2004.06.008

Sætre, R., 1999. Features of the central Norwegian shelf circulation. Cont. Shelf Res. 19. https://doi.org/10.1016/S0278-4343(99)00041-2

Sakshaug, E., 2004. Primary and Secondary Production in the Arctic Seas, in: Stein, P.D.R., MacDonald, D.R.W. (Eds.), The Organic Carbon Cycle in the Arctic Ocean. Springer Berlin Heidelberg, pp. 57–81. https://doi.org/10.1007/978-3-642-18912-8_3

Sallon, A., Michel, C., Gosselin, M., 2011. Summertime primary production and carbon export in the southeastern Beaufort Sea during the low ice year of 2008. Polar Biol. 34. https://doi.org/10.1007/s00300-011-1055-5

Sarmiento, Jorge L, Gruber, Nicolas, 2006. Oceanic carbon cycle, atmospheric CO2, and climate, in: Sarmiento, J. L., Gruber, N. (Eds.), Ocean Biogeochemical Dynamics. Princeton University Press.

Schaffer, J., Kanzow, T., von Appen, W.-J., Albedyll, L. von, Arndt, J.E., Roberts, D.H., 2020. Bathymetry constrains ocean heat supply to Greenland's largest glacier tongue. Nat. Geosci. 13. https://doi.org/10.1038/s41561-019-0529-x

Schaffer, J., von Appen, W.-J., Dodd, P.A., Hofstede, C., Mayer, C., de Steur, L., Kanzow, T., 2017. Warm water pathways toward Nioghalvfjerdsfjorden Glacier, Northeast Greenland. J. Geophys. Res. Oceans 122, 4004–4020. https://doi.org/10.1002/2016JC012462

Schauer, U., Fahrbach, E., Osterhus, S., Rohardt, G., 2004. Arctic warming through the Fram Strait: Oceanic heat transport from 3 years of measurements. J. Geophys. Res. Oceans 109. https://doi.org/10.1029/2003JC001823

Schauer, U., Loeng, H., Rudels, B., Ozhigin, V.K., Dieck, W., 2002. Atlantic Water flow through the Barents and Kara Seas. Deep Sea Res. Part Oceanogr. Res. Pap. 49. https://doi.org/10.1016/S0967-0637(02)00125-5

Sejr, M.K., Stedmon, C.A., Bendtsen, J., Abermann, J., Juul-Pedersen, T., Mortensen, J., Rysgaard, S., 2017. Evidence of local and regional freshening of Northeast Greenland coastal waters. Sci. Rep. 7. https://doi.org/10.1038/s41598-017-10610-9

Serreze, M.C., Barrett, A.P., Slater, A.G., Woodgate, R.A., Aagaard, K., Lammers, R.B., Steele, M., Moritz, R., Meredith, M., Lee, C.M., 2006. The large-scale freshwater cycle of the Arctic. J. Geophys. Res. Oceans 111. https://doi.org/10.1029/2005JC003424

Sheldon, R.W., Evelyn, T.P.T., Parsons, T.R., 1967. On the occurrence and formation of Small particles in seawater. Limnol. Oceanogr. 12. https://doi.org/10.4319/lo.1967.12.3.0367

Shu, Q., Wang, Q., Årthun, M., Wang, S., Song, Z., Zhang, M., Qiao, F., 2022. Arctic Ocean Amplification in a warming climate in CMIP6 models. Sci. Adv. 8. https://doi.org/10.1126/sciadv.abn9755

Siegel, D.A., Fields, E., Buesseler, K.O., 2008. A bottom-up view of the biological pump: Modeling source funnels above ocean sediment traps. Deep Sea Res. Part Oceanogr. Res. Pap. 55. https://doi.org/10.1016/j.dsr.2007.10.006

Silberberger, M.J., Koziorowska-Makuch, K., Reiss, H., Kędra, M., 2024. Trophic niches of macrobenthos: Latitudinal variation indicates climate change impact on ecosystem functioning. Glob. Change Biol. 30. https://doi.org/10.1111/gcb.17100

Skagseth, Ø., Furevik, T., Ingvaldsen, R., Loeng, H., Mork, K.A., Orvik, K.A., Ozhigin, V., 2008. Volume and heat transports to the Arctic Ocean via the Norwegian and Barents Seas, in: Dickson, R.R., Meincke, J., Rhines, P. (Eds.), Arctic–Subarctic ocean fluxes: defining the role of the Northern Seas in climate. Springer, pp. 45–64.

Slagstad, D., Wassmann, P.F.J., Ellingsen, I., 2015. Physical constrains and productivity in the future Arctic Ocean. Front. Mar. Sci. 2. https://doi.org/10.3389/fmars.2015.00085

Smedsrud, L.H., Muilwijk, M., Brakstad, A., Madonna, E., Lauvset, S.K., Spensberger, C., Born, A., Eldevik, T., Drange, H., Jeansson, E., Li, C., Olsen, A., Skagseth, Ø., Slater, D.A., Straneo, F., Våge, K., Årthun, M., 2022. Nordic seas heat loss, Atlantic inflow, and Arctic sea ice cover over the last century. Rev. Geophys. 60. https://doi.org/10.1029/2020RG000725

Smith Jr., W.O., 1995. Primary productivity and new production in the Northeast Water (Greenland) Polynya during summer 1992. J. Geophys. Res. Oceans 100. https://doi.org/10.1029/94JC02764

Smith, W., Gosselin, M., Legendre, L., Wallace, D., Daly, K., Kattner, G., 1997. New production in the Northeast Water Polynya: 1993. J. Mar. Syst. 10. https://doi.org/10.1016/S0924-7963(96)00067-X

Smith, W.O., Barber, D.G., 2007. Polynyas and Climate Change: A view to the future, in: Smith, W.O., Barber, D.G. (Eds.), Elsevier Oceanography Series, Polynyas: Windows to the world. Elsevier, pp. 411–419. https://doi.org/10.1016/S0422-9894(06)74013-2

Sneed, W.A., Hamilton, G.S., 2016. Recent changes in the Norske Øer Ice Barrier, coastal Northeast Greenland. Ann. Glaciol. 57. https://doi.org/10.1017/aog.2016.21

Sokolova, M.N., 1994. Euphausiid "dead body rain" as a source of food for abyssal benthos. Deep Sea Res. Part Oceanogr. Res. Pap. 41. https://doi.org/10.1016/0967-0637(94)90052-3

Soltwedel, T., Bauerfeind, E., Bergmann, M., Bracher, A., Budaeva, N., Busch, K., Cherkasheva, A., Fahl, K., Grzelak, K., Hasemann, C., Jacob, M., Kraft, A., Lalande, C., Metfies, K., Nöthig, E.-M., Meyer, K., Quéric, N.-V., Schewe, I., Włodarska-Kowalczuk, M., Klages, M., 2016. Natural variability or anthropogenically-induced variation? Insights from 15 years of multidisciplinary observations at the arctic marine LTER site HAUSGARTEN. Ecol. Indic., The value of long-term ecosystem research (LTER): Addressing global change ecology using site-based data 65. https://doi.org/10.1016/j.ecolind.2015.10.001

Steer, A., Divine, D., 2023. Sea ice concentrations in the northern Barents Sea and the area north of Svalbard at Nansen Legacy stations during 2017-2021. https://doi.org/10.21334/NPOLAR.2023.24F2939C

Straneo, F., Sutherland, D.A., Holland, D.M., Gladish, C., Hamilton, G.S., Johnson, H.L., Rignot, E., Xu, Y., Koppes, M., 2012. Characteristics of ocean waters reaching Greenland's glaciers. Ann. Glaciol. 53. https://doi.org/10.3189/2012AoG60A059

Stroeve, J., Notz, D., 2018. Changing state of Arctic sea ice across all seasons. Environ. Res. Lett. 13. https://doi.org/10.1088/1748-9326/aade56

Sumata, H., de Steur, L., Gerland, S., Divine, D.V., Pavlova, O., 2022. Unprecedented decline of Arctic sea ice outflow in 2018. Nat. Commun. 13. https://doi.org/10.1038/s41467-022-29470-7

Sun, M.-Y., Clough, L.M., Carroll, M.L., Dai, J., Ambrose, W.G., Lopez, G.R., 2009. Different responses of two common Arctic macrobenthic species (*Macoma balthica* and *Monoporeia affinis*) to phytoplankton and ice algae: Will climate change impacts be species specific? J. Exp. Mar. Biol. Ecol. 376. https://doi.org/10.1016/j.jembe.2009.06.018

Sverdrup, H.U., 1953. On conditions for the vernal blooming of phytoplankton. ICES J. Mar. Sci. 18. https://doi.org/10.1093/icesjms/18.3.287

Szczepanek, M., Silberberger, M.J., Koziorowska-Makuch, K., Nobili, E., Kędra, M., 2021. The response of coastal macrobenthic food-web structure to seasonal and regional variability in organic matter properties. Ecol. Indic. 132. https://doi.org/10.1016/j.ecolind.2021.108326

Takahashi, T., Sutherland, S.C., Wanninkhof, R., Sweeney, C., Feely, R.A., Chipman, D.W., Hales, B., Friederich, G., Chavez, F., Sabine, C., Watson, A., Bakker, D.C.E., Schuster, U., Metzl, N., Yoshikawa-Inoue, H., Ishii, M., Midorikawa, T., Nojiri, Y., Körtzinger, A., Steinhoff, T., Hoppema, M., Olafsson, J., Arnarson, T.S., Tilbrook, B., Johannessen, T., Olsen, A., Bellerby, R., Wong, C.S., Delille, B., Bates, N.R., de Baar, H.J.W., 2009. Climatological mean and decadal change in surface ocean pCO2, and net sea–air CO2 flux over the global oceans. Deep Sea Res. Part II Top. Stud. Oceanogr., Surface Ocean CO2 Variability and Vulnerabilities 56. https://doi.org/10.1016/j.dsr2.2008.12.009

Tande, K.S., 1991. Calanus in North Norwegian fjords and in the Barents Sea. Polar Res. 10.

Thornton, D.C.O., 2002. Diatom aggregation in the sea: mechanisms and ecological implications. Eur. J. Phycol. 37. https://doi.org/10.1017/S0967026202003657

Tremblay, J.-É., Bélanger, S., Barber, D.G., Asplin, M., Martin, J., Darnis, G., Fortier, L., Gratton, Y., Link, H., Archambault, P., Sallon, A., Michel, C., Williams, W.J., Philippe, B., Gosselin, M., 2011. Climate forcing multiplies biological productivity in the coastal Arctic Ocean. Geophys. Res. Lett. 38. https://doi.org/10.1029/2011GL048825

Trudnowska, E., Lacour, L., Ardyna, M., Rogge, A., Irisson, J.O., Waite, A.M., Babin, M., Stemmann, L., 2021. Marine snow morphology illuminates the evolution of phytoplankton blooms and determines their subsequent vertical export. Nat. Commun. 12. https://doi.org/10.1038/s41467-021-22994-4

Turner, J.T., 2015. Zooplankton fecal pellets, marine snow, phytodetritus and the ocean's biological pump. Prog. Oceanogr. 130. https://doi.org/10.1016/j.pocean.2014.08.005

Utermöhl, H., 1958. Zur Vervollkommnung der quantitativen Phytoplankton-Methodik. SIL Commun. (1953-1996) 9. https://doi.org/10.1080/05384680.1958.11904091

Verdugo, P., Alldredge, A.L., Azam, F., Kirchman, D.L., Passow, U., Santschi, P.H., 2004. The oceanic gel phase: a bridge in the DOM–POM continuum. Mar. Chem., New Approaches in Marine Organic Biogeochemistry: A Tribute to the Life and Science of John I. Hedges 92. https://doi.org/10.1016/j.marchem.2004.06.017

Verdugo, P., Santschi, P.H., 2010. Polymer dynamics of DOC networks and gel formation in seawater. Deep Sea Res. Part II Top. Stud. Oceanogr., Ecological and Biogeochemical Interactions in the Dark Ocean 57. https://doi.org/10.1016/j.dsr2.2010.03.002

Vernet, M., Ellingsen, I.H., Seuthe, L., Slagstad, D., Cape, M.R., Matrai, P.A., 2019. Influence of phytoplankton advection on the productivity along the Atlantic Water inflow to the Arctic Ocean. Front. Mar. Sci. 6. https://doi.org/10.3389/fmars.2019.00583

von Appen, W.-J., Waite, A.M., Bergmann, M., Bienhold, C., Boebel, O., Bracher, A., Cisewski, B., Hagemann, J., Hoppema, M., Iversen, M.H., Konrad, C., Krumpen, T., Lochthofen, N., Metfies, K., Niehoff, B., Nöthig, E.-M., Purser, A., Salter, I., Schaber, M., Scholz,

D., Soltwedel, T., Torres-Valdes, S., Wekerle, C., Wenzhöfer, F., Wietz, M., Boetius, A., 2021. Sea-ice derived meltwater stratification slows the biological carbon pump: results from continuous observations. Nat. Commun. 12. https://doi.org/10.1038/s41467-021-26943-z

Vonnahme, T.R., Klausen, L., Bank, R.M., Michellod, D., Lavik, G., Dietrich, U., Gradinger, R., 2022. Light and freshwater discharge drive the biogeochemistry and microbial ecology in a sub-Arctic fjord over the Polar night. Front. Mar. Sci. 9. https://doi.org/10.3389/fmars.2022.915192

Wadhams, P., 1981. The ice cover in the Greenland and Norwegian seas. Rev. Geophys. 19. https://doi.org/10.1029/RG019i003p00345

Wassmann, P., 1998. Retention versus export food chains: processes controlling sinking loss from marine pelagic systems, in: Tamminen, T., Kuosa, H. (Eds.), Eutrophication in Planktonic Ecosystems: Food Web Dynamics and Elemental Cycling. Springer Netherlands, Dordrecht, pp. 29–57. https://doi.org/10.1007/978-94-017-1493-8_3

Wassmann, P., Olli, K., Riser, C.W., Svensen, C., 2003. Ecosystem function, biodiversity and vertical Flux regulation in the twilight zone, in: Wefer, G., Lamy, F., Mantoura, F. (Eds.), Marine Science Frontiers for Europe. Springer Berlin Heidelberg, Berlin, Heidelberg, pp. 279–287. https://doi.org/10.1007/978-3-642-55862-7_19

Wassmann, P., Reigstad, M., 2011. Future Arctic Ocean Seasonal Ice Zones and implications for pelagic-benthic coupling. Oceanography 24. https://doi.org/10.5670/oceanog.2011.74

Wassmann, P., Reigstad, M., Haug, T., Rudels, B., Carroll, M.L., Hop, H., Gabrielsen, G.W., Falk-Petersen, S., Denisenko, S.G., Arashkevich, E., 2006. Food webs and carbon flux in the Barents Sea. Prog. Oceanogr. 71. https://doi.org/10.1016/j.pocean.2006.10.003

Weber, T., Cram, J.A., Leung, S.W., DeVries, T., Deutsch, C., 2016. Deep ocean nutrients imply large latitudinal variation in particle transfer efficiency. Proc. Natl. Acad. Sci. 113. https://doi.org/10.1073/pnas.1604414113

Wekerle, C., Krumpen, T., Dinter, T., von Appen, W.-J., Iversen, M.H., Salter, I., 2018. Properties of sediment trap catchment areas in Fram Strait: Results from Lagrangian modeling and remote sensing. Front. Mar. Sci. 5. https://doi.org/10.3389/fmars.2018.00407

Wexels Riser, C., Reigstad, M., Wassmann, P., Arashkevich, E., Falk-Petersen, S., 2007. Export or retention? Copepod abundance, faecal pellet production and vertical flux in the marginal ice zone through snap shots from the northern Barents Sea. Polar Biol. 30. https://doi.org/10.1007/s00300-006-0229-z

Wexels Riser, C., Wassmann, P., Olli, K., Pasternak, A., Arashkevich, E., 2002. Seasonal variation in production, retention and export of zooplankton faecal pellets in the marginal ice zone and central Barents Sea. J. Mar. Syst., Seasonal C-cycling variability in the open and ice-covered waters of the Barents Sea 38. https://doi.org/10.1016/S0924-7963(02)00176-8

Wiedmann, I., Ershova, E., Bluhm, B.A., Nöthig, E.-M., Gradinger, R.R., Kosobokova, K., Boetius, A., 2020. What feeds the benthos in the arctic basins? Assembling a carbon budget for the deep Arctic Ocean. Front. Mar. Sci. 7. https://doi.org/10.3389/fmars.2020.00224

Wiedmann, I., Reigstad, M., Marquardt, M., Vader, A., Gabrielsen, T.M., 2016. Seasonality of vertical flux and sinking particle characteristics in an ice-free high arctic fjord—Different from subarctic fjords? J. Mar. Syst. 154. https://doi.org/10.1016/j.jmarsys.2015.10.003

Wiedmann, I., Reigstad, M., Sundfjord, A., Basedow, S., 2014. Potential drivers of sinking particle's size spectra and vertical flux of particulate organic carbon (POC): Turbulence, phytoplankton, and zooplankton. J. Geophys. Res. Oceans 119, https://doi.org/10.1002/2013JC009754

Wietz, M., Bienhold, C., Metfies, K., Torres-Valdés, S., von Appen, W.-J., Salter, I., Boetius, A., 2021. The polar night shift: seasonal dynamics and drivers of Arctic Ocean microbiomes revealed by autonomous sampling. ISME Commun. 1. https://doi.org/10.1038/s43705-021-00074-4

Wollenburg, J.E., Katlein, C., Nehrke, G., Nöthig, E.-M., Matthiessen, J., Wolf- Gladrow, D.A., Nikolopoulos, A., Gázquez-Sanchez, F., Rossmann, L., Assmy, P., Babin, M., Bruyant, F., Beaulieu, M., Dybwad, C., Peeken, I., 2018. Ballasting by cryogenic gypsum enhances carbon export in a Phaeocystis under-ice bloom. Sci. Rep. 8. https://doi.org/10.1038/s41598-018-26016-0

Wright, S.W., Jeffrey, S.W., 1997. High-resolution HPLC system for chlorophylls and carotenoids of marine phytoplankton., in: Jeffrey, S.W., Mantoura, R.F.C., Wright, S.W. (Eds.), Phytoplankton Pigments in Oceanography: Guidelines to Modern Methods. Unesco Pub., Paris, pp. 327–341.

Zhang, Y., Zhuang, Y., Ji, Z., Chen, J., Bai, Y., Wang, B., Jin, H., 2023. Impacts of Atlantic water intrusion on interannual variability of the phytoplankton community structure in the summer season of Kongsfjorden, Svalbard under rapid Arctic change. Mar. Environ. Res. 192. https://doi.org/10.1016/j.marenvres.2023.106195

Zhulay, I., Iken, K., Renaud, P.E., Kosobokova, K., Bluhm, B.A., 2023. Reduced efficiency of pelagic–benthic coupling in the Arctic deep sea during lower ice cover. Sci. Rep. 13. https://doi.org/10.1038/s41598-023-33854-0

Ziegler, A.F., Bluhm, B.A., Renaud, P.E., Jørgensen, L.L., 2023. Weak seasonality in benthic food web structure within an Arctic inflow shelf region. Prog. Oceanogr. 217. https://doi.org/10.1016/j.pocean.2023.103109

8 Research Papers

Paper I

ELEMENTA
Science of the Anthropocene

RESEARCH ARTICLE

Weakened pelagic–benthic coupling on an Arctic outflow shelf (Northeast Greenland) suggested by benthic ecosystem changes

Yasemin V. Bodur[1,2,*] , Paul E. Renaud[3], Lidia Lins[4], Luana Da Costa Monteiro[4], William G. Ambrose Jr.[5], Janine Felden[6], Thomas Krumpen[7], Frank Wenzhöfer[1,8], Maria Włodarska-Kowalczuk[9], and Ulrike Braeckman[4]

Arctic marine ecosystems are becoming more boreal due to climate change. Predictions of ecosystem change focus mainly on Arctic inflow or interior shelves, with few comprehensive studies on Arctic outflow regions. During September–October 2017, soft-bottom communities were sampled and benthic ecosystem processes were quantified at 12 stations on the Northeast Greenland shelf (outflow shelf) and compared to the last regional ecosystem study, conducted in 1992 and 1993. The benthic habitat was characterized in terms of sediment granulometry, pigment concentrations, and porewater chemistry (dissolved inorganic carbon, nutrients). Total abundance and biomass of macrobenthos and meiobenthos, bacterial abundance, porewater dissolved inorganic carbon and ammonium concentrations were higher on the outer shelf compared to locations adjacent to the Nioghalvfjerdsfjorden glacier at 79°N and the inner shelf stations (e.g., macrofauna: 1,964–2,952 vs. 18–1,381 individuals m^{-2}). These results suggest higher benthic production in the outer parts of the NEG shelf. This difference was also pronounced in macrobenthic and meiobenthic community structure, which was driven mainly by food availability (pigments with 1.3–4.3 vs. 0.3–0.9 μg g^{-1} sediment, higher total organic carbon content and bacterial abundance). Compared to the early 1990s, warmer bottom water temperatures, increased number of sea-ice-free days and lower sediment pigment concentrations in 2017 were accompanied by decreased polychaete and increased nematode abundance and diversity, and a different community structure of nematode genera. The present study confirms previous reports of strong pelagic-benthic coupling on the NEG shelf, but highlights a possible weakening since the early 1990s, with a potential shift in importance from macrofauna to meiofauna in the benthic community. Increasing inflow of Atlantic water and decreasing volume transport and thickness of sea ice through the Fram Strait, probably affecting the Northeast Water Polynya, may be responsible, suggesting ecosystem-wide consequences of continued changes in sea-ice patterns on Arctic shelves.

[1] Max Planck Institute for Marine Microbiology, Bremen, Germany

[2] Department of Arctic and Marine Biology, UiT—The Arctic University of Norway, Tromsø, Norway

[3] Akvaplan-niva, Tromsø, Norway

[4] Marine Biology Research Group, Ghent University, Ghent, Belgium

[5] Coastal Carolina University, Conway, SC, USA

[6] MARUM, Center for Marine Environmental Sciences, University Bremen, Bremen, Germany

[7] Alfred Wegener Institute Helmholtz Centre for Polar and Marine Research, Sea Ice Physics, Bremerhaven, Germany

[8] HGF-MPG Group for Deep Sea Ecology and Technology, Alfred Wegener Institute Helmholtz Centre for Polar and Marine Research, Bremerhaven, Germany

[9] Department of Marine Ecology, Institute of Oceanology, Polish Academy of Sciences, Sopot, Poland

*Corresponding author:
Email: yasemin.bodur@uit.no

1. Introduction

The marine environment in the Arctic is characterized by the high seasonality of the solar cycle and sea-ice dynamics, which in turn determine the dynamics of nutrient availability and primary production and with that, the availability of food in the ecosystem. Pathways of secondary production in high latitude ecosystems depend on the match of timing between this seasonal primary production and pelagic consumer development (Sakshaug et al., 2009; Meire et al., 2016). Pelagic mineralization patterns determine the amount of organic matter (OM) that ultimately sinks to the seafloor and serves as food for benthic communities (Graf, 1989; Jensen et al., 1990; Wassmann and Reigstad, 2011; Wiedmann et al., 2020). A strong dependency of benthic ecosystems on pelagic-benthic coupling in the Arctic has been documented for fjord (McMahon et al., 2006) and shelf systems (Grebmeier

et al., 1988; Ambrose and Renaud, 1995; Carmack and Wassmann, 2006; Renaud et al., 2008), as well as for the deep Arctic Ocean (Degen et al., 2015; Wiedmann et al., 2020).

The vertical export of OM in the Arctic Ocean varies regionally, with marginal ice zones and polynyas regarded as particularly productive sites (Spies, 1987; Sakshaug and Skjoldal, 1989; Niebauer et al., 1990; Piepenburg, 2005; Grebmeier and Barry, 2007; Wassmann and Reigstad, 2011). Pelagic variations in primary production are usually reflected in the availability of OM at the seafloor and determine the variability of benthic communities (Piepenburg et al., 1997; Bourgeois et al., 2016). Pelagic processes, both physical (e.g., lateral advection) and biological (zooplankton grazing, microbial recycling), influence the pelagic export (Grebmeier and Barry, 1991), with significant impacts on the functioning of underlying benthic communities (Morata et al., 2015).

Changing sea-ice dynamics in the Arctic are expected to have significant consequences for the composition and timing of OM production, with potential impacts on the quality and quantity of food reaching the benthos (Piepenburg, 2005; Carmack and Wassmann, 2006; Wassmann and Reigstad, 2011; Smith et al., 2013; Mäkelä et al., 2017; Hoffmann et al., 2018), and on the fate of the OM at the seafloor (Braeckman et al., 2018). The Arctic sea-ice extent is declining at an accelerating rate (Overland and Wang, 2013; Comiso et al., 2017; Onarheim et al., 2018; Meredith et al., 2019), resulting in an expansion of open-water areas across the Arctic (Overland and Wang, 2013; Barnhart et al., 2016; Comiso et al., 2017; Onarheim et al., 2018). Accordingly, the export of sea ice through Fram Strait, as well as the sea-ice thickness off Northern Greenland, have declined significantly during the last two decades (Spreen et al., 2020; Sumata et al., 2022). Moreover, the heat transport toward the high North through warming water masses (Spielhagen et al., 2011; Beszczynska-Möller et al., 2012; Polyakov et al., 2020; Skagseth et al., 2020; Smedsrud et al., 2022) and enhanced glacial melt, especially from Greenland's glaciers (Rignot and Kanagaratnam, 2006; Nick et al., 2013), are further effects that coincide with climate change. Alterations in ocean temperature and sea-ice cover will also affect the dynamics of seasonal ice zones and polynyas (April et al., 2019), which are hotspots of the food supply for benthic communities (Grebmeier and Barry, 2007), and most likely lead to drastic changes in Arctic ecosystems through all trophic levels (Wassmann et al., 2011).

A longer period of light availability through reduced sea-ice cover might fuel phytoplankton blooms (Arrigo et al., 2008), but the establishment of a bloom and the export of OM depends on multiple factors such as nutrient availability and vertical mixing, induced for example by wind stress (Ardyna et al., 2014). Despite an overall increase in primary production by 30% in the Arctic during the course of the last two decades, primary production on outflow shelves has either decreased or shown no change (Arrigo and van Dijken, 2015). An efficient transport of OM to the seafloor will most likely be influenced by whether locally changing sea-ice dynamics will favor a stratified or mixed regime in the water column (von

Appen et al., 2021). Moreover, sea-ice algae can contribute substantially to total primary production (Horner and Schrader, 1982; Hegseth, 1998) and are regarded as a food source with higher nutritional value (Falk-Petersen et al., 1998; McMahon et al., 2006).

During the first biological observations in the early 1990s, a tight pelagic-benthic coupling was reported for the Northeast Greenland (NEG) shelf, especially within the Northeast Water (NEW) Polynya, located on the northern part of the shelf (Ambrose and Renaud, 1995; Hobson et al., 1995; Piepenburg et al., 1997; Rowe et al., 1997). Within the NEW Polynya, higher primary production and/ or reduced pelagic mineralization resulted in higher benthic production compared to the ice-covered southern part of the NEG shelf (Ambrose and Renaud, 1995; Stirling, 1997). Benthic communities were strongly associated with OM input from the pelagic realm (Piepenburg et al., 1997), and thick ice algal aggregates potentially served as a rich energy source (Gutt, 1995; Bauerfeind et al., 1997). Since these findings, no further biological studies have been carried out in this region. At that time, the Norske Øer Ice Barrier (NØIB) in front of Nioghalvfjerdsfjorden (79°N Glacier), hindered investigations on benthic communities near the glacier.

Today, glacial melt, increasing sea-ice melt and thinning, as well as stronger input of warm Atlantic Water, are acting in concert in altering the NEG shelf between 77°N and 81°N. Since 2003, glaciers around NEG have undergone sustained thinning, and the seasonal floating tongue of the 79°N Glacier, the largest marine-terminating glacier on the NEG shelf, retreated by more than 100 m yr^{-1} between 2001 and 2011 (Khan et al., 2014). Increasing temperatures have led to seasonal break-up events of the NØIB fast ice cover, which historically broke up only in intervals of several decades (Reeh et al., 2001). The NØIB not only stabilizes the floating glacier tongue and constrains its melting, but also blocks advection of sea ice into the NEW Polynya region. As a result, the NEW Polynya, which has been recurring seasonally for at least 1,000 years (Syring et al., 2020), has become a less obvious phenomenon in the last decade: the patterns in sea-ice cover have become much more dynamic, with a more extensive open water area (Reeh et al., 2001; Smith and Barber, 2007; International Space Science Institute [ISSI], 2008; Reeh, 2017). Moreover, NEG receives a substantial amount of freshwater from the southward sea ice and from freshwater transport through Fram Strait, which, together with glacial meltwater, has already led to a substantial freshening of the coastal subsurface waters in this area (Sejr et al., 2017). Therefore, the NEG outflow shelf is especially susceptible to stratification (Carmack and Wassmann, 2006). Additionally, there is an increasing influence of warm Atlantic Water on the shelf (Schaffer et al., 2017).

For the first time since 1993, a reassessment of the spatial patterns of benthic communities and their ecosystem functions was carried out on the NEG shelf during a field campaign in 2017. To investigate their response to ongoing glacial melt, sea-ice thinning and stronger input of Atlantic Water, we compared environmental conditions,

benthic oxygen uptake and remineralization processes, and benthic community parameters (abundance of macrofauna, meiofauna, and bacteria, and macrofaunal and meiofaunal biomass and community composition) with patterns described in 1992 and 1993 during investigations carried out with USCGC *Polar Sea* and R/V *Polarstern*. We hypothesized that increasing stratification and the disappearance of the NEW Polynya resulted in a decoupling of the benthos from the pelagic environment with decreased OM supply to the seafloor, and consequently reduced abundances and functions of benthic communities on the NEG outflow shelf.

2. Materials and methods
2.1. Study site
The NEG continental shelf extends more than 300 km from the coastline (**Figure 1**). Between 77°N and 81°N, two troughs are present: the Westwind Trough in the north and the Norske Trough in the south, which together

half-encircle shallow banks of water depths <200 m located approximately in the middle of the shelf (Arndt et al., 2015; Schaffer et al., 2017). The bathymetry of the trough system provides a valley between the shelf break of the Norske Trough in the south and the shelf break of the Westwind Trough in the north, allowing warm and saline Atlantic Intermediate Water (AIW) originating from the recirculation into the East Greenland Current to enter the NEG shelf via the Norske Trough (Schaffer et al., 2017). AIW occupies depths below 150–200 m (subsurface AIW) and circulates in an anticyclonic way across the shelf (Bourke et al., 1987).

As part of the Northeast Greenland Ice Shelf, the 79°N Glacier has a large floating ice tongue that fills the entire interior of the 79°N Fjord (Thomsen et al., 1997). Underneath is a trough with a maximum depth of more than 900 m, where subglacial melting takes place with a mean melt rate as fast as 8 m yr^{-1} (Mayer et al., 2000). Water warmer than 1°C below the 79°N Glacier (Wilson and
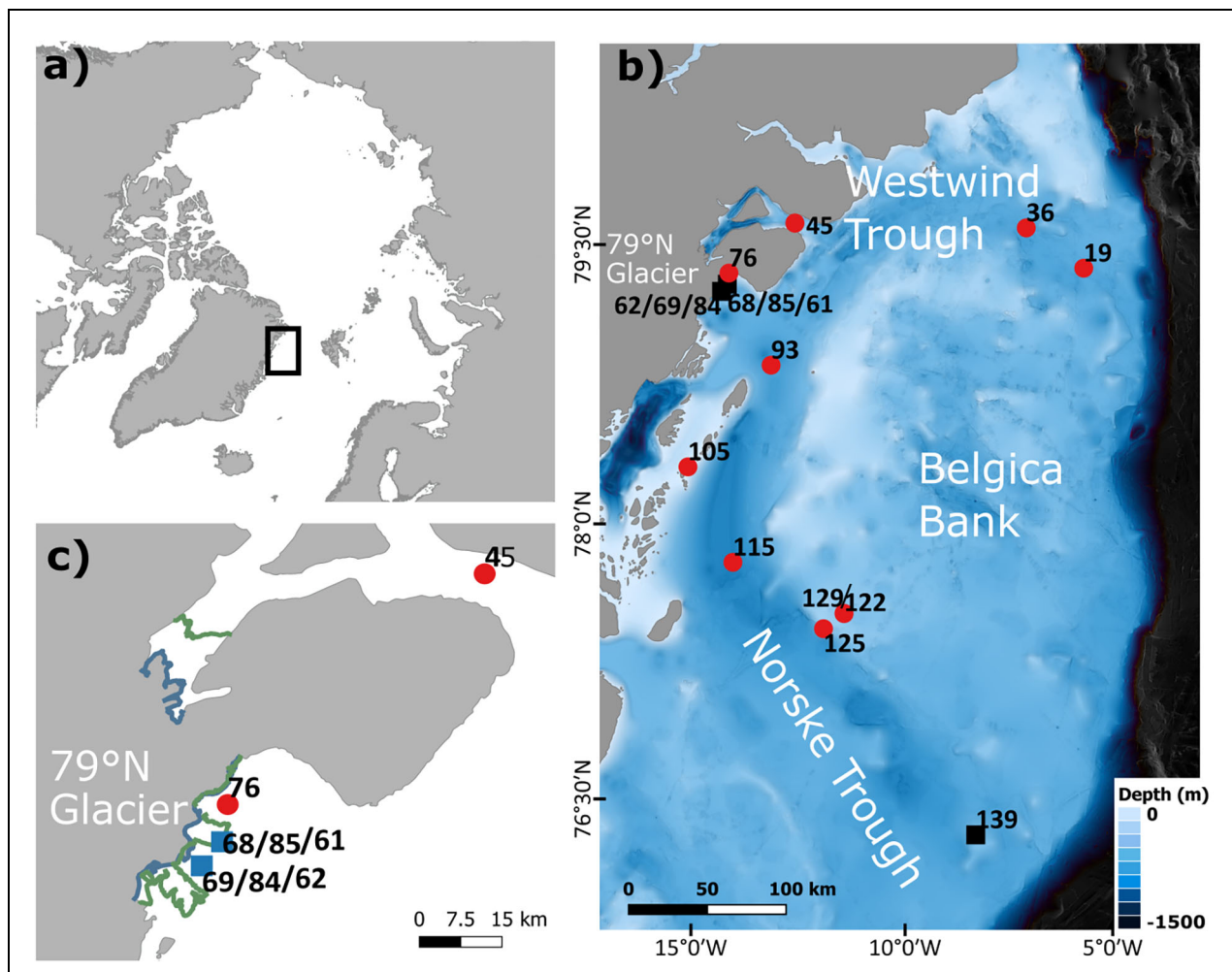

Figure 1. Sampling locations on the Northeast Greenland shelf during 2017. (a) Overview map showing the location of the study area in the Arctic. (b) Station locations from the R/V *Polarstern* cruise PS109 in 2017. Red dots indicate multicorer stations and black rectangles indicate stations where a benthic lander was also used. (c) Closeup of the Glacier stations with calving front from 1990 (green) and 2017 (blue). Background bathymetry is based on the International Bathymetric Chart of the Arctic Ocean (Jakobsson et al., 2020), Coastlines were obtained from Wessel and Smith (1996). Calving front data from 1990 (green line) and 2016 (blue line) were retrieved from the Environmental Earth Observation IT GmbH (ENVEO, 2017).

Straneo, 2015) causes basal melting in this cavity (Mayer et al., 2000; Straneo et al., 2012; Schaffer et al., 2017). Modified AIW leaves the glacier cavity through the calving front and through the Djmphna Sund (Schaffer, 2017), which is located north of the glacier front. The AIW throughout the whole trough system has warmed. In the period between 1979–1999 and 2000–2016, the Norske Trough experienced a temperature increase of 0.5°C (Schaffer et al., 2017; Mayer et al., 2018; Schaffer et al., 2020).

At around 79°30′N, the NØIB, a semi-permanent landfast sea-ice cover and at one time one of the largest areas of landfast ice on Earth (Hughes et al., 2011), was observed to hinder the advection of sea ice into the NEW Polynya at its southern extent (Minnett et al., 1997). The polynya used to open in April or May and close around September (Schneider and Budéus, 1994). It varied in size, located around 80°N in the Westwind Trough, and was reported occasionally to cover an area of 44,000 km^2 (Wadhams, 1981). Two break-ups of the NØIB were observed until 2001, namely in the 1950s and in 1997, which led to an extended open-water area and enhanced calving of the 79°N Glacier (Reeh et al., 2001). Between 2002 and 2005, the NØIB broke up every summer (Hughes et al., 2011).

2.2. Sampling and laboratory analyses

Samples were taken in September and October 2017 during cruise PS109 of the R/V *Polarstern* at 17 multiple corer (MUC) and lander stations at water depths between 140 m and 645 m. Because different deployments of instruments at the same aimed position received individual station numbers, some stations were pooled (namely 69/84/62, 68/85/61, and 122/129), resulting in 12 locations that are henceforth referred to as "stations" (**Figure 1b**, Table S1). Three stations were located in the Westwind Trough, 5 stations in the Norske Trough, and 3 stations close to the 79°N Glacier (Table S1). One station (locations 122 and 129) was located on the shallow Belgica Bank (water depths of 140 m and 139 m, respectively). At each station, a camera-equipped MUC (TV-MUC; core area of 0.007 m^2) was deployed to collect sediment cores for ex situ measurements of oxygen consumption and sediment sampling. Additional in situ oxygen flux measurements were performed with an autonomous benthic lander at three of these stations, one at the outer Norske Trough (Station 139) and two at the margin of the 79°N Glacier (Stations 68 and 69; Table S1). In the following, lander stations are denoted with the suffix "-L" to distinguish them from MUC stations.

CTD profiles (Kanzow et al., 2018) for each benthic station were obtained for temperature and salinity. When a CTD profile was not taken directly at the benthic station, the data from the CTD closest to the station was used (maximum distance to the nearest CTD was 31.5 km at Station 139). At Station 68/85/61, the closest CTD (distance of 13 km) was at a location with a depth of 400 m, so the data from 150 m depth, which was the depth of the benthic station, was taken as bottom water. Bottom water temperatures ranged between −1.07°C and 1.76°C and salinities between 33.96 and 34.94.

2.2.1. Sediment solid–phase parameters

Upon arrival on deck, the upper 5 cm of three MUC cores were sampled in 1 cm intervals with 5 mL cut-off syringes for granulometry, porosity, benthic pigments (chlorophyll *a* (Chl *a*), phaeopigments and fucoxanthin), total organic carbon (TOC), and total nitrogen (TN). Because these cores originated from the same deployment, they are technically pseudoreplicates. Time constraints, however, did not allow for truly replicated deployments. For granulometry, the sediment was sliced in 1 cm intervals and stored in 20 mL scintillation vials or plastic bags. Grain size spectra were assessed by laser diffraction (Malvern Instruments, Malvern, UK; Braeckman, 2023a). Porosity samples were stored in 5 mL cut-off syringes wrapped in aluminum foil. In the laboratory, the samples were sliced in 1 cm sediment depth intervals and the wet mass of the sediment samples was measured and then dried at 60°C in a drying oven. Porosity was calculated by the difference between the wet and dry mass of the samples after Dalsgaard et al. (2000; Braeckman, 2023b).

Chl *a*, phaeopigments (phaeophorbide *a* and phaeophytin *a*) and fucoxanthin were subsampled with 10 mL cut-off syringes, which were pushed gently into the sediment until reaching 5 cm depth, and stored at −80°C. In the laboratory, the samples were sliced in 1 cm horizons and analyzed using high performance liquid chromatography after Wright and Jeffrey (1997; Braeckman, 2023c). Quantities are expressed as microgram pigment per gram of dry sediment ($\mu g\ g^{-1}$). The chloroplastic pigment equivalent (CPE) was calculated as the sum of Chl *a* and phaeopigments.

TOC and TN were determined by treating an aliquot of dried sample with hydrochloric acid until no more bubbles were observed, to remove inorganic carbon prior to analysis. Percent TOC and TN were determined in sediments dried at 250°C using a ELTRA CS2000 Carbon Analyzer (Braeckman, 2023d).

For comparison with the earlier studies, CPE and TOC were converted to grams per meter squared using porosity and sediment density (2.55 g cm^{-3}) in the following equation:

$$\frac{\mu g\ \text{CPE or TOC}}{g\ (\text{dry sediment})} \times (1 - \text{porosity}) \times \text{density} \times 1\ \text{cm} \times 10,000$$

2.2.2. Sediment porewater parameters

At each station, two MUC cores with pre-drilled holes were mounted on the MUC for porewater extractions. Samples for measuring porewater chemistry (DIC, nutrients, sulfate and sulfide concentrations) were collected with Rhizon samplers (pore size 0.2 μm, Rhizosphere, Wageningen, Netherlands) by inserting them carefully into the pre-drilled holes on the retrieved MUC cores with depth intervals of 1 cm until 10 cm sediment depth, and 2 cm intervals until 20 cm sediment depth. The porewater of the two MUC cores was pooled; a total of 9 mL porewater for each depth interval was retrieved in this manner.

To determine the concentration of dissolved inorganic carbon (DIC), 2 mL porewater was sampled in glass vials pre-treated with HgCl$_2$ and stored at 4°C. DIC

concentrations were measured using a flow injection system equipped with the Spark Optimas auto-sampler (model 820, Ambacht, Netherlands). For the analysis of porewater nutrients, 4 mL of porewater was transferred to acid-washed Sarstedt Vials, stored at $-20°C$ and further subsampled in the home lab before analysis (4 mL for phosphate, silicate and ammonium, 1 mL for nitrate and nitrite). Samples were analysed with a Continuous Segmented Flow Analyser (QuAAtro39, SEAL Analytical; Braeckman and Felden, 2023).

2.2.3. Sediment oxygen profiles and oxygen fluxes at the sediment–water interface

For the assessment of ex situ fluxes at the sediment-water interface, part of the overlying water from three cores was removed and stored at in situ temperature separately, while the height of the remaining water above the sediment was adjusted to 10 cm by gently pushing the sediment vertically upwards without disturbing the surface sediment layer. The cores were transferred to a temperature-controlled water bath where the temperature had been adjusted to the in situ values in the bottom water at the respective station (information retrieved from shipboard sensors). The overlying water was homogenized with a magnetic stirrer, and the water surface was gently streamed with a soft air stream to aerate the overlying water.

For the quantification of diffusive oxygen uptake (DOU), two oxygen microprofiles were measured simultaneously, ideally within 2 h of sampling (in some cases >24 h, namely Stations 139, 85, 84, and 76) and for each sediment core with 2 oxygen optodes (Pyroscience, Firesting; tip size 50 μm) mounted on an autonomous microprofiler module. The sensors were two-point calibrated using on-board signals recorded in air-saturated surface seawater and anoxic, dithionite-spiked bottom water at in situ temperature (Felden et al., 2023).

After microprofiling, total oxygen uptake (TOU) was assessed from the decrease in oxygen concentration in the overlying water over time for approximately 48 h (at least 36 h). The cores were closed with no air bubbles in the overlying water, and magnetic stirrers ensured the homogenization of the overlying water. An oxygen optode (Pyroscience, Firesting) measured the oxygen concentration continuously in the overlying water (measuring interval of 60 s, calibrated as described above). Total sediment oxygen flux was determined as the decrease in oxygen concentration in the water phase, which was read from the continuous oxygen sensor data. The incubation was terminated at ≤80% initial $[O_2]$ (Braeckman and Wenzhöfer, 2023).

To quantify in situ fluxes at the sediment-water interface, an autonomous benthic lander equipped with three benthic chambers (area of 0.04 m^2), a sediment profiler and a Niskin bottle were deployed at selected stations. Upon arrival at the seafloor and a waiting time of 4 h after the lander deployment to allow resuspended matter to settle (Glud et al., 1994; Tengberg et al., 1995; Donis et al., 2016), the lander chambers were driven slowly into the sediment. The lander chambers enclosed 20 × 20 cm of sediment and about 10–15 cm of overlying water

(depending on the final orientation of the lander). The enclosed overlying water was gently stirred to avoid stagnation. A syringe sampler collected overlying water samples at regular times for the analysis of nutrients and DIC, while an Aanderaa optode (4330, Aanderaa Instruments, Norway, two-point calibrated as described above) continuously measured the oxygen concentration in the overlying water every 10 min during the total incubation time of around 48 h.

At the end of the incubation, chambers were closed and the incubated sediment was retrieved with the lander from the seafloor. On board, the volume of overlying water in the chambers was estimated from the surface and the height of the overlying water body, measured with a ruler at 6 to 8 positions within each chamber and subsampled for the above-mentioned sediment parameters.

Simultaneously to the chamber incubations, electrochemical oxygen microsensors (adapted and customized after Revsbech, 1989, and calibrated with a two-point calibration) measured in situ oxygen profiles at 3–5 points. The bottom water oxygen concentration (taken from the Niskin bottle and estimated by Winkler titration) was used as the first calibration point. When the sensor had reached the anoxic zone of the sediment, the sensor signal at this point was taken as the second calibration point. Otherwise, the sensor signal in an anoxic solution of sodium dithionite was used. The maximum profiling depth of the profiler during in situ measurement was 180 mm, with profiling resolution of 100 μm.

Both ex situ (MUC cores) and in situ (lander) DOU fluxes across the sediment-water interface were calculated from running average-smoothed oxygen profiles using Fick's first law (Glud et al., 1994). Ex situ TOU fluxes were calculated from the initial linear decrease in O_2 concentration versus time (first 30 h) in the enclosed overlying water body (Glud et al., 1994). Due to issues with optodes, in situ TOU fluxes could only be measured at Station 139-L.

2.3. Benthic community parameters
2.3.1. Bacterial abundance

The upper 5 cm of the sediment was sampled with a 10 mL cut-off syringe and sliced into 1 cm layers, corresponding to 2 mL marked on the syringe. Each slice was transferred to a scintillation vial, and fixed by adding 9 mL of filtered (0.22 μm) 3% (final concentration) formaldehyde-artificial seawater solution. Afterwards, the samples were diluted further with the same solution, filtered through polycarbonate filters (0.2 μm, Whatman Nuclepore Track-Etch Membrane) and stained with a 0.001% acridine orange solution after Hobbie et al. (1977). Single cell abundances were estimated from counts of at least 30 grids for 2 replicate filters per sample with a Zeiss Axiophot microscope (Germany) and a 100× oil immersion objective lens (Zeiss Plan-Apochromat, Germany; Bodur et al., 2023a). For each 1 cm layer, quantities are expressed in cells mL^{-1} (equivalent to 1 cc wet sediment) after accounting for all dilution steps. For summed layers, 0–5 cm, used as an environmental variable (Section 2.5.1), quantities are expressed in cells cm^{-2}.

2.3.2. Macrofaunal and meiofaunal communities

At the end of the ex situ incubations, the MUC cores were opened and meiofaunal communities were sampled with a cut-off 10 mL syringe (area 1.89 cm^2) to 5 cm sediment depth. This subsample was further sliced in 5 horizons of 1 cm. The leftover sediment in the MUC core was sliced into 0–5 cm and 5–10 cm layers and sieved over a 500 μm mesh to collect macrofauna. Sediments from lander chambers were sieved entirely on a 500 μm mesh. Samples were stored in 4% seawater-buffered formaldehyde in Kautex bottles at room temperature.

In the lab, the samples were stained with Rose Bengal. Macrofaunal individuals were identified to the lowest possible taxon level. The blotted wet formalin weight of macrofaunal individuals was determined with a DeltaRange XP56 or AX205 precision balance (Mettler Toledo, Ohio, USA), depending on the organism size and weight. It should be noted that, because of the extremely small size of some specimens, the evaporation of water led to a steady decrease of weight on the precision balance. Polychaetes were removed from their tubes before weighing, and molluscs were weighed with their shells. Other encrusting and calcifying organisms such as bryozoans were also weighed with their tests, such that their biomass is most likely overestimated. Colonial animals such as Bryozoa and Hydrozoa were weighed for biomass estimations but excluded for density and community analysis. When no head was present in the sample but body segments were, polychaete taxa were counted as one specimen due to the general low abundance of specimens in the samples. Nematoda and other worms that inhabited foraminifera tests (Nematoda, small Nemertea) were excluded from the biomass and density calculations as they were not part of the macrofaunal communities (Bodur et al., 2023b).

For the representation of total biomass, the wet weight of individuals >1,000 mg was removed in order to reduce skewing of the data: 1 individual of *Ctenodiscus crispatus* (5,773 mg, Station 139), *Ophiopleura borealis* (3,048 mg, Station 68), *Allantactis parasitica* (3,018 mg, Station 139), *Priapulus bicaudatus* (2,846 mg, Station 36), and *Ophiocten sericeum* (1,471 mg, Station 129). All other individuals were <712 mg. We preferred removing these outliers instead of transforming the data.

Samples from the 5–10 cm sediment depth from the stations with the highest faunal abundance (Stations 36, 125, and 129) were checked for presence of fauna. Only one body part of a specimen of Maldanidae was found in one sample from Station 36; therefore, sediment depths >5 cm were not considered further for community analyses.

Meiofauna were extracted from the samples by triple density centrifugation with the colloidal silica polymer LUDOX TM 40 (Heip et al., 1985) and rinsed with freshwater on stacked 1 mm and 32 μm mesh sieves. The fraction retained on the 32 μm mesh sieve was preserved in 4% Li$_2$CO$_3$-buffered formalin and stained with Rose Bengal. All metazoan meiobenthic organisms were classified at higher taxonomic levels and counted under a stereoscopic microscope (Leica MZ 8, 16×5×; Da Costa Monteiro et al., 2023a). All Nematodes of each sample were handpicked with a fine needle, transferred to glycerine (De Grisse I, II, and III; Seinhorst, 1959), mounted on glass slides, identified to genus level based on the Nemys website (Nemys, 2022), and allocated to functional feeding groups based on Wieser (1953) as selective deposit feeders (1A), non-selective deposit feeders (1B), epistratum feeders (2A) or predators/scavengers (2B; Da Costa Monteiro et al., 2023b).

2.4. Data utilized from 1992 and 1993

Data from the early 1990s for bottom water temperature, sediment CPE, TOC content, TOU and Polychaeta and Nematoda abundances were available from campaigns of the US Coast Guard vessel *Polar Sea* between July 18 and August 1, 1992, and from R/V *Polarstern* during cruises PS25 and PS26 between May and August 1993 (Ambrose and Renaud, 1995; Piepenburg et al., 1997; Rowe et al., 1997; Renaud and Ambrose, 2023). A map of the stations from 1992 and 1993 that were used for comparison is given in **Figure 2**. For TOC and CPE content, one subcore (1.9 × 2 cm) from 2–7 replicate boxcores (0.25 m^2) was taken at each station. Three subcores (8 × 15 cm) sampled from each boxcore were taken for Polychaeta and subsequently sieved through 500 μm mesh sieve. For further details see Ambrose and Renaud (1995) and Renaud and Ambrose (2023). Nematodes were sampled with a multicorer, from which one subsample of 50 mL sediment was taken (16.67 cm^2 down to 3 cm depth; see Piepenburg et al., 1997; Preben and Herman, 2023). Benthic respiration was measured in situ by deploying benthic chambers, as well as ex situ with shipboard micro-incubation chambers (Rowe et al., 1997).

2.5. Data processing and statistical analyses

2.5.1. Analysis of benthic environmental and community patterns from 2017

For data analysis, the number of sea-ice-free days within the sampling year was calculated for each of the stations rather than selecting a daily resolution of sea-ice concentration because processes in the upper water column are reflected in the benthic communities after a time lag (Rowe et al., 1997). The applied sea-ice concentration product is provided by CERSAT (Ezraty et al., 2007) on a 12.5 km grid and is based on 85 GHz Special Sensor Microwave/Imager brightness temperatures, using the ARTIST Sea Ice algorithm (Kaleschke et al., 2001). Water depth values were taken from the benthic MUC stations. Values for bottom water temperature and salinity were taken from the deepest point measured by the shipboard CTD (Kanzow et al., 2018). For median grain size and silt fraction at each station, the mean value across all sediment depth layers was taken. Pigment concentrations and single cell abundances were integrated (summed) over the top 0–5 cm sediment. Measurements of environmental parameters, single cell abundances, and macrofaunal communities obtained by landers were taken as additional station data replicates, when available.

A similarity profile routine (SIMPROF) analysis was performed on standardized (scaled to zero mean and unit
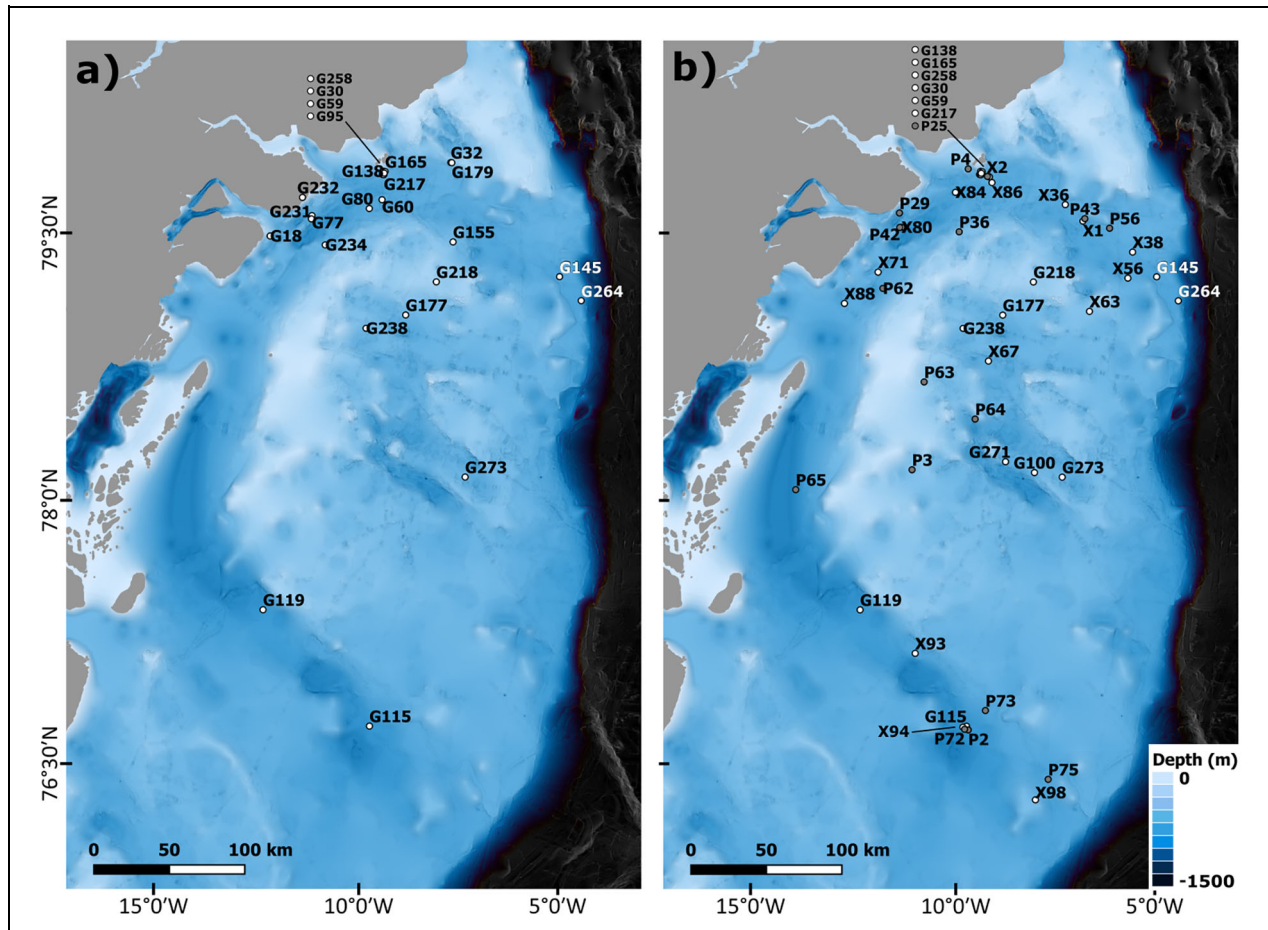
Figure 2. Sampling locations during the 1992 and 1993 USCGC *Polar Sea* and R/V *Polarstern* campaigns. Stations sampled for the (a) Nematoda and (b) Polychaeta data used in this study. Locations taken from Ambrose and Renaud (1995), Piepenburg et al. (1997), and Rowe et al. (1997). Sampling years are distinguished by gray (1992) and white (1993) circles.

variance) environmental variables (number of sea-ice-free days, depth, temperature, salinity, grain size, CPE, TOC, TOC/TN ratio, ammonium, DIC, nitrite, phosphate, silicate and single cell abundances) in order to test a priori how many station groups based on the environment were delineated on a significance level of alpha = 0.05. SIM-PROF is a cluster analysis tool that determines significant clusters of the stations without a priori grouping of samples. Based on these bias-free results, we divided the communities into the regions distinguished by these significant environmental clusters.

A non-parametric ranked Kruskal–Wallis test was performed on each of the ex situ community parameters (macrofaunal abundance, Polychaeta abundance, macrofaunal biomass, and Polychaeta biomass) in order to test whether the communities at the different stations could be distinguished by environmentally different regions ("sites"; the station clusters formerly delineated by the SIMPROF test based on environmental variables). Kruskal–Wallis was used because no dataset was normally distributed even after transformation and the sample size per group was small.

Two correspondence analyses (CA) were performed on the relative abundances of macrofauna and meiofauna

to visualize the differences in community structure among stations. No transformation was applied to the community datasets. Standardized environmental variables were fitted on top of the species relative abundance ordination to indicate which environmental variables contributed the most to the observed patterns in species abundance.

2.5.2. Comparison with data from the early 1990s

The number of sea-ice-free days within the sampling year at each of the stations was calculated as described in Section 2.5.1 for the years 1992, 1993, and 2017. The available environmental (bottom water temperature, sediment CPE and TOC content, number of ice-free days) and community parameters (total Nematoda and Polychaeta abundance) between 1992, 1993, and 2017 were displayed with barplots. Subsequently, a CA was performed on relative family abundances (abundance of a family in a sample divided by the total abundance of all families in that sample) of Polychaeta from 1992, 1993, and 2017 in order to minimize errors due to the possible variation of species identification between the different sampling campaigns. The same was applied to Nematoda at the genus level, with data from Preben and Herman (2023).

Unidentified taxa were removed from both datasets, and validity of taxa names were checked on marinespecies.org.

A PERMANOVA was performed in order to test whether "time" (sampling years; categorical), "site" (previously delineated by SIMPROF on the 2017 data; categorical), and/or the "interaction between time and site" had a significant effect on the differences among Polychaeta and Nematoda community patterns between the different years (p < 0.05). All statistical analyses were performed using the computing environment R (Version 4.2.2; R Core Team, 2018) with the packages *vegan* (Oksanen et al., 2018) and *clustsig* (Whitaker, 2021).

3. Results

3.1. Environmental characteristics on the NEG shelf

Sea-ice-free days were lowest at the Glacier stations (0 ice-free days) and highest at the stations further away from shore (75–80 ice-free days; Figure S1). Water depth of the stations ranged between 140 m and 502 m. The shallowest stations were Station 122/129 (140 m), which were located on Belgica Bank, and Station 61/85/68 (156 m), located on a shoal directly in front of the glacier margin, peaking from a 300–500 m deep area. In 1992, the location of Station 61/85/68 was still covered by the 79°N Glacier (**Figure 1c**). In general, stations at the Glacier and in the Westwind Trough were shallower than the Norske Trough stations (206–315 m and 354–502 m, respectively). Bottom water salinity and temperature indicated the presence of water of Atlantic origin in the Norske Trough and at the Glacier (1.49–1.76°C; except for shallow Glacier Station 61/85/68), while stations in the Westwind Trough were influenced by cooler and fresher glacially modified water (0.69–0.87°C; Figure S2). The station on Belgica Bank was influenced by cold and fresher water.

Median grain size was lowest at all Glacier stations (9–10 μm) and highest on Belgica Bank (49 μm), followed by the Westwind Trough and outer Norske Trough (21 μm and 23 μm at Stations 19 and 36, and 20 μm and 48 μm at Stations 139 and 129, respectively; Figure S3a). Across the NEG shelf, the silt content was extremely high, with values of around 95% at the Glacier stations and about 80% at the other stations. Average concentrations of all measured pigment compounds in the upper 5 cm (CPE, as the sum of Chl *a* and phaeopigments, and fucoxanthin) were highest in the Westwind Trough, where the CPE range was 1.3–4.3 μg g^{-1} sediment (Figure S3b and c). At all other sites the range of values was 0.3–0.8 μg g^{-1} sediment, with similar ranges at the Glacier stations compared to the Norske Trough. TOC concentrations were very low at the Glacier stations (0.91–1.48 g m^{-2}) and highest in the Westwind Trough (2.96–3.81 g m^{-2}; Figure S3e). When single cell abundances (bacterial cells mL^{-1}; Figure S4) in all sediment sections, 0–5 cm, were summed, the abundances were lowest at all Glacier stations (2–4 × 10^9 cells cm^{-2}) and highest in the Westwind Trough (8 × 10^9–1 × 10^{10} cells cm^{-2}). Based on environmental variables, the SIMPROF analysis identified 4 spatially defined, distinct groups (Westwind Trough, 79°N Glacier, Norske Trough, and Belgica Bank; Figure S5).

3.2. Benthic processes

Total oxygen uptake was very low across all sites (**Figure 3**). Highest uptake rates were measured at Station 45 in the Dijmphna Sound, and at Station 139/139-L in the outer Norske Trough (2.17 and 1.64 mmol m^{-2} d^{-1}, respectively). Lowest uptake was measured at Stations 125 and 85 (around 1.2 mmol m^{-2} d^{-1}). Diffusive oxygen uptake was highest at Station 85/68-L (3.74 mmol m^{-2} d^{-1}) and lowest at Stations 93 and 125 (1.3 and 1 mmol m^{-2} d^{-1}, respectively).

Porewater nutrient concentrations were generally low (Figure S6). Sulfate and sulfide were not detected in the sampled cores. Overall, the Westwind Trough revealed
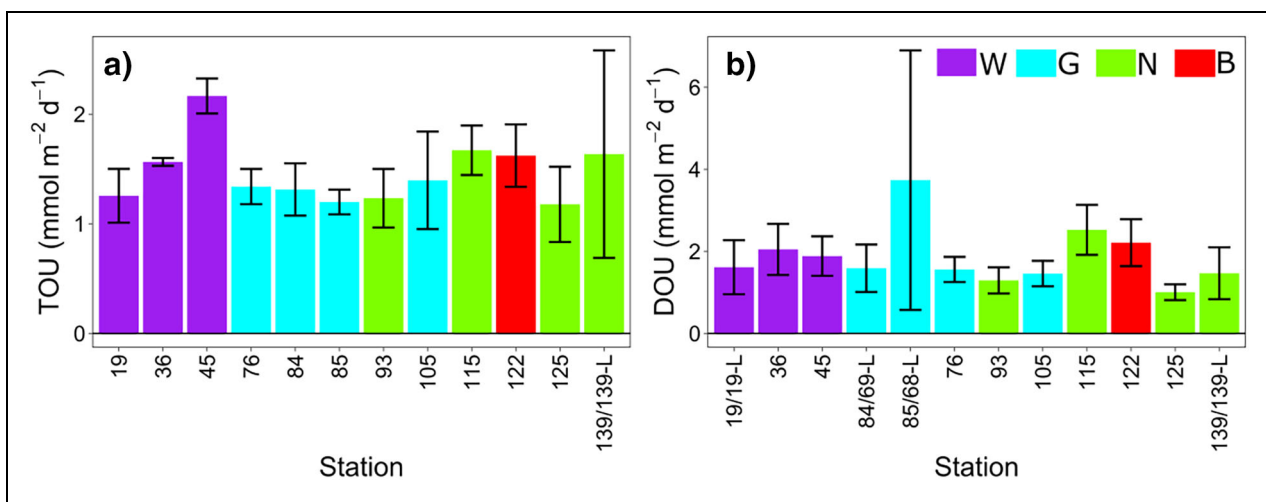

Figure 3. Ex situ total (TOU) and dissolved oxygen uptake (DOU) at the sediment-water interface. Means and standard deviations (error bars) for (a) TOU (n = 2–3, except for pooled station 139/139-L where n = 6) and (b) DOU (n = 10–12, except for pooled stations 19/19-L, 84/69-L, 85/68-L and 139/139-L, where n > 20) are given for each station. Colors represent the 4 sites statistically identified by the SIMPROF analysis based on standardized environmental data (Figure S5): Westwind Trough (W), 79°N Glacier (G), Norske Trough (N), and Belgica Bank (B).

different nutrient profiles than observed at all other sites. Ammonium concentrations were highest at Westwind Trough stations, where values increased with sediment depth (data not shown). At all other stations, ammonium concentrations were close to 0. Highest concentrations of nitrate were present at Norske Trough Stations 139 (103.0 mmol m^{-3}), 115 (89.9 mmol m^{-3}), and 125 (85.6 mmol m^{-3}). Nitrite was not detected at most of the Norske Trough stations, except Station 93. The range of nitrite concentrations at Westwind Trough stations was $0.3–0.6$ mmol m^{-3}, while at the Glacier stations the range was $0–0.2$ mmol m^{-3}. Phosphate was present overall in low concentrations of $3.2–14.4$ mmol m^{-3}. DIC concentrations did not differ much across sites, varying between 5.58 mol m^{-3} and 8.89 mol m^{-3} across all sites. Silicate exhibited the highest concentrations in the Westwind Trough.

3.3. Benthic community characteristics

In total, 319 macrofaunal individuals from ex situ and 115 from in situ samples were identified, belonging to 109 and 62 distinct taxa, respectively. Polychaeta was the most represented phylum in abundance, with Maldanidae being the most abundant polychaete family. The most abundant macrofaunal species was *Boltenia ovifera* (Ascidiacea), with an average of 757 ind m^{-2} at Station 125, followed by juvenile Bivalvia at Station 19, with an average of 571 ind m^{-2}. All other macrofaunal taxa occurred with average densities lower than 571 ind m^{-2} (fewer than 4 individuals per sample). One of the triplicate samples at Glacier Station 85 did not contain any macrofaunal individuals except for a single colonial Bryozoan specimen (*Escharella sp.*), which could not be weighed due to its small size and fragility. Total macrofaunal densities were high ($1,809–2,762$ ind m^{-2}) at Station 122/129 on the Belgica Bank, at all stations in the Westwind Trough, at Station 125 in the Norske Trough, and at Glacier Station 76 (**Figure 4a**, Table S2). At all other stations macrofaunal densities were lower than 1,381 ind m^{-2}. Similar to density, biomass was the highest on Belgica Bank with 44.0 g m^{-2}, followed by the Westwind Trough ($8.4–22.3$ g m^{-2}) and lowest at the Glacier ($0.8–5.7$ g m^{-2}; **Figure 4e**). The non-parametric Kruskal–Wallis test performed on ex situ community parameters did not reveal significant differences among sites based on macrofaunal abundance ($p = 0.08$), Polychaeta abundance ($p = 0.32$), macrofaunal biomass ($p = 0.05$), and Polychaeta biomass ($p = 0.09$).

The highest densities of meiofauna were found in the Westwind Trough and on the Belgica Bank ($2,707$ ind cm^{-2} at Station 36 and 2,175 ind 10 cm^{-2} at Station 122; **Figure 4e**). The lowest densities were found at the Glacier stations ($693–737$ ind 10 cm^{-2}) and in the inner Norske Trough at Station 93 (466 ind 10 cm^{-2}). Across all stations, Nematoda comprised more than 85% of the meiofauna and their abundance pattern largely followed that of the total meiofaunal densities. Analyses on functional feeding groups did not show any pattern among stations (data not shown).

3.4. Relationship of benthic community parameters and environmental variables

Westwind and Norske Trough stations were distinct in the correspondence analysis plots for both macrofauna and meiofauna. In the CA based on macrofaunal density from ex situ MUC cores, the eigenvalues of the first and second correspondence axes (CA1 and CA2) accounted for 15% and 14% of the total variation each (Table S3, **Figure 5a**), together explaining 29% of the overall variation. The Westwind Trough stations correlated positively with higher CPE, TOC and single cell abundances, while the Norske Trough stations correlated negatively with these parameters. The Glacier stations grouped with the Norske Trough stations. The only vectors that were significantly correlated to the displayed ordination were CPE ($R^2 = 0.82$, $p = 0.007$), salinity ($R^2 = 0.75$, $p = 0.010$), and TOC ($R^2 = 0.67$, $p = 0.044$).

The CA based on meiofaunal relative density showed that the Westwind Trough stations, similarly to macrofaunal communities, were characterized by higher CPE, TOC, and single cell abundances compared to the Norske Trough (Table S3, **Figure 5b**). Here, CA1 and CA2 together explained a much higher fraction of the overall station variance compared to macrofaunal relative density (CA1 = 34% and CA2 = 29%). Only CPE was significantly correlated with the displayed ordination ($R^2 = 0.74$, $p = 0.009$).

3.5. Comparison to the early 1990s

Overall, Polychaeta densities were 4.8 times lower, and Nematoda densities 3.4 times higher, in 2017 compared to the early 1990s (**Figure 6a** and **b**). These differences were much more pronounced in the Westwind Trough ($3,494$ ind m^{-2} in the 1990s vs. 703 ind m^{-2} in 2017 for Polychaeta and 264 ind 10 cm^{-2} in the 1990s vs. 2,053 ind 10 cm^{-2} in 2017 for Nematoda) than in the Norske Trough (861 ind m^{-2} in the 1990s vs. 537 ind m^{-2} in 2017 for Polychaeta and 45 ind 10 cm^{-2} in the 1990s vs. 1,214 ind 10 cm^{-2} in 2017 for Nematoda). While TOC concentrations, as well as TOU, were relatively similar between the early 1990s and 2017 ($0.31–1.45$ g m^{-2} and $0.46–1.31$ g m^{-2} for TOC in the early 1990s and in 2017, respectively; $11–148$ µmol m^{-2} h^{-1} and $49–100$ µmol m^{-2} h^{-1} for TOU in 1993 and in 2017, respectively; **Figure 6c** and **d**), CPE was 9.9 times higher in the early 1990s compared to 2017 (**Figure 6f**). Bottom water temperature across all stations sampled in 2017 was 2.8 times higher compared to the stations in the 1990s (**Figure 6e**).

A CA performed on abundances of Polychaeta families from the 1990s and 2017 displays that the stations from 2017 group on the left side of the ordination, while the stations from the 1990s group on the right side (**Figure 7a** and Table S4). In total, the first two axes explain 28.9% of the total variation. In particular, the stations on the Belgica Bank (122 and 129) clearly group further apart from all other stations.

The CA based on Nematoda genera shows a much stronger distinction between 2017 and 1993; the two years are clearly separated along the CA1, explaining
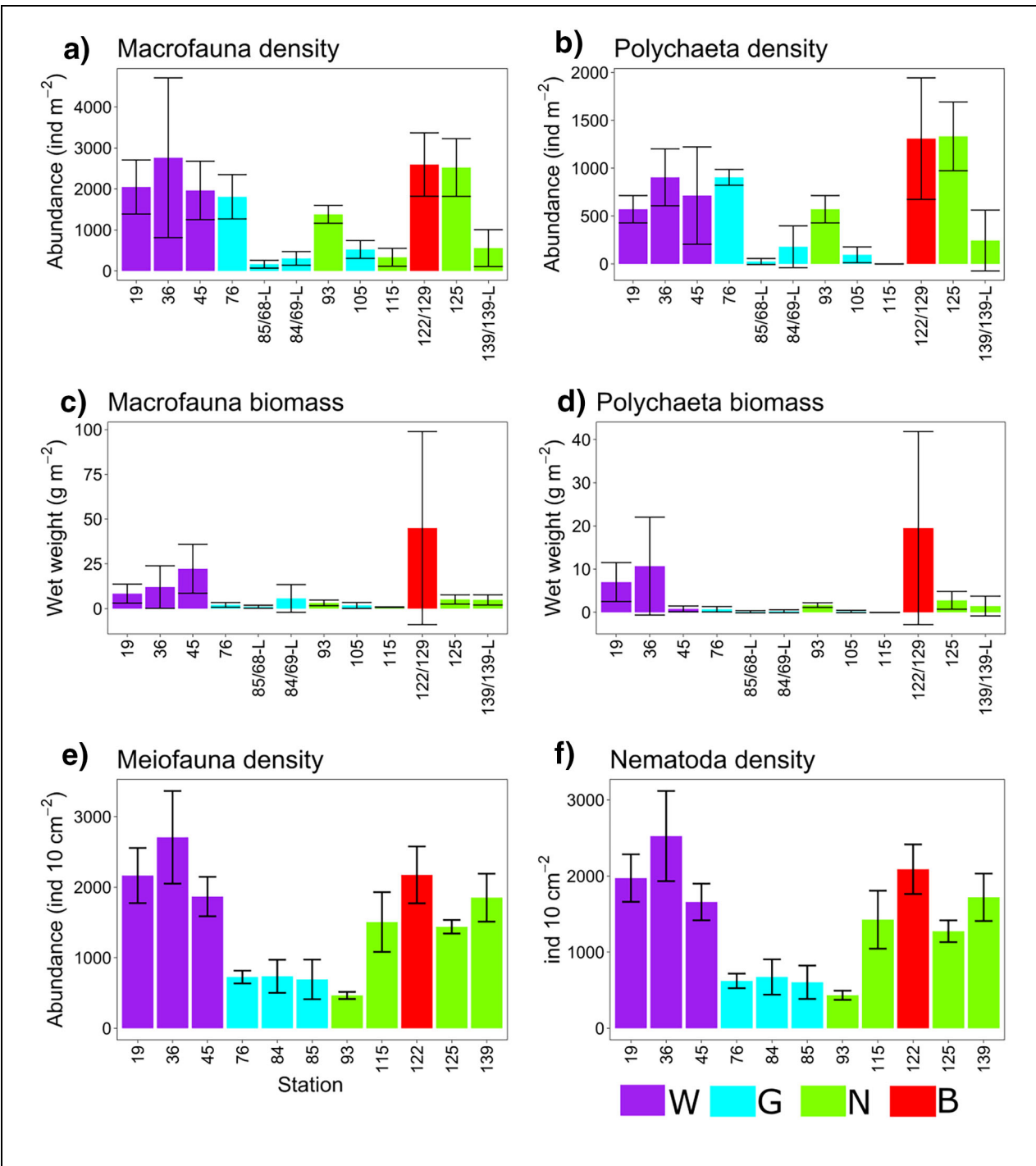
Figure 4. Macrofaunal and meiofaunal community parameters at each station. Means and standard deviations (error bars) are shown for (a, b, e, f) abundance (density) data and (c, d) biomass data (n = 3, except for pooled stations 85/68-L, 84/69-L, 122/129, 139/139-L, where n = 6). Colors represent the 4 sites statistically identified by the SIMPROF analysis based on standardized environmental data (Figure S5): Westwind Trough (W), 79°N Glacier (G), Norske Trough (N), and Belgica Bank (B). However, differences among sites based on these community parameters were not significant.

22.2% of the total variation (**Figure 7b** and Table S4). The number of observed genera was much higher in 2017, with 155 genera identified versus 79 genera identified in 1993. Along CA2, all stations except for the Westwind stations are grouped together, while there is a gradient for the Westwind stations from the Glacier toward the outer part of the

trough. In the 1990s, a distinction between the Westwind and the Norske Trough stations is visible along the CA2. A PERMANOVA performed on each of the datasets (Polychaeta and Nematoda) revealed significant differences based on time, site, and the interaction between time and site, with p-values < 0.03 (**Table 1**).
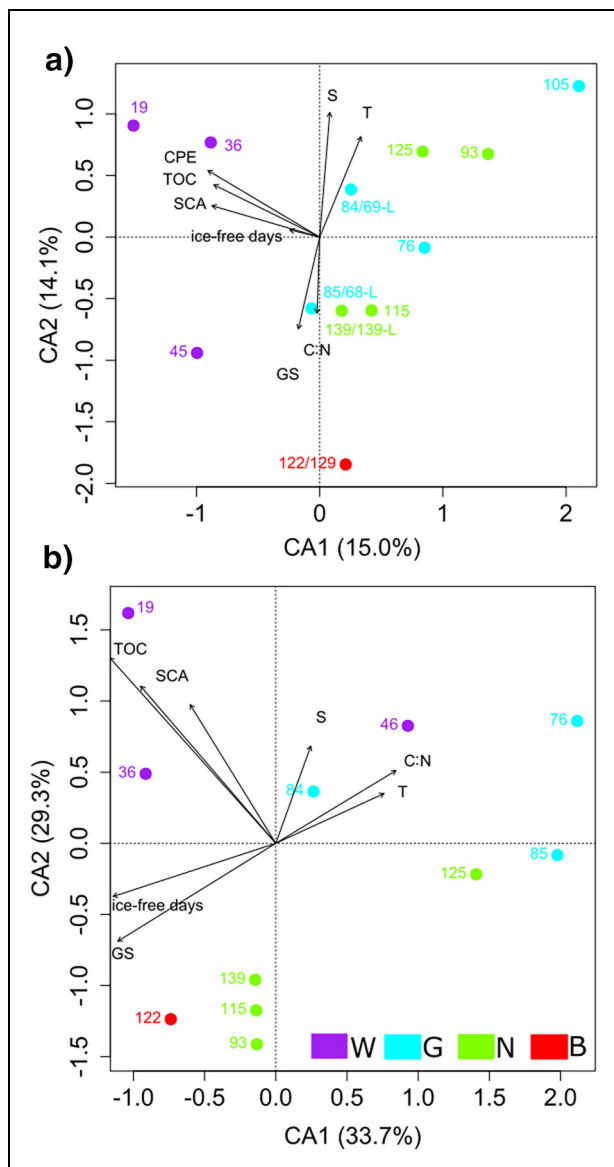
Figure 5. Visualization of the correspondence analysis for macrofaunal and meiofaunal communities with environmental parameters. Relative abundances of (a) macrofauna and (b) meiofauna with standardized environmental parameters fitted onto their ordination as supplementary variables. Colors represent the 4 sites statistically identified by the SIMPROF analysis based on standardized environmental data (Figure S5): Westwind Trough (W), 79°N Glacier (G), Norske Trough (N), and Belgica Bank (B). Tested environmental parameters are number of sea-ice-free days (ice-free days), sediment TOC:TN ratio (C:N), chloroplastic pigment equivalent (CPE), grain size (GS), single cell abundances (SCA), bottom water salinity (S) and temperature (T).

4. Discussion

4.1. Regional variations on the NEG shelf: Stronger pelagic-benthic coupling in the Westwind Trough

Marked regional differences in sediment organic matter content on the NEG shelf matched those in benthic biota. The Westwind Trough displayed the highest CPE and TOC content and highest single cell abundances. The strongest regional contrasts in abundance and biomass of benthic macrofauna and meiofauna were observed between the stations closest to the 79°N Glacier and the coast and those in the Westwind and outer Norske Trough area. Close to the Glacier, densities and biomass of macrofauna and meiofauna were the lowest. The similar responses of the different faunistic groups (macrofauna and meio-fauna) to the strongest contrasts in environmental variables (CPE and TOC content), and CPE being the only parameter that was significantly correlated to both ordinations, suggest that food availability is the main driver of the structure of these communities (**Figure 5**; Piepenburg et al., 1997). These results add to an extensive body of evidence linking spatial patterns in benthic community structure with those of pelagic productivity on Arctic shelves (Grebmeier and Barry, 1991; Ambrose and Renaud, 1995; Carroll et al., 2008).

Our data suggest that the reason for the lower abundance and biomass of benthic infauna in the areas closer to the 79°N Glacier is, as mentioned above, lower food input compared to the Westwind and outer Norske Troughs. These differences in food availability are similarly reflected in different benthic Foraminifera communities between the inner and the outer NEG shelf (Davies et al., 2023). Arctic benthic community structure is highly dependent on annual patterns of carbon export from primary production in the upper water column. In contrast, respiration of benthic communities on the NEG shelf is coupled to OM pulses (Rowe et al., 1997). This relationship is tightly driven by sea-ice dynamics. The stations in the Westwind Trough and outer Norske Trough are located in the marginal ice zone (Figure S1) where the number of sea-ice-free days was higher compared to the Glacier stations and the innermost Norske Trough Stations 93 and 105 which are close to the coast. Benthic communities feature especially high abundance and biomass at the marginal ice zone (Hoffmann et al., 2018), and higher faunal abundance, biomass, distinct community structure, and correspondence with higher values of CPE in these regions were also noted in the 1990s (Ambrose and Renaud, 1995; Piepenburg et al., 1997).

The elevated silicate concentrations in the pore water of Westwind Trough sediments are consistent with higher benthic fucoxanthin concentrations, indicating a higher diatom input in Westwind Trough. In addition, ammonium and nitrite concentrations in the porewater were higher in Westwind Trough compared to the other sites (Figure S6), indicative of higher mineralization rates. When oxygen is depleted, nitrate is used as the next suitable electron acceptor in microbial metabolism. Indeed, in Westwind Trough sediments, nitrate was depleted with depth (data not shown; see Braeckman and Felden, 2023), which could point to denitrification taking place in the deeper sediment layers. At all other sites, nitrate was not depleted with depth, and ammonium and silicate concentrations were much lower. These results indicate that nitrate is not consumed in the upper 20 cm of the sediment; that is, microbial metabolism is low. The results from benthic community structure and geochemistry
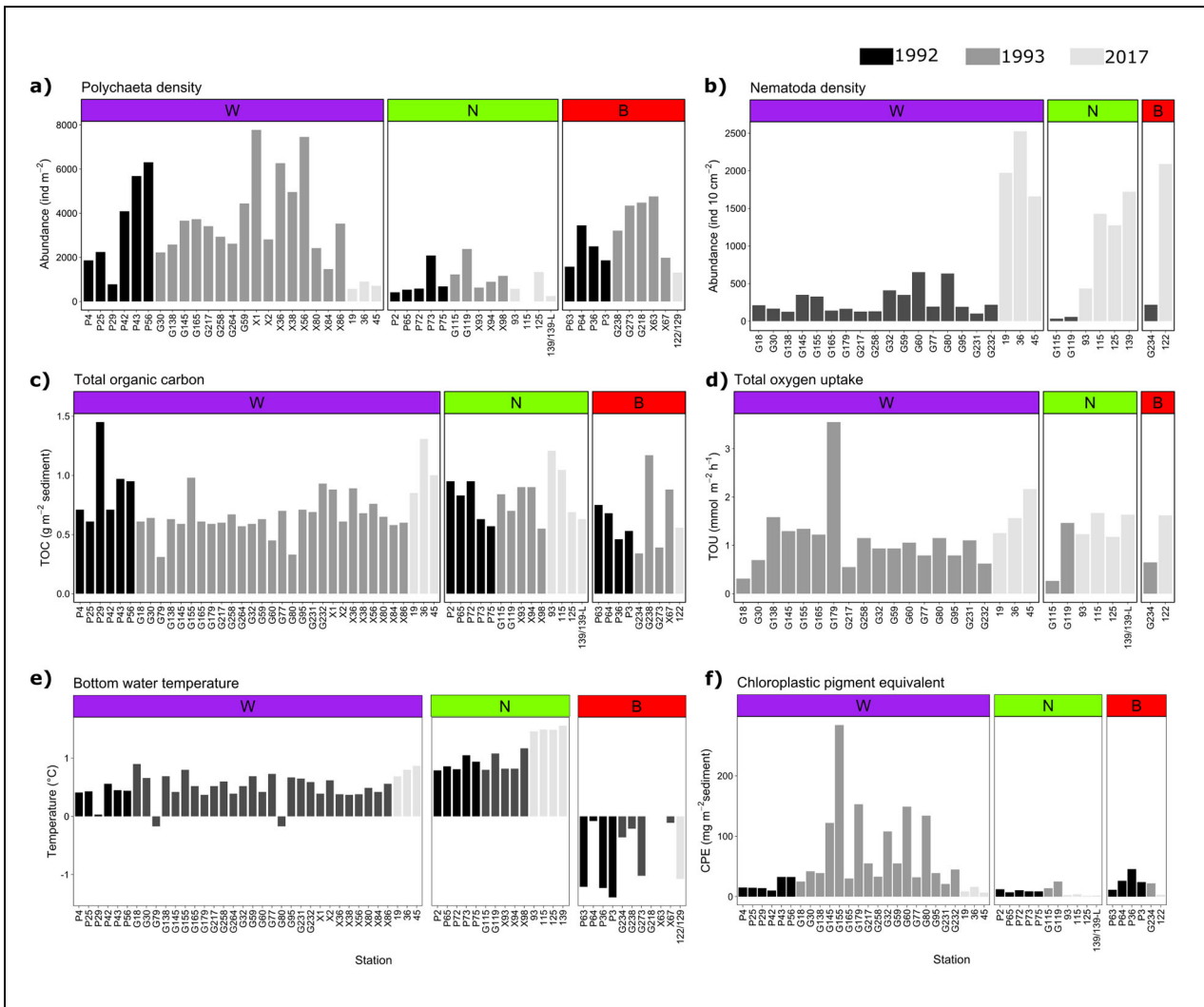
Figure 6. Comparison of benthic community parameters between 1992, 1993, and 2017. Plotted by station number are (a) Polychaeta density, (b) Nematoda density, (c) total organic carbon (TOC), (d) total oxygen uptake (TOU), (e) bottom water temperature, (f) chloroplastic pigment equivalent (CPE). Data from 1992 and 1993 were taken from Ambrose and Renaud (1995) and Piepenburg et al. (1997). Colors represent the sites statistically identified by the SIMPROF analysis based on standardized environmental data (Figure S5): Westwind Trough (W), Norske Trough (N), and Belgica Bank (B).

jointly suggest a tight pelagic-benthic coupling driven by higher diatom fluxes in the Westwind Trough area compared to the Glacier and inner Norske Trough areas. Indeed, primary production and export of algal cells during spring 1993 were also higher in the Westwind Trough, which is located within the NEW Polynya, compared to the Norske Trough, which was ice-covered during that time (Pesant et al., 1996; Pesant et al., 2000).

With benthic pigment concentrations being much higher in the Westwind Trough, the seafloor at this location could still be receiving a higher annual OM input. Uncalibrated ship-based fluorescence measurements in the upper water column during this study indicated similar phytoplankton biomass in the water column of both troughs during the sampling period (Kanzow and Rohardt, 2017), but this similarity likely reflected a consequence of the timing of sampling relative to bloom and/or vertical flux phenologies in the two regions. Another mechanism

could be a "decoupling" of the benthic environment from the pelagic in the Norske Trough due to higher zooplankton grazing (Ambrose and Renaud, 1995). Ashjian et al. (1995) observed that pelagic grazing rates greatly exceeded primary production in both the Westwind and Norske troughs, but especially in the Norske Trough, consistent with reduced food input for the benthos (Ambrose and Renaud, 1995). Possibly pelagic mineralization took place before OM could settle, leaving a lower fraction of the surface production to reach the seafloor in this area. In contrast to the stations within the Norske Trough, the station located on the Belgica Bank showed benthic abundances and biomasses similar to the Westwind Trough, as well as higher benthic remineralization rates (**Figures 3**, **4**, and **S5**), which are most likely due to the shallow depth receiving more settled OM than a deeper trough. Similarly, the stations in the Westwind Trough were shallower (206–315 m) than those in the Norske Trough (354–502 m),
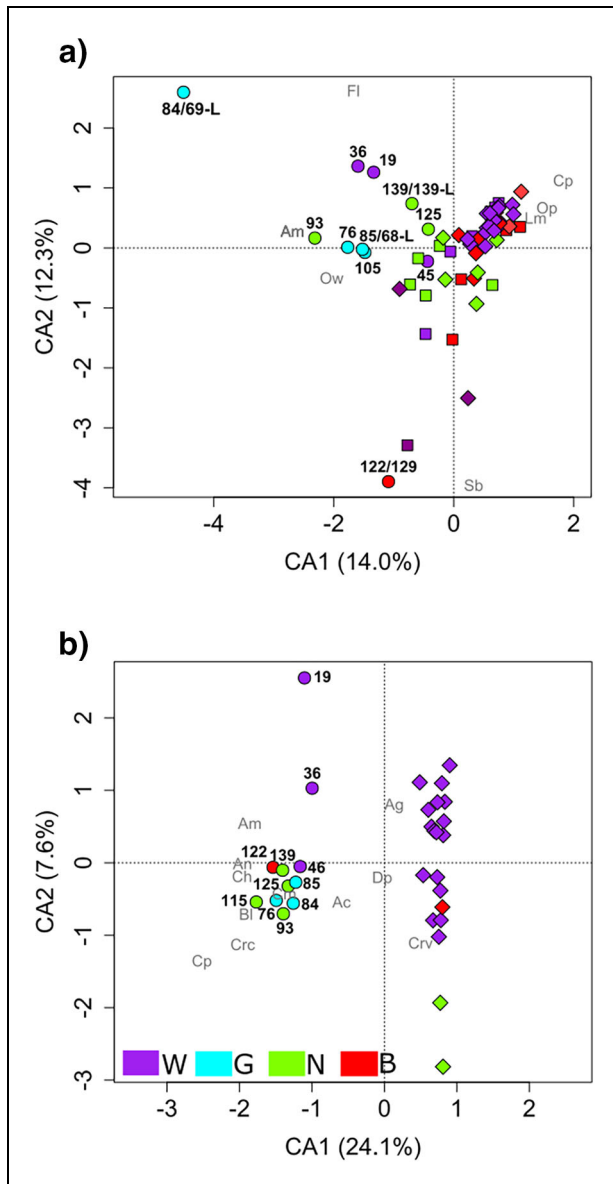
Figure 7. Visualization of the correspondence analysis for Polychaeta and Nematoda with sampling year. Relative abundances of (a) Polychaeta (family level) and (b) Nematoda (genus level) from 1992 (squares), 1993 (diamonds), and 2017 (circles). Symbol colors represent the 4 sites statistically identified by the SIMPROF analysis based on standardized environmental data (Figure S5): Westwind Trough (W), 79°N Glacier (G), Norske Trough (N), and Belgica Bank (B). Abbreviations for the most abundant taxa (Polychaeta families >500 ind m^{-2} and Nematoda genera >30 ind 10 cm^{-2}) are depicted in gray font; station numbers from 2017, in black font. Polychaeta families in (a) are Ampharetidae (Am), Capitellidae (Cp), Flabelligeridae (Fl), Lumbrineridae (Lm), Opheliidae (Op), Oweniidae (Ow) and Sabellidae (Sb). Nematoda genera in (b) are *Acantholaimus* (Ac), *Aegialoalaimus* (Ag), *Amphimonhystrella* (Am), *Anoplostoma* (An), *Bolbolaimus* (Bl), Chromadorita (Ch), *Campylaimus* (Cm), *Capsula* (Cps), *Ceramonema* (Cr), *Cricohalalaimus* (CrC), *Cervonema* (Crv), and *Diplopeltula* (Dp).

possibly explaining more OM settling at this site, with a shorter distance to the seafloor, and hence fueling a richer benthic community.

Both benthic diffusive and total oxygen uptake rates were very low, showing little differentiation among the sites. In general, benthic stations under more productive surface waters on Arctic shelves exhibit higher benthic process rates than stations in less productive regions (Grebmeier and Barry, 1991; Graf et al., 1995; Renaud et al., 2008; Grebmeier et al., 2015). Seasonal patterns in vertical flux of phytodetritus can also be tightly linked with temporal patterns in benthic oxygen utilization (Renaud et al., 2007). Thus, the overall low rates observed here may be representing minimum rates, while a rate measured after a bloom would result in higher rates. By late September–October when these measurements were performed, the spatial variation in seasonal carbon deposition in the area was no longer apparent in processes expected to respond more rapidly than other benthic parameters such as community structure or sediment geochemistry (McMahon et al., 2006; Renaud et al., 2008; Morata et al., 2015). Moreover, sediment oxygen uptake is usually dominated by microbial communities that react more dynamically to seasonal food input than macrofauna and meiofauna (Piepenburg et al., 1995); therefore, a seasonal signal in TOU might have faded toward autumn, while differences in macrofaunal and meiofaunal community structures usually persist over longer time scales.

4.2. Comparing NEG to other Arctic shelves: An oligotrophic outflow shelf

The NEG shelf is an Arctic outflow shelf, transporting Arctic Water into the North Atlantic. Primary production on Arctic outflow shelves is typically highly seasonal, quickly nutrient-limited, and highly variable spatially and interannually (Carmack and Wassmann, 2006). Pelagic primary production rates on the NEG shelf are 1–2 orders of magnitude lower than those on productive inflow shelves such as the shallow Chukchi Sea and deep Barents Sea (Pabi et al., 2008). This lower primary production is also reflected in the amount of fresh OM that arrives at the seafloor. The maximum sediment CPE content observed in this study was indeed an order of magnitude lower than the maximum CPE content in sediments of the shallow Chukchi Sea (McTigue et al., 2015) and Barents Sea at comparable depths to this study (Morata and Renaud, 2008). The overall low Chl *a*:phaeopigment ratios on the NEG shelf (Figure S3d) suggest that OM was in a degraded state. Presumed low input of fresh OM is also reflected in low benthic activity, with TOU values across the NEG shelf comparable to those observed in the 1990s (0.31–3.55 mmol m^{-2} d^{-1} in Piepenburg et al., 1997; 0.72–6.72 mmol m^{-2} d^{-1} in Rowe et al., 1997) and in the deep Arctic Fram Strait (0.5–5.1 mmol m^{-2} d^{-1}; Hoffmann et al., 2018). In contrast, at similar depths (200–500 m) in the inflow Chukchi Sea and Svalbard region, TOU is generally up to 10 times higher (Bourgeois et al., 2017). These comparisons confirm the previous report about this outflow region being oligotrophic (Rowe et al., 1997).

Table 1. Results of the PERMANOVA performed on the community parameters of Polychaeta and Nematoda densities from 1992, 1993, and 2017

Factor Tested	Df[a]	Sum of Squares	R^2	F	Pr(>F)
Polychaeta					
Time	2	2.49	0.17	7.15	0.00
Site	5	2.92	0.20	3.37	0.00
Time and site	5	1.28	0.09	1.48	0.04
Residual	45	7.82	0.54	NA[b]	NA
Total	57	14.51	1.00	NA	NA
Nematoda					
Time	1	2.85	0.40	23.78	0.00
Site	3	0.80	0.11	2.21	0.01
Time and site	2	0.53	0.08	2.21	0.02
Residual	24	2.88	0.41	NA	NA
Total	30	7.06	1.00	NA	NA

[a]Degrees of freedom.

[b]Not applicable.

In accordance, the abundance of macrofauna on the NEG shelf was generally low compared to Arctic inflow shelf regions. Locations where densities were the highest (all stations in the Westwind Trough, and stations in the outer Norske Trough, far from the 79°N Glacier) featured similar densities to sites with low food availability recorded in Svalbard fjords (76–250 m water depths; Włodarska-Kowalczuk and Pearson, 2004) and the western Barents Sea (Carroll et al., 2008). Although the spatial scale in our study and distances between stations were large (55–150 km distances between stations on the shelf), compositional differences among benthic communities were relatively small (**Figure 5**). The circulation of AIW in the trough system might lead to very similar hydrographic conditions among stations. In contrast, benthic communities along a transect of only a few kilometers in the glacial fjord of Kongsfjorden featured conspicuous differences (Włodarska-Kowalczuk et al., 2005; Bourgeois et al., 2016). Open-shelf benthic systems, however, have higher species diversity and higher numbers of rare species compared to fjord systems (Włodarska-Kowalczuk et al., 2012), and differences among sites emerge at much larger distances (Cochrane et al., 2012), which is in accordance with our findings.

Surprisingly, this study did not show clear dominance patterns in the macrofaunal communities, but all species were present in low abundance (<4 ind. 0.007 m^{-2}). The same pattern was observed in the samples from the early 1990s (Ambrose and Renaud, 1995). Often, benthic communities are dominated by a few species in high densities (e.g., Włodarska-Kowalczuk and Pearson, 2004; Blanchard et al., 2013); however, the infaunal communities on the NEG shelf appear to be highly diverse with very low densities. This finding agrees with the observation that North Greenland features comparatively high species richness

among the Arctic marine ecoregions (Piepenburg et al., 2011). Meiofaunal communities in this study, on the other hand, were strongly dominated by nematodes, as is usually the case in other benthic ecosystems (Gerlach, 1971; Włodarska-Kowalczuk et al., 2016; Hoffmann et al., 2018; Veit-Köhler et al., 2018).

4.3. A possible weakening of pelagic-benthic coupling on the NEG shelf since the 1990s

We found strong contrasts in physical parameters of the sediment as well as in community structure between the early 1990s and 2017 (present study). A 0.5°C temperature increase of the bottom water in the Norske Trough in 2000–2016 compared to 1979–1999 (Schaffer et al., 2017; see also **Figure 6e**) and lower sediment pigment content (**Figure 6f**) were striking. A strong influence of warm Atlantic Water and absence of sea ice can be related to a higher amount of degraded material reaching the seafloor, due to a more active microbial loop and higher grazing pressure in the pelagic environment (Dybwad et al., 2022). CPE concentrations for the upper 2 cm of the sediment varied between 7.2 mg m^{-2} and 45.6 mg m^{-2} across the whole NEG shelf between July and August in the early 1990s (Ambrose and Renaud, 1995), while in this study (conducted in September–October, 2017), highest concentrations were found in the Westwind Trough, with values of 7.38–18.0 mg m^{-2}. At all other sites, CPE concentrations were close to 0. While this pattern could reflect a seasonal effect, the consistently low macrofaunal densities in 2017 suggest that a seasonal effect is not the only reason, because macrofaunal community structure reflects ecosystem processes on a longer time scale, especially in oligotrophic areas like the NEG shelf.

Macrofaunal abundances in 1992 were nearly 5× higher than we observed in 1992. In contrast, Nematoda

abundances were 3.4 times higher in 2017 than recorded in 1993, and a much higher diversity of nematode genera was observed in 2017 (157 identified in 2017 vs. 77 identified in 1993). Nematoda in deep-sea polar regions have been shown to prefer bacteria over fresh phytoplankton (Ingels et al., 2010), so the shift observed here could be linked with lower quality as well as quantity of the food supply from surface waters. The CAs based on meiofaunal and macrofaunal abundances (**Figure 5**) showed less variation in benthic community structure across the shelf in 2017 compared to the strong spatial differences between the Westwind and Norske troughs in the 1990s (Piepenburg et al., 1997), suggesting a homogenization of the shelf communities. This change in an already oligotrophic shelf system appears to indicate a system more closely resembling a deep-sea community, with few hotspots of food supply to the seafloor and predominance of smaller biota in sediments (e.g., Górska et al., 2020). Similarly, during the campaigns in the 1990s benthic foraminifera communities across the NEG shelf were dominated by calcified species, while in 2017 agglutinated species were dominating (Davies et al., 2023). The spread of stations in the CA plot, however, also suggests that between-study differences in taxonomic identification of fauna, particularly for nematodes, may have contributed to variability. Stations are completely separated by sampling period and show a similar latitudinal gradient, which suggests either wholesale community changes such that even the most oligotrophic stations in both sampling occasions shifted or an inconsistency in naming of organisms. This "identifier bias" is not uncommon in the literature (e.g., Bluhm et al., 2011). We took several measures to reduce potential bias, such as checking and harmonizing species names on marinespecies.org for both datasets, selecting coarse taxonomic resolutions (family level for polychaetes and genus level for nematodes), and using relative abundance for the data analysis (taxon number divided by total number of individuals at the respective station).

Some of the differences between the early 1990s and our study may be a consequence of sampling season or simply intra-annual variability, especially with regard to sea-ice cover. Samples were taken during different months in both studies (March–August in 1992/1993 vs. September–October in 2017). Upon reaching the seafloor, phytodetritus can be consumed rapidly by the benthos (Morata et al., 2015) and a pigment signal from a spring bloom in surface sediments can fade with time. Spring bloom timing may also have changed due to differences in seasonality in ice cover. An earlier bloom in 2017 may have resulted in an earlier benthic food consumption, which would in turn lead to a lower detection of pigment concentrations late in the year than it did before. Sejr et al. (2000), for example, showed an increase in macrofaunal abundance in Young Sound from mid-July to mid-August, coupled with changes in primary production. The low Chl *a*:phaeopigment ratios in the sediment from our study indicate that sediment pigments reflect older or more processed phytodetritus. Assuming a lack of secondary bloom, the pigment content of the sediment would be expected to be higher in July–August and more depleted in September–October.

Our observations of slightly higher oxygen uptake in 2017 compared to 1993 (63.7 μmol m^{-2} h^{-1} vs. 44.8 μmol m^{-2} h^{-1}) appears to contradict the assumption that an earlier spring bloom during the 1993 sampling campaign would fuel a rapid consumption and oxygen uptake in contrast to 2017. Although polychaete recruitment was seasonally variable, no synchrony between recruitment and pulsed sedimentation of organic material was detected (Ambrose and Renaud, 1997). Even if seasonal signals can be detected in oxygen uptake rates (Morata et al., 2015), seasonal patterns are not usually integrated in the community structure of macrofauna and meiofauna in the Arctic (Kędra et al., 2012; Berge et al., 2015; Włodarska-Kowalczuk et al., 2016).

What, then, may be responsible for the observed changes across this shelf region over the span of 25 years? As observed everywhere in the Arctic, the extent of sea-ice cover on the NEG shelf is shrinking, with an increasing ice-free period during summer (Stroeve et al., 2012). On the NEG shelf, however, interannual variability of sea-ice concentration evaluated between 1995 and 2017 was large, showing no obvious trend. However, the thickness of sea ice transported onto the NEG shelf through Fram Strait has decreased drastically since the last decade (Spreen et al., 2020; Sumata et al., 2022). There is an increasing influence of freshwater layering on the NEG shelf (Sejr et al., 2017), which may lead to decreased nutrient concentrations (Li et al., 2009) and subsequent lower primary production, ultimately resulting in lower export of OM to the seafloor (von Appen et al., 2021). Moreover, the NØIB in the south of the 79°N Glacier, a land-fast ice barrier that keeps the NEW Polynya in place and prevents calving of the glacier, is breaking up seasonally more often due to increasing summer temperatures in the area (Reeh et al., 2001; Smith and Barber, 2007). The ice barrier prevented surface currents from advecting sea ice into the Westwind Trough, which kept an open water area in place. In the early 1990s, this polynya was strongly related to abundance patterns of benthos and was characterized by tight pelagic-benthic coupling in the Westwind Trough, compared to a weaker pelagic-benthic coupling in the Norske Trough (Ambrose and Renaud, 1995; Brandt, 1995; Hobson et al., 1995; Piepenburg et al., 1997). Without the NØIB barrier, the sea-ice cover across the NEG shelf becomes more variable, likely reducing the differentiation between the Westwind Trough and Norske Trough. Pelagic-benthic coupling may have weakened in the region due to a more recurrent break-up of the polynya (ISSI, 2008; Reeh, 2017).

One scenario of the effects of shrinking ice cover in the Arctic is that the longer exposure to sunlight will result in a longer season for phytoplankton growth and higher production rates (Arrigo et al., 2008), thus to a higher food input for the benthos. This study indicates that a different scenario might be happening on the NEG shelf. Due to climate warming, Arctic sea ice melts earlier in the year, and the ice-free period is prolonged (Overland and Wang, 2013). Primary production starts earlier in the year and

sunlight could be available to phytoplankton for a longer period of time, but primary production might not be high throughout this period as nutrients would be consumed earlier during peak bloom in early spring (Wassmann and Reigstad, 2011). Lower nutrient concentrations favor smaller phytoplankton with lower carbon export efficiency (Li et al., 2009). During the early 1990s massive assemblages of under-ice algae were recorded underneath first-year ice sheets on the NEG shelf, dominated by the diatom *Melosira arctica* (Gutt, 1995), which could have provided important food pulses for benthic communities during ice melt in spring during that time (Bauerfeind et al., 1997).

The wider time window for pelagic primary production and increasing stratification increases in turn the time available for heterotrophic pelagic consumers to exploit this primary resource by extended grazing periods and population growth (Olli et al., 2007). Accordingly, the current Arctic marine ecosystem, characterized locally by highly seasonal and short-term "pulses" of organic carbon production and deposition (Grebmeier and Barry, 1991), may shift to one where a smaller share of primary production may be available for export. If the input of warmer AIW introduces more Atlantic zooplankton species onto the NEG shelf, enhanced grazing could lead to a "decoupling" of the benthic system from the pelagic productivity. In fact, the carbon demand of pelagic heterotrophs on the NEG shelf was reported to exceed the estimated local primary production (Carmack and Wassmann, 2006). Such an imbalance could also have led to the homogenization of the benthic communities between the Norske and the Westwind Trough, compared to the early 1990s when differences between benthic community compositions were far more conspicuous. A shift away from pelagic-benthic coupling has been predicted for Arctic ecosystems (Grebmeier and Barry, 1991) and has been reported for the Northern Bering Sea, with a northward shift of the pelagic-dominated ecosystem that was previously limited to the southeastern Bering Sea (Grebmeier et al., 2006). Our results are consistent with the new scenario of reduced food input to the benthos, although the mechanism proposed here is speculative. The extent to which our findings of change in the region are due to broader ecosystem change to be found throughout the Arctic is unclear. Just as in the early 1990s, this study provides only a snapshot of pigment concentrations and benthic community parameters. Annual patterns need to be further resolved empirically in order to be able to state clear conclusions about climate change-related ecosystem shifts.

5. Conclusions
Revisiting the NEG shelf 25 years after the first benthic studies there has demonstrated that, despite the decrease in sea-ice cover and variability in the NEW Polynya, the area is still an oligotrophic Arctic outflow shelf. Macrobenthic and meiobenthic communities in 2017 exhibited high diversity across the shelf but low abundances and activity. Pelagic-benthic coupling remained most pronounced in Westwind Trough, while food availability was lowest close to the 79°N Glacier. However, sediment pigment content had decreased markedly since the early 1990s, along with a reduction in polychaete densities, while nematode density and diversity had increased. These results may be due to a weakening of pelagic-benthic coupling, leading to input of pelagic organic matter in a lower quantity and more degraded state, possibly driven by a local change in the strength of the NEW Polynya or the stratification regime.

Data accessibility statement
All data used were published on PANGAEA (www.pangaea.de) and cited within this manuscript.

Supplemental files
The supplemental files for this article can be found as follows:
Tables S1–S4. Figures S1–S6. docx

Competing interests
The authors declare no competing interests.

Author contributions
UB, FW, JF planned and conducted the fieldwork and in situ measurements. YVB analyzed single cell abundances, counted and identified macrofaunal abundances and determined their biomass. UB and MWK contributed to macrofaunal identifications. LL and LDCM counted and identified meiofauna and Nematoda. TK provided sea-ice data and their interpretation. PER and WGA provided data from the early 1990s and their interpretation. YVB

analysed all data. YVB, PER, and UB drafted this manuscript. All authors revised and contributed to its finalization and approved of the submitted version.

References

Ambrose, WG, Renaud, PE. 1995. Benthic response to water column productivity patterns: Evidence for benthic-pelagic coupling in the Northeast Water Polynya. *Journal of Geophysical Research: Oceans* **100**(C3): 4411–4421. DOI: http://dx.doi.org/10.1029/94JC01982.

Ambrose, WG, Renaud, PE. 1997. Does a pulsed food supply to the benthos affect polychaete recruitment patterns in the Northeast Water Polynya? *Journal of Marine Systems* **10**(1–4): 483–495. DOI: http://dx.doi.org/10.1016/S0924-7963(96)00053-X.

April, A, Montpetit, B, Langlois, D. 2019. Linking the open water area of the North Open Water Polynya to climatic parameters using a multiple linear regression prediction model. *Atmosphere-Ocean* **57**(2): 91–100. DOI: http://dx.doi.org/10.1080/07055900.2019.1598332.

Ardyna, M, Babin, M, Gosselin, M, Devred, E, Rainville, L, Tremblay, J-É. 2014. Recent Arctic Ocean Sea ice loss triggers novel fall phytoplankton blooms. *Geophysical Research Letters* **41**(17): 6207–6212. DOI: http://dx.doi.org/10.1002/2014GL061047.

Arndt, JE, Jokat, W, Dorschel, B, Myklebust, R, Dowdeswell, JA, Evans, J. 2015. A new bathymetry of the Northeast Greenland continental shelf: Constraints on glacial and other processes. *Geochemistry, Geophysics, Geosystems* **16**(10): 3733–3753. DOI: http://dx.doi.org/10.1002/2015GC005931.

Arrigo, KR, van Dijken, G, Pabi, S. 2008. Impact of a shrinking Arctic ice cover on marine primary production. *Geophysical Research Letters* **35**(19). DOI: http://dx.doi.org/10.1029/2008GL035028.

Arrigo, KR, van Dijken, GL. 2015. Continued increases in Arctic Ocean primary production. *Progress in Oceanography* **136**: 60–70. DOI: http://dx.doi.org/10.1016/j.pocean.2015.05.002.

Ashjian, CJ, Smith, SL, Lane, PVZ. 1995. The Northeast Water Polynya during summer 1992: Distribution and aspects of secondary production of copepods. *Journal of Geophysical Research: Oceans* **100**(C3): 4371–4388. DOI: http://dx.doi.org/10.1029/94JC02199.

Barnhart, KR, Miller, CR, Overeem, I, Kay, JE. 2016. Mapping the future expansion of Arctic open water. *Nature Climate Change* **6**: 280–285. DOI: http://dx.doi.org/10.1038/nclimate2848.

Bauerfeind, E, Garrity, C, Krumbholz, M, Ramseier, RO, Voβ, M. 1997. Seasonal variability of sediment trap collections in the Northeast Water Polynya. Part 2. Biochemical and microscopic composition of sedimenting matter. *Journal of Marine Systems* **10**: 371–389. DOI: https://doi.org/10.1016/S0924-7963(96)00069-3.

Berge, J, Daase, M, Renaud, PE, Ambrose, WG, Darnis, G, Last, KS, Leu, E, Cohen, JH, Johnsen, G, Moline, MA, Cottier, F, Varpe, Ø, Shunatova, N, Bałazy, P, Morata, N, Massabuau, J-C, Falk-Petersen, S, Kosobokova, K, Hoppe, CJM, Węsławski, JM, Kukliński, P, Legeżyńska, J, Nikishina, D, Cusa, M, Kędra, M, Włodarska-Kowalczuk, M, Vogedes, D, Camus, L, Tran, D, Michaud, E, Gabrielsen, TM, Granovitch, A, Gonchar, A, Krapp, R, Callesen, TA. 2015. Unexpected levels of biological activity during the polar night offer new perspectives on a warming Arctic. *Current Biology* **25**(19): 2555–2561. DOI: http://dx.doi.org/10.1016/j.cub.2015.08.024.

Beszczynska-Möller, A, Fahrbach, E, Schauer, U, Hansen, E. 2012. Variability in Atlantic water temperature and transport at the entrance to the Arctic Ocean, 1997–2010. *ICES Journal of Marine Science* **69**(5): 852–863. DOI: http://dx.doi.org/10.1093/icesjms/fss056.

Blanchard, AL, Parris, CL, Knowlton, AL, Wade, NR. 2013. Benthic ecology of the northeastern Chukchi Sea. Part I. Environmental characteristics and macrofaunal community structure, 2008–2010. *Continental Shelf Research* **67**: 52–66. DOI: http://dx.doi.org/10.1016/j.csr.2013.04.021.

Bluhm, BA, Ambrose, WG, Bergmann, M, Clough, LM, Gebruk, AV, Hasemann, C, Iken, K, Klages, M, MacDonald, IR, Renaud, PE, Schewe, I, Soltwedel, T, Włodarska-Kowalczuk, M. 2011. Diversity of the Arctic deep-sea benthos. *Marine Biodiversity* **41**: 87–107. DOI: http://dx.doi.org/10.1007/s12526-010-0078-4.

Bodur, YV, Deja, K, Górska, B, Kędra, M, Kukliński, P, Legeżyńska, J, Pawlowska, J, Ronowicz, M, Włodarska-Kowalczuk, M, Braeckman, U. 2023a. Benthic macrofauna and foraminifera (>500 μm) diversity, abundance and biomass on the Northeast Greenland (NEG) shelf sediments during POLARSTERN cruise PS109. PANGAEA. DOI: https://doi.pangaea.de/10.1594/PANGAEA.959134.

Bodur, YV, Felden, J, Braeckman, U. 2023b. Single prokaryotic cell abundances of the Northeast Greenland (NEG) shelf sediments from POLARSTERN cruise PS109. PANGAEA. DOI: https://doi.pangaea.de/10.1594/PANGAEA.959552.

Bourgeois, S, Archambault, P, Witte, U. 2017. Organic matter remineralization in marine sediments: A Pan-Arctic synthesis. *Global Biogeochemical Cycles* **31**(1): 190–213. DOI: http://dx.doi.org/10.1002/2016GB005378.

Bourgeois, S, Kerhervé, P, Calleja, MLl, Many, G, Morata, N. 2016. Glacier inputs influence organic matter composition and prokaryotic distribution in a high Arctic fjord (Kongsfjorden, Svalbard). *Journal of Marine Systems* **164**: 112–127. DOI: http://dx.doi.org/10.1016/j.jmarsys.2016.08.009.

Bourke, RH, Newton, JL, Paquette, RG, Tunnicliffe, MD. 1987. Circulation and water masses of the East Greenland shelf. *Journal of Geophysical Research: Oceans* **92**(C7): 6729–6740. DOI: http://dx.doi.org/10.1029/JC092iC07p06729.

Braeckman, U. 2023a. Grain size analysis of the Northeast Greenland (NEG) shelf sediments from POLARSTERN cruise PS109. PANGAEA. DOI: https://doi.pangaea.de/10.1594/PANGAEA.959546.

Braeckman, U. 2023b. Porosity of the Northeast Greenland (NEG) shelf sediments from POLARSTERN cruise PS109. PANGAEA. DOI: https://doi.pangaea.de/10.1594/PANGAEA.959550.

Braeckman, U. 2023c. Sedimentary pigments on the Northeast Greenland (NEG) Shelf from Polarstern cruise PS109. PANGAEA. DOI: https://doi.pangaea.de/10.1594/PANGAEA.959548.

Braeckman, U. 2023d. Total organic nitrogen (TON) and total organic carbon (TOC) concentration of the Northeast Greenland (NEG) shelf sediments from POLARSTERN cruise PS109. PANGAEA. DOI: https://doi.pangaea.de/10.1594/PANGAEA.959554.

Braeckman, U, Felden, J. 2023. Porewater nutrients of the Northeast Greenland (NEG) shelf sediments from POLARSTERN cruise PS109. PANGAEA. DOI: https://doi.pangaea.de/10.1594/PANGAEA.959549.

Braeckman, U, Janssen, F, Lavik, G, Elvert, M, Marchant, H, Buckner, C, Bienhold, C, Wenzhöfer, F. 2018. Carbon and nitrogen turnover in the Arctic deep sea: In situ benthic community response to diatom and coccolithophorid phytodetritus. *Biogeosciences Discussions* **15**: 6537–6557. DOI: http://dx.doi.org/10.5194/bg-2018-264.

Braeckman, U, Wenzhöfer, F. 2023. Ex situ total oxygen uptake of the Northeast Greenland (NEG) shelf sediments from POLARSTERN cruise PS109. PANGAEA. DOI: https://doi.pangaea.de/10.1594/PANGAEA.959553.

Brandt, A. 1995. Peracarid fauna (Crustacea, Malacostraca) of the Northeast Water Polynya off Greenland: Documenting close benthic-pelagic coupling in the Westwind Trough. *Marine Ecology Progress Series* **121**: 39–51. DOI: http://dx.doi.org/10.3354/meps121039.

Carmack, E, Wassmann, P. 2006. Food webs and physical–biological coupling on pan-Arctic shelves: Unifying concepts and comprehensive perspectives. *Progress in Oceanography* **71**(2–4): 446–477. DOI: http://dx.doi.org/10.1016/j.pocean.2006.10.004.

Carroll, ML, Denisenko, SG, Renaud, PE, Ambrose Jr, WG. 2008. Benthic infauna of the seasonally ice-covered western Barents Sea: Patterns and relationships to environmental forcing. *Deep Sea Research Part II: Topical Studies in Oceanography* **55**: 2340–2351.

Cochrane, SKJ, Pearson, TH, Greenacre, M, Costelloe, J, Ellingsen, IH, Dahle, S, Gulliksen, B. 2012. Benthic fauna and functional traits along a Polar Front transect in the Barents Sea—Advancing tools for ecosystem-scale assessments. *Journal of Marine Systems* **94**: 204–217. DOI: http://dx.doi.org/10.1016/j.jmarsys.2011.12.001.

Comiso, JC, Meier, WN, Gersten, R. 2017. Variability and trends in the Arctic Sea ice cover: Results from different techniques. *Journal of Geophysical Research: Oceans* **122**(8): 6883–6900. DOI: http://dx.doi.org/10.1002/2017JC012768.

Da Costa Monteiro, L, Lins, L, Braeckman, U. 2023a. Benthic meiofauna diversity on the Northeast Greenland (NEG) shelf during POLARSTERN cruise PS109. PANGAEA. DOI: https://doi.pangaea.de/10.1594/PANGAEA.959357.

Da Costa Monteiro, L, Lins, L, Braeckman, U. 2023b. Nematoda diversity and functional feeding groups on the Northeast Greenland (NEG) shelf during POLARSTERN cruise PS109. PANGAEA. DOI: https://doi.pangaea.de/10.1594/PANGAEA.959351.

Dalsgaard, T, Nielsen, LP, Brotas, V, Viaroli, P, Underwood, G, Nedwell, D, Sundbäck, K, Rysgaard, S, Miles, A, Bartoli, M, Dong, L, Thornton, D, Ottosen, L, Castaldelli, G, Risgaard-Petersen, N. 2000. *Protocol handbook for NICE-Nitrogen cycling in estuaries: A project under the EU research programme.* Silkeborg, Denmark: Marine Science and Technology Program (MAST III), National Environmental Research Institute.

Davies, J, Lloyd, J, Pearce, C, Seidenkrantz, M-S. 2023. Distribution of modern benthic foraminiferal assemblages across the Northeast Greenland continental shelf. *Marine Micropaleontology* **184**: 102273. DOI: http://dx.doi.org/10.1016/j.marmicro.2023.102273.

Degen, R, Vedenin, A, Gusky, M, Boetius, A, Brey, T. 2015. Patterns and trends of macrobenthic abundance, biomass and production in the deep Arctic Ocean. *Polar Research* **34**(1): 24008. DOI: http://dx.doi.org/10.3402/polar.v34.24008.

Donis, D, McGinnis, DF, Holtappels, M, Felden, J, Wenzhoefer, F. 2016. Assessing benthic oxygen fluxes in oligotrophic deep sea sediments (HAUSGARTEN observatory). *Deep Sea Research Part I: Oceanographic Research Papers* **111**: 1–10.

Dybwad, C, Lalande, C, Bodur, YV, Henley, SF, Cottier, F, Ershova, EA, Hobbs, L, Last, KS, Dąbrowska, AM, Reigstad, M. 2022. The influence of sea ice cover and Atlantic Water advection on annual particle export north of Svalbard. *Journal of Geophysical Research: Oceans* **127**(10): e2022JC018897. DOI: http://dx.doi.org/10.1029/2022JC018897.

ENVEO. 2017. Greenland calving front dataset, 1990–2016, v2.0, Greenland Ice Sheet CCI. ENVEO. Available at http://cryoportal.enveo.at/data/. Accessed February 04, 2018.

Ezraty, R, Girard-Ardhuin, F, Piolle, J, Kaleschke, L, Heygster, G. 2007. *Arctic & Antarctic sea ice concentration and Arctic sea ice drift estimated from Special Sensor MIcrowave data—User's manual V2.1.* France: Departement d'Oceanographie Physique et Spatiale, IFREMER, Brest.

Falk-Petersen, S, Sargent, JR, Henderson, J, Hegseth, EN, Hop, H, Okolodkov, YB. 1998. Lipids and fatty acids in ice algae and phytoplankton from the Marginal Ice Zone in the Barents Sea. *Polar Biology* **20**:

41–47. DOI: http://dx.doi.org/10.1007/s00300 0050274.

Felden, J, **Wenzhöfer, F**, **Braeckman, U.** 2023. Ex situ diffusive oxygen uptake of the Northeast Greenland (NEG) shelf sediments from POLARSTERN cruise PS109. PANGAEA. DOI: https://doi.pangaea.de/10.1594/PANGAEA.959545.

Gerlach, SA. 1971. On the importance of marine meiofauna for benthos communities. *Oecologia* **6**: 176–190. DOI: http://dx.doi.org/10.1007/BF00 345719.

Glud, RN, **Gundersen, JK**, **Barker Jørgensen, B**, **Revsbech, NP**, **Schulz, HD.** 1994. Diffusive and total oxygen uptake of deep-sea sediments in the eastern South Atlantic Ocean: *In situ* and laboratory measurements. *Deep Sea Research Part I: Oceanographic Research Papers* **41**(11–12): 1767–1788. DOI: http://dx.doi.org/10.1016/0967-0637(94)90072-8.

Górska, B, **Soltwedel, T**, **Schewe, I**, **Włodarska-Kowalczuk, M.** 2020. Bathymetric trends in biomass size spectra, carbon demand, and production of Arctic benthos (76–5561 m, Fram Strait). *Progress in Oceanography* **186**: 102370. DOI: http://dx.doi.org/10.1016/j.pocean.2020.102370.

Graf, G. 1989. Benthic-pelagic coupling in a deep-sea benthic community. *Nature* **341**: 437–439. DOI: http://dx.doi.org/10.1038/341437a0.

Graf, G, **Gerlach, SA**, **Linke, P**, **Queisser, W**, **Ritzrau, W**, **Scheltz, A**, **Thomsen, L**, **Witte, U.** 1995. Benthic-pelagic coupling in the Greenland-Norwegian Sea and its effect on the geological record. *Geologische Rundschau* **84**: 49–58. DOI: http://dx.doi.org/10.1007/BF00192241.

Grebmeier, J, **McRoy, C**, **Feder, H.** 1988. Pelagic-benthic coupling on the shelf of the northern Bering and Chukchi Seas. I. Food supply source and benthic biomass. *Marine Ecology Progress Series* **48**: 57–67. DOI: http://dx.doi.org/10.3354/meps048057.

Grebmeier, J, **Overland, JE**, **Moore, SE**, **Farley, EV**, **Carmack, EC**, **Cooper, LW**, **Frey, KE**, **Helle, JH**, **McLaughlin, FA**, **McNutt, SL.** 2006. A major ecosystem shift in the Northern Bering Sea. *Science* **311**(5766): 1461–1464. DOI: http://dx.doi.org/10.1126/science.1121365.

Grebmeier, JM, **Barry, JP.** 1991. The influence of oceanographic processes on pelagic-benthic coupling in polar regions: A benthic perspective. *Journal of Marine Systems* **2**(3–4): 495–518. DOI: http://dx.doi.org/10.1016/0924-7963(91)90049-Z.

Grebmeier, JM, **Barry, JP.** 2007. Benthic processes in polynyas, in Smith, WO, Barber, DG eds., *Elsevier oceanography series, polynyas: Windows to the world*: 363–390. DOI: http://dx.doi.org/10.1016/S0422-9894(06)74011-9.

Grebmeier, JM, **Bluhm, BA**, **Cooper, LW**, **Danielson, SL**, **Arrigo, KR**, **Blanchard, AL**, **Clarke, JT**, **Day, RH**, **Frey, KE**, **Gradinger, RR**, **Kędra, M**, **Konar, B**, **Kuletz, KJ**, **Lee, SH**, **Lovvorn, JR**, **Norcross, BL**, **Okkonen, SR.** 2015. Ecosystem characteristics and processes facilitating persistent macrobenthic

biomass hotspots and associated benthivory in the Pacific Arctic. *Progress in Oceanography* **136**: 92–114. DOI: http://dx.doi.org/10.1016/j.pocean.2015.05.006.

Gutt, J. 1995. The occurrence of sub-ice algal aggregations off northeast Greenland. *Polar Biology* **15**: 247–252. DOI: http://dx.doi.org/10.1007/BF00239844.

Hegseth, EN. 1998. Primary production of the northern Barents Sea. *Polar Research* **17**: 113–123. Available at https://onlinelibrary.wiley.com/doi/abs/10.1111/j.1751-8369.1998.tb00266.x.

Heip, C, **Vincx, M**, **Vranken, G.** 1985. The ecology of marine nematodes, in Barnes, H, Barnes, M eds., *Oceanography and marine biology, an annual review.* Aberdeen, UK: Aberdeen University Press: 399–489.

Hobbie, JE, **Daley, RJ**, **Jasper, S.** 1977. Use of nuclepore filters for counting bacteria by fluorescence microscopy. *Applied and Environmental Microbiology* **33**: 1225–1228.

Hobson, KA, **Ambrose, WG**, **Renaud, PR.** 1995. Sources of primary production, benthic-pelagic coupling, and trophic relationships within the northeast Water Polynya: Insights from ∂13C and ∂15N analysis. *Marine Ecology Progress Series* **128**: 1–10.

Hoffmann, R, **Braeckman, U**, **Hasemann, C**, **Wenzhöfer, F.** 2018. Deep-sea benthic communities and oxygen fluxes in the Arctic Fram Strait controlled by sea-ice cover and water depth. *Biogeosciences* **15**: 1–40. DOI: http://dx.doi.org/10.5194/bg-2017-537.

Horner, R, **Schrader, GC.** 1982. Relative contributions of ice algae, phytoplankton, and benthic microalgae to primary production in nearshore regions of the Beaufort Sea. *Arctic* **35**(4): 485–503. DOI: http://dx.doi.org/10.14430/arctic2356.

Hughes, NE, **Wilkinson, JP**, **Wadhams, P.** 2011. Multi-satellite sensor analysis of fast-ice development in the Norske Øer Ice Barrier, Northeast Greenland. *Annals of Glaciology* **52**: 151–160. DOI: http://dx.doi.org/10.3189/172756411795931633.

Ingels, J, **Van den Driessche, P**, **De Mesel, I**, **Vanhove, S**, **Moens, T**, **Vanreusel, A.** 2010. Preferred use of bacteria over phytoplankton by deep-sea nematodes in polar regions. *Marine Ecology Progress Series* **406**: 121–133. DOI: http://dx.doi.org/10.3354/meps08535.

International Space Science Institute. 2008. Arctic change and polynyas: Focus on the Northeast Water Polynya and North Water Polynya/Nares Strait system team. Available at http://www.issibern.ch/teams/Polynya/. Accessed November 2, 2018.

Jakobsson, M, **Mayer, LA**, **Bringensparr, C**, **Castro, CF**, **Mohammad, R**, **Johnson, P**, **Ketter, T**, **Accettella, D**, **Amblas, D**, **An, L**, **Arndt, JE**, **Canals, M**, **Casamor, JL**, **Chauché, N**, **Coakley, B**, **Danielson, S**, **Demarte, M**, **Dickson, M-L**, **Dorschel, B**, **Dowdeswell, JA**, **Dreutter, S**, **Fremand, AC**, **Gallant, D**, **Hall, JK**, **Hehemann, L**, **Hodnesdal, H**, **Hong, J**, **Ivaldi, R**, **Kane, E**, **Klaucke, I**, **Krawczyk, DW**, **Kristoffersen, Y**, **Kuipers, BR**, **Millan, R**, **Masetti, G**, **Morlighem, M**, **Noormets, R**, **Prescott, MM**,

Rebesco, M, Rignot, E, Semiletov, I, Tate, AJ, Travaglini, P, Velicogna, I, Weatherall, P, Weinrebe, W, Willis, JK, Wood, M, Zarayskaya, Y, Zhang, T, Zimmermann, M, Zinglersen, KB. 2020. The International Bathymetric Chart of the Arctic Ocean version 4.0. *Scientific Data* **7**(1): 176. DOI: http://dx.doi.org/10.1038/s41597-020-0520-9.

Jensen, M, Lomstein, E, Sørensen, J. 1990. Benthic NH_4^+ and NO_3^- flux following sedimentation of a spring phytoplankton bloom in Aarhus Bight, Denmark. *Marine Ecology Progress Series* **61**: 87–96. DOI: http://dx.doi.org/10.3354/meps061087.

Kaleschke, L, Lüpkes, C, Vihma, T, Haarpaintner, J, Bochert, A, Hartmann, J, Heygster, G. 2001. SSM/I sea ice remote sensing for mesoscale ocean-atmosphere interaction analysis. *Canadian Journal of Remote Sensing* **27**(5): 526–537. DOI: http://dx.doi.org/10.1080/07038992.2001.10854892.

Kanzow, T, Rohardt, G. 2017. CTD raw data files from POLARSTERN cruise PS109, link to tar-archive. PANGAEA. DOI: http://dx.doi.org/10.1594/PANGAEA.883366.

Kanzow, T, Schaffer, J, Rohardt, G. 2018. Physical oceanography during POLARSTERN cruise PS109 (ARK-XXXI/4). PANGAEA. DOI: http://dx.doi.org/10.1594/PANGAEA.885358.

Kędra, M, Kuliński, K, Walkusz, W, Legeżyńska, J. 2012. The shallow benthic food web structure in the high Arctic does not follow seasonal changes in the surrounding environment. *Estuarine, Coastal and Shelf Science* **114**: 183–191. DOI: http://dx.doi.org/10.1016/j.ecss.2012.08.015.

Khan, SA, Kjær, KH, Bevis, M, Bamber, JL, Wahr, J, Kjeldsen, KK, Bjørk, AA, Korsgaard, NJ, Stearns, LA, van den Broeke, MR, Liu, L, Larsen, NK, Muresan, IS. 2014. Sustained mass loss of the northeast Greenland ice sheet triggered by regional warming. *Nature Climate Change* **4**: 292–299. DOI: http://dx.doi.org/10.1038/nclimate2161.

Li, WKW, McLaughlin, FA, Lovejoy, C, Carmack, EC. 2009. Smallest algae thrive as the Arctic Ocean freshens. *Science* **326**(5952): 539. DOI: http://dx.doi.org/10.1126/science.1179798.

Mäkelä, A, Witte, U, Archambault, P. 2017. Ice algae versus phytoplankton: Resource utilization by Arctic deep sea macroinfauna revealed through isotope labelling experiments. *Marine Ecology Progress Series* **572**: 1–18. DOI: http://dx.doi.org/10.3354/meps12157.

Mayer, C, Reeh, N, Jung-Rothenhäusler, F, Huybrechts, P, Oerter, H. 2000. The subglacial cavity and implied dynamics under Nioghalvfjerdsfjorden Glacier, NE-Greenland. *Geophysical Research Letters* **27**(15): 2289–2292. DOI: http://dx.doi.org/10.1029/2000GL011514.

Mayer, C, Schaffer, J, Hattermann, T, Floricioiu, D, Krieger, L, Dodd, PA, Kanzow, T, Licciulli, C, Schannwell, C. 2018. Large ice loss variability at Nioghalvfjerdsfjorden Glacier, Northeast-Greenland.

Nature Communications **9**: 2768. DOI: http://dx.doi.org/10.1038/s41467-018-05180-x.

McMahon, K, Ambrose, WG, Johnson, B, Sun, M, Lopez, G, Clough, L, Carroll, M. 2006. Benthic community response to ice algae and phytoplankton in Ny Ålesund, Svalbard. *Marine Ecology Progress Series* **310**: 1–14. DOI: http://dx.doi.org/10.3354/meps310001.

McTigue, ND, Bucolo, P, Liu, Z, Dunton, KH. 2015. Pelagic-benthic coupling, food webs, and organic matter degradation in the Chukchi Sea: Insights from sedimentary pigments and stable carbon isotopes. *Limnology and Oceanography* **60**: 429–445. DOI: http://dx.doi.org/10.1002/lno.10038.

Meire, L, Mortensen, J, Rysgaard, S, Bendtsen, J, Boone, W, Meire, P, Meysman, FJR. 2016. Spring bloom dynamics in a subarctic fjord influenced by tidewater outlet glaciers (Godthåbsfjord, SW Greenland): Spring in a subarctic fjord. *Journal of Geophysical Research: Biogeosciences* **121**(6): 1581–1592. DOI: http://dx.doi.org/10.1002/2015JG003240.

Meredith, M, Sommerkorn, M, Cassota, S, Derksen, C, Ekaykin, A, Hollowed, A, Kofinas, G, Mackintosh, A, Melbourne-Thomas, J, Muelbert, MMC, Ottersen, G, Pritchard, H, Schuur, EAG. 2019. Polar regions, in Pörtner, HO, Roberts, DC, Masson-Delmotte, V, Zhai, P, Tignor, M, Poloczanska, ES, Mintenbeck, K, Alegría, A, Nicolai, M, Okem, A, Petzold, J, Rama, B, Weyer, NM eds., *IPCC special report on the ocean and cryosphere in a changing climate*. Cambridge University Press: 203–320. DOI: http://dx.doi.org/10.1017/9781009157964.

Minnett, PJ, Bignami, F, Böhm, E, Budéus, G, Galbraith, PS, Gudmandsen, P, Hopkins, TS, Ingram, RG, Johnson, MA, Niebauer, HJ, Ramseier, RO, Schneider, W. 1997. A summary of the formation and seasonal progression of the Northeast Water Polynya. *Journal of Marine Systems* **10**(1–4): 79–85. DOI: http://dx.doi.org/10.1016/S0924-7963(96)00060-7.

Morata, N, Michaud, E, Włodarska-Kowalczuk, M. 2015. Impact of early food input on the Arctic benthos activities during the polar night. *Polar Biology* **38**: 99–114. DOI: http://dx.doi.org/10.1007/s00300-013-1414-5.

Morata, N, Renaud, PE. 2008. Sedimentary pigments in the western Barents Sea: A reflection of pelagic–benthic coupling? *Deep Sea Research Part II: Topical Studies in Oceanography* **55**(20–21): 2381–2389. DOI: http://dx.doi.org/10.1016/j.dsr2.2008.05.004.

Nemys eds. 2022. Nemys: World database of nematodes. DOI: http://dx.doi.org/10.14284/366.

Nick, FM, Vieli, A, Andersen, ML, Joughin, I, Payne, A, Edwards, TL, Pattyn, F, van de Wal, RSW. 2013. Future sea-level rise from Greenland's main outlet glaciers in a warming climate. *Nature* **497**: 235–238. DOI: http://dx.doi.org/10.1038/nature12068.

Niebauer, HJ, Alexander, V, Henrichs, S. 1990. Physical and biological oceanographic interaction in the

spring bloom at the Bering Sea marginal ice edge zone. *Journal of Geophysical Research: Oceans* **95**(C12): 22229–22241. DOI: http://dx.doi.org/10.1029/JC095iC12p22229.

Oksanen, J, Blanchet, FG, Friendly, M, Kindt, R, Legendre, P, McGlinn, D, Minchin, PR, O'Hara, RB, Simpson, GL, Solymos, P, Stevens, MHH, Szoecs, E, Wagner, H. 2018. Vegan: Community ecology package, version 2.5. Available at https://CRAN.R-project.org/package=vegan. Accessed August 22, 2018.

Olli, K, Wassmann, P, Reigstad, M, Ratkova, TN, Arashkevich, E, Pasternak, A, Matrai, P, Knulst, J, Tranvik, L, Klais, R, Jacobsen, A. 2007. The fate of production in the central Arctic Ocean—Top-down regulation by zooplankton expatriates? *Progress in Oceanography* **72**(1): 84–113. DOI: http://dx.doi.org/10.1016/j.pocean.2006.08.002.

Onarheim, IH, Eldevik, T, Smedsrud, LH, Stroeve, JC. 2018. Seasonal and regional manifestation of Arctic Sea ice loss. *Journal of Climate* **31**(12): 4917–4932. DOI: http://dx.doi.org/10.1175/JCLI-D-17-0427.1.

Overland, JE, Wang, M. 2013. When will the summer Arctic be nearly sea ice free? *Geophysical Research Letters* **40**(10): 2097–2101. DOI: http://dx.doi.org/10.1002/grl.50316.

Pabi, S, van Dijken, GL, Arrigo, KR. 2008. Primary production in the Arctic Ocean, 1998–2006. *Journal of Geophysical Research: Oceans* **113**: C8. DOI: http://dx.doi.org/10.1029/2007JC004578.

Pesant, S, Legendre, L, Gosselin, M, Bjornsen, PK, Fortier, L, Michaud, J, Nielsen, TG. 2000. Pathways of carbon cycling in marine surface waters: The fate of small-sized phytoplankton in the Northeast Water Polynya. *Journal of Plankton Research* **22**(4): 779–801. DOI: http://dx.doi.org/10.1093/plankt/22.4.779.

Pesant, S, Legendre, L, Gosselin, M, Smith, R, Kattner, G, Ramseier, R. 1996. Size-differential regimes of phytoplankton production in the Northeast Water Polynya (77°–81°N). *Marine Ecology Progress Series* **142**: 75–86. DOI: http://dx.doi.org/10.3354/meps142075.

Piepenburg, D. 2005. Recent research on Arctic benthos: Common notions need to be revised. *Polar Biology* **28**(10): 733–755. DOI: http://dx.doi.org/10.1007/s00300-005-0013-5.

Piepenburg, D, Ambrose, WG, Brandt, A, Renaud, PE, Ahrens, MJ, Jensen, P. 1997. Benthic community patterns reflect water column processes in the Northeast Water polynya (Greenland). *Journal of Marine Systems* **10**(1–4): 467–482. DOI: http://dx.doi.org/10.1016/S0924-7963(96)00050-4.

Piepenburg, D, Archambault, P, Ambrose, WG, Blanchard, AL, Bluhm, BA, Carroll, ML, Conlan, KE, Cusson, M, Feder, HM, Grebmeier, JM, Jewett, SC, Lévesque, M, Petryashev, VV, Sejr, MK, Sirenko, BI, Włodarska-Kowalczuk, M. 2011. Towards a pan-Arctic inventory of the species diversity of the macro- and megabenthic fauna of the Arctic shelf

seas. *Marine Biodiversity* **41**: 51–70. DOI: http://dx.doi.org/10.1007/s12526-010-0059-7.

Piepenburg, D, Blackburn, T, von Dorrien, C, Gutt, J, Hall, P, Hulth, S, Kendall, M, Opalinski, K, Rachor, E, Schmid, M. 1995. Partitioning of benthic community respiration in the Arctic (northwestern Barents Sea). *Marine Ecology Progress Series* **118**: 199–213. DOI: http://dx.doi.org/10.3354/meps118199.

Polyakov, IV, Alkire, MB, Bluhm, BA, Brown, KA, Carmack, EC, Chierici, M, Danielson, SL, Ellingsen, I, Ershova, EA, Gårdfeldt, K, Ingvaldsen, RB, Pnyushkov, AV, Slagstad, D, Wassmann, P. 2020. Borealization of the Arctic Ocean in response to anomalous advection from sub-Arctic seas. *Frontiers in Marine Science* **7**: 491. DOI: http://dx.doi.org/10.3389/fmars.2020.00491.

Preben, J, Herman, R. 2023. Abundance of nematoda genera on the Northeast Greenland shelf collected between May and August 1993 with USCG Polar Sea and R/V Polarstern (ARK VIII/2). PANGAEA. DOI: http://dx.doi.org/10.1594/PANGAEA.959509.

R Core Team. 2018. R: A language and environment for statistical computing. Vienna, Austria: R Foundation for Statistical Computing. Available at https://www.R-project.org/. Accessed August 20, 2018.

Reeh, N. 2017. Greenland ice shelves and ice tongues, in Copland, L, Mueller, D eds., *Arctic ice shelves and ice islands.* Springer: 75–106. DOI: http://dx.doi.org/10.1007/978-94-024-1101-0.

Reeh, N, Thomsen, HH, Higgins, AK, Weidick, A. 2001. Sea ice and the stability of north and northeast Greenland floating glaciers. *Annals of Glaciology* **33**: 474–480. DOI: http://dx.doi.org/10.3189/172756401781818554.

Renaud, PE, Ambrose, WGJ. 2023. Benthic polychaeta diversity on the Northeast Greenland (NEG) shelf collected between July–August 1992 and between May and August 1993. DOI: http://dx.doi.org/10.1594/PANGAEA.959541.

Renaud, PE, Morata, N, Carroll, ML, Denisenko, SG, Reigstad, M. 2008. Pelagic–benthic coupling in the western Barents Sea: Processes and time scales. *Deep Sea Research Part II: Topical Studies in Oceanography* **55**(20–21): 2372–2380. DOI: http://dx.doi.org/10.1016/j.dsr2.2008.05.017.

Renaud, PE, Riedel, A, Michel, C, Morata, N, Gosselin, M, Juul-Pedersen, T, Chiuchiolo, A. 2007. Seasonal variation in benthic community oxygen demand: A response to an ice algal bloom in the Beaufort Sea, Canadian Arctic? *Journal of Marine Systems* **67**: 1–12. DOI: http://dx.doi.org/10.1016/j.jmarsys.2006.07.006.

Revsbech, NP. 1989. An oxygen microsensor with a guard cathode. *Limnology and Oceanography* **34**(2): 474–478. DOI: http://dx.doi.org/10.4319/lo.1989.34.2.0474.

Rignot, E, Kanagaratnam, P. 2006. Changes in the velocity structure of the Greenland ice sheet. *Science* **311**:

986–990. DOI: http://dx.doi.org/10.1126/science.1121381.

Rowe, GT, Boland, GS, Escobar-Briones, EG, Cruz-Kaegi, ME, Newton, A, Piepenburg, D, Walsh, I, Deming, J. 1997. Sediment community biomass and respiration in the Northeast water polynya, Greenland: A numerical simulation of benthic lander and spade core data. *Journal of Marine Systems* **10**: 497–515. DOI: http://dx.doi.org/10.1016/S0924-7963(96)00065-6.

Sakshaug, E, Johnsen, G, Kristiansen, S, von Quillfeldt, CH, Rey, F, Slagstad, D, Thingstad, F. 2009. Phytoplankton and primary production, in Sakshaug, E, Johnsen, G, Kovacs, KM eds., *Ecosystem Barents Sea*. Trondheim, Norway: Tapir Academic Press: 167–208.

Sakshaug, E, Skjoldal, HR. 1989. Life at the ice edge. *Ambio* **18**: 60–67.

Schaffer, J, Kanzow, T, von Appen, W-J, Albedyll, L, von Arndt, JE, Roberts, DH. 2020. Bathymetry constrains ocean heat supply to Greenland's largest glacier tongue. *Nature Geoscience* **13**: 227–231. DOI: http://dx.doi.org/10.1038/s41561-019-0529-x.

Schaffer, J, von Appen, W-J, Dodd, PA, Hofstede, C, Mayer, C, de Steur, L, Kanzow, T. 2017. Warm water pathways toward Nioghalvfjerdsfjorden Glacier, Northeast Greenland. *Journal of Geophysical Research: Oceans* **122**(5): 4004–4020. DOI: http://dx.doi.org/10.1002/2016JC012462.

Schneider, W, Budéus, G. 1994. The Northeast Water Polynya (Greenland Sea) I. A physical concept of its generation. *Polar Biology* **14**: 1–9.

Seinhorst, JW. 1959. A rapid method for the transfer of nematodes from fixative to anhydrous glycerin. *Nematologica* **4**: 67–69.

Sejr, MK, Jensen, KT, Rysgaard, S. 2000. Macrozoobenthic community structure in a high-Arctic East Greenland fjord. *Polar Biology* **23**: 792–801. DOI: http://dx.doi.org/10.1007/s003000000154.

Sejr, MK, Stedmon, CA, Bendtsen, J, Abermann, J, Juul-Pedersen, T, Mortensen, J, Rysgaard, S. 2017. Evidence of local and regional freshening of Northeast Greenland coastal waters. *Scientific Reports* **7**: 13183. DOI: http://dx.doi.org/10.1038/s41598-017-10610-9.

Skagseth, Ø, Eldevik, T, Årthun, M, Asbjørnsen, H, Lien, VS, Smedsrud, LH. 2020. Reduced efficiency of the Barents Sea cooling machine. *Nature Climate Change* **10**: 661–666. DOI: http://dx.doi.org/10.1038/s41558-020-0772-6.

Smedsrud, LH, Muilwijk, M, Brakstad, A, Madonna, E, Lauvset, SK, Spensberger, C, Born, A, Eldevik, T, Drange, H, Jeansson, E, Li, C, Olsen, A, Skagseth, Ø, Slater, DA, Straneo, F, Våge, K, Årthun, M. 2022. Nordic seas heat loss, Atlantic inflow, and Arctic sea ice cover over the last century. *Reviews of Geophysics* **60**(1): e2020RG000725. DOI: http://dx.doi.org/10.1029/2020RG000725.

Smith, KL, Ruhl, HA, Kahru, M, Huffard, CL, Sherman, AD. 2013. Deep ocean communities impacted by changing climate over 24 y in the abyssal northeast Pacific Ocean. *Proceedings of the National Academy of Sciences* **110**(49): 19838–19841. DOI: http://dx.doi.org/10.1073/pnas.1315447110.

Smith, WO, Barber, DG. 2007. Polynyas and climate change: A view to the future, in Smith, WO, Barber, DG eds., *Elsevier oceanography series, polynyas: Windows to the world*. Elsevier: **74**: 411–419. DOI: http://dx.doi.org/10.1016/S0422-9894(06)74013-2.

Spielhagen, RF, Werner, K, Sørensen, SA, Zamelczyk, K, Kandiano, E, Budeus, G, Husum, K, Marchitto, TM, Hald, M. 2011. Enhanced modern heat transfer to the Arctic by warm Atlantic Water. *Science* **331**(6016): 450–453. DOI: http://dx.doi.org/10.1126/science.1197397.

Spies, A. 1987. Phytoplankton in the Marginal Ice Zone of the Greenland Sea during summer, 1984. *Polar Biology* **7**: 195–205. DOI: http://dx.doi.org/10.1007/BF00287416.

Spreen, G, de Steur, L, Divine, D, Gerland, S, Hansen, E, Kwok, R. 2020. Arctic sea ice volume export through Fram Strait from 1992 to 2014. *Journal of Geophysical Research: Oceans* **125**(6): e2019JC016039. DOI: http://dx.doi.org/10.1029/2019JC016039.

Stirling, I. 1997. The importance of polynyas, ice edges, and leads to marine mammals and birds. *Journal of Marine Systems* **10**(1–4): 9–21. DOI: http://dx.doi.org/10.1016/S0924-7963(96)00054-1.

Straneo, F, Sutherland, DA, Holland, DM, Gladish, C, Hamilton, GS, Johnson, HL, Rignot, E, Xu, Y, Koppes, M. 2012. Characteristics of ocean waters reaching Greenland's glaciers. *Annals of Glaciology* **53**(60): 202–210. DOI: http://dx.doi.org/10.3189/2012AoG60A059.

Stroeve, JC, Serreze, MC, Holland, MM, Kay, JE, Malanik, J, Barrett, AP. 2012. The Arctic's rapidly shrinking sea ice cover: A research synthesis. *Climatic Change* **110**: 1005–1027. DOI: http://dx.doi.org/10.1007/s10584-011-0101-1.

Sumata, H, de Steur, L, Gerland, S, Divine, DV, Pavlova, O. 2022. Unprecedented decline of Arctic Sea ice outflow in 2018. *Nature Communications* **13**: 1747. DOI: http://dx.doi.org/10.1038/s41467-022-29470-7.

Syring, N, Stein, R, Fahl, K, Vahlenkamp, M, Zehnich, M, Spielhagen, RF, Niessen, F. 2020. Holocene changes in sea-ice cover and polynya formation along the eastern North Greenland shelf: New insights from biomarker records. *Quaternary Science Reviews* **231**: 106173. DOI: http://dx.doi.org/10.1016/j.quascirev.2020.106173.

Tengberg, A, De Bovee, F, Hall, P, Berelson, W, Chadwick, D, Ciceri, G, Crassous, P, Devol, A, Emerson, S, Gage, J. 1995. Benthic chamber and profiling landers in oceanography—A review of design, technical solutions and functioning. *Progress in Oceanography* **35**(3): 253–294.

Thomsen, HH, **Reeh, N**, **Olesen, OB**, **Boggild, CE**, **Starzer, W**, **Weidick, A**, **Higgins, AK.** 1997. The Nioghalvfjerdsfjorden glacier project, North-East Greenland: A study of ice sheet response to climatic change. *Geology of Greenland Survey Bulletin* **176**: 95–103.

Veit-Köhler, G, **Durst, S**, **Schuckenbrock, J**, **Hauquier, F**, **Durán Suja, L**, **Dorschel, B**, **Vanreusel, A**, **Martínez Arbizu, P.** 2018. Oceanographic and topographic conditions structure benthic meiofauna communities in the Weddell sea, Bransfield Strait and Drake Passage (Antarctic). *Progress in Oceanography* **162**: 240–256. DOI: http://dx.doi.org/10.1016/j.pocean.2018.03.005.

von Appen, W-J, **Waite, AM**, **Bergmann, M**, **Bienhold, C**, **Boebel, O**, **Bracher, A**, **Cisewski, B**, **Hagemann, J**, **Hoppema, M**, **Iversen, MH**, **Konrad, C**, **Krumpen, T**, **Lochthofen, N**, **Metfies, K**, **Niehoff, B**, **Nöthig, E-M**, **Purser, A**, **Salter, I**, **Schaber, M**, **Scholz, D**, **Soltwedel, T**, **Torres-Valdes, S**, **Wekerle, C**, **Wenzhöfer, F**, **Wietz, M**, **Boetius, A.** 2021. Sea-ice derived meltwater stratification slows the biological carbon pump: Results from continuous observations. *Nature Communications* **12**: 7309. DOI: http://dx.doi.org/10.1038/s41467-021-26943-z.

Wadhams, P. 1981. The ice cover in the Greenland and Norwegian seas. *Reviews of Geophysics* **19**(3): 345–393. DOI: http://dx.doi.org/10.1029/RG019i003p00345.

Wassmann, P, **Reigstad, M.** 2011. Future Arctic Ocean seasonal ice zones and implications for pelagic-benthic coupling. *Oceanography* **24**(3): 220–231. DOI: http://dx.doi.org/10.5670/oceanog.2011.74.

Wessel, P, **Smith, WHF.** 1996. A global, self-consistent, hierarchical, high-resolution shoreline database. *Journal of Geophysical Research: Solid Earth* **101**(B4): 8741–8743. DOI: http://dx.doi.org/10.1029/96JB00104.

Whitaker, D. 2021. Clustsig. Available at https://github.com/douglaswhitaker/clustsig. Accessed November 9, 2022.

Wiedmann, I, **Ershova, E**, **Bluhm, BA**, **Nöthig, EM**, **Gradinger, RR**, **Kosobokova, K**, **Boetius, A.** 2020. What feeds the benthos in the Arctic basins? Assembling a carbon budget for the deep Arctic Ocean. *Frontiers in Marine Science* **7**: 224. DOI: http://dx.doi.org/10.3389/fmars.2020.00224.

Wieser, W. 1953. Die Beziehung zwischen Mundhöhlengestalt, Ernährungsweise und Vorkommen bei freilebenden marinen Nematoden: Eine ökologisch-morphologische studie. *Arkiv för zoologi* **2**(Ser 4): 439–484.

Wilson, NJ, **Straneo, F.** 2015. Water exchange between the continental shelf and the cavity beneath Nioghalvfjerdsbræ (79 North Glacier). *Geophysical Research Letters* **42**(18): 7648–7654. DOI: http://dx.doi.org/10.1002/2015GL064944.

Włodarska-Kowalczuk, M, **Górska, B**, **Deja, K**, **Morata, N.** 2016. Do benthic meiofaunal and macrofaunal communities respond to seasonality in pelagial processes in an Arctic fjord (Kongsfjorden, Spitsbergen)? *Polar Biology* **39**: 2115–2129. DOI: http://dx.doi.org/10.1007/s00300-016-1982-2.

Włodarska-Kowalczuk, M, **Pearson, TH.** 2004. Soft-bottom macrobenthic faunal associations and factors affecting species distributions in an Arctic glacial fjord (Kongsfjord, Spitsbergen). *Polar Biology* **27**: 155–167. DOI: http://dx.doi.org/10.1007/s00300-003-0568-y.

Włodarska-Kowalczuk, M, **Pearson, TH**, **Kendall, MA.** 2005. Benthic response to chronic natural physical disturbance by glacial sedimentation in an Arctic fjord. *Marine Ecology Progress Series* **303**: 31–41. DOI: http://dx.doi.org/10.3354/meps303031.

Włodarska-Kowalczuk, M, **Renaud, PE**, **Węsławski, JM**, **Cochrane, SK**, **Denisenko, SG.** 2012. Species diversity, functional complexity and rarity in Arctic fjordic versus open shelf benthic systems. *Marine Ecology Progress Series* **463**: 73–87. DOI: http://dx.doi.org/10.3354/meps09858.

Wright, SW, **Jeffrey, SW.** 1997. High-resolution HPLC system for chlorophylls and carotenoids of marine phytoplankton, in Jeffrey, SW, Wright, SW, Mantoura, RFC eds., *Phytoplankton pigments in oceanography: Guidelines to modern methods*. Paris, France: UNESCO Pub.

Elem Sci Anth is a peer-reviewed open access journal published by University of California Press.

OPEN ACCESS

Paper II

Seasonal patterns of vertical flux in the northwestern Barents Sea under Atlantic Water influence and sea-ice decline

Yasemin V. Bodur [a,*], Paul E. Renaud [b], Lucie Goraguer [c], Martí Amargant-Arumí [a], Philipp Assmy [c], Anna Maria Dąbrowska [d], Miriam Marquardt [a], Angelika H.H. Renner [e], Agnieszka Tatarek [d], Marit Reigstad [a]

[a] *UiT – the Arctic University of Norway, Tromsø, Norway*
[b] *Akvaplan-niva, Tromsø, Norway*
[c] *Norwegian Polar Institute, Tromsø, Norway*
[d] *Institute of Oceanology Polish Academy of Science (IOPAN), Poland*
[e] *Institute of Marine Research, Tromsø, Norway*

ARTICLE INFO

ABSTRACT

The northern Barents Sea is a productive Arctic inflow shelf with a seasonal ice cover and as such, a location with an efficient downward export of particulate organic matter through the biological carbon pump. The region is under strong influence of Atlantification and sea-ice decline, resulting in a longer open water and summer period. In order to understand how these processes influence the biological carbon pump, it is important to identify the seasonal and spatial dynamics of downward vertical flux of particulate organic matter. In 2019 and 2021, short-term sediment traps were deployed between 30 and 200 m depth along a latitudinal transect in the northwestern Barents Sea during March, May, August and December. Vertical flux of particulate organic carbon, $\delta^{13}C$ and $\delta^{15}N$ values, Chl-a, protists and fecal pellets were assessed. We identified a clear seasonal pattern, with highest vertical flux in May and August (178 $\pm$ 202 and 159 $\pm$ 79 mg C m^{-2} d^{-1}, respectively). Fluxes in December and March were < 45 mg C m^{-2} d^{-1}. May was characterized by diatom- and Chl a-rich fluxes and high spatial variability, while fluxes in August had a higher contribution of fecal pellets and small flagellates, and were spatially more homogenous. Standing stocks of suspended particulate organic matter were highest in August, suggesting a more efficient retention system in late summer. The strong latitudinal sea-ice gradient and the influence of Atlantic Water probably led to the high spatial variability of vertical flux in spring, due to their influence on primary productivity. We conclude that the efficiency of the biological carbon pump in a prolonged open-water period depends on the reworking of small, slow sinking material into efficiently sinking fecal pellets or aggregates, and the occurrence of mixing.

1. Introduction

The Barents Sea is the largest inflow shelf of the Arctic Ocean, and with an annual primary production of 20–200 g C m^{-2} yr^{-1} it is also one of the most productive Arctic shelf seas (Wassmann et al., 2006; Sakshaug et al., 2009). Over the last decades, the northern Barents Sea has experienced the largest sea ice loss across the Arctic Ocean (Screen and Simmonds, 2010; Onarheim et al., 2018; Smedsrud et al., 2022). Moreover, the heat and inflow of warm (>2 °C) and saline (>35.06 g kg^{-1}) Atlantic Water (AW) in this region is increasing (Oziel et al., 2020; Polyakov et al., 2020; Skagseth et al., 2020; Ingvaldsen et al., 2021;

Smedsrud et al., 2022; AW definition following Sundfjord et al., 2020). This "Atlantification" is predicted to have significant consequences for the marine ecosystem in this region and thus, for the cycling and export of organic carbon (Wassmann and Reigstad, 2011).

Over the last century, the uptake of atmospheric CO₂ by the Arctic Ocean has increased by around 30% (Smedsrud et al., 2022). An especially tight pelagic-benthic coupling has been documented in the marginal sea-ice zone (MIZ) in the northern Barents Sea (Wassmann et al., 2006). Thus, the biological carbon pump in the Barents Sea is an important sink for anthropogenic carbon as well as a crucial food source for benthic communities in the region (Carroll et al., 2008). It is therefore important to

---

investigate the strength of the biological carbon pump across the marginal or seasonal ice zone today, in order to evaluate potential responses to future climate change.

As a consequence of earlier ice melt and later onset of freezing, earlier phytoplankton blooms and a longer productive period in the MIZ are predicted (Ellingsen et al., 2008; Slagstad et al., 2015; Polyakov et al., 2020), resulting in longer summer conditions (Wassmann and Reigstad, 2011). While remote sensing from satellites have shown an increase of annual primary production in the northern Barents Sea (Arrigo and van Dijken 2015; Dalpadado et al. 2014; Lewis et al. 2020), the stratification regime and nutrient availability will most likely determine whether there will be an increase or a decrease in a future warmer central and southern Barents Sea (Slagstad et al., 2011; Mousing et al., 2023).

The efficiency of the biological carbon pump depends not only on primary production, but on a number of regulating mechanisms, such as grazing and fecal pellet production by zooplankton, aggregation and disaggregation of particles, microbial processes, ballasting by minerals, vertical mixing and stratification of the upper water column (De La Rocha and Passow, 2007; Turner, 2015; Iversen, 2023). Since retention processes dominate in the pelagic realm, vertical flux is typically "attenuated" sharply in surface waters, and usually less than 10% of primary production reaches below the mesopelagic zone (Martin et al., 1987; Wassmann et al., 2003). Highest export has most often been measured during peak bloom events in spring (Reigstad et al., 2008; Dybwad et al., 2021). While nutrients decrease as the season proceeds, the carbon flux is increasingly dominated by regenerated material orginating from blooms of lower magnitude with a higher fraction of small cells during summer (late bloom scenarios; Reigstad et al., 2008; Dybwad et al., 2021; Trudnowska et al., 2021). Small cells usually sink less efficiently and are more often coupled to a tight microbial food web, leading to higher retention in the surface water column (Wassmann et al., 2006) and a reduced efficiency of the biological carbon pump. Thus, a prolonged summer season and increased light availability for primary production will not necessarily result in higher export of carbon (Wassmann and Reigstad, 2011). However, if a sufficiently high amount of small and reworked particles is present and vertical flux attenuation is weak, these particles can contribute significantly to vertical flux (Wiedmann et al., 2014).

As an Arctic inflow shelf, the northern Barents Sea is under strong influence of AW, which impacts physical and biological properties in the region such as amplified warming, reduced sea ice thickness, enhanced upper ocean mixing, nutrient supply, advection of organic material and increased primary production (Polyakov et al., 2020; Skagseth et al., 2020; Ingvaldsen et al., 2021). Another consequence is that boreal zooplankton are expanding northwards in the Barents Sea (Ellingsen et al., 2008; Drinkwater, 2011; Dalpadado et al., 2012; Fossheim et al., 2015; Eriksen et al., 2017), altering pelagic communities and their functions (Renaud et al., 2018). These changing properties are termed "Atlantification". Increased metabolic activity due to warming (Wohlers et al., 2009) and an increase of grazers could lead to enhanced degradation of organic matter in the water column. On the other hand, grazers can enhance vertical flux by packaging the production into fast-sinking fecal pellets (Wexels Riser et al., 2008), which can substantially contribute to vertical flux in the Barents Sea (Wiedmann et al., 2014; Dybwad et al., 2022).

Only a few studies have been carried out in the Arctic Ocean that integrate the effects of temporal (seasonal), spatial and depth gradients of vertical flux and its composition (e.g. Olli et al., 2002; Reigstad et al., 2008; Dybwad et al., 2021), and we are aware of only 3 studies that deployed short-term sediment traps at revisited stations (Lalande et al., 2016a; Walker et al., 2022; Wiedmann et al., 2016). However, these are from Arctic fjords and do not integrate spatial variability. In order to fill this gap for the seasonally ice-covered northern Barents Sea, we revisited stations along a latitudinal transect in 2019 and 2021 during different seasons reflecting potential changes in drivers most strongly impacted by climate change (sea ice, water masses). Short-term sediment traps were deployed to assess daily vertical flux patterns and its composition. We attempted to 1. describe seasonal and spatial patterns in vertical flux, 2. identify the importance of environmental (sea ice, water mass) and biological drivers contributing to the observed patterns and 3. explore the implications of these results in a changing Arctic Ocean.

2. Methods

2.1. Study area and short-term sediment trap deployment

The study was carried out within the framework of the Norwegian research project The Nansen Legacy. Fieldwork took place in August and December 2019, and March and May 2021 at 6 stations following a transect between 75° and 85°N along the 30°E meridian in the northern Barents Sea (Fig. 1) aboard the Norwegian icebreaker *RV Kronprins Haakon*.

Stations P1, P2, P4, and P5 were on the shelf whereas P6 was on the northern Barents Sea slope and P7 was in the Nansen Basin (Fig. 1). The northern Barents Sea shelf is around 300 m deep, while two stations on the shelf (P2 and P5) were located on shallower banks and are <200 m deep. The positions of stations P6 and P7 varied somewhat due to ice conditions during the different cruises. Thus, the depth at station P6 varied between ~800–1500 m while station P7 in the Nansen Basin had a water depth of >3000 m (Table 1).

Atlantic Water (AW) enters the central and northern Barents Sea via two pathways (Fig. 1). One pathway is through the Barents Sea Opening between mainland Norway and Bjørnøya towards the southern Barents Sea, where P1 is situated, and continuing eastwards (Ingvaldsen et al., 2002; Ingvaldsen et al., 2004). The second pathway follows the continental slope first west then north of Svalbard (Beszczynska-Möller et al. 2012). From there, AW enters the northern Barents Sea through two troughs on either side of Kvitøya (Lind and Ingvaldsen, 2012; Lundesgaard et al., 2022).

During the sampling campaigns, station P1 was influenced by warm and saline AW or modified AW (mAW: AW that has lost heat; Sundfjord et al., 2020) throughout the water column. In August, P1 displayed presence of warm (<0°C) Polar Water at the surface (wPW; Sundfjord et al. 2020). wPW is usually PW that is warmed by AW from below, or by solar radiation at the surface. Stations P2, P4 and P5 were mainly characterized by Polar Water (PW), with wPW dominating below 100 m during March and above 40 m during August. During March and May, stations P6 and P7 were dominated by wPW below ~ 50 m, while PW dominated at the surface. In August and December, a deep core of AW was present below 100 m at these stations.

Short-term drifting sediment traps (KC Denmark, aspect ratio > 6) were deployed during each sampling campaign at 6 depths (30, 40, 60, 90, 120 and 200 m) for a duration between 18 and 38 h, with longer deployment times during periods of low vertical flux. At stations shallower than 250 m, the deepest trap was at 120 m. In order to ensure settling of particles into the traps, the cylinders were filled with pre-filtered (0.7 μm GF/F Whatman) high-density bottom water. The traps were deployed without poison in open water, sea ice leads or anchored to a sea ice floe, depending on the sea ice conditions at the station.

2.2. Subsampling for biogeochemical and biological analysis

After sediment trap retrieval, the content of all traps (2 or 4 cylinders) at each depth were pooled and kept cold and dark until subsamples were taken for size fractionated chlorophyll *a* (Chl-*a*; Bodur et al. 2023a–d), fecal pellets (FP; Bodur et al. 2023e–h), protist community composition (Bodur et al. 2023i–l), particulate organic carbon and particulate nitrogen (POC and PN; Bodur et al. 2023m–p), and stable isotopes (SI; Bodur et al. 2023q–t).
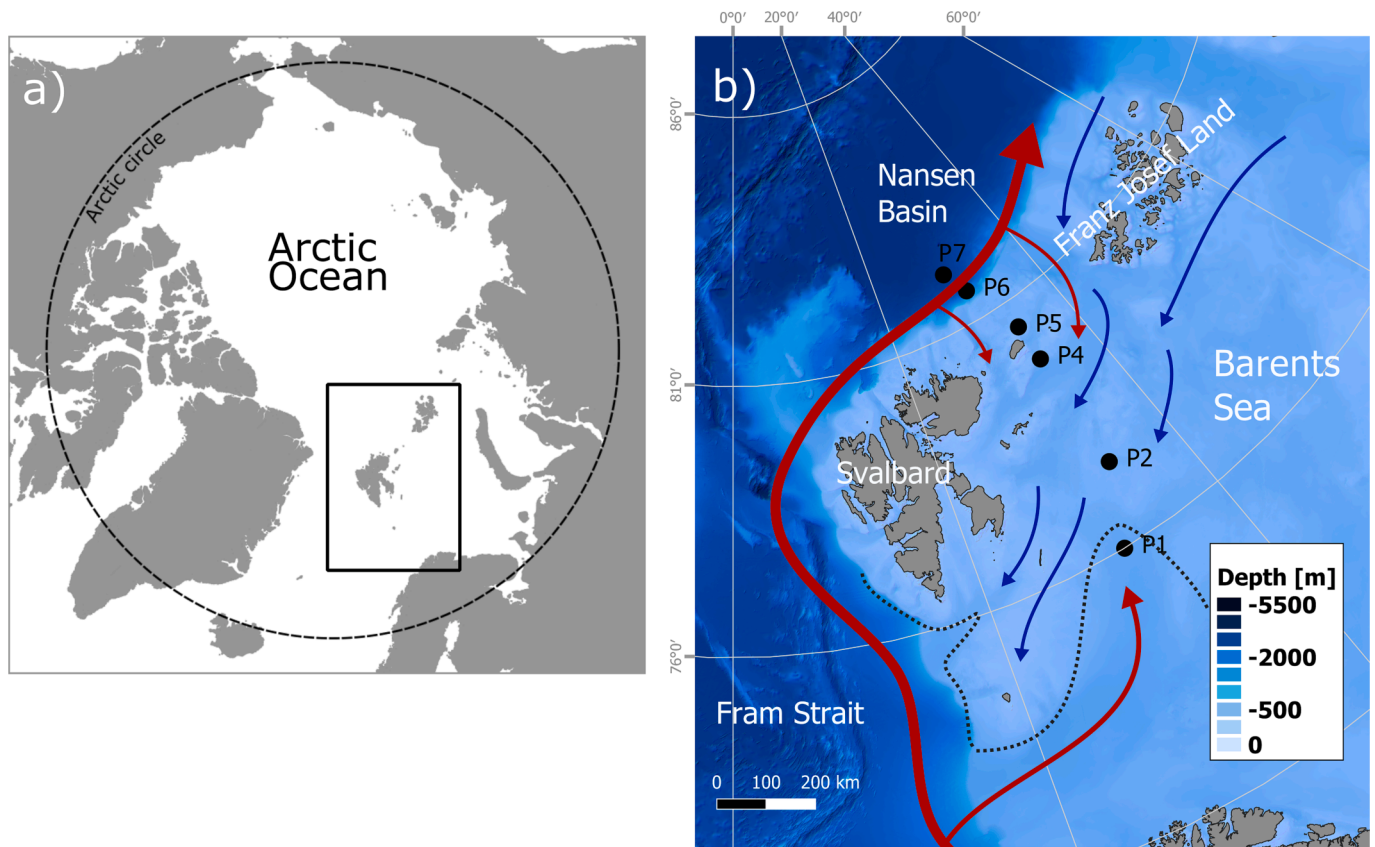
Fig. 1. Map of the a) Arctic Ocean, showing the study area in the black rectangle, and b) nominal sampling locations in the central and northwestern Barents Sea during August 2019, December 2019, March 2021 and May 2021, general patterns of inflowing Atlantic Water along and onto the shelf (red arrows), general patterns of surface Polar Water (blue arrows) and approximate location of the Polar Front (dashed line, after Onarheim and Teigen 2018). For actual sampling locations during each individual cruise see Table 1. Bathymetry obtained from the International Bathymetric Chart of the Arctic Ocean (IBCAO; Jakobsson et al., 2020) and coastlines from Wessel & Smith (1996), plotted with QGIS 3.28.2.

Table 1

Sampling locations and details for short-term sediment trap deployments during August and December 2019 and March and May 2021 in the northwestern Barents Sea. Daily sea ice concentration data for station locations were retrieved from Steer and Divine (2023) and mean % ice cover is calculated from the 4 weeks preceding the respective sampling date. Chl-*a* data was retrieved from Vader (2022a–d), and the depth of Chl-*a* maximum is shown within paranthesis.

Station	Latitude	Longitude	Deployment date	Depth (m)	Deployment duration (hours)	Mean % ice cover	Max susp. Chl a (mg m^{-3})
P1	76.00	31.22	08.08.2019	325	23.55	0 ± 0	1.22 (55 m)
P4	79.78	33.97	13.08.2019	330	19.10	8 ± 17	1.37 (30 m)
P5	80.50	33.88	15.08.2019	157	20.67	92 ± 8	2.57 (20 m)
P6	81.57	31.22	18.08.2019	861	18.15	96 ± 4	1.29 (10 m)
P7	81.93	29.16	21.08.2019	3312	24.75	96 ± 5	1.74 (10 m)
P4	79.82	34.17	08.12.2019	271	27.77	100 ± 1	0.02 (121 m)
P7 (DEEP-ICE)	82.06	29.22	01.12.2019	3433	41.75	98 ± 2	0.04 (20 m)
P4	79.74	33.88	09.03.2021	334	38.72	97 ± 3	N.A.[a]
P5	80.52	33.99	12.03.2021	162	25.80	85 ± 20	0.01 (30 m)
P6	81.54	31.02	14.03.2021	789	27.13	28 ± 34	0.02 (10 m)
P7	82.00	29.98	16.03.2021	3299	33.53	20 ± 35	0.02 (10 m)
P1	76.00	31.22	01.05.2021	326	11.97	0 ± 0	1.66 (50 m)
P2	77.50	33.96	02.05.2021	188	11.68	21 ± 31	1.29 (50 m)
P4	79.75	33.97	04.05.2021	359	26.75	71 ± 33	2.13 (50 m)
P5	80.50	34.07	07.05.2021	162	25.85	96 ± 4	0.69 (10 m)
P6	81.56	30.76	09.05.2021	1557	23.3	92 ± 7	3.17 (30 m)
P7	82.12	29.13	13.05.2021	3369	26.12	96 ± 4	0.29 (90 m)

[a] Not available.

Subsamples for Chl-*a* were filtered in triplicates onto GF/F (Whatman, 0.7 μm) filters and filtered volumes ranged from 100 to 300 ml depending on the amount of material in the traps. Additional samples for Chl-*a* were filtered on 10 μm polycarbonate filters (Millipore) to quantify the contribution from larger cells.

Triplicates of 250–1000 ml were filtered for POC/PN and SI, respectively, onto pre-combusted GF/F filters. POC samples were stored at −20 °C and SI samples at −80 °C until further processing.

250 ml from each depth was fixed with hexamethylenetetramine-buffered 37% formaldehyde (final pH = 7) to a final concentration of

4% for microscopic inspection of fecal pellets, and 100 ml was fixed with a mixture of glutaraldehyde-lugol for protist examination (Rousseau et al., 1990).

2.3. Biogeochemical analysis

Size-fractionated Chl-*a* (0.7 and 10 μm) was extracted from the filters in 100% methanol at 4 °C after filtration and measured on board within 12–24 h after sampling (modified after Holm-Hansen and Riemann, 1978) with a pre-calibrated Turner Design AU-10 fluorometer in 2019 and Turner Triology in 2021 before and after acidification with 5% HCl. Concentrations of Chl-*a* pigments and their phaeopigment degradation products were calculated according to Holm-Hansen and Riemann (1978).

Filters for POC and PN were dried for 24 h at 60° C and subsequently acid fumed (HCl) for 24 h in order to remove all inorganic carbon. Afterwards, the samples were again dried for 24 h at 60° C, transferred to tin capsules and measured with an Exeter Analytical CE440 CHN elemental analyzer.

Standards for isotopic ratios for carbon and nitrogen were Vienna PeeDee belemnite and air, respectively. Alanine (JALA, Fischer Scientific) was used for internal quality assurance with an analytical precision of $\delta^{13}C_{VPDB}$ = -20.59 ± 0.05 ‰ (n = 47 runs) and $\delta^{15}N_{AIR}$ = -3.16 ± 0.10 ‰ (n = 57 runs), respectively. L-glutamic acid (JGLUT, Fischer Scientific) and glycine (POPPGLY, Fischer Scientific) were used as internal reference material. Internal references and quality assurance for $\delta^{13}C_{VPDB}$ were calibrated against calcium carbonate (NBS19) and lithium carbonate (LSVEC) with consensus values 1.95 ‰ and −46.6 ‰, respectively, and for $\delta^{15}N_{AIR}$ against L-glutamic acid (USGS40 and USGS41) with consensus values −4.52 ‰ and 47.57 ‰, respectively.

2.4. Analysis of vertical flux particle composition

Protists, including phyto- and protozooplankton, were identified to the lowest possible taxonomic level in accordance with the World Register of Marine Species (WoRMS) and counted under an inverted light microscope (Nikon Eclipse TE-300 and Ti-S) using the Utermöhl method (Utermöhl, 1958; Edler and Elbrächter, 2010). Between 23 and 2301 cells (December and May, respectively) were counted per sample (mean: 531 ± 595 cells per sample across all sample dates and stations). Abundances were converted to carbon biomass based on published geometric relationships for biovolume conversion (Hillebrand et al., 1999) and biovolume to carbon conversion factors (Menden-Deuer and Lessard, 2000). Radiolaria (12 recorded instances with < 4 individuals counted) and Foraminifera (1 instance with 1 count) were kept in the community composition data, but were removed from biomass estimations as no size measurements were available and thus carbon estimates could not be made for these groups.

Depending on their density in the sample, subsamples of 25–100 ml were taken for fecal pellet analysis and settled in Utermöhl sedimentation chambers for 24 h. Subsequently they were counted and the length and width of each fecal pellet were measured using a Leica inverted microscope. The condition of each pellet was noted (intact, end piece or mid piece). Long and cylindrical pellets were attributed to calanoid copepods, small ellipsoid pellets to appendicularians, and larger strings with cut ends to euphausiids (Dybwad et al. 2021). Larger and irregularly shaped ellipsoid pellets were attributed to chaetognaths (Dilling and Alldredge 1993; Giesecke et al. 2010). Micropellets were ignored because they can be difficult to distinguish from protozoans or detritus.

Based on the pellet types, the volume for each pellet was calculated and their carbon content was assessed using empirical conversion factors of 94.3 μg C mm^{-3} for copepod, 45.1 μg C mm^{-3} for krill and 25.1 μg C mm^{-3} for appendicularian pellets after Wexels Riser et al. (2007), 12.73 μg C mm^{-3} for chaetognath pellets after Giesecke et al. (2010) and 69.4 μg C mm^{-3} for unidentified pellets after Riebesell et al. (1995).

The percentage contribution of fecal pellet carbon (FPC) and protist carbon (PC) to total POC are estimates using empirically determined conversion factors, largely from other locations and seasons as stated above. This sometimes resulted in higher FPC or PC estimations than total measured POC. Manno et al. (2015) showed that FPC content can be lower in late autumn/winter in the Southern Ocean and Franco-Santos et al. (2018) demonstrated different FPC content under contrasting nutrient conditions; however, Urban-Rich (1997) showed that there was no difference in carbon to volume ratio between food types and different locations.

2.5. Statistical analyses

All statistical analyses were performed in the computing software R (version 4.2.2), using the vegan package (Oksanen et al., 2018). An unconstrained correspondence analysis (CA) was performed on log-transformed protist community data in order to downweigh stations with high abundances. A second CA was run on biomass data. In order to delineate which groups (diatoms, dinoflagellates, ciliates, *Phaeocystis*, other flagellates) dominated the vertical flux at the respective stations during each season, they were plotted on top of the ordination. To understand how POC fluxes were related to the protist community composition, they were displayed by isolines.

In order to describe how bulk flux characteristics differed at each station during each season, a principal component analysis (PCA) on scaled (centered to mean of zero) flux variables (POC, POC:PN ratio, FPC, PC, protist abundance, Chl-*a*, % of Chl-*a* > 10 μm, Chl-*a*:Phaeopigment ratio) was performed. Subsequently, environmental (sea ice, salinity, temperature and water mass) and suspended biological (integrated suspended POC, POC:PN ratio, Chl-*a*, Chl-*a*:Phaeogiment ratio, % of Chl-*a* > 10 μm, integrated protist abundance and biomass) parameters were fitted on top of the ordination in order to visualize how they may be related to the vertical flux patterns. The fitted data were standardized prior to analysis.

Environmental and biological parameters were retrieved for all seasonal cruises from the following sources: CTD data for salinity and temperature, from Gerland (2022); Ludvigsen (2022); Reigstad (2022) and Søreide (2022); water masses were assigned according to Sundfjord et al. (2020); suspended POC data were obtained from Marquardt et al. (2022a–d); suspended Chl-*a* data, from Vader (2022a–d); and suspended protist diversity, from Assmy et al. (2022a–d). Sea ice concentration data for station locations were retrieved from Steer and Divine (2023), which uses AMSR-2 and AMSR-E sea ice concentration products, and the mean sea ice concentration from one month prior to sampling at the respective station was computed and used for the PCA analysis.

3. Results

3.1. Seasonal and spatial patterns of sinking particulate organic matter

In May and August, vertical flux of POC averaged across all stations was similar, but the variability among stations was higher in May than in August (178 ± 199 and 159 ± 97 mg C m^{-2} d^{-1}, respectively; Fig. 2). By contrast, mean chlorophyll *a* (Chl-*a*) fluxes differed substantially between seasons (Fig. 3), with highest vertical flux in May (mean 8 ± 11 mg Chl-*a* m^{-2} d^{-1}), followed by August (mean 1 ± 0.4 mg Chl-*a* m^{-2} d^{-1}).

Highest POC fluxes were measured during May at P1 with no attenuation (604 ± 18 mg C m^{-2} d^{-1} across all depths) and at P6 with high POC fluxes at 30 m (416 mg C m^{-2} d^{-1}) that attenuated by 50% at 60 m. At all other stations, POC fluxes were much lower and did not change much with depth (68 ± 28 mg C m^{-2} d^{-1} across all stations and depths). Similar to the patterns in POC, Chl-*a* fluxes were highest during May at P1, with very high values of 32 ± 1 mg Chl-*a* m^{-2} d^{-1} across all depths, and at 30 m at P6 (25 mg Chl-*a* m^{-2} d^{-1}), while they were much lower at all other stations and depths (1.8 ± 1.4 mg Chl-*a* m^{-2} d^{-1}).
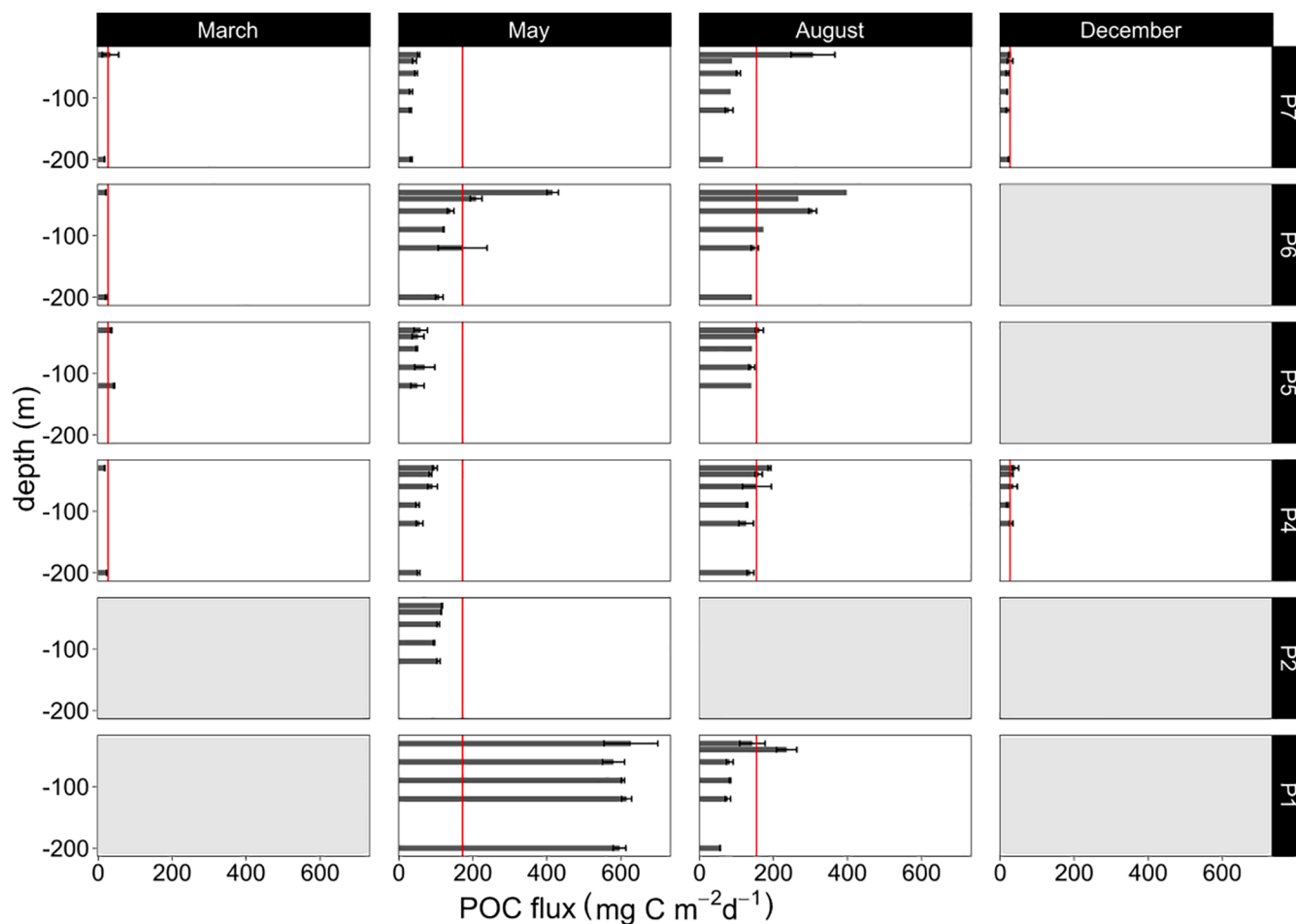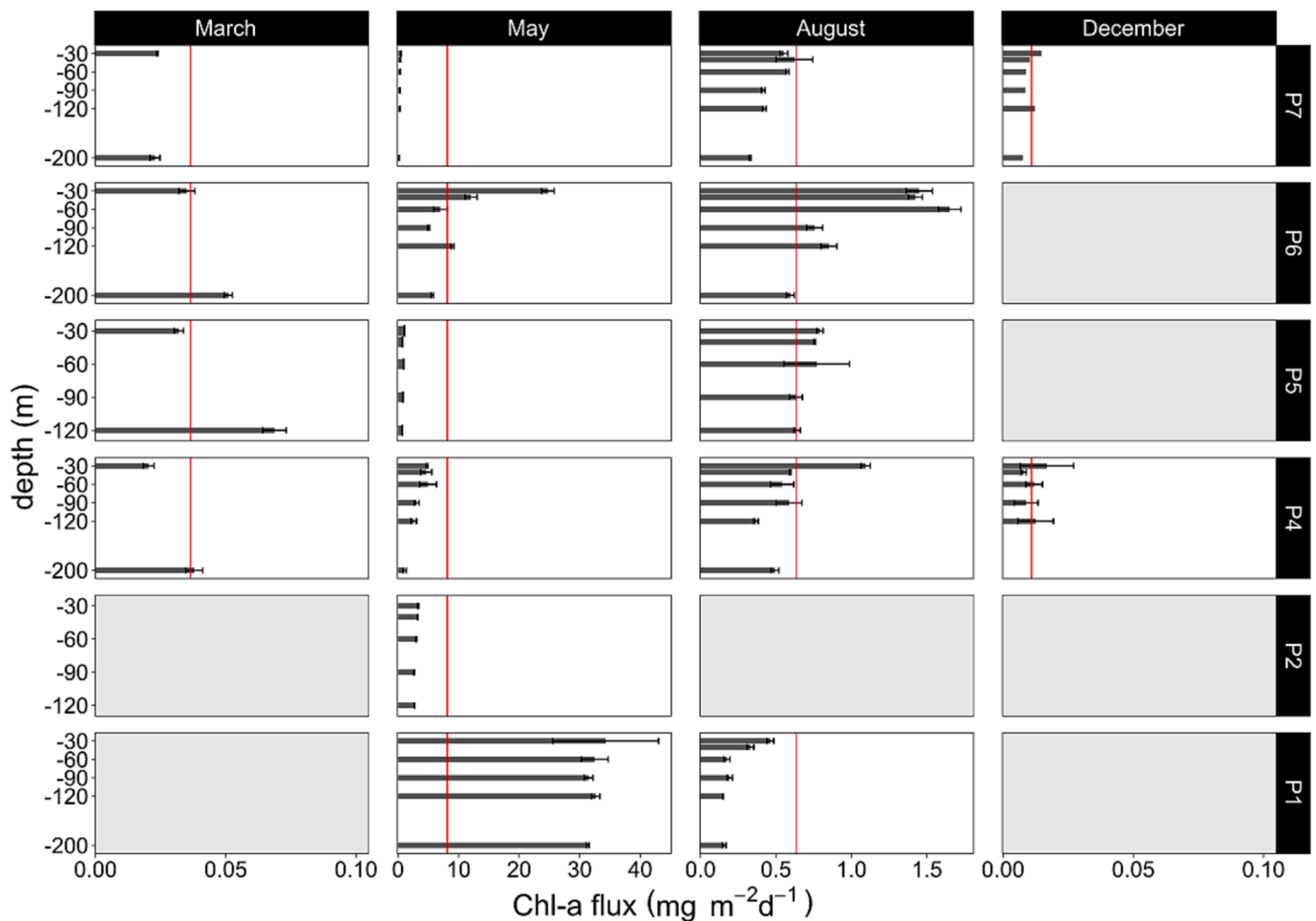
Fig. 2. Mean vertical POC fluxes and standard deviations of three replicate sub-samples across all seasons and stations in the northwestern Barents Sea. Red vertical lines depict the mean vertical flux across all depths and stations for the respective season. Stations are presented according to their position along the latitudinal gradient from south (P1) to north (P7).

In August, highest vertical POC fluxes were observed at 30 m at the northernmost stations, P6 and P7 (531 and 307 mg m^{-2} d^{-1}), but at both stations, fluxes were attenuated quickly by 50% and 30% at 40 m, respectively. At all other stations, there was little attenuation, and average fluxes were 137 $\pm$ 44 mg C m^{-2} d^{-1} across all stations and depths. Chl-*a* fluxes ranged between 0.1 at P1 and 1.7 mg Chl-*a* m^{-2} d^{-1} at P6.

In December and March, average POC flux across all stations and depths was 27 $\pm$ 7 and 27 $\pm$ 9 mg C m^{-2} d^{-1}, respectively. Chl-*a* fluxes during both months were < 0.03 mg Chl-*a* m^{-2} d^{-1}. During March, at the shelf stations (P4, P5) and on the shelf break (P6) POC and Chl-*a* fluxes at 120 or 200 m were slightly elevated. POC fluxes were 1–8 mg C m^{-2} d^{-1} higher relative to 30 m.

In May, POM was most depleted in ^{15}N, with a mean δ^{15}N value of +3.09 $\pm$ 1.15 ‰, indicating fresher OM (Fig. 4). Over the course of the season (May, August, December, March) POM became more and more enriched in ^{15}N, until highest values of δ^{15}N were present in March (mean of +8.92 $\pm$ 0.57 ‰ across all stations). A high variation among stations in May is visible along the δ^{13}C axis, with lowest δ^{13}C values at P2 (−28.89 ‰) and P7 (−28.29 ‰) and highest values at P1 and P6 (~−21 ‰). With progressing season, values for all stations converge along the δ^{13}C axis. While in August the range in δ^{13}C values among stations was already lower (between −27.28 ‰ at P4 and −21.95 ‰ at P6), in December, δ^{13}C among all stations varied only between −26.42 ‰ and –23.59 ‰. In March, δ^{13}C values were between −23.80 and −25.72 ‰ at P7 at 30 m. At all the other stations, however, samples

more enriched in ^{13}C were measured at the 120 and 200 m traps at P4, P5 and P6 (−21.77 to −21.38 ‰).

3.2. Composition and drivers of vertical flux

For May and August, carbon conversions applied to fecal pellets and protists occasionally led to overestimates of the contribution of protist carbon (PC) and fecal pellet carbon (FPC) to total POC, resulting in estimates > 100% of total POC. The contribution of PC to total POC was highly variable during May and August across the transect, with 2 – 98% in May across all stations and depths, 8 – 100% in August, <15% in December and < 3% in March. (Fig. 5). Fecal pellet carbon made up a significant fraction of total POC flux during May and August, particularly at P4, P5, and P6 where it contributed up to 100%, while at the other stations it usually contributed < 30%. In both March and December, there were few recognizable cells or fecal pellets, resulting in a higher amount of detritus contributing to bulk POC (>94% in March and > 65% in December). In March, there was a slightly higher number of recognizable cells at depth compared to the surface. In December, up to 5 mg C m^{-2} d^{-1} (10–25% total POC flux) could be attributed to PC, mostly from ciliates.

During degradation of organic matter, N is remineralised faster than C, resulting in increased POC:PN ratios of more degraded material. Ratios were highest in winter (6 – 10 in March and 8 – 11 in December) and lowest in spring (5 – 7 across all stations and depth; except for at P7 where ratios were very high, ranging between 8 and 11 across all depths;

Fig. 3. Mean vertical Chl-*a* fluxes and standard deviations of three replicate sub-samples across all seasons and stations in the northwestern Barents Sea. Red vertical lines depict the mean vertical flux across all depths and stations for the respective season. Stations are presented according to their position along the latitudinal gradient from south (P1) to north (P7). Note the different scales on the x-axes.

Fig. 6). POC:PN ratios usually increased with depth across all seasons and stations, except for in March at stations P4 and P6. Chl-*a*:Phaeo ratios reflect the freshness of algal material since phaeopigments are a degradation product of Chl-*a*. The Chl-*a*:Phaeo ratios were highest in May, ranging between 1.3 (P4) – 4.8 (P1), also showing high variability among stations. In August, ratios ranged between 0.5 and 2.3 and decreased with depth, while in March they were between 0.1 and 2. In December, Chl-*a*:Phaeo ratios were lowest, with < 0.003 across all stations. Chl-*a*:POC ratios reflects the contribution of photosynthetic algae to the organic matter pool. They were low in March, August and December, with ratios < 0.007. In contrast, in May they varied between 0.006 at P7 to 0.06 at P4. The percentage of total Chl-*a* found in cells larger than 10 μm (% Chl-*a* > 10 μm) was generally higher in May than in August (69% ± 0.3 and 49% ± 0.2, respectively; Figure S1).

To identify key drivers and similarities of the protist community contributing to the vertical flux, two correspondence analyses (CA) were performed on protist cell and biomass fluxes, respectively. The patterns of the two CAs were very similar and therefore the results are not shown for biomass fluxes. All fitted protist groups were significantly correlated with the ordination (p < 0.003). The two first axes of the CA explained a low, but similar amount of the total variance (8.8 and 6.2%, respectively; Fig. 7, Table S1) and indicated a clear seasonal gradient in their combination.

In anti-clockwise direction, stations in May, which were mostly aligned along the second CA axis, were followed by stations in August that correlated negatively with the first CA axis, then followed by

stations in December and finally stations March, which were both negatively correlated with the second CA axis. This lead to a separation of all stations by productivity along the second CA axis, with August and productive May stations positively correlated with the axis, and the winter (December and March) and less productive May stations negatively correlated. Along the first axis, stations were separated by the different protist groups, with May stations strongly driven by diatoms, while in August they were driven by *Phaeocystis*, ciliates, dinoflagellates and other flagellates.

The gradient in POC flux clearly increased with high diatom abundances in May (isolines; Fig. 7), whereas the winter communities indicated lower POC fluxes across stations. This clear gradient was also reflected in Chl-*a* flux (not shown).

A PCA biplot of the measured vertical flux parameters is shown in Fig. 8a and identifies seasonal characteristics of the vertical flux. Along the first axis (explaining 44.7% of the total variance among samples), stations are clearly separated by vertical flux gradients: May and August grouped on the right-hand side, strongly driven by high POC fluxes, while the winter fluxes are grouped further to the left on this axis, driven by high POC:PN ratios. Along the second axis (explaining 20.1% of the variance), fluxes in August are separated from May. While vertical flux in August was strongly driven by high protist abundance, protist biomass and fecal pellet carbon, vertical flux in May was driven by fresher material, indicated by high Chl-*a*, mainly large cells (defined by % Chl-*a* > 10 μm), and high Chl-*a*:Phaeopigments ratios.
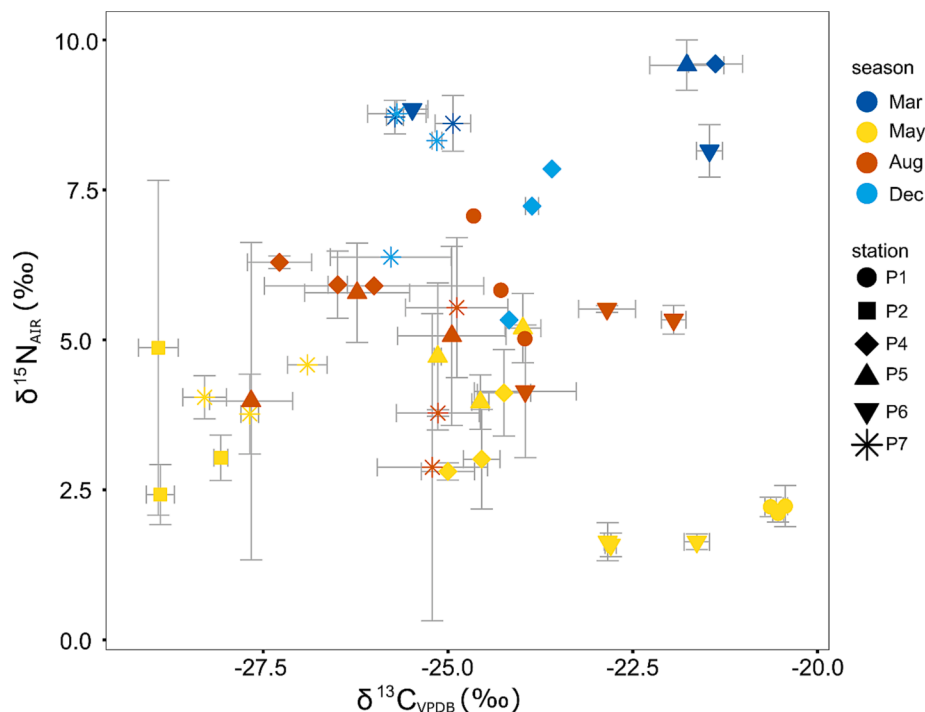
Fig. 4. $\delta^{13}C_{VPDB}$ and $\delta^{15}N_{AIR}$ values for sediment trap particulate organic matter across all seasons and stations in the northern Barents Sea. Seasons are distinguished by color and stations by symbols. Standard deviations are depicted by grey errorbars and are based on 2-3 replicates.

When environmental (sea ice, salinity, temperature and water mass) and biological parameters (integrated suspended POC, POC:PN ratio, Chl-*a*, Chl-*a*:Phaeogiment ratio, % of Chl-*a* > 10 μm, integrated protist abundance and biomass) are fitted on top of this ordination, AW is associated with vertical flux in August, while modified AW (mAW) is associated with vertical flux in May. Integrated suspended Chl-*a* correlates with the fluxes in May, while suspended POC correlates with fluxes in August. Along the first axis, temperature and suspended integrated Chl-*a* (Fig. 8b) as well as Chl-*a* flux (Fig. 8a) are pointing in the same directions, while along the second axis total suspended POC and % of Chl-*a* > 10 μm are pointing into opposite directions. High suspended POC:PN ratios are correlated with the vertical flux in winter. All fitted variables except for POC:PN, protist abundance and protist biomass were significantly correlated to the ordination (p < 0.02).

4. Discussion

Vertical flux of particulate organic matter measured in the northwestern Barents Sea in August and December 2019 and March and May 2021 displayed strong seasonal differences in vertical flux magnitude with highest values during the productive season from early spring to summer. Moreover, we identified conspicuous differences in the composition and quality of vertical flux between spring (May) and summer (August). Interestingly, during May we did not observe a strictly latitudinal gradient of vertical flux patterns following the northwards retreat of the sea ice edge. Instead, we measured high vertical flux under pack-ice at one of the northernmost regions, possibly influenced by the warm Atlantic Water flowing eastwards along the Barents Sea shelf break.

4.1. Characterizing spring and summer during heterogenous conditions in the seasonally ice-covered northern Barents Sea

The identified strong seasonal pattern is consistent with previous seasonal vertical flux measurements conducted with short-term sediment traps in the same region (Andreassen and Wassmann, 1998; Olli

et al., 2002), and other regions in the Arctic (Dezutter et al., 2021; Dybwad et al., 2021; Fadeev et al., 2021; Koch et al., 2020; Lalande et al., 2016a,b; Nöthig et al., 2015). Highest POC fluxes were measured in May and August (Fig. 2), moving from a fresh, diatom-derived flux in spring (May) to a vertical flux dominated by small and increasingly heterotrophic cells in summer (August), especially by *Phaeocystis* (Figs. 7, 8 and S2). In August, Chl-*a* fluxes, Chl-*a*:POC and Chl-*a*:Phaeo ratios were lower than in May (Fig. 7), indicating reduced algal biomass and freshness of the sinking OM during summer. In winter (December and March), vertical flux was negligible (Fig. 2) and was mostly comprised of unidentifiable detritus (Fig. 5), suggesting low export from a heterotrophic pelagic system dominated by ciliates and heterotrophic flagellates.

This seasonal pattern was also reflected in the increasingly positive $\delta^{15}N$ values of sinking organic matter (OM) with progressing season from spring to winter, where each sampling period was clearly separated along the $\delta^{15}N$ axis (Fig. 4). When nitrate is abundant, algal cells preferentially take up the lighter ^{14}N isotope, which leads to POM being depleted in ^{15}N (Peterson and Fry 1987; Tamelander et al. 2009). Accordingly, we measured the lowest $\delta^{15}N$ values across the whole transect during spring (May), when nutrients were abundant and the increasing incident light started to allow for primary production (Figure S3). With progressing season, nutrients became increasingly reduced, which led to an intensified uptake of the heavier isotope, and increasingly regenerated and degraded material in the water column towards winter further led to OM enriched in ^{15}N. This result is consistent with year-round sediment trap measurements from the Bransfield Basin (Antarctica), with lowest $\delta^{15}N$ values during the productive season and increasing enrichment towards winter (Khim et al. 2013).

Bloom and vertical flux patterns are highly seasonal in the Arctic (Wassmann et al., 2006; Leu et al., 2011; Leu et al., 2015), which can lead to different timing of seasonal stages at different locations, depending on the sea ice cover. Accordingly, revisiting the same transect revealed advanced and delayed seasonalities at each of the stations within the same sampling campaign. This was especially evident in May.
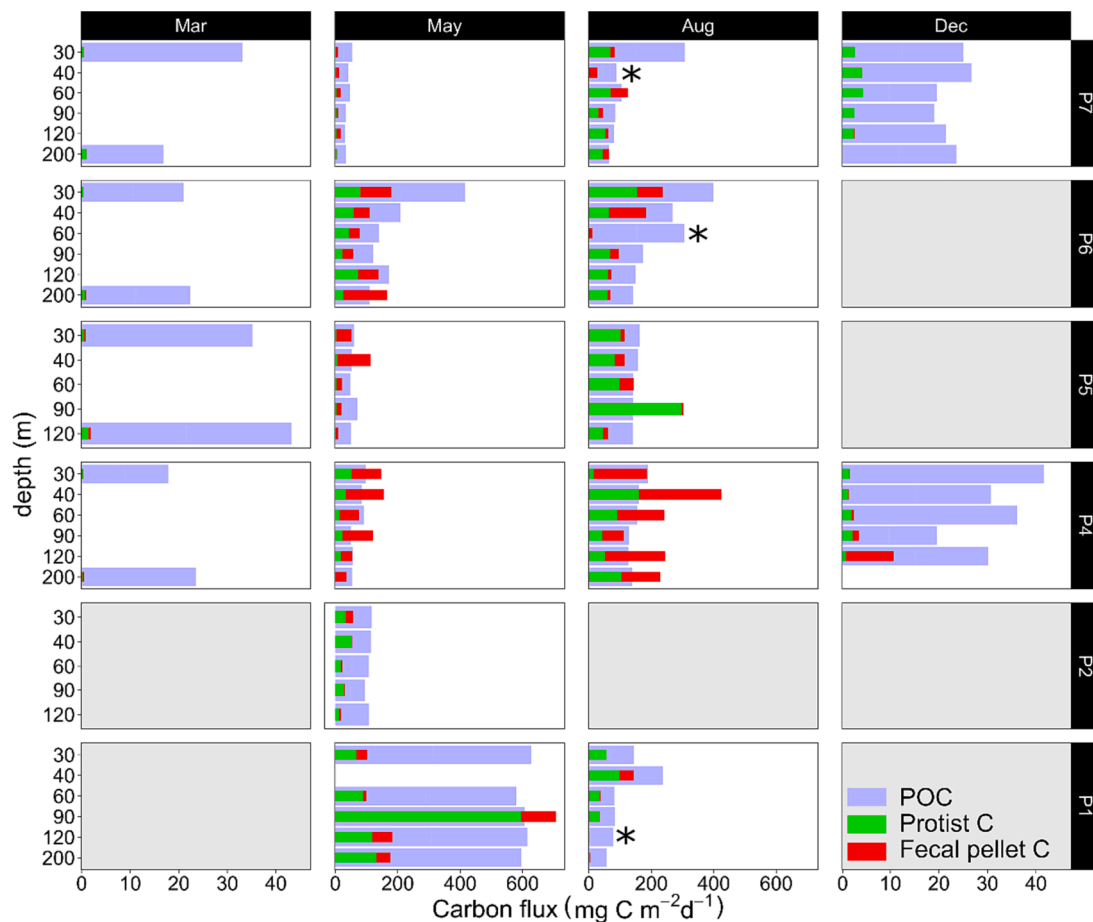
Fig. 5. Composition of vertical flux across all seasons and stations in the northwestern Barents Sea. Thick blue bars show the total POC, overlying green and red bars show the estimated contributions of protist (PC) and fecal pellet carbon (FPC), respectively. Note that for PC and FPC, carbon conversions can sometimes lead to overestimates, leading to estimations > 100% of total POC. * No PC data available from August P1-120 m, P6-60 m and P7-40 m. Note the different scales on the x-axes.

POC fluxes ranging between ∼ 30 and 600 mg C m^{-2} d^{-1} in May are in accordance with previously shown high spatial variability in spring within the region, though our range is lower than previously reported (∼100 – 870 mg C m^{-2} d^{-1}, Reigstad et al., 2008; 200 – 1500 mg C m^{-2} d^{-1}, Olli et al., 2002; and 400 – 1100 mg C m^{-2} d^{-1} below 100 m, Andreassen & Wassmann, 1998; Wassmann, 1998). While the southernmost station P1 displayed the highest fluxes measured during all seasons, fluxes at the northernmost station P7 were similar to those in March (Figs. 2, 8) or during the pre-bloom period in the same area (Olli et al., 2002) and North of Svalbard (Dybwad et al., 2021). This suggests that during our sampling time in May, "spring" had started in the southern part of the transect (P1), while P7 was still in a "winter" pre-bloom state. Spring blooms often follow the northward retreat of the sea ice, with southern stations experiencing local blooms along the MIZ earlier in the year (Wassmann, 2018; Castro de la Guardia et al., 2023; this issue). The ice edge reached all the way to P2 in May, reducing incident light for primary production further north, although nutrients were abundant at the surface (Figure S3, Jones et al., 2023; this issue). By contrast, we observed highest fluxes at P1, which was not ice-covered. In the northern Barents Sea, "spring" (i.e. early and peak bloom conditions), occurs from mid-May until July, depending on sea-ice conditions (Reigstad et al., 2008). Accordingly, the timing of sampling in May certainly resulted in a wide span in pelagic conditions and characteristic fluxes, from spring bloom to winter pre-bloom regimes. By contrast, the highest vertical flux along the transect during August was present at the northernmost stations P6 and P7, while lowest fluxes were measured at the southernmost station P1, consistent with the northward

retreat of the sea ice edge. Accordingly, May and August framed the start and the end of a productive period in the northern Barents Sea, as May displayed early spring and August late summer conditions.

In general, vertical flux patterns of OM became more uniform across the different locations in August compared to May (means of 159 ± 97 and 178 ± 199 mg C m^{-2} d^{-1} across the transect, respectively; Fig. 2). In May, the high range of Chl-*a* flux, Chl-*a*:Phaeo ratios, Chl-*a*:POC ratios (Fig. 5) and the δ^{13}C variation, when station locations were clearly separated along a wide range on the δ^{13}C axis (Fig. 4; range of 8.46 ‰), demonstrate a high spatial and compositional variability of vertical flux patterns during spring. Over the course of the season and increasingly open water area, this variability among stations is reduced. In August, δ^{13}C variation already had a smaller range of 5.72 ‰ and POC fluxes across the transect were more comparable (Fig. 5). It is also evident from the close grouping of the stations in the multivariate data visualizations during summer compared to their large distance during May (Figs. 7 and 8). Highest integrated suspended stocks of POC were observed across the transect during August (Fig. 8b; Marquardt et al., 2022a; Marquardt et al., 2022d), although vertical flux was not higher in this month compared to May. This suggests that a smaller fraction of the suspended OM is sinking in August compared to May, and with that a less efficient export of OM in summer. However, it also demonstrates that bulk export was sustained under summer conditions, even though the composition of vertical flux differed between the two seasons. Early and peak phytoplankton bloom conditions in spring usually lead to short, but intense diatom-driven export events of OM along the MIZ, in contrast to post-bloom scenarios in summer when the open water area is extended, nutrients are depleted and smaller,
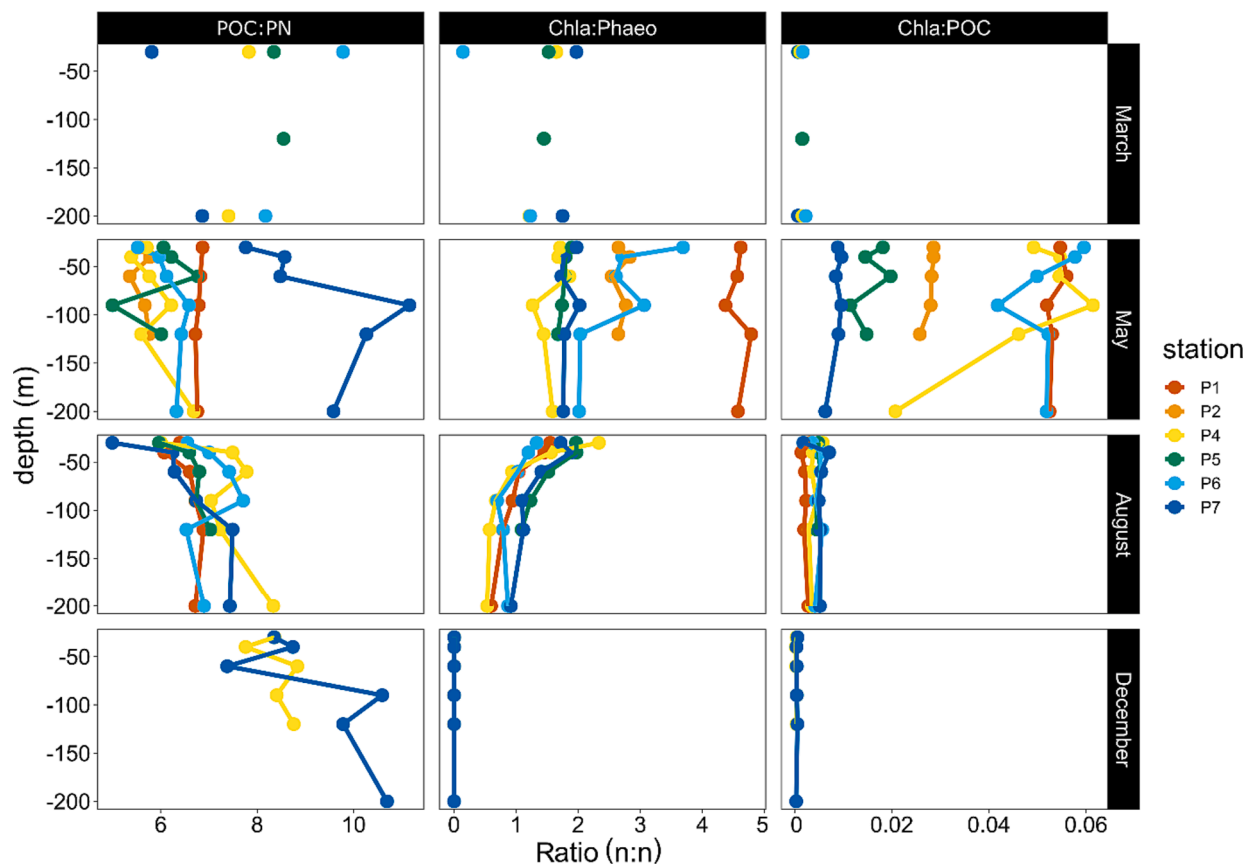
Fig. 6. POC:PN (left), Chl-a:Phaeopigments (mid) and Chl-a:POC ratios (right panel) of vertical flux across all seasons (facets) and stations (colors) in the northwestern Barents Sea.

less efficiently sinking cells dominate in the pelagic environment (Olli et al., 2002; Reigstad et al., 2008; Dybwad et al., 2021). While fluxes in May were strongly driven by large cells (Figure S1) and fresh Chl-*a* -rich material, fluxes in August were driven by high fecal pellet and small heterotrophic protist cell fluxes (Figs. S2, 8a). Small and presumably less efficiently sinking cells can contribute significantly to POC fluxes if they are abundant enough (Wiedmann et al., 2014) or packaged into fast-sinking fecal pellets (Wexels Riser et al., 2007; Dybwad et al., 2021). Even with progressing season, while the protist composition of vertical flux changes and protist carbon flux decreases (Kohlbach et al., 2023, this issue), bulk export can be sustained by detritus (and potentially fecal pellets) if sufficiently enough material escapes retention processes in the water column (Wassmann et al., 2003; Amargant-Arumí et al., this issue).

4.2. High vertical flux under pack ice in early spring

Vertical flux patterns during May did not strictly follow a latitudinal gradient consistent with the sea ice cover, as high fluxes at P6 under pack ice demonstrate. Similar to P1, at P6 high Chl-*a* fluxes were strongly associated with diatoms and were reflected in the high % Chl-*a* > 10 µm and high Chl-*a*:Phaeo ratios, indicating fresh material from a sinking diatom bloom (Fig. 7a and 8). At both P1 and P6, we also measured the least negative $\delta^{13}C$ values of ~ –22 ‰, which is in the range recorded earlier for $\delta^{13}C$ values in sinking OM in the Barents Sea under bloom conditions (~–21 ‰; Tamelander et al., 2009). In the early stage of a bloom, the lighter ^{12}C in dissolved inorganic caron (DIC) is quickly taken up, which leads to an accumulation of the heavier ^{13}C isotope in decreasing DIC concentrations as primary production continues. This is reflected in POM that becomes enriched in ^{13}C with increasing primary production (Rau et al., 1992).
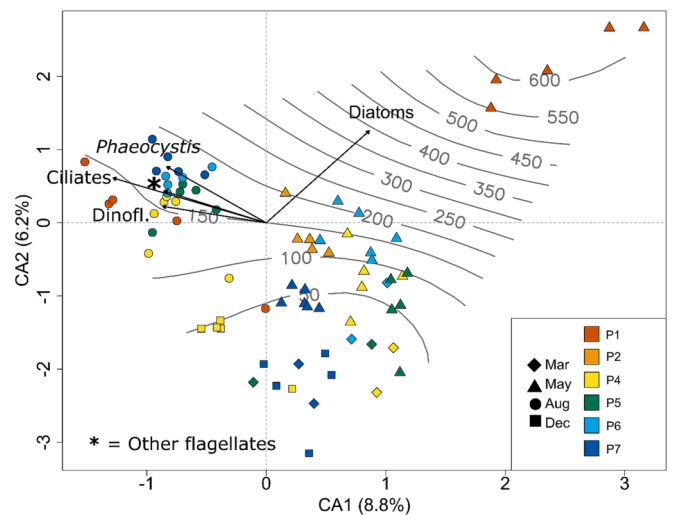
Fig. 7. Visualization of the Correspondence Analysis results on log-transformed protist cell fluxes (species level), with total cell fluxes of the different groups (Diatoms, Dinoflagellates, Ciliates, *Phaeocystis pouchetii* and other flagellates) plotted on top. Symbols represent seasons and colors represent stations. Isolines of POC fluxes are plotted on top of the ordination.

The AW inflow to the Arctic Ocean along the Barents Sea shelf break north of Svalbard may have led to favorable conditions for primary production at P6 early in the season. The heat of AW results in more fragile and mobile sea ice in this region, potentially leading to a higher occurrence of leads and large open-water areas (Onarheim et al., 2014; Ivanov et al., 2016; Renner et al., 2018). In fact, under-ice blooms are
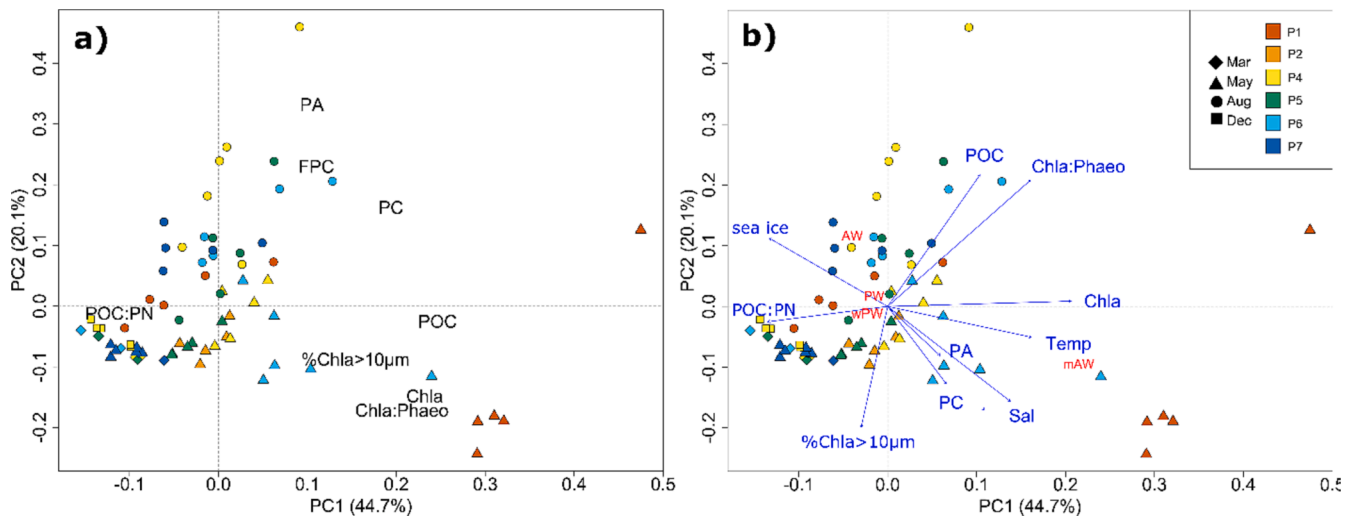
Fig. 8. Visualization of the Principal component analyses (PCA) performed on components of vertical flux from all seasons and stations. a) PCA of vertical flux components. POC = particulate organic carbon flux, POC:PN = POC to particulate nitrogen ratio, PA = protist abundance (cell flux), PC = protist carbon flux, FPC = fecal pellet carbon flux, Chla = Chlorophyll *a* flux, Chla:Phaeo = Chl-*a*:Phaeopigment ratio. b) PCA of vertical flux components (same as in a)), with environmental and suspended integrated biological parameters plotted on top. POC = integrated suspended particulate organic carbon, POC:PN = integrated suspended POC to particulate nitrogen ratio, PA = integrated suspended protist abundance, PC = integrated suspended protist carbon, Chla = integrated suspended Chlorophyll *a*, Chla: Phaeo = integrated suspended Chl-*a*:Phaeopigment ratio, % Chl-*a* > 10 μm = % of integrated suspended Chl-*a* > 10 μm, sea ice = mean sea ice concentration during one month before sampling. Water masses: AW = Atlantic water, mAW = modified AW, PW = Polar Water, wPW = warm PW.

observed under pack ice below meltponds or in leads, which are difficult to capture with satellite measurements (Assmy et al., 2017; Ardyna et al., 2020), although they can lead to subsequent vertical flux (Dybwad et al., 2021). Indeed, primary production measured locally was > 150 mg C m^{-2} d^{-1} during the time of the sediment trap deployment (pers. comm. Martí Amargant-Arumí, UiT The Arctic University of Norway), which is in the range of what has been measured earlier in the northern Barents Sea during spring blooms (Hegseth, 1998).

The community composition in the sediment traps at P6 suggests that a mix of ice-associated and pelagic diatoms were sinking at P6 in May. The ice-associated centric diatom *Thalassiosira bioculata* and pennate species such as *Nitzschia frigida, Fragilariopsis cylindricus* and *Navicula* spp. were present in sediment traps deployed 1 m below the sea ice at that station (Bodur et al., 2023l) as well as at 30 m. These ice-associated species were also present in the sea ice at this station (Marquardt et al., 2023, this issue). Below 60 m, pelagic diatoms such as *Chaetoceros fur-cillatus* dominated the community composition in the sediment traps. Moreover, there was a second peak in POC flux with higher Chl-*a*:Phaeo ratios at 120 m depth (Figs. 2 and 5). These findings suggest that the vertical flux at P6 may have originated from a mixture of a local under-ice bloom and an advected bloom. While it is difficult to disen-tangle the exact origin of sinking OM at this location, the patterns demonstrate that vertical flux in the northern Barents Sea does not strictly follow a northward retreating sea-ice gradient, but that the AW inflow and sea-ice cover drive its seasonality in concert, especially at the locations situated in the AW pathway (P1 and P6).

4.3. Vertical flux regulation by zooplankton: Fecal pellet flux and potential grazer mismatch

At several stations during May and August, we did not measure a typical attenuation curve of vertical flux (Martin et al., 1987). This could indicate that during the sediment trap deployments the OM was either remineralized above 30 m and we did not capture this, or OM was not degraded within the upper 100 m (Wassmann et al. 2003). At P1 during May, a possible mismatch between grazers and primary production could be the reason for high suspended standing stocks, high vertical flux of Chl-*a* and few identified fecal pellets down to 200 m. Indeed, zooplankton abundance and biomass was at a minimum in March and

May, and lowest biomass during May were observed at P1 (Wold et al., 2023, this issue). A storm that simultaneously induced strong vertical mixing resulted in the transport of a high amount of ungrazed diatoms to, and probably below, 200 m depth, was most likely responsible for the lack of flux attentuation observed.

FPC contributions to POC fluxes were highest during summer and at the shelf stations north of the Polar Front (P4, P5), where we also noted a high amount of FP already at 30 m and little change of FPC flux with depth (Fig. 5), together with a lack of attenuation in POC fluxes (Fig. 2). Usually, vertical flux is attenuated within the upper 100 m (Wassmann et al., 2003), but these observations might indicate that high grazing pressure was already present above 30 m, leading to fast retention of OM at the surface and a subsequent lack of POC attenuation below this depth. Highest zooplankton abundance and biomass during summer (July and August) support this observation (Wold et al., 2023, this issue). FPC flux probably played an important role during summer when small cells that usually sink less efficiently are exported by packaging into fast-sinking fecal pellets (Turner, 2015; Wiedmann et al., 2016; von Appen et al., 2021). Highest seasonal POC fluxes can occur where there is a large contribution of FPC (Dybwad et al., 2021). Accordingly, FPC flux probably mediated an efficient export through packaging at these sta-tions during summer when less efficiently sinking small flagellates and *Phaeocystis* dominated vertical flux (Fig. 8a, A2), or grazing reduced OM already above 30 m depth.

4.4. Elevated vertical flux at depth during March

During March, sinking OM below 100 m at the stations north of the Polar Front (P4, P5, P6) was highly enriched in ^{13}C and was within the range of the AW-influenced stations P1 and P6 during May, although POC fluxes below 45 mg C m^{-2} d^{-1} clearly mirrored a winter state. Moreover, Chl-*a* and POC fluxes at 120 and 200 m depth were slightly elevated relative to fluxes at 30 m. This indicates either resuspension from sediments or influence of different water masses at depth compared to the surface, since there was clearly no local vertical export of OM. Below 100 m, the presence of wPW (PW mixed with AW; after Sundfjord et al., 2020) could point towards an influence of AW at depth which shows elevated δ^{13}C values during early winter. In fact, AW is advected onto the northern Barents Sea shelf from the continental slope between

100 and 200 m and its inflow is seasonally highly variable, usually strongest between autumn and early March (Lundesgaard et al., 2022). The influence of this AW inflow probably became more conspicuous during March when compared to surface fluxes, since local biological processes are at their minima and would otherwise mask the $\delta^{13}C$ signal.

5. Summary and future implications

To the best of our knowledge, this study is the first that used short-term sediment traps along a revisited latitudinal transect during different seasons in order to investigate spatial and seasonal trends of daily vertical flux patterns in the seasonally ice-covered northwestern Barents Sea. Short-term sediment traps are particularly suited for investigating daily vertical flux (Buesseler et al., 2007; Baker et al., 2020); however, their use requires considerable ship time, is costly and especially challenging under ambient conditions in the Arctic.

We identified high spatial variability in vertical flux patterns in the northwestern Barents Sea region during early spring, spanning from peak bloom to late winter conditions, while with decreasing sea ice and increasing open water areas towards summer, vertical flux patterns became spatially more homogenous. These differences are driven by sea ice and the impact of AW, and led to the detection of high vertical flux events on the shelf break during both seasons. During late summer, higher concentrations of suspended POC but similar bulk fluxes compared to spring indicate a less efficient carbon pump. We suggest that fecal pellets played an important role for facilitating export during summer, leading to low attenuation of vertical flux at some stations below 30 m. During early spring, a wind-driven mixing event and a possible grazer mismatch led to an efficient transport of fresh OM down to at least 200 m. It should be noted that short-term deployments will not fully capture the seasonal cycle across such a large latitudinal gradient. Vertical fluxes of particulate organic matter during spring shown in this study were likely underestimated due to the ephemeral nature of the phytoplankton spring bloom. However, we were able to demonstrate (1) strong quantitative differences between the productive season in spring/summer and winter, and (2) differences in vertical flux composition between May and August.

With decreasing sea ice in the region, the northern Barents Sea will probably experience an earlier start of the summer season (Wassmann and Reigstad, 2011) with a less efficient carbon pump (i.e. a lower fraction of the suspended OM exported) and a higher contribution of *Phaeocystis*, flagellates and detritus to vertical flux. Nevertheless, a less efficient export over a prolonged productive season may still lead to high annual carbon export if vertical flux is sustained through the efficient packaging of small cells into fast-sinking fecal pellets or aggregates, and/or through mixing events.

The common notion that vertical flux strictly follows the sea-ice gradient and associated MIZ blooms is challenged, as vertical flux events under pack-ice might be common but are difficult to measure, especially in the region north of Svalbard where sea ice conditions are highly variable. With thinner ice cover and the increasing influence of AW, these export events are probably more likely to occur early in the season at locations still under consolidated ice cover before the onset of an MIZ bloom.

Declaration of Competing Interest

The authors declare that they have no known competing financial interests or personal relationships that could have appeared to influence the work reported in this paper.

Data availability

All data used for the research has been cited within the document.

Appendix A. Supplementary material

Supplementary data to this article can be found online at https://doi.org/10.1016/j.pocean.2023.103132.

References

Amargant-Arumí, M., Müller, O., Bodur, Y.V., Ntino, I.-V., Vonnahme, T., Assmy, P., Kohlbach, D., Chierici, M., Jones, E., Olsen, L.M., Tsagaraki, T.M., Reigstad, M., Bratbak, G., Gradinger, R. Interannual differences in sea ice regime in the northwestern Barents Sea cause major changes in summer pelagic production and export mechanisms. Prog. Oceanogr. (in review).

Andreassen, I., Wassmann, P., 1998. Vertical flux of phytoplankton and particulate biogenic matter in the marginal ice zone of the Barents Sea in May 1993. Mar. Ecol. Prog. Ser. 170 https://doi.org/10.3354/meps170001.

Ardyna, M., Mundy, C.J., Mayot, N., Matthes, L.C., Oziel, L., Horvat, C., Leu, E., Assmy, P., Hill, V., Matrai, P.A., Gale, M., Melnikov, I.A., Arrigo, K.R., 2020. Under-Ice Phytoplankton Blooms: Shedding Light on the "Invisible" Part of Arctic Primary Production. Front. Mar. Sci. 7 https://doi.org/10.3389/fmars.2020.608032.

Arrigo, K.R., van Dijken, G.L., 2015. Continued increases in Arctic Ocean primary production. Prog. Oceanogr. 136 https://doi.org/10.1016/j.pocean.2015.05.002.

Assmy, P., Fernández-Méndez, M., Duarte, P., Meyer, A., Randelhoff, A., Mundy, C.J., Olsen, L.M., Kauko, H.M., Bailey, A., Chierici, M., Cohen, L., Doulgeris, A.P., Ehn, J. K., Fransson, A., Gerland, S., Hop, H., Hudson, S.R., Hughes, N., Itkin, P., Johsen, G., King, J.A., Koch, B.P., Koenig, Z., Kwasniewski, S., Laney, S.R., Nicolaus, M., Pavlov, A.K., Polashenski, C.M., Provost, C., Rösel, A., Sandbu, M., Spreen, G., Smedsrud, L.H., Sundfjord, A., Taskjelle, T., Tatarek, A., Wiktor, J., Wagner, P.M., Wold, A., Steen, H., Granskog, M.A., 2017. Leads in Arctic pack ice enable early phytoplankton blooms below snow-covered sea ice. Sci. Rep. 7 https://doi.org/10.1038/srep40850.

Assmy, P., Gradinger, R., Edvardsen, B., Wiktor, J., Tatarek, A., Dąbrowska, A.M., 2022a. Phytoplankton biodiversity Nansen Legacy Q4. Norwegian Polar Institute. https://doi.org/10.21334/npolar.2022.5c40d100.

Assmy, P., Gradinger, R., Edvardsen, B., Wold, A., Goraguer, L., Wiktor, J., 2022b. Phytoplankton biodiversity Nansen Legacy Q1. Norwegian Polar Institute. https://doi.org/10.21334/npolar.2022.e6521515.

Assmy, P., Gradinger, R., Edvardsen, B., Wold, A., Goraguer, L., Wiktor, J., Tatarek, A., Dąbrowska, A.M., 2022c. Phytoplankton biodiversity Nansen Legacy Q3. Norwegian Polar Institute. https://doi.org/10.21334/npolar.2022.dadccf78.

Assmy, P., Gradinger, R., Edvardsen, B., Wold, A., Goraguer, L., Wiktor, J., Tatarek, A., Smoła, Z., 2022d. Phytoplankton biodiversity Nansen Legacy Q2. Norwegian Polar Institute. https://doi.org/10.21334/npolar.2022.9c05c643.

Baker, C.A., Estapa, M.L., Iversen, M., Lampitt, R., Buesseler, K., 2020. Are all sediment traps created equal? An intercomparison study of carbon export methodologies at the PAP-SO site. Prog. Oceanogr. 184 https://doi.org/10.1016/j.pocean.2020.102317.

Beszczynska-Möller, A., Fahrbach, E., Schauer, U., Hansen, E., 2012. Variability in Atlantic water temperature and transport at the entrance to the Arctic Ocean, 1997–2010. ICES J. Mar. Sci. 69 https://doi.org/10.1093/icesjms/fss056.

Bodur, Y.V., Amargant-Arumí, M., Reigstad, M., 2023a. Downward vertical flux of size-fractionated Chlorophyll-a and phaeopigments in the northern Barents Sea during August 2019, Nansen Legacy cruise 2019706 Q3. UiT The Arctic University of Norway. https://doi.org/10.11582/2023.00102.

Bodur, Y.V., Amargant-Arumí, M., Reigstad, M., 2023b. Downward vertical flux of size-fractionated Chlorophyll-a and phaeopigments in the northern Barents Sea during December 2019, Nansen Legacy cruise 2019711 Q4. UiT The Arctic University of Norway. https://doi.org/10.11582/2023.00103.

Bodur, Y.V., Amargant-Arumí, M., Reigstad, M., 2023c. Downward vertical flux of size-fractionated Chlorophyll-a and phaeopigments in the northern Barents Sea during March 2021, Nansen Legacy cruise 2021703 Q1. UiT The Arctic University of Norway. https://doi.org/10.11582/2023.00104.

Bodur, Y.V., Amargant-Arumí, M., Reigstad, M., 2023d. Downward vertical flux of size-fractionated Chlorophyll-a and phaeopigments in the northern Barents Sea during May 2021, Nansen Legacy cruise 2021704 Q2. UiT The Arctic University of Norway. https://doi.org/10.11582/2023.00105.

Bodur, Y.V., Amargant-Arumí, M., Reigstad, M., 2023e. Downward fecal pellet flux measured from short-term sediment traps during August 2019 in the northern Barents Sea as part of the Nansen Legacy project, cruise 2019706 Q3. UiT The Arctic University of Norway. https://doi.org/10.11582/2023.00108.

Bodur, Y.V., Amargant-Arumí, M., Reigstad, M., 2023f. Downward fecal pellet flux measured from short-term sediment traps during December in the northern Barents Sea as part of the Nansen Legacy project, cruise 2019711 Q4. UiT The Arctic University of Norway. https://doi.org/10.11582/2023.00106.

Bodur, Y.V., Amargant-Arumí, M., Reigstad, M., 2023g. Downward fecal pellet flux measured from short-term sediment traps during March 2021 in the northern Barents Sea as part of the Nansen Legacy project, cruise 2021703 Q1. UiT The Arctic University of Norway. https://doi.org/10.11582/2023.00086.

Bodur, Y.V., Amargant-Arumí, M., Reigstad, M., 2023h. Downward fecal pellet flux measured from short-term sediment traps during May 2021 in the northern Barents Sea as part of the Nansen Legacy project, cruise 2021704 Q2. UiT The Arctic University of Norway. https://doi.org/10.11582/2023.00107.

Bodur, Y.V., Dąbrowska, A.M., Tatarek, A, Wiktor, J.M., Goraguer, L., Amargant-Arumí, M., Reigstad, M., 2023i. Downward vertical flux of protist cells and biomass in the northern Barents Sea during August 2019, Nansen Legacy cruise 2019706 Q3. UiT The Arctic University of Norway. https://doi.org/10.11582/2023.00088.

Bodur, Y.V., Dąbrowska, A.M., Tatarek, A, Wiktor, J.M., Goraguer, L., Amargant-Arumí, M., Reigstad, M., 2023j. Downward vertical flux of protist cells and biomass in the northern Barents Sea during December 2019, Nansen Legacy cruise 2019711 Q4. UiT The Arctic University of Norway. https://doi.org/10.11582/2023.00089.

Bodur, Y.V., Dąbrowska, A.M., Tatarek, A, Wiktor, J.M., Goraguer, L., Amargant-Arumí, M., Reigstad, M., 2023k. Downward vertical flux of protist cells and biomass in the northern Barents Sea during March 2021, Nansen Legacy cruise 2021703 Q1. UiT The Arctic University of Norway. https://doi.org/10.11582/2023.00090.

Bodur, Y.V., Dąbrowska, A.M., Tatarek, A, Wiktor, J.M., Goraguer, L., Amargant-Arumí, M., Reigstad, M., 2023l. Downward vertical flux of protist cells and biomass in the northern Barents Sea during May 2021, Nansen Legacy cruise 2021704 Q2. UiT The Arctic University of Norway. https://doi.org/10.11582/2023.00091.

Bodur, Y.V., Marquardt, M., Dubourg, P., Amargant, M., Reigstad, M., 2023m. Downward vertical flux of particulate organic carbon (POC) and nitrogen (PON) in the northern Barents Sea during May 2021, Nansen Legacy cruise 2021704 Q2. UiT The Arctic University of Norway. https://doi.org/10.11582/2023.00096.

Bodur, Y.V., Marquardt, M., Dubourg, P., Amargant-Arumí, M., Reigstad, M., 2023n. Downward vertical flux of particulate organic carbon (POC) and nitrogen (PON) in the northern Barents Sea during August 2019, Nansen Legacy cruise 2019706 Q3. UiT The Arctic University of Norway. https://doi.org/10.11582/2023.00093.

Bodur, Y.V., Marquardt, M., Dubourg, P., Amargant-Arumí, M., Reigstad, M., 2023o. Downward vertical flux of particulate organic carbon (POC) and nitrogen (PON) in the northern Barents Sea during December 2019, Nansen Legacy cruise 2019711 Q4. UiT The Arctic University of Norway. https://doi.org/10.11582/2023.00094.

Bodur, Y.V., Marquardt, M., Dubourg, P., Amargant-Arumí, M., Reigstad, M., 2023p. Downward vertical flux of particulate organic carbon (POC) and nitrogen (PON) in the northern Barents Sea during March 2021, Nansen Legacy cruise 2021703 Q1. UiT The Arctic University of Norway. https://doi.org/10.11582/2023.00095.

Bodur, Y.V., Renaud, P.E., Amargant-Arumí, M., Reigstad, M., 2023q. Stable isotopic composition (d13C and d15N) of sinking particulate matter measured from short-term sediment traps in the northern Barents Sea during August 2019, Nansen Legacy cruise 2019706 Q3. UiT The Arctic University of Norway. https://doi.org/10.11582/2023.00097.

Bodur, Y.V., Renaud, P.E., Amargant-Arumí, M., Reigstad, M., 2023r. Stable isotopic composition (d13C and d15N) of sinking particulate matter measured from short-term sediment traps in the northern Barents Sea during December 2019, Nansen Legacy cruise 2019711 Q4. UiT The Arctic University of Norway. https://doi.org/10.11582/2023.00098.

Bodur, Y.V., Renaud, P.E., Amargant-Arumí, M., Reigstad, M., 2023s. Stable isotopic composition (d13C and d15N) of sinking particulate matter measured from short-term sediment traps in the northern Barents Sea during March 2021, Nansen Legacy cruise 2021703 Q1. UiT The Arctic University of Norway. https://doi.org/10.11582/2023.00099.

Bodur, Y.V., Renaud, P.E., Amargant-Arumí, M., Reigstad, M., 2023t. Stable isotopic composition (d13C and d15N) of sinking particulate matter measured from short-term sediment traps in the northern Barents Sea during May 2021, Nansen Legacy cruise 2021704 Q2. UiT The Arctic University of Norway. https://doi.org/10.11582/2023.00100.

Buesseler, K.N., Antia, A., Chen, M., Fowler, S., Gardner, W., Gustafsson, O., Harada, K., Michaels, A., van der Loeff, M.R., Sarin, M.M., Steinberg, D.K., Trull, T., 2007. An assessment of the use of sediment traps for estimating upper ocean particle fluxes. J. Mar. Res. 65 https://doi.org/10.1357/002224007781567621.

Carroll, J., Zaborska, A., Papucci, C., Schirone, A., Carroll, M.L., Pempkowiak, J., 2008. Accumulation of organic carbon in western Barents Sea sediments. Deep Sea Res. Part II 55. https://doi.org/10.1016/j.dsr2.2008.05.005.

Castro de la Guardia, L., Hernández Fariñas, T., Marchese, C., Amargant-Arumí, M., Myers, P.G., Bélanger, S., Assmy, P., Gradinger, R.R., Duarte, P., 2023. Assessing net primary production in the northwestern Barents Sea using in situ, remote sensing and modelling approaches. Prog. Oceanogr. (under review).

Dalpadado, P., Ingvaldsen, R.B., Stige, L.C., Bogstad, B., Knutsen, T., Ottersen, G., Ellertsen, B., 2012. Climate effects on Barents Sea ecosystem dynamics. ICES J. Mar. Sci. 69 https://doi.org/10.1093/icesjms/fss063.

Dalpadado, P., Arrigo, K.R., Hjøllo, S.S., Rey, F., Ingvaldsen, R.B., Sperfeld, E., van Dijken, G.L., Stige, L.C., Olsen, A., Ottersen, G., 2014. Productivity in the Barents Sea - response to recent climate variability. PLoS One 9. https://doi.org/10.1371/journal.pone.0095273.

De La Rocha, C.L., Passow, U., 2007. Factors influencing the sinking of POC and the efficiency of the biological carbon pump. Deep Sea Res. Part II 54. https://doi.org/10.1016/j.dsr2.2007.01.004.

Dezutter, T., Lalande, C., Darnis, G., Fortier, L., 2021. Seasonal and interannual variability of the Queen Maud Gulf ecosystem derived from sediment trap measurements. Limnol. Oceanogr. 66 https://doi.org/10.1002/lno.11628.

Dilling, L., Alldredge, A., 1993. Can chaetognath fecal pellets contribute significantly to carbon flux? Mar. Ecol. Prog. Ser. 92 https://doi.org/10.3354/meps092051.

Drinkwater, K.F., 2011. The influence of climate variability and change on the ecosystems of the Barents Sea and adjacent waters: review and synthesis of recent studies from the NESSAS Project. Prog. Oceanogr. 90 https://doi.org/10.1016/j.pocean.2011.02.006.

Dybwad, C., Assmy, P., Olsen, L.M., Peeken, I., Nikolopoulos, A., Krumpen, T., Randelhoff, A., Tatarek, A., Wiktor, J.M., Reigstad, M., 2021. Carbon export in the seasonal sea ice zone north of Svalbard from winter to late summer. Front. Mar. Sci. 7 https://doi.org/10.3389/fmars.2020.525800.

Dybwad, C., Lalande, C., Bodur, Y.V., Henley, S.F., Cottier, F., Ershova, E.A., Hobbs, L., Last, K.S., Dąbrowska, A.M., Reigstad, M., 2022. The influence of sea ice cover and Atlantic Water advection on annual particle export north of Svalbard. J. Geophys. Res. Oceans 127. https://doi.org/10.1029/2022JC018897.

Edler, L., Elbrächter, M., 2010. The Utermöhl method for quantitative phytoplankton analysis. In: Microscopic and Molecular Methods for Quantitative Phytoplankton Analysis. Unesco Pub, pp. 13–20.

Ellingsen, I.H., Dalpadado, P., Slagstad, D., Loeng, H., 2008. Impact of climatic change on the biological production in the Barents Sea. Clim. Change 87. https://doi.org/10.1007/s10584-007-9369-6.

Eriksen, E., Skjoldal, H.R., Gjøsæter, H., Primicerio, R., 2017. Spatial and temporal changes in the Barents Sea pelagic compartment during the recent warming. Prog. Oceanogr. 151 https://doi.org/10.1016/j.pocean.2016.12.009.

Fadeev, E., Rogge, A., Ramondenc, S., Nöthig, E.-M., Wekerle, C., Bienhold, C., Salter, I., Waite, A.M., Hehemann, L., Boetius, A., Iversen, M.H., 2021. Sea ice presence is linked to higher carbon export and vertical microbial connectivity in the Eurasian Arctic Ocean. Commun. Biol. 4 https://doi.org/10.1038/s42003-021-02776-w.

Fossheim, M., Primicerio, R., Johannesen, E., Ingvaldsen, R.B., Aschan, M.M., Dolgov, A. V., 2015. Recent warming leads to a rapid borealization of fish communities in the Arctic. Nat. Clim. Chang. 5 https://doi.org/10.1038/nclimate2647.

Franco-Santos, R.M., Auel, H., Boersma, M., De Troch, M., Meunier, C.L., Niehoff, B., 2018. Bioenergetics of the copepod Temora longicornis under different nutrient regimes. J. Plankton Res. 40 https://doi.org/10.1093/plankt/fby016.

Gerland, S., 2022. CTD data from Nansen Legacy Cruise - Seasonal Cruise Q1. Norwegian Polar Institute. https://doi.org/10.21335/NMDC-1491279668.

Giesecke, R., González, H.E., Bathmann, U., 2010. The role of the chaetognath Sagitta gazellae in the vertical carbon flux of the Southern Ocean. Polar Biol. 33 https://doi.org/10.1007/s00300-009-0704-4.

Hegseth, E.N., 1998. Primary production of the northern Barents Sea. Polar Res. 17 https://doi.org/10.1111/j.1751-8369.1998.tb00266.x.

Hillebrand, H., Dürselen, C.-D., Kirschtel, D., Pollingher, U., Zohary, T., 1999. Biovolume calculation for pelagic and benthic microalgae. J. Phycol. 35 https://doi.org/10.1046/j.1529-8817.1999.3520403.x.

Holm-Hansen, O., Riemann, B., 1978. Chlorophyll a determination: Improvements in methodology. Oikos 30. https://doi.org/10.2307/3543338.

Ingvaldsen, R.B., Asplin, L., Loeng, H., 2004. The seasonal cycle in the Atlantic transport to the Barents Sea during the years 1997–2001. Cont. Shelf Res. 24 https://doi.org/10.1016/j.csr.2004.02.011.

Ingvaldsen, R.B., Assmann, K.M., Primicerio, R., Fossheim, M., Polyakov, I.V., Dolgov, A, V., 2021. Physical manifestations and ecological implications of Arctic Atlantification. Nat. Rev. Earth. Environ. 2. Nature Publishing Group. https://doi.org/10.1038/s43017-021-00228-x.

Ingvaldsen, R., Loeng, H., Asplin, L., 2002. Variability in the Atlantic inflow to the Barents Sea based on a one-year time series from moored current meters. Cont. Shelf Res. 22 https://doi.org/10.1016/S0278-4343(01)00070-X.

Ivanov, V., Alexeev, V., Koldunov, N.V., Repina, I., Sandø, A.B., Smedsrud, L.H., Smirnov, A., 2016. Arctic Ocean heat impact on regional ice decay: A suggested positive feedback. J. Geophys. Res. Oceans 46. https://doi.org/10.1175/JPO-D-15-0144.1.

Iversen, M.H., 2023. Carbon export in the ocean: a biologist's perspective. Annu Rev Mar Sci 15. https://doi.org/10.1146/annurev-marine-032122-035153.

Jakobsson, M., Mayer, L.A., Bringensparr, C., Castro, C.F., Mohammad, R., Johnson, P., Ketter, T., Accettella, D., Amblas, D., An, L., Arndt, J.E., Canals, M., Casamor, J.L., Chauché, N., Coakley, B., Danielson, S., Demarte, M., Dickson, M.-L., Dorschel, B., Dowdeswell, J.A., Dreutter, S., Fremand, A.C., Gallant, D., Hall, J.K., Hehemann, L., Hodnesdal, H., Hong, J., Ivaldi, R., Kane, E., Klaucke, I., Krawczyk, D.W., Kristoffersen, Y., Kuipers, B.R., Millan, R., Masetti, G., Morlighem, M., Noormets, R., Prescott, M.M., Rebesco, M., Rignot, E., Semiletov, I., Tate, A.J., Travaglini, P., Velicogna, I., Weatherall, P., Weinrebe, W., Willis, J.K., Wood, M., Zarayskaya, Y., Zhang, T., Zimmermann, M., Zinglersen, K.B., 2020. The International Bathymetric Chart of the Arctic Ocean Version 4.0. Sci. Data 7. https://doi.org/10.1038/s41597-020-0520-9.

Jones, E.M., Chierici, M., Fransson, A., Assmann, K.M., Renner, A.H.H., Lødemel, H.H., 2023. Inorganic carbon and nutrient dynamics in the marginal ice zone of the Barents Sea: seasonality and implications for ocean acidification. Prog. Oceanogr. (Journal Preprint). https://doi.org/10.1016/j.pocean.2023.103131.

Khim, B.-K., Dunbar, R., Kim, D., 2013. δ15N values of settling biogenic particles in the eastern Bransfield Basin (west Antarctic) and their records for the surface-water condition. Geosci. J. 17 https://doi.org/10.1007/s12303-013-0032-0.

Turner, J.T., 2015. Zooplankton fecal pellets, marine snow, phytodetritus and the ocean's biological pump. Prog. Oceanogr. 130 https://doi.org/10.1016/j.pocean.2014.08.005.

Urban-Rich JL. 1997. Latitudinal variations in the contribution by copepod fecal pellets to organic carbon and amino acid flux. [Ann Arbor, United States]: University of Maryland. Available at https://www.proquest.com/docview/304350779/abstract/451E5A796DF848E3PQ/1. Accessed 2022 Oct 8.

Utermöhl, H., 1958. Zur Vervollkommnung der quantitativen Phytoplankton-Methodik. SIL Communications 1953–1996, 9. https://doi.org/10.1080/05384680.1958.11904091.

Vader, A., 2022a. Chlorophyll A and phaeopigments Nansen Legacy cruise 2021704. University Centre in Svalbard. https://doi.org/10.21335/NMDC-966499899.

Vader, A., 2022b. Chlorophyll A and phaeopigments Nansen Legacy cruise 2019706. University Centre in Svalbard. https://doi.org/10.21335/NMDC-1109067467.

Vader, A., 2022c. Chlorophyll A and phaeopigments Nansen Legacy cruise 2019711. University Centre in Svalbard. https://doi.org/10.21335/NMDC-226850212.

Vader, A., 2022d. Chlorophyll A and phaeopigments Nansen Legacy cruise 2021703. University Centre in Svalbard. https://doi.org/10.21335/NMDC-983908955.

von Appen, W.-J., Waite, A.M., Bergmann, M., Bienhold, C., Boebel, O., Bracher, A., Cisewski, B., Hagemann, J., Hoppema, M., Iversen, M.H., Konrad, C., Krumpen, T., Lochthofen, N., Metfies, K., Niehoff, B., Nöthig, E.-M., Purser, A., Salter, I., Schaber, M., Scholz, D., Soltwedel, T., Torres-Valdes, S., Wekerle, C., Wenzhöfer, F., Wietz, M., Boetius, A., 2021. Sea-ice derived meltwater stratification slows the biological carbon pump: results from continuous observations. Nat. Commun. 12, 7309. https://doi.org/10.1038/s41467-021-26943-z.

Walker, E.Z., Wiedmann, I., Nikolopoulos, A., Skarðhamar, J., Jones, E.M., Renner, A.H. H., 2022. Pelagic Ecosystem Dynamics between Late Autumn and the Post Spring Bloom in a Sub-Arctic Fjord. Elem. Sci. Anth. 10 https://doi.org/10.1525/elementa.2021.00070.

Wassmann, P., 1998. Retention versus export food chains: processes controlling sinking loss from marine pelagic systems. In: Tamminen, T., Kuosa, H. (Eds.), Eutrophication in Planktonic Ecosystems: Food Web Dynamics and Elemental Cycling. Springer Netherlands, Dordrecht, pp. 29–57. https://doi.org/10.1007/978-94-017-1493-8_3.

Wassmann, P., Olli, K., Riser, C.W., Svensen, C., 2003. Ecosystem function, biodiversity and vertical Ffux regulation in the twilight zone. In: Wefer, G., Lamy, F., Mantoura, F. (Eds.), Marine Science Frontiers for Europe. Springer Berlin

Heidelberg, Berlin, Heidelberg, pp. 279–287. https://doi.org/10.1007/978-3-642-55862-7_19.

Wassmann, P., Reigstad, M., Haug, T., Rudels, B., Carroll, M.L., Hop, H., Gabrielsen, G. W., Falk-Petersen, S., Denisenko, S.G., Arashkevich, E., 2006. Food webs and carbon flux in the Barents Sea. Prog. Oceanogr. 71.

Wassmann, P., Reigstad, M., 2011. Future Arctic Ocean Seasonal Ice Zones and implications for pelagic-benthic coupling. Oceanogr. 24 https://doi.org/10.5670/oceanog.2011.74.

Wassmann P., 2018. At the Edge- Current Knowledge from the Northernmost European Rim, Facing the Vast Expanse of the Hitherto Ice-Covered Arctic Ocean. Stamsund: Orkana.

Wessel, P., Smith, W.H.F., 1996. A global, self-consistent, hierarchical, high-resolution shoreline database. J. Geophys. Res. Solid Earth 101. https://doi.org/10.1029/96JB00104.

Wexels Riser, C., Reigstad, M., Wassmann, P., Arashkevich, E., Falk-Petersen, S., 2007. Export or retention? Copepod abundance, faecal pellet production and vertical flux in the marginal ice zone through snap shots from the northern Barents Sea. Polar Biol. 30 https://doi.org/10.1007/s00300-006-0229-z.

Wexels Riser, C., Wassmann, P., Reigstad, M., Seuthe, L., 2008. Vertical flux regulation by zooplankton in the northern Barents Sea during Arctic spring. Deep Sea Res. Part II 55. https://doi.org/10.1016/j.dsr2.2008.05.006.

Wiedmann, I., Reigstad, M., Sundfjord, A., Basedow, S., 2014. Potential drivers of sinking particle's size spectra and vertical flux of particulate organic carbon (POC): Turbulence, phytoplankton, and zooplankton. J. Geophys. Res. Oceans 119. https://doi.org/10.1002/2013JC009754.

Wiedmann, I., Reigstad, M., Marquardt, M., Vader, A., Gabrielsen, T.M., 2016. Seasonality of vertical flux and sinking particle characteristics in an ice-free high arctic fjord—different from subarctic fjords? J. Mar. Syst. 154 https://doi.org/10.1016/j.jmarsys.2015.10.003.

Wohlers, J., Engel, A., Zöllner, E., Breithaupt, P., Jürgens, K., Hoppe, H.-G., Sommer, U., Riebesell, U., 2009. Changes in biogenic carbon flow in response to sea surface warming. Proc. Natl. Acad. Sci. USA 106. Proc. Natl. Acad. Sci. https://doi.org/10.1073/pnas.0812743106.

Wold, A., Hop, H., Svensen, C., Søreide, J., Assmann, K.M., Ormancyk, M., Kwasniewski, S., 2023. Atlantification influences zooplankton communities seasonally in the northern Barents Sea and Arctic Ocean. Prog. Oceanogr. (Journal Preprint). https://doi.org/10.1016/j.pocean.2023.103133.

Paper III

9 Appendix

Table S1: List of short-term sediment trap data used in Figure 6. Asterisks depict POC values that were read from a figure, and therefore represent approximate values. Trap deployment depths vary between 90–150m (depending on the available data); but in some cases, POC flux values were taken from shallower depths when the seafloor was <100m, or from deployments during winter (the low fluxes were compared with deeper fluxes to confirm no change in vertical flux with depth)

Region	Reference	Area	Deployment Latitude [ºN]	Deployment Longitude [ºE]	Deployment Date	Trap Depth [m]	POC flux
BS	Andreassen et al. 1996	Northern Svalbard, offshelf	78.98	6.02	02.07.1991	100	25.00*
BS	Andreassen et al. 1996	Northern Svalbard, offshelf	79.02	8.58	04.07.1991	100	35.00*
BS	Andreassen et al. 1996	Northern Svalbard, offshelf	81.28	18.62	11.07.1991	100	15.00*
BS	Andreassen et al. 1996	Northern Svalbard, offshelf	81.67	29.80	16.07.1991	100	75.00*
BS	Andreassen et al. 1996	Northern Svalbard, offshelf	81.53	30.58	18.07.1991	100	25.00*
BS	Andreassen et al. 1996	Northern Svalbard, offshelf	81.43	30.92	15.07.1991	100	20.00*
BS	Andreassen et al. 1996	Northern Svalbard, offshelf	80.33	29.15	22.07.1991	60	45.00*
BS	Andreassen & Wassmann 1998	Central BS	76.37	32.73	19.05.1993	100	305.21
BS	Andreassen & Wassmann 1998	Central BS	75.08	32.05	21.05.1993	100	330.46
BS	Andreassen & Wassmann 1998	Central BS	74.97	31.70	23.05.1993	100	370.52
BS	Andreassen & Wassmann 1998	Central BS	73.73	31.00	25.05.1993	100	202.23

BS	Dybwad et al. 2020	Northern Svalbard, offshelf	83.02	17.38	30.01.2015	100	19.36
BS	Dybwad et al. 2020	Northern Svalbard, offshelf	82.83	21.10	14.03.2015	100	39.76
BS	Dybwad et al. 2020	Northern Svalbard, offshelf	82.72	15.25	26.04.2015	100	56.77
BS	Dybwad et al. 2020	Northern Svalbard, offshelf	81.62	12.00	10.05.2015	100	153.67
BS	Dybwad et al. 2020	Northern Svalbard, offshelf	81.39	8.81	18.05.2015	100	64.47
BS	Dybwad et al. 2020	Northern Svalbard, offshelf	80.70	7.27	30.05.2015	100	73.51
BS	Dybwad et al. 2020	Northern Svalbard, offshelf	80.76	12.05	12.06.2015	100	164.51
BS	Dybwad et al. 2020	Northern Svalbard, offshelf	80.51	7.85	16.06.2015	100	243.65
BS	Dybwad et al. 2020	Northern Svalbard, offshelf	79.97	10.65	19.05.2014	90	309.68
BS	Dybwad et al. 2020	Northern Svalbard, offshelf	79.76	9.14	23.05.2014	90	171.13
BS	Dybwad et al. 2020	Northern Svalbard, offshelf	79.78	6.16	25.05.2014	90	228.46
BS	Dybwad et al. 2020	Northern Svalbard, offshelf	79.97	10.74	09.08.2014	90	214.59
BS	Dybwad et al. 2020	Northern Svalbard, offshelf	80.86	14.95	14.08.2014	90	156.58
BS	Dybwad et al. 2020	Northern Svalbard, offshelf	80.69	15.42	14.08.2014	90	108.41

BS	Dybwad et al. 2020	Northern Svalbard, offshelf	81.17	19.13	28.05.2015	90	472.07
BS	Dybwad et al. 2020	Northern Svalbard, offshelf	81.39	17.59	31.05.2015	90	261.79
BS	Dybwad et al. 2020	Northern Svalbard, offshelf	81.62	19.43	03.06.2015	90	225.54
BS	Dybwad et al. 2020	Northern Svalbard, offshelf	81.23	19.43	06.06.2015	90	512.66
BS	Dybwad et al. 2020	Northern Svalbard, offshelf	81.92	13.46	11.06.2015	90	31.22
BS	Dybwad et al. 2020	Northern Svalbard, offshelf	82.21	7.59	15.06.2015	90	31.32
BS	Dybwad et al. 2020	Northern Svalbard, offshelf	81.89	9.73	17.06.2015	90	35.31
BS	Dybwad et al. 2020	Northern Svalbard, offshelf	81.35	13.61	19.06.2015	90	149.50
BS	Olli et a. 2002	Central BS	72.55	30.98	23.03.1998	90	60.32
BS	Olli et a. 2002	Central BS	73.77	31.88	21.03.1998	90	30.31
BS	Olli et a. 2002	Central BS	76.39	33.21	19.03.1998	90	26.24
BS	Olli et a. 2002	Central BS	72.50	30.95	28.05.1998	90	766.07
BS	Olli et a. 2002	Central BS	73.79	31.64	26.05.1998	90	746.82
BS	Olli et a. 2002	Central BS	74.80	32.46	24.05.1998	90	552.66
BS	Olli et a. 2002	Central BS	75.61	33.06	22.05.1998	90	429.29
BS	Olli et a. 2002	Central BS	76.02	32.99	20.05.1998	90	344.31
BS	Olli et a. 2002	Central BS	73.80	31.78	09.07.1999	90	163.47
BS	Olli et a. 2002	Central BS	75.12	32.29	08.07.1999	90	206.31
BS	Olli et a. 2002	Central BS	77.08	33.82	06.07.1999	90	199.46
BS	Olli et a. 2002	Central BS	77.65	34.21	04.07.1999	90	118.74

BS	Olli et a. 2002	Central BS	78.24	34.23	02.07.1999	90	105.14
BS	Reigstad et al. 2008	Central/northern BS	75.54	30.28	10.07.2003	90	122.71
BS	Reigstad et al. 2008	Central/northern BS	78.23	27.32	13.07.2003	90	344.72
BS	Reigstad et al. 2008	Central/northern BS	79.04	25.70	15.07.2003	90	222.26
BS	Reigstad et al. 2008	Central/northern BS	77.05	29.17	18.07.2003	90	145.74
BS	Reigstad et al. 2008	Central/northern BS	82.42	29.43	23.07.2004	90	58.14
BS	Reigstad et al. 2008	Central/northern BS	79.38	28.70	27.07.2004	90	117.01
BS	Reigstad et al. 2008	Central/northern BS	79.82	29.73	29.07.2004	90	219.47
BS	Reigstad et al. 2008	Central/northern BS	81.13	16.32	20.05.2005	90	350.99
BS	Reigstad et al. 2008	Central/northern BS	77.14	29.95	25.05.2005	90	208.33
BS	Reigstad et al. 2008	Central/northern BS	77.43	41.05	28.05.2005	90	80.09
BS	Reigstad et al. 2008	Central/northern BS	75.68	31.80	31.05.2005	90	720.16
BS	Wassmann et al. 1990	Central BS	75.00	28.62	27.05.1987	100	223.00
BS	Wassmann et al. 1990	Central BS	75.00	28.62	02.06.1987	100	198.00
BS	Wassmann et al. 1990	Central BS	74.48	31.52	21.05.1987	100	97.00
BS	Wassmann et al. 1990	Central BS	74.48	31.52	28.05.1987	100	64.00
BS	Wassmann et al. 1994	Central BS	73.00	31.25	7.1988	90	96.60
BS	Wassmann et al. 1994	Central BS	75.00	28.00	7.1988	100	126.40
BS	Wiedmann et al. 2014	Central BS	78.10	28.13	22.06.2011	90	247.12

BS	Wiedmann et al. 2014	Central BS	76.95	29.71	24.06.2011	90	170.26
BS	Wiedmann et al. 2014	Central BS	76.49	29.86	25.06.2011	90	198.36
BS	Wiedmann et al. 2014	Central BS	74.91	30.00	27.06.2011	90	262.29
BS	Amargant-Arumí et al. 2023	northern BS	76.16	30.97	09.08.2018	90	221.52
BS	Amargant-Arumí et al. 2023	northern BS	77.57	33.88	10.08.2018	90	168.93
BS	Amargant-Arumí et al. 2023	northern BS	79.82	33.81	14.08.2018	90	135.27
BS	Amargant-Arumí et al. 2023	northern BS	83.32	31.52	17.08.2018	90	143.38
BS	Bodur et al. 2023	northern BS	79.74	33.88	09.03.2021	30	17.83
BS	Bodur et al. 2023	northern BS	80.52	33.99	12.03.2021	30	35.19
BS	Bodur et al. 2023	northern BS	81.54	31.02	14.03.2021	30	21.00
BS	Bodur et al. 2023	northern BS	82.00	29.98	16.03.2021	30	33.14
BS	Bodur et al. 2023	northern BS	76.00	31.22	01.05.2021	90	605.67
BS	Bodur et al. 2023	northern BS	77.50	33.96	02.05.2021	90	94.73
BS	Bodur et al. 2023	northern BS	79.75	33.97	04.05.2021	90	50.28
BS	Bodur et al. 2023	northern BS	80.50	34.07	07.05.2021	90	69.81
BS	Bodur et al. 2023	northern BS	81.56	30.76	09.05.2021	90	120.89
BS	Bodur et al. 2023	northern BS	82.12	29.13	13.05.2021	90	32.55

BS	Bodur et al. 2023	northern BS	76.00	31.22	08.08.2019	90	82.34
BS	Bodur et al. 2023	northern BS	79.76	33.97	13.08.2019	90	128.47
BS	Bodur et al. 2023	northern BS	80.50	33.88	15.08.2019	90	141.50
BS	Bodur et al. 2023	northern BS	81.57	31.22	18.08.2019	90	172.88
BS	Bodur et al. 2023	northern BS	81.93	29.16	21.08.2019	90	83.96
BS	Bodur et al. 2023	northern BS	79.82	34.17	08.12.2019	90	19.54
BS	Bodur et al. 2023	northern BS	82.06	29.22	01.12.2019	90	18.98
AO	Olli et al. 2007	Deep AO	87.97	154.28	26.07.2001	90	41.73
AO	Olli et al. 2007	Deep AO	88.92	-2.03	02.08.2001	90	63.19
AO	Olli et al. 2007	Deep AO	88.75	-1.67	05.08.2001	90	
AO	Olli et al. 2007	Deep AO	88.57	3.79	09.08.2001	90	74.84
AO	Olli et al. 2007	Deep AO	88.51	-0.36	12.08.2001	90	
AO	Olli et al. 2007	Deep AO	88.29	-4.54	16.08.2001	90	46.15
AO	Olli et al. 2007	Deep AO	88.25	-8.17	18.08.2001	90	26.66
CS	Lalande et al. 2007a & b	Chukchi Sea – slope	72.64	-158.69	30.05.2004	60	59.47
CS	Lalande et al. 2007a & b	Chukchi Sea – slope	72.72	-158.40	31.05.2004	60	5.41
CS	Lalande et al. 2007a & b	Chukchi Sea – slope	72.85	-158.21	02.06.2004	100	9.01
CS	Lalande et al. 2007a & b	Chukchi Sea – slope	72.06	-154.62	13.06.2004	100	625.29
CS	Lalande et al. 2007a & b	Chukchi Sea – slope	71.92	-154.86	16.06.2004	100	623.49
CS	Lalande et al. 2007a & b	Chukchi Sea – slope	71.91	-154.97	25.07.2004	100	414.46
CS	Lalande et al. 2007a & b	Chukchi Sea – slope	72.18	-153.92	06.08.2004	100	380.22

CS	Lalande et al. 2007a & b	Chukchi Sea – slope	72.82	-158.26	12.08.2004	100	108.12
CS	Lalande et al. 2007a & b	Chukchi Sea – slope	73.05	-157.99	14.08.2004	100	138.75
CS	O'Daly et al. 2020	Chukchi/Bering Sea	63.30	-168.45	07.06.2018	30	2200.00
CS	O'Daly et al. 2020	Chukchi/Bering Sea	64.98	-168.88	11.06.2018	30	1180.00
CS	O'Daly et al. 2020	Chukchi/Bering Sea	67.67	-168.84	14.06.2018	30	1390.00
CS	O'Daly et al. 2020	Chukchi/Bering Sea	67.47	-166.21	13.06.2018	30	480.00
CS	O'Daly et al. 2020	Chukchi/Bering Sea	68.19	-167.31	15.06.2018	30	340.00
CS	O'Daly et al. 2020	Chukchi/Bering Sea	69.04	-168.82	16.06.2018	30	340.00
CS	O'Daly et al. 2020	Chukchi/Bering Sea	68.96	-166.90	17.06.2018	30	170.00
CS	Baumann et al. 2013, 2014, Moran et al. 2012	eastern Bering Sea	56.23	-171.07	31.03.2008	100	72.98
CS	Baumann et al. 2013, 2014, Moran et al. 2012	eastern Bering Sea	57.76	-174.91	22.04.2008	100	76.04
CS	Baumann et al. 2013, 2014, Moran et al. 2012	eastern Bering Sea	58.59	-176.62	25.04.2008	100	96.59
CS	Baumann et al. 2013, 2014, Moran et al. 2012	eastern Bering Sea	55.29	-167.94	06.07.2008	100	344.90
CS	Baumann et al. 2013, 2014, Moran et al. 2012	eastern Bering Sea	56.24	-171.11	15.07.2008	100	147.22
CS	Baumann et al. 2013, 2014,	eastern Bering Sea	58.42	-174.47	21.07.2008	100	314.09

	Moran et al. 2012						
CS	Baumann et al. 2013, 2014, Moran et al. 2012	eastern Bering Sea	56.26	-171.08	23.04.2009	100	198.22
CS	Baumann et al. 2013, 2014, Moran et al. 2012	eastern Bering Sea	59.51	-175.10	26.04.2009	100	514.47
CS	Baumann et al. 2013, 2014, Moran et al. 2012	eastern Bering Sea	59.55	-175.16	29.04.2009	100	736.84
CS	Baumann et al. 2013, 2014, Moran et al. 2012	eastern Bering Sea	59.57	-175.28	30.04.2009	100	796.84
CS	Baumann et al. 2013, 2014, Moran et al. 2012	eastern Bering Sea	59.44	-174.22	01.05.2009	100	1948.86
CS	Baumann et al. 2013, 2014, Moran et al. 2012	eastern Bering Sea	55.43	-168.06	19.06.2009	100	694.49
CS	Baumann et al. 2013, 2014, Moran et al. 2012	eastern Bering Sea	56.05	-171.30	23.06.2009	100	533.39
CS	Baumann et al. 2013, 2014, Moran et al. 2012	eastern Bering Sea	58.23	-174.57	25.06.2009	100	416.44
CS	Baumann et al. 2013, 2014, Moran et al. 2012	eastern Bering Sea	59.90	-178.79	03.07.2009	100	224.89
CS	Baumann et al. 2013, 2014, Moran et al. 2012	eastern Bering Sea	59.90	-178.91	19.05.2010	100	866.22
CS	Baumann et al. 2013, 2014,	eastern Bering Sea	58.21	-174.25	21.05.2010	100	208.13

	Moran et al. 2012						
CS	Baumann et al. 2013, 2014, Moran et al. 2012	eastern Bering Sea	55.44	-168.06	28.05.2010	100	48.83
CS	Baumann et al. 2013, 2014, Moran et al. 2012	eastern Bering Sea	59.89	-178.90	06.06.2010	100	244.71
CS	Baumann et al. 2013, 2014, Moran et al. 2012	eastern Bering Sea	56.26	-171.11	12.06.2010	100	84.87
CS	Baumann et al. 2013, 2014, Moran et al. 2012	eastern Bering Sea	55.43	-168.06	21.06.2010	100	1245.54
CS	Baumann et al. 2013, 2014, Moran et al. 2012	eastern Bering Sea	56.26	-171.12	26.06.2010	100	713.23
CS	Baumann et al. 2013, 2014, Moran et al. 2012	eastern Bering Sea	58.26	-174.56	28.06.2010	100	344.36
CS	Baumann et al. 2013, 2014, Moran et al. 2012	eastern Bering Sea	59.90	-178.86	04.07.2010	100	213.18
CA	Amiel et al. 2002, Huston & Deming 2002	North Water	78.36	-74.32	13.07.1998	100	191.01
CA	Amiel et al. 2002, Huston & Deming 2002	North Water	78.02	-74.85	19.07.1998	100	394.64
CA	Amiel et al. 2002, Huston & Deming 2002	North Water	77.00	-72.66	18.07.1998	100	191.01
CA	Amiel et al. 2002, Huston & Deming 2002	North Water	76.28	-74.39	04.07.1998	100	682.96

CA	Amiel et al. 2002, Huston & Deming 2002	North Water	76.42	-77.34	08.07.1998	100	491.95
CA	Amiel et al. 2002, Huston & Deming 2002	North Water	78.02	-73.85	02.09.1999	100	72.08
CA	Amiel et al. 2002, Huston & Deming 2002	North Water	77.00	-72.66	05.09.1999	100	113.53
CA	Amiel et al. 2002, Huston & Deming 2002	North Water	76.28	-71.99	07.09.1999	100	95.51
CA	Amiel et al. 2002, Huston & Deming 2002	North Water	76.28	-74.39	28.08.1999	100	91.90
CA	Fortier et al. 2002	Barrow Strait	74.74	-95.99	10.05.1994	90	83.00*
CA	Fortier et al. 2002	Barrow Strait	74.74	-95.99	15.05.1994	90	75.00*
CA	Fortier et al. 2002	Barrow Strait	74.74	-95.99	20.05.1994	90	75.00*
CA	Fortier et al. 2002	Barrow Strait	74.74	-95.99	25.05.1994	90	194.00*
CA	Fortier et al. 2002	Barrow Strait	74.74	-95.99	30.05.1994	90	260.00*
CA	Fortier et al. 2002	Barrow Strait	74.74	-95.99	01.06.1994	90	110.00*
CA	Fortier et al. 2002	Barrow Strait	74.74	-95.99	10.06.1994	90	200.00*
CA	Fortier et al. 2002	Barrow Strait	74.74	-95.99	12.06.1994	90	230.00*
CA	Fortier et al. 2002	Barrow Strait	74.74	-95.99	16.06.1994	90	313.00*
CA	Fortier et al. 2002	Barrow Strait	74.74	-95.99	20.06.1994	90	340.00*
CA	Fortier et al. 2002	Barrow Strait	74.74	-95.99	25.06.1994	90	450.00*
CA	Fortier et al. 2002	Barrow Strait	74.74	-95.99	01.07.1994	90	490.00*

CA	Fortier et al. 2002	Barrow Strait	74.74	-95.99	05.07.1994	90	430.00*
CA	Fortier et al. 2002	Barrow Strait	74.74	-95.99	10.07.1994	90	254.00*
CA	Fortier et al. 2002	Barrow Strait	74.44	-97.30	20.05.1995	90	63.00*
CA	Fortier et al. 2002	Barrow Strait	74.44	-97.30	25.05.1995	90	20.00*
CA	Fortier et al. 2002	Barrow Strait	74.44	-97.30	28.05.1995	90	10.00*
CA	Fortier et al. 2002	Barrow Strait	74.44	-97.30	01.06.1995	90	20.00*
CA	Fortier et al. 2002	Barrow Strait	74.44	-97.30	05.06.1995	90	125.00*
CA	Fortier et al. 2002	Barrow Strait	74.44	-97.30	10.06.1995	90	45.00*
CA	Fortier et al. 2002	Barrow Strait	74.44	-97.30	15.06.1995	90	190.00*
CA	Fortier et al. 2002	Barrow Strait	74.44	-97.30	05.07.1995	90	90.00*
CA	Juul-Pedersen	Disko Bay	69.23	-53.55	01.06.2001	100	599.30
HB	Lapoussière et al. 2009	Hudson Bay	62.28	-71.99	23.09.2005	100	63.90
HB	Lapoussière et al. 2009	Hudson Bay	62.65	-80.06	26.09.2005	100	63.40
HB	Lapoussière et al. 2009	Hudson Bay	79.17	-60.18	28.09.2005	100	37.70
HB	Lapoussière et al. 2009	Hudson Bay	55.33	-78.23	30.09.2005	50	50.00*
HB	Lapoussière et al. 2009	Hudson Bay	58.40	-83.29	06.10.2005	100	70.40
HB	Lapoussière et al. 2009	Hudson Bay	59.01	-87.62	11.10.2005	100	47.10
HB	Lapoussière et al. 2009	Hudson Bay	60.00	-91.95	13.10.2005	50	50.00*
HB	Lapoussière et al. 2009	Hudson Bay	61.06	-86.19	16.10.2005	100	69.40

BF	Miquel et al. 2015	Mackenzie slope	71.33	-132.56	14.08.2009	150	4.00*
BF	Miquel et al. 2015	Mackenzie slope	71.78	-130.73	22.08.2009	150	5.00*
BF	Miquel et al. 2015	Mackenzie slope	71.32	-127.50	20.08.2009	150	7.50*
BF	Juul-Pedersen et al. 2010	Amundsen Gulf	70.79	-127.62	23.09.2002	50	45.00*
BF	Juul-Pedersen et al. 2010	Mackenzie slope	71.46	-133.73	28.09.2002	50	30.00*
BF	Juul-Pedersen et al. 2010	Mackenzie shelf	70.11	-133.47	01.10.2002	50	85.00*
BF	Juul-Pedersen et al. 2010	Mackenzie shelf	70.84	-133.64	05.10.2002	50	70.00*
BF	Juul-Pedersen et al. 2010	Amundsen Gulf	71.26	-128.53	06.10.2002	50	45.00*
BF	Juul-Pedersen et al. 2010	Amundsen Gulf	70.74	-124.24	09.10.2002	50	80.00*
BF	Juul-Pedersen et al. 2010	Amundsen Gulf	71.55	-126.99	09.10.2003	50	75.00*
BF	Juul-Pedersen et al. 2010	Amundsen Gulf	70.59	-127.23	11.10.2003	50	65.00*
BF	Juul-Pedersen et al. 2010	Amundsen Gulf	70.64	-123.12	13.10.2003	50	45.00*
BF	Juul-Pedersen et al. 2010	Amundsen Gulf	70.63	-123.17	06.06.2004	50	15.00*
BF	Juul-Pedersen et al. 2010	Amundsen Gulf	70.91	-125.58	09.06.2004	50	15.00*
BF	Juul-Pedersen et al. 2010	Amundsen Gulf	70.79	-127.00	18.06.2004	50	90.00*
BF	Juul-Pedersen et al. 2010	Mackenzie shelf	71.05	-133.77	30.06.2004	50	87.00*
BF	Juul-Pedersen et al. 2010	Mackenzie shelf	70.02	-138.58	03.07.2004	50	258.40*
BF	Juul-Pedersen et al. 2010	Mackenzie shelf	70.67	-135.63	08.07.2004	50	126.50*

BF	Juul-Pedersen et al. 2010	Amundsen Gulf	71.12	-125.84	18.07.2004	50	60.00*
BF	Juul-Pedersen et al. 2010	Amundsen Gulf	70.32	-124.84	01.08.2004	50	75.00*
BF	Juul-Pedersen et al. 2010	Amundsen Gulf	70.58	-122.63	09.08.2004	50	40.00*
LS	Drits et al. 2021	Laptev Sea	77.17	114.67	31.08.2017	45	62.80
LS	Drits et al. 2021	Laptev Sea	75.41	115.44	01.09.2017	30	74.30
LS	Drits et al. 2021	Laptev Sea	75.81	130.50	03.09.2017	25	65.00
LS	Drits et al. 2021	Laptev Sea	74.25	130.50	03.09.2017	20	53.50
LS	Drits et al. 2021	Laptev Sea	78.00	105.33	23.08.2018	100	21.80
LS	Drits et al. 2021	Laptev Sea	77.65	115.60	23.08.2018	100	43.40
LS	Drits et al. 2021	Laptev Sea	77.17	114.67	24.08.2018	45	24.70
KS	Drits et al. 2017	Kara Sea	73.11	61.20	31.08.2015	75	16.60
KS	Drits et al. 2017	Kara Sea	74.78	66.59	01.09.2015	140	17.10
KS	Drits et al. 2017	Kara Sea	76.53	71.37	09.09.2015	130	92.60
ESS	Drits et al. 2021	East Siberian Sea	73.13	154.95	06.09.2017	18	49.20
ESS	Drits et al. 2021	East Siberian Sea	74.89	164.09	07.09.2017	35	33.40
FS	Reigstad (unpublished)	Fram Strait	79.80	-2.40	14.04.2003	90	19.69
FS	Reigstad (unpublished)	Fram Strait	79.62	-2.09	16.04.2003	90	12.53
NEG	Reigstad (unpublished)	NEG shelf	77.50	-6.14	21.04.2003	90	12.22
NEG	Reigstad (unpublished)	NEG shelf	76.99	-6.65	23.04.2003	90	9.53
FS	Reigstad (unpublished)	Fram Strait	79.00	0.00	23.05.2003	90	223.50
FS	Reigstad (unpublished)	Fram Strait	76.97	-2.62	27.05.2003	90	212.61
NEG	Reigstad (unpublished)	NEG shelf	77.54	-6.98	21.04.2004	90	10.64

NEG	Reigstad (unpublished)	NEG shelf	77.45	-7.30	23.04.2004	90	7.08
NEG	Reigstad (unpublished)	NEG shelf	76.95	-11.91	28.04.2004	90	8.00
NEG	Reigstad (unpublished)	NEG shelf	74.91	-13.39	03.05.2004	90	8.09
FS	Reigstad (unpublished)	Fram Strait	79.61	-2.38	16.05.2004	90	8.81
FS	Reigstad (unpublished)	Fram Strait	79.58	-3.68	18.05.2004	90	8.11
FS	Reigstad (unpublished)	Fram Strait	78.94	-2.46	21.05.2004	90	24.77
FS	Reigstad (unpublished)	Fram Strait	78.74	-2.40	23.05.2004	90	32.55